RADIOLYSIS CALCULATIONS AND HYDROGEN PEROXIDE MEASUREMENTS FOR THE MIT BWR COOLANT CHEMISTRY LOOP

by

LIN-WEN HU

S.M., Nuclear Engineering (1991)
National Tsing-Hua University
Taiwan, R.O.C.

Submitted to the Department of
Nuclear Engineering
in Partial Fulfillment of the Requirements
for the Degree of

Master of Science in Nuclear Engineering
at the
Massachusetts Institute of Technology
May 1993

Signature of Author _____
Department of Nuclear Engineering
May 7, 1993

Certified by _____
Professor Scott A. Simonson, Nuclear Engineering
Thesis Supervisor

Certified by _____
Professor Emeritus Michael J. Driscoll, Nuclear Engineering
Thesis Reader

Accepted by ____ _____
Professor Allan F. Henry
Chairman, Department Committee on Graduate Students

RADIOLYSIS CALCULATIONS AND HYDROGEN PEROXIDE MEASUREMENTS FOR THE MIT BWR COOLANT CHEMISTRY LOOP

by

LIN-WEN HU

Submitted to the Department of Nuclear Engineering
in partial fulfillment of the requirements for the Degree of Master of Science in
Nuclear Engineering

Abstract

This thesis summarizes calculations related to experiments of water radiolysis effects, principally O_2, H_2 and H_2O_2 production, conducted at the MIT Nuclear Reactor Laboratory for the BWR Coolant Chemistry Loop (BCCL). This loop has been used in a series of in-pile runs to evaluate the effects of a variety of organic and inorganic additives under both normal and hydrogen water chemistry.

A computer code, RADICAL, is used for the radiolysis calculations. An extensive series of parametric studies are reported, which attempt, unsuccessfully, to explain why measured O_2, H_2 and H_2O_2 concentrations exceed consensus calculated values by a factor of two or more. However, the calculations in this work are in relatively good agreement with those of other laboratories.

Hydrogen peroxide measurement methods are also reviewed/evaluated in this thesis. A method involving dissociation using MnO_2 was tested, using both recirculation mode and once-through mode flow path, to measure oxygen, hence hydrogen peroxide concentrations. The experiments have demonstrated that the accuracy of this method is within $\pm$ 20 %.

Thesis Supervisor : Scott A. Simonson
Title : Assistant Professor of Nuclear Engineering
Thesis Reader : Michael J. Driscoll
Title : Professor of Nuclear Engineering (Emeritus)

Acknowledgements

The completion of this thesis is due to the contributions of the MIT BCCL group. Among the members, Professor Emeritus Michael Driscoll and Professor Scott Simonson have been unfailingly helpful in both radiolysis calculations and hydrogen peroxide measurements. Their support, guidance and valuable suggestions are greatly appreciated.

I would like to express my sincere gratitude to many other people for making this thesis possible.

Thanks go to Gordon Kohse, Ernesto Cabello and Miles Kafka for their technical support for building the hydrogen peroxide measurement loop and for Orbisphere maintenance.

I am also indebted to John Chun for his support with the RADICAL code, and Bruce Hilton for the valuable discussions about the BCCL experiments. Their patience and assistance has encourged me during this research.

Special thanks go to Sam Yam. His constant inspiration and support will be long remembered.

The most important appreciation goes to my family, for being there whenever I need them.

Table of Contents

Chapter Page

List of Figures

Figure Page

List of Tables

Table Page

Chapter 1
Introduction

1.1 Foreword

An in-pile loop for coolant radiolysis studies in an environment similar to that in a BWR core has been constructed and operated at the MIT Nuclear Reactor Laboratory (O-1) (R-1). Aspects of particular interest here are measurements of the concentrations of the principal radiolysis products, H_2, O_2, and H_2O_2 under both normal and hydrogen water chemistries. Nitrogen-16 carryover and electrochemical corrosion potential (ECP) are also routinely measured, but analysis of such data are outside the scope of this report.

One of the objectives of this work is to calculate, using state-of-the-art methods and basic data, species concentrations for comparison with experimental data with two applications in mind:

(a) to assist in planning and interpretation of the experiments
(b) to use the experimental data as a guide to refinement of high temperature radiolysis data and computational models

As part of the first objective we seek to determine just how well the MIT BWR Coolant Chemistry Loop (BCCL) simulates a full scale BWR, and how sensitive results are likely to be to differences in key parameters of design and operation. In the second category we will be focusing on plausible ways to account for the higher than calculated H_2O_2 concentrations experienced in all runs to date.

Hydrogen Peroxide measurement methods are also introduced in this thesis. A "MnO_2 method" was tested for two different configurations – recirculation and once-through; both are shown to be accurate with ± 20 %. The MnO_2 method will be used to supplement the current colorimetric method in the Summer 1993 campaign, so that experimental results can be verified, particularly if an abnormal hydrogen peroxide concentration is measured. A reagent injection method is also to be evaluated using colorimetric reagent in the injected sample cooling line, so that thermal/surface decomposition can be avoided, or greatly reduced, during hydrogen peroxide sampling.

In addition to their intrinsic merit, both objectives are also relevant to achievement of the goals of two other in-pile research projects at the MITNRL: The construction and operation of facilities to test ECP and crack-growth sensors and measure irradiation

assisted stress corrosion cracking. These projects require the simulation of BWR coolant environments (i.e. an inherently two phase situation) using loops operated under single phase (liquid) conditions.

It should be also noted that this thesis is an amplification of a prior report by the same author (H-2), and both supplements and supercedes this early submission.

1.2 Background

The as-built version of the BCCL is documented in Refs (R-1) and (O-1) in considerable detail. Figure 1.1 is a schematic showing its principal features. Basically it consists of a 0.25 inch ID titanium feedwater line supplying preheated water to a Zircaloy in-pile U-tube in which boiling is induced by a combination of gamma and electric heating. The two phase mixture flows into a separator plenum from which vapor and liquid effluent are extracted. The return lines are scanned for N-16 activity, and are then remixed in a regenerative heat exchanger before being returned to the makeup storage tank. The cover gas in this tank can be varied to control system chemistry, and a separate chemical injection system is provided to effect more substantial changes. ECP electrodes are incorporated in the separator plenum and in an external autoclave in the liquid letdown line. A cooled sample extraction system is used to draw samples from the plenum liquid effluent line for analysis of H_2O_2. Nodalization of this system for computer calculations is discussed in Chapter 2.

Several aspects are of special interest relative to current objectives. While the original conceptual design of the BCCL attempted close simulation of a BWR, including the capability for corrosion product radionuclide deposition studies, the focus evolved more toward its use for "clean" experiments involving radiolysis chemistry. Thus the loop studied in this report is once-through and employs titanium as its principal material of construction. This permits addition of controlled amounts of transition metals (Fe, Mn, Cu, Zn, etc..) to assess their effect on system chemistry. Later phases of our research program call for conversion to a recirculating version, and replacement of titanium by steel, in a step-by-step approach to a more realistic BWR analog.

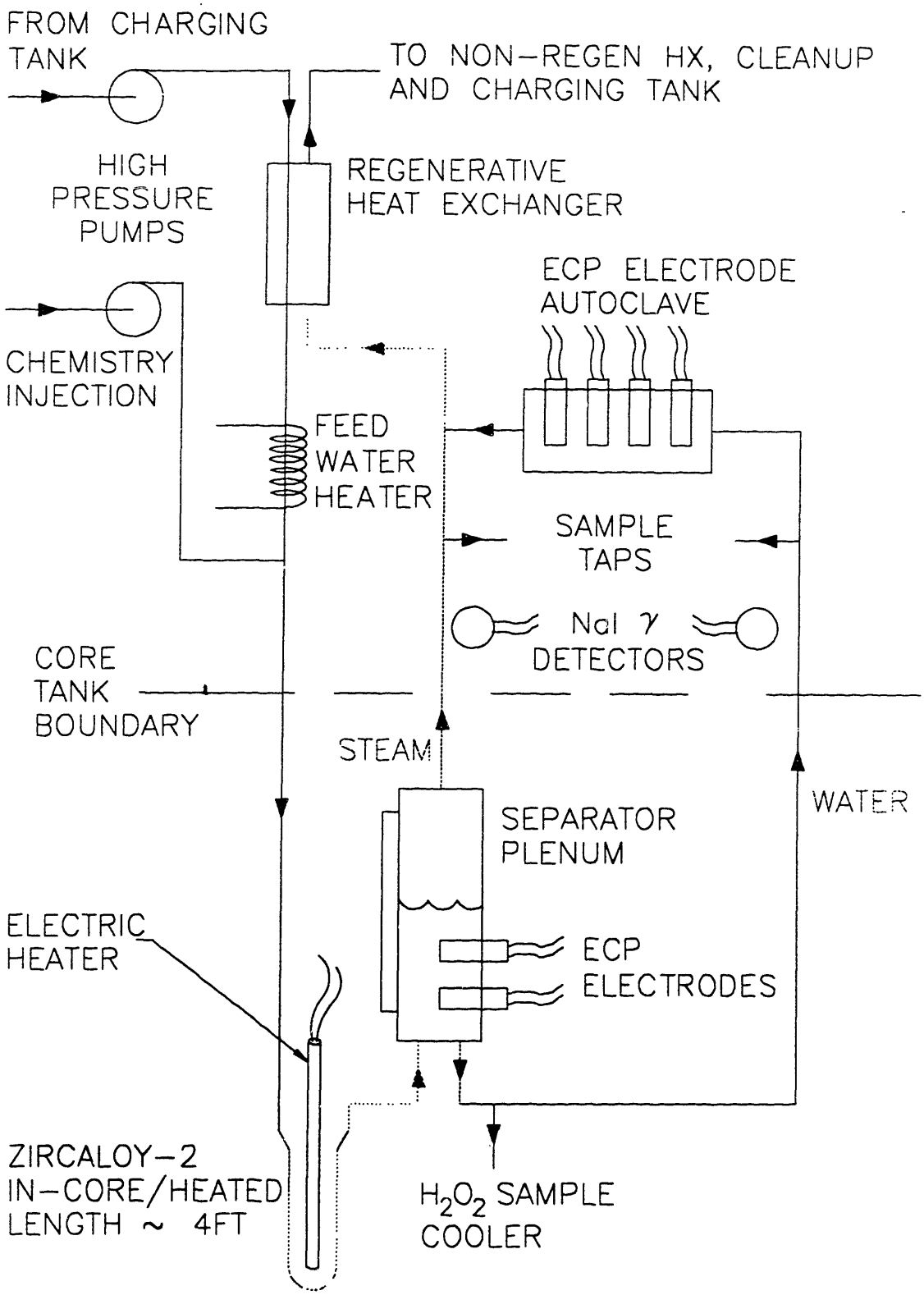

Figure 1.1 Schematic of BWR Coolant Chemistry Loop

1.3 Organization of This Thesis

The next two chapters describe the input to (in BCCL specific terms) and capabilities of, the MIT RADICAL program, which was used to carry out all of the calculation work in this thesis. Particular emphasis is given to some of the fine points involved in the use of this code. Loop nodalization is described in sufficiently general terms to permit others to calculate BCCL performance using other programs. Note that Appendix F supplements the user's manual provided in J. Chun's thesis (C-1).

Chapter 4 reports the results of an extensive series of parametric studies carried out to establish the dominant design and operating parameters, so that proper attention can be paid to their precise quantification for the final round of simulation runs reported in Chapter 5. As might be anticipated, the magnitude of the in-core neutron and gamma dose rates proved to be the key data. Appendices C and D describe our efforts to better define this information.

Chapter 5 presents the results of main interest: the concentrations of radiolytic species (H_2, O_2, H_2O_2), together with a set of comparisons with BCCL data. Chapter 6 reviews and evaluates hydrogen peroxide measurement methods. Design and tests for the hydrogen peroxide measurement facility to be used in the summer 1993 campaign are included in this chapter. Chapter 7 identifies a course of action which should resolve some of the main discrepancies between the experimental data and the calculation results.

Chapter 2
The MIT BCCL

2.1 Introduction

The loop has already been described in schematic fashion in Chapter 1. Our interest here is in the details necessary to translate its physical characteristics into a computer model. Part of the information required to do so relates to the environment in which it operates inside the MIT reactor core and pool above the core: specifically the neutron and gamma dose profiles. Within the loop itself, the thermal-hydraulic and mass transfer characteristics are of principal interest.

Uncertainties will be discussed as appropriate, as a prelude to the parameter studies in Chapter 4, where the extent to which they lead to uncertainty in the results of our calculations will be evaluated.

2.2 Description of System

Figure 2.1 shows a schematic, focusing on the in-thimble components. As can be seen, with the exception of the outlet plenum, the design is quite simple, consisting of quarter inch diameter tubing: titanium ex-core, and Zircaloy-2 in-core. Table 2.1 gives the properties of this tubing. The titanium tubing in question has now experienced several months of hot operations, including several cleanouts with HNO_3, so that a well developed oxide film is in place. Fresh Zircaloy tubing is used for each campaign, to reduce handling dose to those refurbishing and re-assembling the loop internals.

Figure 2.2 shows a more detailed section view of the outlet plenum, showing how the vapor-liquid inlet mixture is turned 90° to aid in separation and reduce carryover. A slotted exit tube serves as a moisture de-entrainment device. Measured carryover is about 2 wt %. Since H_2 and O_2 concentrations in the vapor are roughly fifty times those in the liquid phase in the plenum, this level of carryover is not significant. Carryunder is another matter. While not yet accurately measured, several percent appears unavoidable, which means that "liquid" effluent will have most of its H_2 and O_2 contributed by entrained vapor.

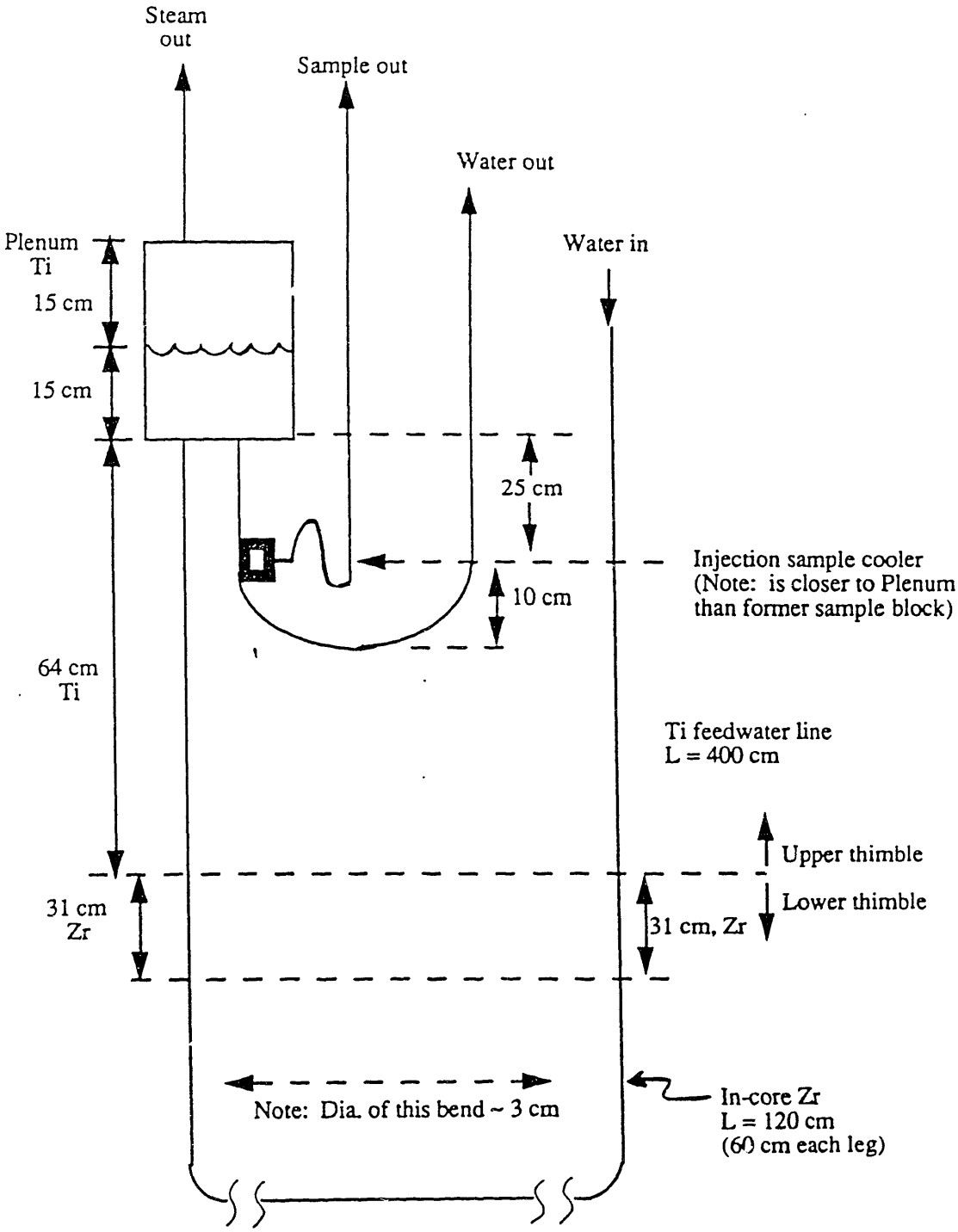

Figure 2.1 Layout of BCCL In-Thimble Components (not to scale)

Table 2.1

Properties of Loop Materials

Titanium Tubing (Thimble Internals)

Type: CP Grade 2

Lengths: (See Nodal Diagram)

OD: 1/4 inch

ID: 0.194 inch (0.48 cm)

Impurities (Mfgr. Spec.), Typical:

Fe	0.03%
O	0.11%
N	0.006%
H	14 ppm

Residual Elements

Each < 0.10%

Total < 0.40%

Zircaloy Tubing

Type: Zircaloy-2

Length: 60 inches

OD: 5/16 inch

ID: 0.257 inch (0.67 cm)

COMPOSITION:	ppm (NAA)*
Cr	984 ± 18
Fe	1450 ± 70
Co	0.5 ± 0.07
Hf	48 ± 4
Zr	BALANCE

NAA = measured using neutron activation analysis

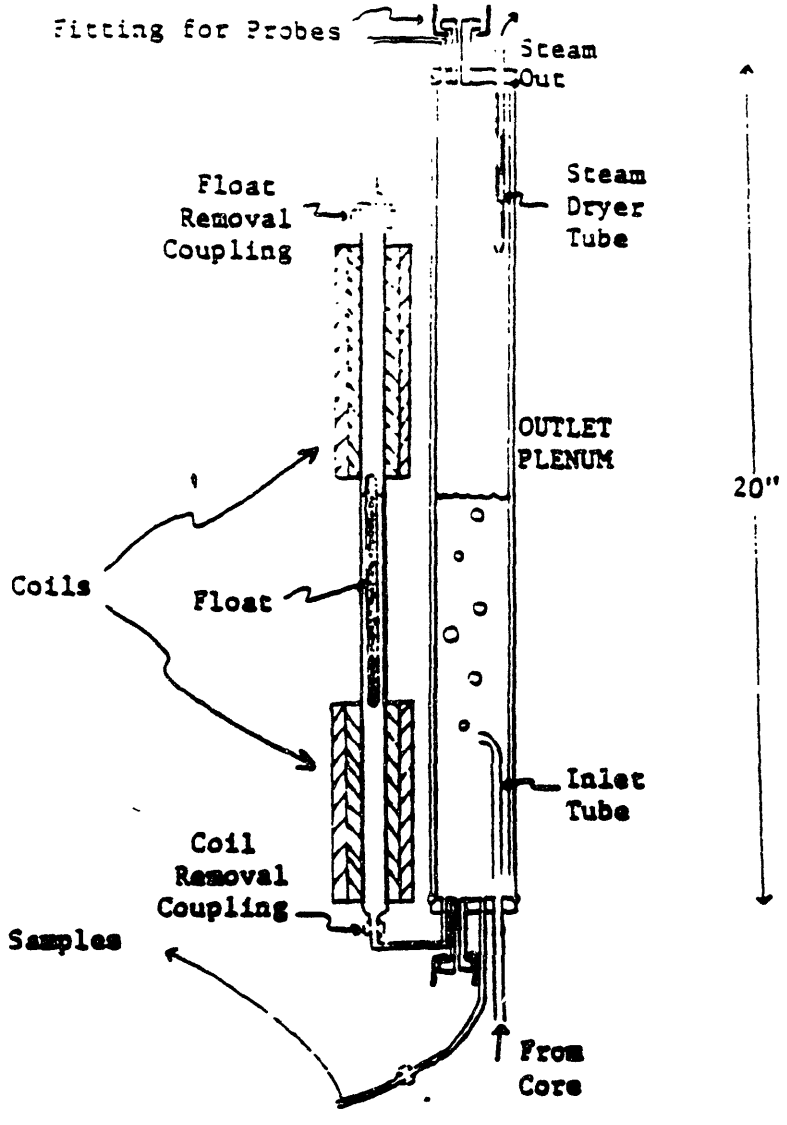

Figure 2.2 Details of BCCL Plenum

Figure 2.3 is an ex-thimble nodal diagram. Table 2.2 lists the geometry and inlet/outlet temperatures of the components. This ex-thimble model has not yet been included in the present calculation. However, it provides the possibility to simulate the entire BCCL loop in the future.

Several features of the system external to the core tank thimble are worthly of note:

(1) The effluent vapor and liquid streams are combined in a regenerative heat exchanger. Thus the only high-flow rate, low temperature effluent stream accessible to instrumentation is a reconstituted mixture. In view of the key role of carryunder, a segregated liquid sample would be of little value, in any event.

(2) Cold high flow rate samples are needed for the Orbisphere O_2 and H_2 meters. Hence only the combined letdown stream, the feedwater recycle stream, and a recirculation side stream on the makeup tank can be analyzed using these devices.

(3) Full flow ion exchange cleanup is provided on the letdown line, and makeup tank cover gas is circulated through a catalytic recombiner and then sparged through the water inventory. Measurements on the tank inventory using an on-line IC unit confirm that anion impurities are present only at ppb levels (which implies similar bounds on their associated cations)

(4) Virtually no peroxide can complete a full loop circuit when the system is operating at high temperature; when the entire system is cold however, several ppm can accumulate in the makeup tank.

The perishable nature of H_2O_2 required that special measures be taken to obtain a useful measurement of this species. The sample in question is extracted from the plenum liquid effluent line and cooled as quickly as possible to stop both thermal and wall-induced decomposition of H_2O_2. Originally heat was rejected by conduction to the thimble wall (October 1990 campaign), but more recently a system which employs injection of cold water, followed by a sample-to-water heat exchanger has been used. Even so, about half of the H_2O_2 is lost in the sampling process. Since H_2O_2 is presumed to be non-volatile, carryunder does not interfere with this measurement.

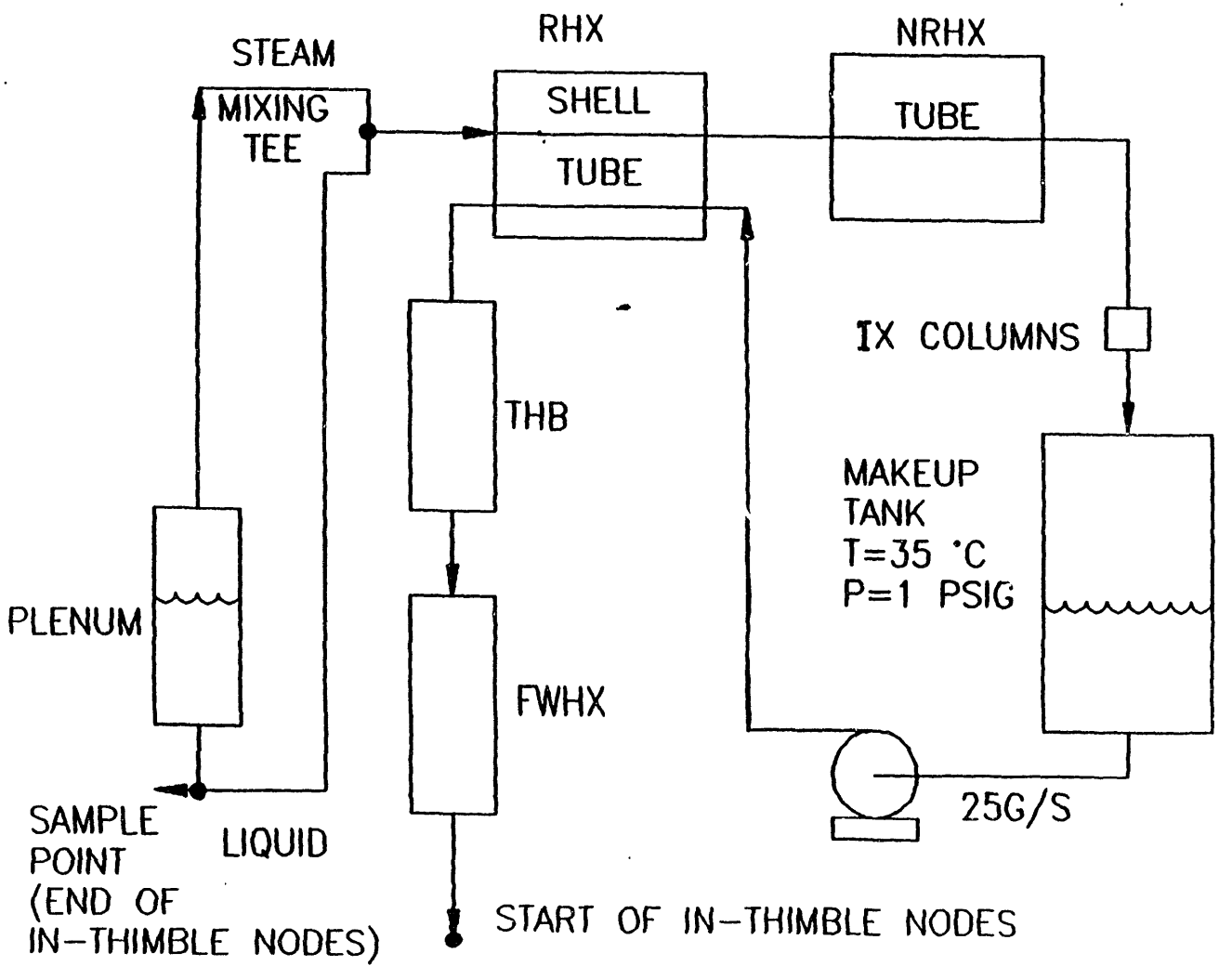

Figure 2.3 Ex-thimble Nodal Daigram

NODAL DIAGRAM OF BCCL MAKEUP/LETDOWN SYSTEM
(Principal features only)

MAKEUP

Component	Length (cm)	ID (cm)	Tin/Tout C
Line to RHX	338	0.48	38/38
Feedwater RHX	610	0.48	38/263
Line to thermal Ballast	78	0.48	263/263
Thermal Ballast (THB)	467	0.48	263/263
Line to FWHX	74	0.48	263/263
FWHX	460	0.48	263/280
Line to Thimble	994	0.48	280/280

LETDOWN

Liquid to Tee (1)(2)	706	0.48	289/285
Steam in Plenum	25	1.27	289/289
Steam to Tee (1)	642	0.48	289/285
Tee to RHX	536	0.48	285/285
RHX	610	d_H = 0.45 Annulus	285/100
NRHX	610	0.48	100/32
Line to Makeup	231	0.48	32/32

Note: All lines are Titanium (Except for ~ 100 cm nulon to/from makeup tank)
(1) Includes N-16 Plena
(2) Dose Rate: $D_\gamma \leq 43.20$ R/s, $D_n \leq 0.006$ R/s; zero elsewhere

Table 2.2 Geometry and inlet/outlet temperatures of the ex-thimble components

Cooled, low flow rate samples are also extracted from the vapor and liquid effluent lines after they exit the MIT Reactor core tank. They are primarily useful for special measurements, such as carryover and carryunder.

To summarize, then, the most useful samples are the combined effluent (for O_2 and H_2), and the plenum outlet line (for H_2O_2). This should be kept in mind when comparing experimental and computed values. A further limitation in most runs to date has been the unreliable performance of the H_2 analyzer proior to the Summer 1992 campaign. Thus major emphasis must be placed on H_2O_2 and O_2. One would expect that (in the absence of oxidizing or reducing additives) H_2 and O_2 are present in stoichiometric amounts at the point where effluent re-enters the makeup tank, because H_2O_2 has decomposed, and other radiolytic species are short lived.

2.3 Characterization of Environment

The magnitudes of the neutron and gamma dose rates are arguably the most important input data to a computer simulation. Two principal issues are addressed here: development of best-estimate values for the MITR-II, and comparison with the corresponding values for a representative BWR core.

The MIT Research Reactor operates at a power density of 70 KW/liter, and the core is approximately 50 volume percent each H_2O and Al (the highly enriched uranium fuel constitutes less than one volume percent). As such it provides neutron and gamma dose rates roughly comparable to those in a LWR. There are, however, important differences, most of them traceable to the virtual absence of U-238, which absorbs neutron energy by inelastic scattering, and, because of its high density, is an important sink for gamma energy in LWR cores. Appendix C discusses how this affects the dose absorbed by H_2O.

Basically three different sources of data can be marshaled to address the present task:

(a) experimental measurements made during MITR-II startup operations in the mid-1970's, and in the past several years as part of the design phase of in-pile facility development

(b) basic energy balance calculations (see Appendix C) considering yields in fission and other nuclear processes, and energy absorption by core constituents

(c) state-of-the-art Monte Carlo code computations, carried out on behalf of the present study using the MCNP program

The experimental data is most useful for establishing spatial profiles. Figures 2.4 and 2.5 and Table 2.3 summarize the most pertinent information in this category: an in-core gamma traverse by Boerigter (B-1) an above-core gamma traverse by Outwater *et al.* (O-2), and in-core gamma heating measurements by Zaker (Z-1). Our present assessment is that the absolute values in these reports are somewhat uncertain because the measurements were made at low reactor power and extrapolated to full power. The contribution by fission product decay gammas is the principal issue. The measured doses are also in non-aqueous detectors or dosimeters.

Energy balances are useful in that they illuminate possible sources of error and help set upper or lower limit bounds. Simple estimates of this sort, however, can not easily amount for the effect of leakage in the small MITR core, which has an equivalent spherical radius of only 25 cm. Detailed consideration of the ingredients of the gamma energy balance also suggest another important difference between the MITR and a BWR: the former usually operates on a 4 days up/3 days down schedule for an average capacity factor of about 60%, whereas the latter ideally run at 100% power for a year or more at a stretch. Hence in the MITR gamma balance the decay gamma contribution should be reduced accordingly.

Finally, there is the Monte Carlo method, which, if done carefully and consistently, should yield the best estimates we are likely to get. Figures C.2 and C.3 show MCNP traverses for gamma and neutron doses in the H_2O of the MITR core and the BCCL loop,respectively. Table 2.4 summarizes the core average results, both as-computed and as-corrected for fission product decay gammas. These average results are calculated from the curve fit functions, which are obtained from MCNP data, as shown in Table C.2. Note that the MCNP runs were for a fresh core before any fission product buildup. Also shown in Table 2.3 are comparable BWR values computed for the unit cell shown in Appendix C.

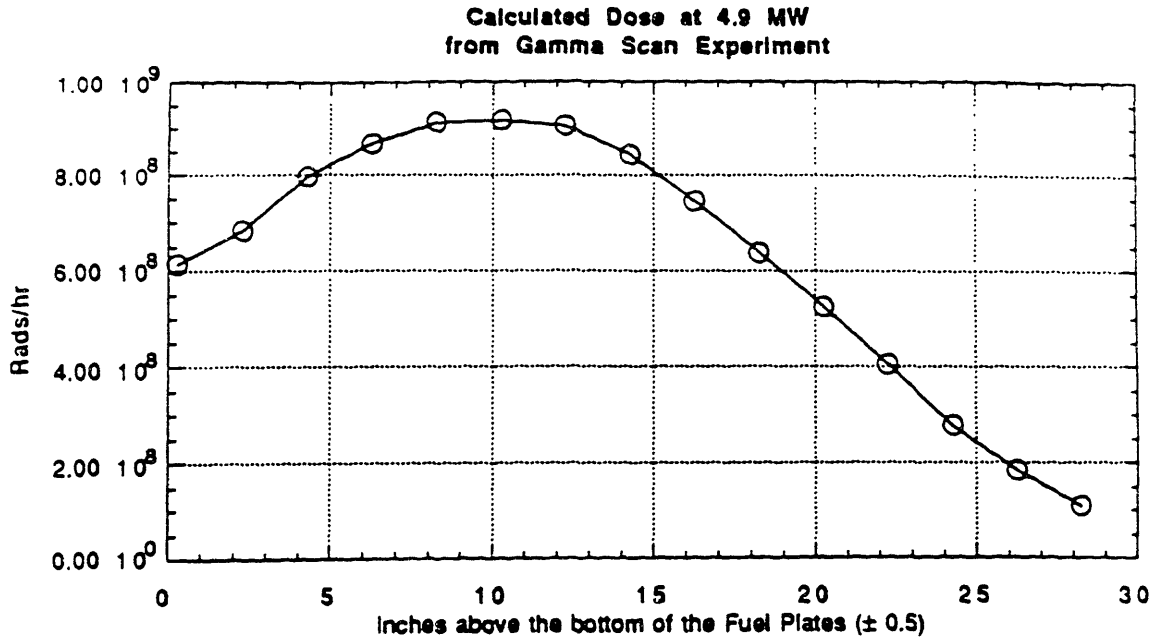

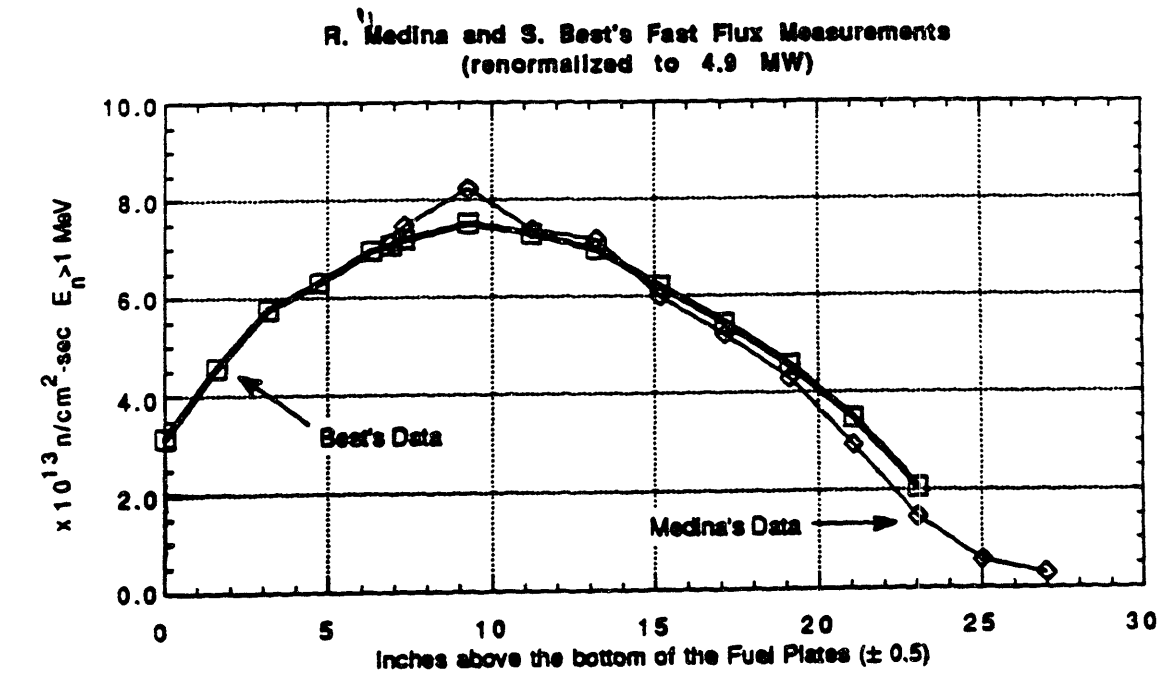

Figure 2.4 Gamma and Fast Neutron Profiles in the MITR

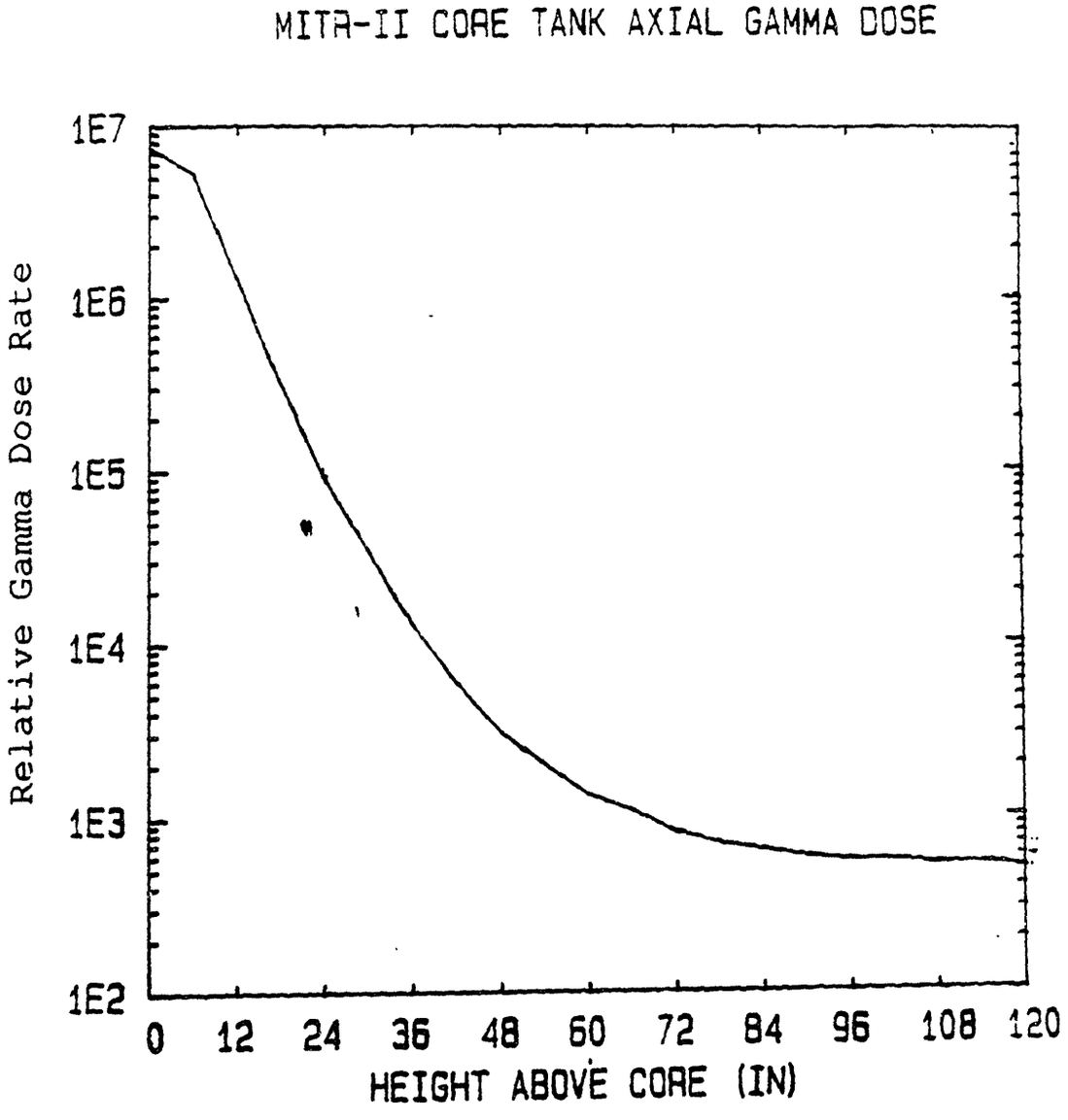

Figure 2.5 Gamma Dose Rate Measured in the MITR-II Core Tank at 1 kW

Table 2.3

Total Dose Rate Extrapolated to 5 MW
Measured In the ICSA of MITR-II (Z-1)

Total Dose / Position	R_C^T, carbon watt/gm	R_{Al}^T, Aluminum watt/gm	R_{Be}^T, Beryllium watt/gm
0	2.442	2.262	2.336
	± 0.006	± 0.007	± 0.002
15	2.527	2.262	2.602
	± 0.005	± 0.007	± 0.002
20	2.595	2.380	2.816
	± 0.008	± 0.006	± 0.003
25	2.711	2.484	2.908
	± 0.009	± 0.008	± 0.004
35	2.554	2.331	2.602
	± 0.006	± 0.007	± 0.003
45	2.037	1.994	2.418
	± 0.005	± 0.003	± 0.002
55	1.610	1.474	1.673
	± 0.004	± 0.004	± 0.002

Notes

- ICSA = In-core sample assembly in fuel position B4
- Position = cm above bottom of ICSA, which is 2-3 inches below bottom of fuel element
- Measurements done at 2-3.5 MW using adiabatic calorimeters and extrapolated to 5 MW
- Percent of total heating due to neutrons (estimated) is ~ 10%, 5%, 20% in C, Al, Be, respectively
- Al value is corrected for thermal neutron captures

Table 2.4

Summary of Dose Rate Values (Core Axial Average in H_2O)

Best-estimate (Monte Carlo) Dose Rates in BCCL H2O

$D_n = 2.0 \times 10^5$ R/s*

$D_\gamma = 0.9 \times 10^5$ R/s*

BWR (Monte Carlo) @ 51 Kw/l

$D_n = 3.02 \times 10^5$ R/s

$D_\gamma = 1.12 \times 10^5$ R/s

BWR (GE) @ 51 Kw/l

$D_n = 2.86 \times 10^5$ R/s

$D_\gamma = 1.04 \times 10^5$ R/s

MITR Core (Monte Carlo)

$D_n = 2.5 \times 10^5$ R/s

$D_\gamma = 1.7 \times 10^5$ R/s

CONCLUSIONS:

- BCCL gamma dose rate is same as BWR
- BCCL neutron dose rate is 2/3 that of BWR
- Attenuation of core neutrons and gammas by BCCL structure must be accounted for

* Compare to 1991 nodal diagram (Fig. 6.1) values of
$D_n = 1.1 \times 10^5$ R/s
$D_\gamma = 1.1 \times 10^5$ R/s

2.4 Loop Thermal-Hydraulics

The time spent in-core, together with the ambient dose rates, determines total absorbed dose. Hence loop thermal hydraulics are an important consideration. Most of our prior computations have assumed a particularly simple model of core flow, in which quality varies linearly from the start-of-boiling locus to the core exit. As part of the present study a more thorough investigation of this aspect and other boiling characteristics were undertaken.

Core Residence Time

Integrated dose is proportional to core-average dose rate times in-core residence time. The latter parameter can be estimated from:

$$t = \frac{L\rho}{\dot{m}''} \tag{2.1}$$

where $\dot{m}''$ = mass flux, $g/cm^2\ s$
L = length of core, cm
ρ = average density of fluid in core (~0.45 g/cm^3)

We may compare a BWR and the BCCL assuming they have the same axial void profiles as a function of normalized position. Appropriate data and results are

	$\dot{m}''$, $g/cm^2\ s$	L, cm	t, second
BWR	200	366	0.82
BCCL	75	120	0.72

Thus the residence time in the BCCL in core region is only 13% shorter than that in a full scale BWR. It would be possible to reduce the flow rate to achieve an exact match if this were thought worthwhile: for example to allow equal times for diffusion, mass transfer and chemical reaction.

Thus the principal factors leading to different integrated doses are the differences in dose rates for neutrons and gammas between the BCCL and a representative BWR.

Residence Time in Plenum

The residence time of liquid in the outlet separator plenum is readily estimated from the liquid volume.

$$V = \frac{\pi}{4} d^2 L = \frac{\pi}{4}(3.36)^2(15) = 133 \text{ cm}^3$$

and the liquid mass flow rate

$$\dot{m}_\ell = \dot{m}(1-x) = 25(1-0.15) = 21.25 \text{g/s}$$

at a liquid density,

$$\rho = 0.74 \text{ g/cm}^3$$

one has

$$t_l = \frac{\rho V}{\dot{m}_l} = 4.6 \text{ s}$$

This is considerably longer than the in-core residence time, and ample for the completion of most post-irradiation reactions.

It should be reiterated, however, that the current plenum model employed in the loop simulation is quite crude: perfect liquid/vapor phase separation is assumed at the entrance to the plenum without subsequent mass transfer between the two phases.

The vapor phase volume in the plenum is roughly comparable to that of the liquid phase, but the density is a factor of 19 lower, hence even at 15% quality, the vapor residence time is shorter: ~ 1.4 seconds.

Homogeneous Boiling Model

The thermal-hydraulic model used in RADICAL is a homogeneous boiling model which calculates quality from the energy balance equation and uses Bankoff's equation to correlate the corresponding void fraction and slip ratio. The Bankoff equation is :

$$V_f = \frac{K}{1 - \frac{\rho_g}{\rho_\ell}\left(1 - \frac{1}{q}\right)}$$

$$S_\ell = \frac{V_g}{V_\ell} = \frac{1 - V_f}{K - V_f} \tag{2.2}$$

$$A_g = V_f A_o$$

$$A_\ell = A_o - A_g$$

where K = flow parameter = 0.71+0.00143P
P = pressure (atm)
ρ_ℓ = density of liquid (g/cc)
ρ_g = density of vapor (g/cc)
A_0 = cross sectional area of the channel (cm^2)
A_ℓ = cross sectional area occupied by liquid (cm^2)
A_g = cross sectional area occupied by vapor (cm^2)
q = quality, weight fraction vapor

From a mass balance

$$\rho_g V_f V_g + \rho_\ell (1 - V_f) V_\ell = \rho_\ell V_o \tag{2.3}$$

where V_0= inlet velocity of liquid phase (cm/s)

Then

$$V_\ell = \frac{\rho_\ell V_o}{\rho_g V_f S_\ell + \rho_\ell (1 - V_f)} \tag{2.4}$$

$$V_g = S_\ell V_\ell \tag{2.5}$$

This simple model makes it easy to simulate boiling conditions but doesn't reflect the actual boiling phenomena. For example, the Bankoff equation calculates a void fraction of about 0.8 when quality equals one (all vapor) as shown in Fig. 2.6, which is physically inconsistent. Moreover, the slip ratios fall below zero when the void fraction is greater than 0.8, as shown in Fig. 2.7, which is physically impossible. Also notice that the slip ratio increases to as large as 20 at a void fraction of 0.8: this is far too high, since even though the vapor phase tends to travel faster than the liquid phase, the liquid droplet entrainment in the high void fraction region will suppress the increasing rate of the slip ratio.

Modified Homogeneous Boiling Model

The modified homogeneous boiling model is presented here to show the possibility of improving the boiling model in the radiolysis calculation. It is claimed that the subcooled boiling region, due to thermal non-equilibrium effects, is important in a high pressure system. Experiments showed that the void fraction at the bulk boiling point can be as high as 0.4 (B-2) depending on the system conditions at which the predicted void fraction is zero in the homogeneous boiling model. A slip ratio model as a function of flow patterns is suggested here, since the stripping rate is crucial to radiolysis calculations.

Fig. 2.8 shows a boiling channel with subcooled boiling. Saha and Zuber used experimental data to correlate the point where the onset of nucleate boiling begins (S-2).

$$X_{\ell d} = -0.0022\frac{C_{pf}q''}{h_{fg}}\frac{D_h}{k_f}, \text{ for } Pe < 70{,}000$$

$$X_{\ell d} = -154\frac{q''}{\rho_f h_{fg}}\frac{1}{V_{in}}, \text{ for } Pe \geq 70{,}000 \qquad (2.6)$$

where Z = axial position

X_e = thermal equilibrium quality = $\dfrac{\bar{h} - h_f}{h_{fg}}$

$X_{\ell d}$ = thermal equilibrium quality at Z_d

D_h = heated diameter

V_{in} = liquid inlet velocity

and the Peclet number, $Pe = \dfrac{\rho_\ell V_{in} D_h C_{pf}}{k_f}$

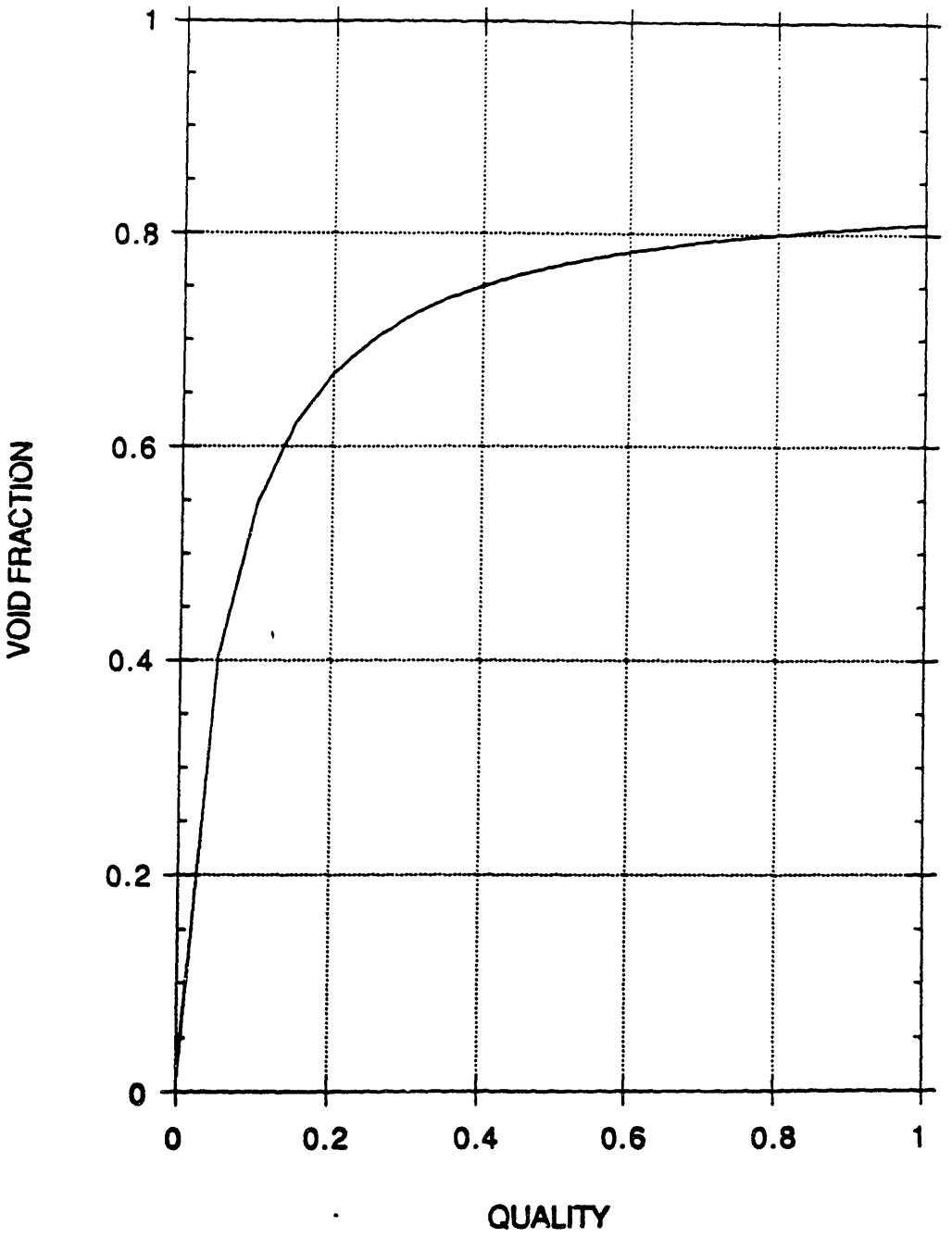

Figure 2.6 Void fraction-quality relation from Bankoff equation at 70 atm

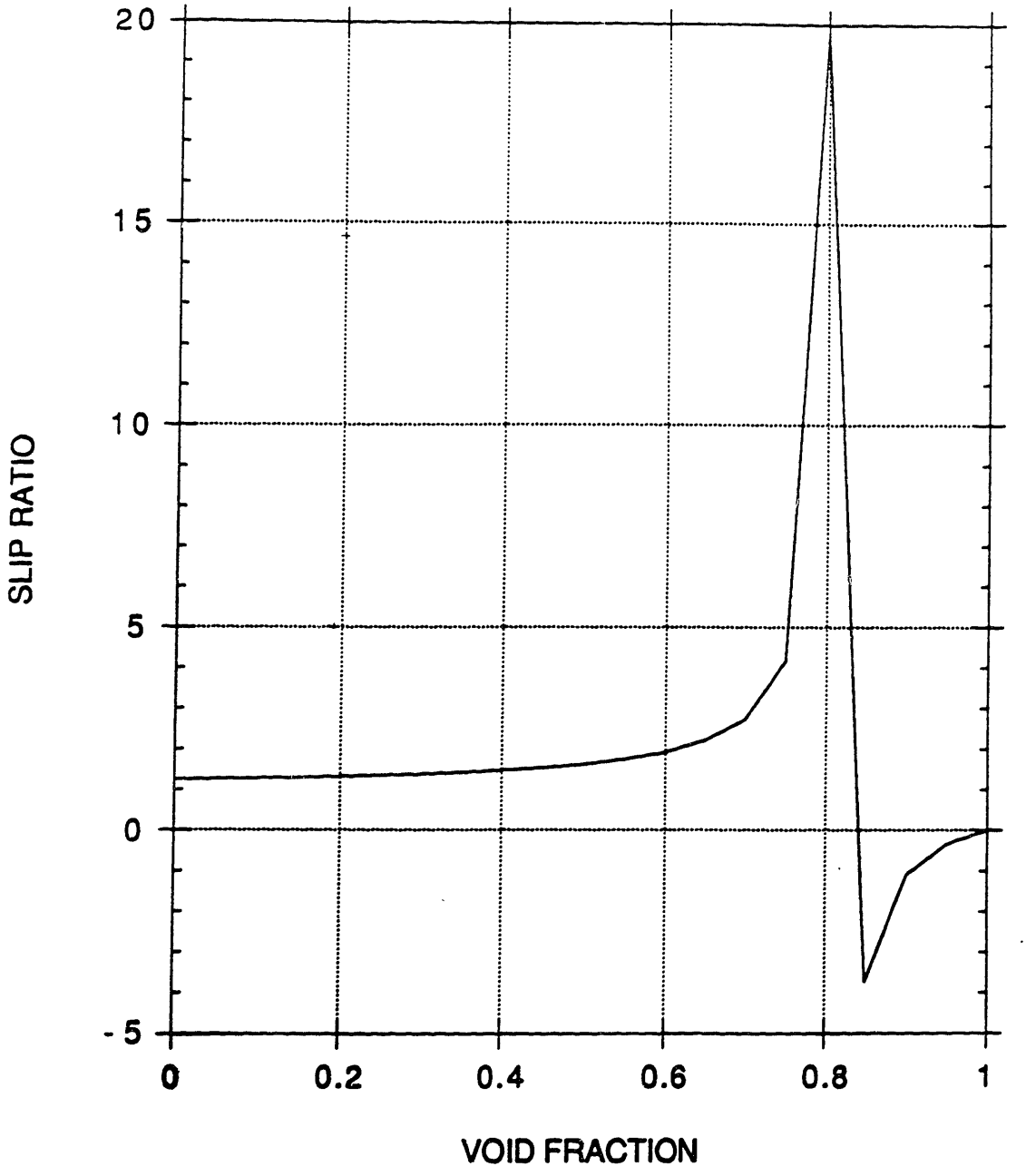

Figure 2.7 Slip ratio-void fraction relation from Bankoff equation at 70 atm

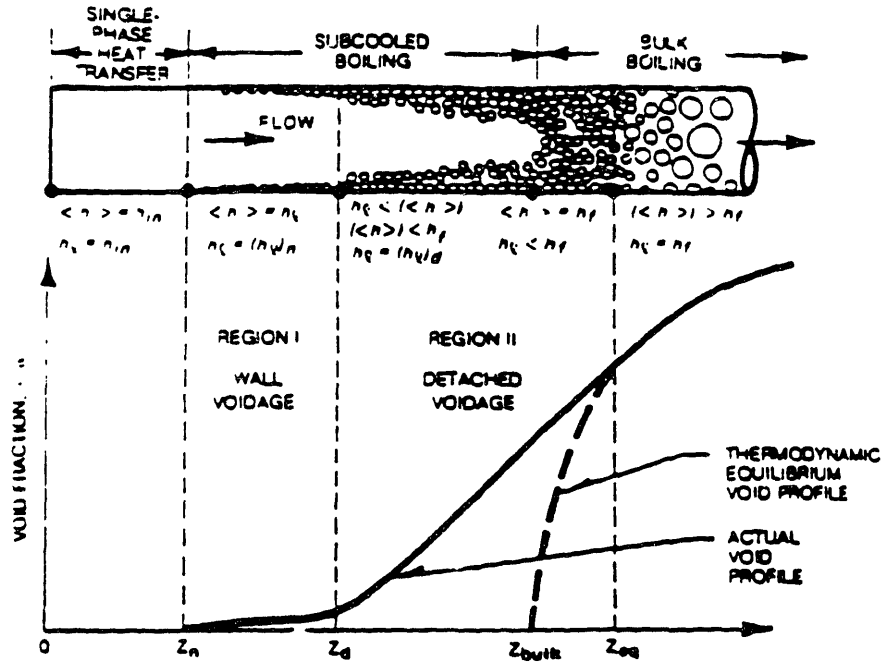

Figure 2.8 Boiling regions in two-phase flow (L-2)

The corresponding Z_d, the position where boiling begins, can be calculated from the energy equation.

$$\because \bar{h} = h_f + x_e h_{fg} = \frac{\pi D_h Z q''}{\rho_\ell V_{in} \frac{\pi}{4} D_h^2} + h_{in}$$

$$\therefore Z_d = \rho_f V_{in} D_h \left(h_f + X_{ed} h_{fg} - h_{in}\right) \frac{4}{q''} \tag{2.7}$$

A simple relation between X , the true quality, and Xe is recommended as follows

$$X(X_e) = \frac{X_e - X_{ed}\left(\frac{X_e}{X_{ed}} - 1\right)}{1 - X_{ed} \exp\left(\frac{X_e}{X_{ed}} - 1\right)} \tag{2.8}$$

The void fraction can be calculated from

$$V_f = \frac{X}{C_o\left[\frac{X(\rho_\ell - \rho_g)}{\rho_\ell} + \frac{\rho_g}{\rho_\ell}\right] + \frac{\rho_g V_{gj}}{G}} \tag{2.9}$$

Note that the above equation can be derived from the mass balance equation.

$$V_f = \frac{1}{1 + \frac{(1-X)}{X} S_\ell \frac{\rho_g}{\rho_\ell}} \tag{2.10}$$

Substituting the slip ratio equation in the drift flux model (L-1) gives

$$S_\ell = C_o + \frac{X(C_o - 1)\rho_\ell}{\rho_g(1-X)} + \frac{\rho_\ell V_{gj}}{G(1-X)} \tag{2.11}$$

where C_0 is the distribution parameter: a value of 1.13 is generally used. V_{gj} is the weighted mean vapor drift velocity which, for upward bubbly churn flow, can be given by

$$V_{gj} = 1.41\left[\frac{\sigma g(\rho_\ell - \rho_g)}{\rho_\ell}\right]^{1/4} \tag{2.12}$$

Notice that if we neglect the local slip between phases (i.e. set V_{gj}=0), Eq. (2.9) and (2.11) yield the same form of equation as Bankoff's equation (2.2), where $1 / C_0$ corresponds to K. A discussion in (I-1) indicates that the local slip can be important under certain circumstances due to bubble distribution effects. This shows the deficiency of Bankoff's equation for accurate thermal-hydraulic simulation.

The advantage of using the slip relations of the drift-flux model is that we can simulate the influence of flow regimes on the slip ratio easily once we determine the local flow regime from flow map criteria. The parameters C_0 and V_{gj} in different flow regimes are listed in Table 2.5

Table 2.5 Zuber and Findlay distribution parameter and drift velocity (D-1)

Type of flow	Distribution parameter C_o	Drift velocity V_{gj}
Bubbly	Circular cross section: $p_R \triangleq \frac{p}{p_c}$	
	$D > 5$ cm $\quad C_o = 1 - 0.5p_R$	
	$D < 5$ cm $\quad p_R < 0.5 \quad C_o = 1.2$	
	$p_R < 0.5 \quad C_o = 1.4 - 0.4p_R$	$V_{gj} = 1.41\left(\frac{\sigma g \Delta\rho}{\rho^2 f}\right)^{\frac{1}{4}}$
	Rectangular cross section: $C_o = 1.4 - 0.4p_R$	
Slug	$C_o = 1.2$	$V_{gj} = 0.35\left(\frac{g\Delta\rho D}{\rho f}\right)^{\frac{1}{2}}$
Annular	$C_o = 1.0$	$V_{gj} = 23\left(\frac{\mu_f j_f}{\rho_g D}\right)^{\frac{1}{2}} \frac{\Delta\rho}{\rho_f}$

BCCL Loop Thermal-Hydraulic Characteristics

The BCCL loop is designed to study BWR in-core water chemistry. Since the boiling process will play an important role in the simulation, a comparison between the BCCL loop and BWR thermal hydraulic characteristics will be given in this section.

Heat Transfer

The in-core U-tube of the BCCL loop is heated by a combination of gamma and electric heating. Currently in RADICAL we assume the quality profile of the flow (thus the heat flux profile from the lead bath to the test section) is linear.

Flow regime

The identification of different flow regimes is crucial in obtaining local boiling information. Figure 2.9 is a schematic of the evolution of the flow regimes in a boiling channel.

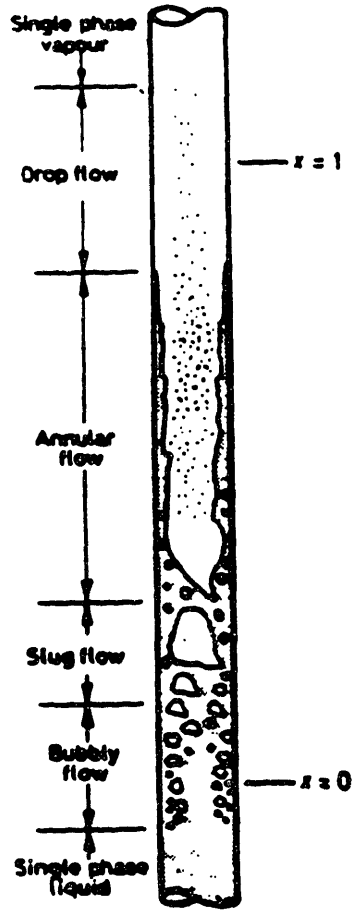

Figure 2.9 Flow patterns in a vertical evaporator tube (C-2)

At the onset of boiling, small bubbles are generated on the heated wall and later escape when the buoyancy force of the bubbles and the drag force exerted by the main flow overcome the friction force and surface tension on the tube wall (L-1). Then slug flow occurs: slugs form from bubble coalescence when a large number of bubbles are generated. The slug travels faster than bubbles because the buoyancy force provides a larger upward force in slug flow. Further downstream is annular flow. The vapor phase tends to travel faster due to smaller interfacial drag between phases. When the vapor velocity reaches a certain limit, liquid droplets which travel at almost the same speed as the vapor occur. The slip ratio thus decreases due to the area average effect even though the liquid film on the wall still proceeds slowly.

Flow pattern maps are generally used to identify flow regimes for given two-phase flow conditions. Taitel and Dukler's work (T-1), based on both theoretical and experimental approaches, is one of the most complete. By using their flow map, calculations show that under the flow condition in the BCCL base case, the flow regime will start as slug flow, then enter the churn flow region, followed by annular flow. In BWRs, bubbly flow occurs before slug flow. The main reason for the difference is that the tube diameter of the BCCL loop is much smaller (~0.67 cm) than the hydraulic diameter of the intra-fuel-pin channel in BWRs (~ 1.6cm). Bubbles cannot exist separately in a small diameter tube.

Therefore the BCCL loop is expected to have a higher slip ratio. However, the fluid in the BCCL loop flows downward in the first half of the loop, which results in a decrease in the slip ratio because the buoyancy force opposes downward flow. The combination of effects probably makes it acceptable to assume the flow condition in the BCCL loop is the same as in BWRs. However, further analysis clearly in order. Table 2.6 is a summary of BCCL loop thermal hydraulic characteristics.

Table 2.6 BCCL loop thermal hydraulic characteristics

Items	BWRs	BCCL
core residence time	0.82 sec.	0.72 sec
coolant	H_2O	H_2O
pressure	~ 70 atm	~ 70 atm
flow direction	upward	down ward -> upward (U-tube)
heat flux distribution	sinusoidal (approximately)	determined by combination of uniform electric heat and cosine gamma heating
flow pattern	bubbly -> slug -> annular	slug -> annular

2.5 Loop Nodalization

Based upon the physical layout of the loop, and a series of parametric studies using the RADICAL code described in the next chapter, the system was broken down into a sequence of nodes at a level of detail thought to be suitable for sufficiently accurate simulation.

A bit of past history is worthy of note. An initial nodalization, shown in Figure 2.10, was defined as a benchmark problem, to permit intercomparison of lab and vendor calculations. It served its purpose, pointing to aspects requiring refinement and to the need for reaching consensus on an improved set of high temperature radiolysis parameters.

The next version, circulated by MIT in early 1992, is shown in Figure 2.11. The major changes are the increase in in-core nodes (from 2 to 6), to permit closer representation of dose profiles, and a reduction in the magnitude of the doses. This version has been used for the parametric studies reported in Chapter 4. Note, however, that the "best-estimate" simulations in Chapter 5 are based upon the newer set of dose rate estimates developed in this chapter.

Support for the generic features of the model embodied in Figure 2.8 is a major subject of the parametric studies in Chapter 4, hence further discussion is postponed until then.

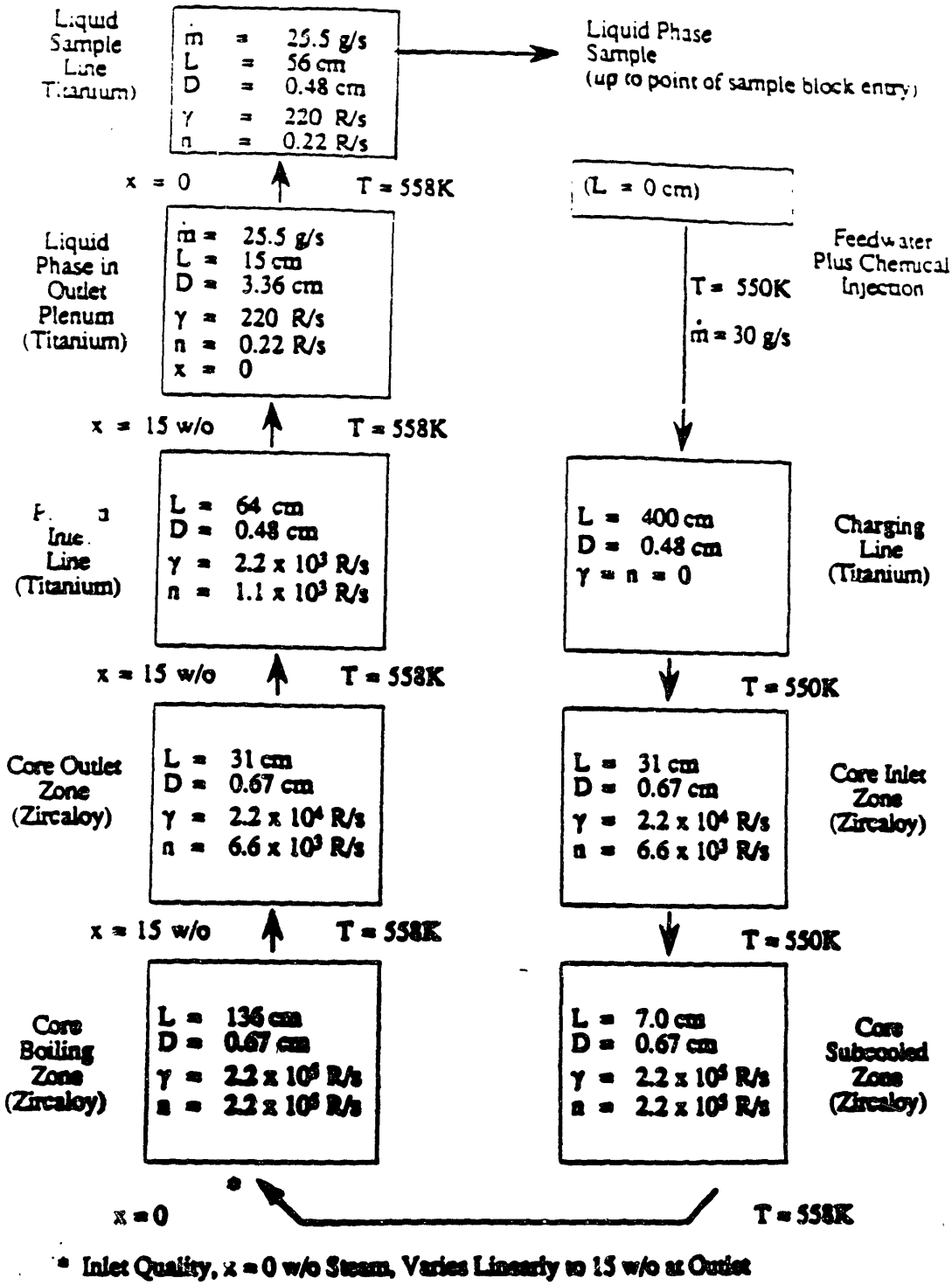

Figure 2.10 Original BWR Loop Nodalization for Simple Benchmark calculations

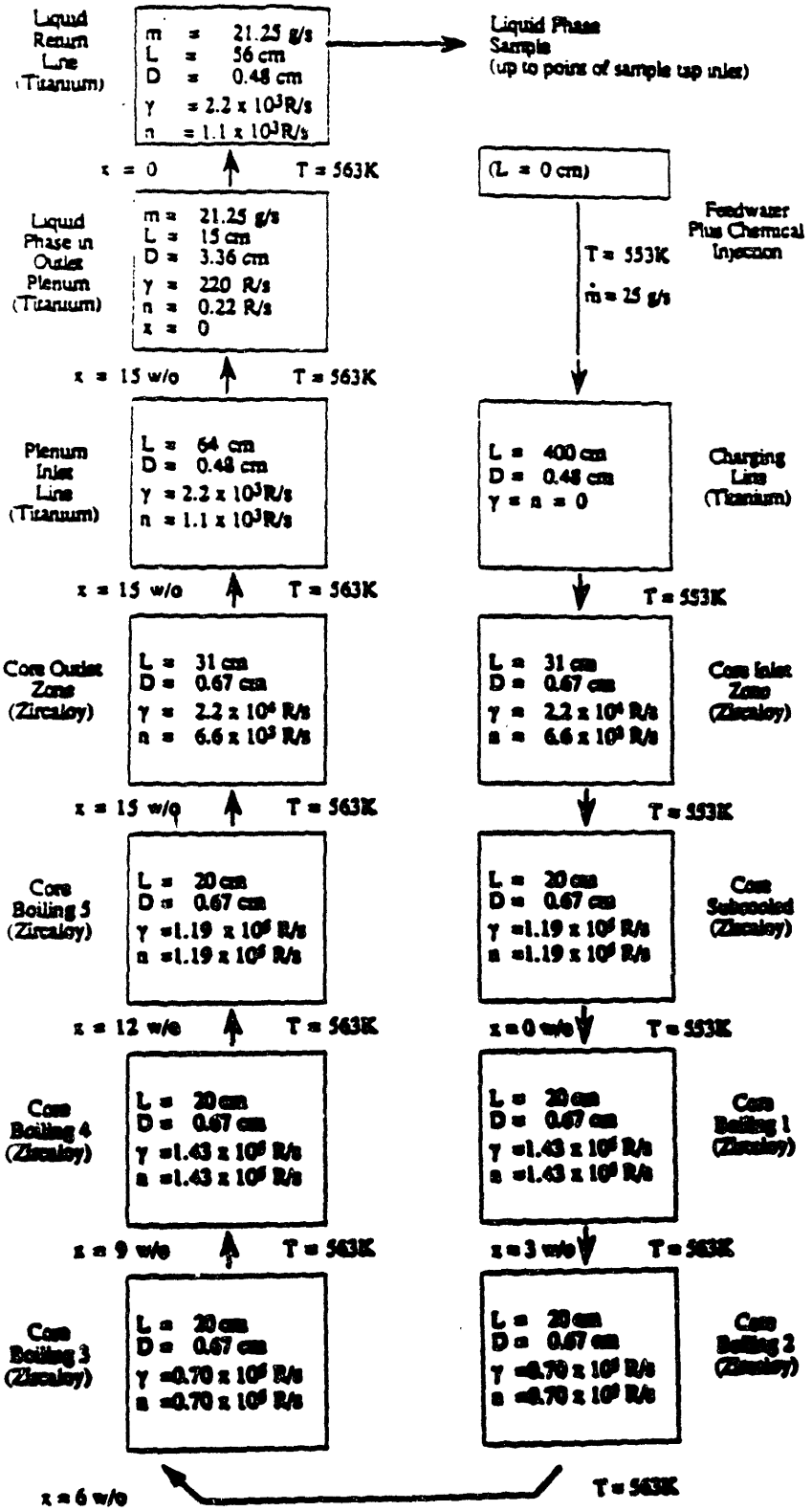

Figure 2.11 Curent BWR Loop Nodalization

2.6 Chapter Summary

This chapter has dealt with development of a description of the BCCL at a level sufficient to permit modelling of the system in state-of-the-art radiolysis programs. Based upon priorities established in an earlier round of parametric studies, the main focus has been placed on characterization of gamma and neutron dose rate profiles. For this task, principal reliance has been placed on a set of monte carlo code (MCNP) calculations of the MITR core, including the loop facility itself.

A review of boiling channel thermal hydraulics was presented to relate the modelling of these phenomena in the RADICAL code and to provide some perspective on the similitude of BCCL and BWR conditions. In particular, in-core residence times were found to be comparable (BCCL ~ 13% shorter). Coupled with the comparable dose rates (BCCL gamma ≅ BWR gamma; BCCL neutron ~ 2/3 BWR neutron), this assures that methods and data sets developed for full scale BWR cores will also apply to the BCCL. The major differences are the smaller hydraulic diameter for the BCCL, hence higher surface-to-volume ratio: 2 cm^{-1} for a BWR core vs 6 cm^{-1} in the BCCL; and the presence of downflow in the inlet leg of the in-core Zircoloy U-tube in the BCCL. Future work should address these two points.

Chapter 3
The RADICAL Program

3.1 Introduction

All of the calculations carried out at MIT to date have employed the RADICAL program, as developed by J. Chun (C-1) for BWR coolant radiolysis calculations, based on earlier work by Simonson (S-1). Mason (M-1) collaborated with Chun to adapt RADICAL to BCCL simulation, and also carried out a variety of parametric studies, most notably an intercomparison of radiolysis data sets.

Reference (C-1) describes the subject code in great detail. The thermal-hydraulic equations in RADICAL are, for the most part, based on the formulations used in the SIMFONY/AQUARY codes as used by Dr. I. Ibe (Hitachi) (C-1). We will not repeat such information here, except for a number of special aspects, such as surface-enhanced H_2O_2 decomposition. Appendix F provides supplementary information to the user's manual in Ref (C-1), to help others who may wish to run the code. The present chapter will also identify a number of fine points involved in correctly defining various input parameters for RADICAL, as required to model the BCCL.

A bit of additional genealogy is in order at this point: the RADICAL code was developed at MIT from an earlier MIT program MITIRAD. The chemical reaction portion of MITIRAD is identical to the many computer codes now being used around the world for radiation chemistry problems: for example, MAKSIMA-CHEMIST, used in Canada; SYMPHONY, used in Japan; FACSIMILE, used in England; and GENKIN, used at Sandia National Laboratory. Thus, there is a strong element of commonalty worldwide, which greatly narrows the potential scope for code-to-code disagreements.

3.2 Summary Description of RADICAL Code

RADICAL was originally developed in VAX FORTRAN 4.2 on the MicroVAX-II under MicroVMS 5.0, and was later converted to the Macintosh version (RADICAL 1.11). It can be run with both systems 6 and 7 on Mac II or above.

The RADICAL code was written with careful attention to its structure and readability; abundant comments and indentations were used. The code is also broken down into a number of nested logical blocks. Once the global code structure is understood, modifying the code should be a straightforward task.

There are several files in RADICAL: the first one is the main code RADICAL.FOR and the second is the global-variable block RADICAL.BLK which contains global constants, variable declarations, and common variable declarations. The third is LSODE.FOR which is a numerical solver for a system of nonlinear differential equations. LSODE was developed at the Lawrence Livermore National Laboratory by Alan C. Hindmarsh. In RADICAL, LSODE is used as a black box which takes parameters and returns the solutions. RADICAL.BLK is inserted in each subroutine of RADICAL.FOR by a non-standard statement INCLUDE so that global variables do not have to be declared in each subroutine. This reduces the code size substantially.

To run the computer code, users first prepare an input file which includes the system descriptions for each node, chemical reactions with activation energies and rate constants and G-values for neutrons and gamma-rays. A sample input file for the BCCL experiment is listed in Appendix B. The procedures for running RADICAL are documented in Appendix F. Users can generate plots of the results easily using KaleidaGraph.

3.3 RADICAL Program Fine Points

Careful attention to several aspects of code input and output are essential, the following points in particular:

(a) The concentrations of the chemical species in RADICAL are in moles/liter. Users have the option of obtaining output in ppb (by mass) by setting the parameter PPBOUT in $CONTROL equal to T (true). The conversion factor used by the code is:

$$\text{ppb} = \left(\frac{\text{moles}}{\text{liter}}\right)\frac{A \cdot 10^6}{\rho} \tag{3.1}$$

where

A = grams per mole for the species in question

ρ = density of fluid phase at the appropriate pressure and temperature (g/cm^3)

Note, however, that RADICAL always divides by water density; hence to obtain vapor (steam) phase concentrations in ppb, the results must be multiplied by the ratio of

liquid to vapor densities (eg. at 553K, the ratio is 18.8). All the simulation results shown in this report have been modified for this point.

(b) The code requires a value for inlet velocity, Vo, for the first component (i.e. node). The inlet velocity of the next component is calculated internally if an input value is not given explicitly. This is done by comparing the sectional flow area assuming mass conservation:

$$V_1 = \left(\frac{D_0}{D_1}\right)^2 V_0, \text{ cm/s} \tag{3.2}$$

where D is the diameter of the node indicated.
However, this does not apply in two-phase flow [See (c)] or for multiple components in parallel. Often confusion arises between "inlet velocity" and "flowrate": the two have no physical connection in RADICAL. Flowrate is used only for multiple components in parallel to weigh exit concentrations.

(c) Furthermore, the inlet velocity, Vo, for each node should be that of liquid in single phase flow. In a two-phase flow component the code calculates the actual local liquid velocity from Vo, the void fraction and the slip ratio. One has:

$$Vo = \frac{\dot{m}}{\rho A_0}, \text{ cm/s} \tag{3.3}$$

where

$\dot{m}$ = mass flow-rate (g/s)
ρ = liquid density at the local temperature and pressure (e.g. saturation), (g/cm^3)
A_0 = cross sectional area of flow channel (cm^2)

(d) The polynomial coefficients for dose and void-fraction shapes are functions of absolute position. For example, if the void fraction at X = 430 is zero in component A, the coefficients must be such that Void Fraction (X = 430) = 0. This is straight-forward until a section length prior to component A is changed. If the section length is reduced by 30, for example, the coefficients must be reevaluated to give Void Fraction (X = 400) = 0.

(e) RADICAL is designed to work for a variety of loop configurations. Its flexibility leaves room for ambiguity. Checking output results for consistency is critical. In particular, check the following for component-to-component continuity:

- Liquid & gas flow velocity
- Temperature
- Concentrations

Also, check dose and void fraction profiles to see if they are as expected.

(f) In comparing rate constants one must keep in mind an important difference in conventions. Some rate constant sets treat H_2O implicitly, whereas others may treat it explicitly; i.e. when H_2O appears as a reactant:

explicit: $[H_2O] = 55.56$ moles/liter at 25°C
implicit: $[H_2O] \equiv 1.0$ at all temperatures
Thus k_o IMPL. = 55.56 x k_o EXPL.

Furthermore, the concentration of H_2O varies with temperature (density). In the explicit treatment this is automatically accounted for if the molarity is computed at the appropriate density. In the implicit treatment in RADICAL one must multiply the tabulated k_o for reactions involving H_2O by the density of H_2O at the temperature of interest (e.g. 0.74 at 285°C). This must be done exogenously by the user, since RADICAL has no internal provision for adjusting the density of water in reaction rate computations.

(g) The H_2O_2 decomposition rate is expressed as (refer to Appendix H)

$$k = k_{th} + \left(\frac{S}{V}\right) \cdot k_{surf} \qquad (3.4)$$

where

k_{th} : thermal (bulk) decomposition rate of H_2O_2 (sec^{-1})
k_{surf} : surface decomposition rate of H_2O_2 (sec^{-1} cm)
S : surface area
V : volume

and for a cylinder,

$$\frac{S}{V} = \frac{\pi DL}{\frac{\pi}{4}D^2L} = \frac{4}{D} \tag{3.5}$$

In RADICAL, a similar equation is used to account for thermal decomposition and surface decomposition.

$$k = k_{th} + \frac{1}{D} \cdot k'_{surf} \tag{3.6}$$

Thus

$$k'_{surf} = 4\, k_{surf} \tag{3.7}$$

Both k_{th} and k'_{surf} are calculated using Arrhenius law (Appendix A) for a certain temperature with given reference reaction rate. Chun (C-1), the author of RADICAL, used Lin's experimental results to calculate $k_{th,0}$ and $k'_{surf,0}$ for the reaction $H_2O_2 \rightarrow 2OH$, which is assumed for computation convenience and is not a true reaction (see Appendix H), for 0.25 inch diameter tubing. The result is

$k_{th,0}$ = 2.0 x10^{-8} (sec $^{-1}$)

Ea_{th} = 7.3 (kJ / mol K)

and

$k'_{surf,0}$ = 5.3 x 10^{-7} (sec $^{-1}$ cm)

Ea_{surf} = 67.0 (kJ / mol K)

for room temperature (25° C)

The decomposition coefficients thus depend on temperature and tube diameter only. Other simulation codes, e.g., FACSIMILE, can treat the surface decomposition coefficient as a function of Reynolds number (including the effects of temperature, diameter and velocity). Please refer to Appendix H for further information on surface decomposition.

(h) One way to deal with fractional reactions in RADICAL is to make up a reaction which leads to the same result as the original reaction. For example, the reaction $H_2O_2 \rightarrow$ 1/2 O_2 + H_2O can't be used directly because the 1/2 coefficient is not acceptable in RADICAL. We can assume a fictitious species X to replace 1/2 O_2 and add another reaction X + X $\rightarrow$ O_2 which has a very large reaction rate so that the reaction will

occur immediately once X is produced. This artifice is recommended to future RADICAL users.

(i) RADICAL uses mole/l concentrations to do its calculations. If a ppb concentration is requested, mole/l will be transformed into ppb for the output. When the liquid density changes mole/l concentrations should be modified by a density ratio to preserve mass balance, but RADICAL doesn't do that. For example at position 451 cm (see Table 5.1) a density change occurs, and RADICAL gives discontinuous ppb output. Hence the ppb concentrations downstream of the core subcooling region (451 cm) must be multiplied by the liquid density ratio to obtain correct concentrations and continuity at the position where the liquid density changes. For example in Table E.7, the original RADICAL output gives a H2 concentration of 431.8 ppb at the inlet of the core boiling 1 region (row 7) which is 1.023 times larger than that at the outlet of the subcooled region at the same position. That result comes from mole/l concentration continuity (which is incorrect for our BCCL simulation) performed by RADICAL at 451 cm.

That is, $\text{mole/l}_{row6} = \text{mole/l}_{row7}$

so,

$$ppb_{row7} = \text{mole/l}_{row6} \cdot \frac{M_{H2}}{\rho_{row7}} = ppb_{row6} \cdot \frac{\rho_{row6}}{\rho_{row7}} \tag{3.8}$$

where ppb_{row7} is the ppb concentration reported by RADICAL

To obtain the correct results, the user should modify the data downstream of row 6 by using the following equation.

$$ppb'_{row\,N} = ppb_{row\,N} \cdot \frac{\rho_{row\,N}}{\rho_{row6}} \tag{3.9}$$

where the subscript "row N" represents all the components downstream of row 6, and $\rho_{row\,N} = \rho_{row\,7}$ in the current best-estimate simulation, since temperature is constant from station downward.

All the best-estimate simulation results shown in Tables E.1 through E.8 in Appendix E and Tables 5.3, 5.4 6.3 and 6.4 have been modified by using eq.(3.9).

(j) The mixed concentration of the chemicals of two components (as shown in Fig. 5.2) are calculated by weighting the separate concentration with volumetric flow rate due to the fact that the concentrations are in mole/l. The relation is shown as follows:

$$C_3 = \frac{(C_1\dot{m}_1+C_2\dot{m}_2)}{\left(\frac{\dot{m}_1}{\rho_1}+\frac{\dot{m}_2}{\rho_2}\right)\rho_3} \tag{3.10}$$

where,

C= concentration of chemical species considered (mole/l)

ρ= water density (g/cc)

ṁ= mass flow rate (g/s)

subscripts 1, 2 and 3 represent stream 1, stream 2 and mixed flow, respectively.

With the above exceptions, the code manual is sufficiently explicit to permit preparation of a reliable set of input data. The sample input of Appendix B can be correlated with the BCCL nodal diagram in Chapter 2 as a further guide to future users.

3.4 Chapter Summary

The present chapter has examined the radiolysis code RADICAL, developed at MIT, with two objectives in mind: to describe key code features and limitations for the benefit of researchers using other programs of this genre, and, in conjunction with appendices B and F, to explain how to employ this code for simulation of the BCCL for the benefit of subsequent users of RADICAL at MIT or elsewhere.

A point of particular interest is that RADICAL uses an empirical method to model surface-induced decomposition of H_2O_2. Also, while not an inherent limitation, the BCCL outlet plenum is crudely modeled (instantaneous separation of the liquid and vapor phases). Another remediable limitation is that only major in-thimble components are modeled. In the future it may be desirable to also model the peroxide sample extraction system and the ex-thimble part of the system (a nodal diagram for this section has been developed, but not input to the code: see chapter 2, Figure 2.3).

Chapter 4
Parametric Studies

4.1 Introduction

The RADICAL code has been employed to study the effect of a wide variety of changes in loop operating parameters, design features, and how the latter are modeled. Several objectives were served in this manner:

(1) the factors which dominate H_2O_2, O_2 and H_2 generation were identified. This, in turn, helps to

   (a) plan and interpret loop experiments
   (b) focus on modeling aspects which deserve refinement in the computer simulation

(2) the accuracy with which dose rates must be determined, both in magnitude and spatial distribution, was established

(3) the sensitivity of the results to basic radiolysis and thermodynamic data was investigated, to identify specific parameters which might account for differences among results computed by MIT and others.

It should be noted, that the parametric studies reported in Tables 4.1, 4.3 and 4.4 were carried out using the loop as defined in Figure 2.11 of Chapter 2, and the data set compiled by J. Chun for his BWR studies (i.e., set no. 1 in Appendix A). The parametric studies in Tables 4.2 and 4.3, carried out after the August 1992 workshop, use the consensus data set agreed to in the workshop (set No 2 in Appendix A). The current consensus estimates of Chapter 5 reflect several differences, which are defined in detail there. Also note that an earlier series of parametric studies were carried out by M. Becker using the simpler nodal diagram of Figure 2.10, as reported in the review meeting held at MIT on January 30, 1992. The results reported here confirm or revise and extend these earlier computations.

4.2 Effects of Major Variables

Table 4.1 documents the results of a series of parametric variations from the base case result for the model described by Figure 2.11. Additional parametric study results for changes in temperature, liquid density and liquid/gas mass transfer coefficients are shown in Tables 4.2, 4.3 and 4.4 , respectively. These tables focus on liquid phase H_2O_2 and O_2 concentrations at the core exit and at the point at which liquid samples are extracted. However, as shown in the sample in Appendix B, more detailed output was normally recorded, and even more is available from the code upon request - see for example Ref. (C-1).

In general, the results exhibit the expected qualitative trends. In particular:

- Oxygen in the feedwater increases the production of H_2O_2 and O_2, but not in direct proportionality

- Conversely, H_2 injection suppresses O_2, and also H_2O_2, but less effectively

- Mass flow rate does not appear to be a particularly sensitive variable, nor does exit quality once it exceeds ~5%. Boiling length is also not a major factor.

- Results are sensitive to neutron dose rate more than they are to gamma dose rate; as a consequence the higher gamma/neutron ratio in the BCCL vs a BWR only moderately skews the results.

- The results differ significantly when G values and kinetics parameters from current data sets are substituted for the base case values. Table 4.5 is a comparison of G-values used by RADICAL, Ibe and GE. A comparison of thermochemical constants used by Ibe and MIT is provided in Table 4.6. The reaction rate constants at operating temperature (563K) are calculated from the Arrhenius equation, Eq. (A-1).

  GE's new neutron G-values are greater than those labeled "RADICAL" by a factor of about 1.5 and the gamma G-values are less by about a factor of 1.2. According to the parametric study results shown in Table 4.1, both of these trends tend to increase peroxide concentration at the core exit. The discrepancy resulting from different reaction sets comes from both the

Table 4.1. Parametric Studies of BCCL Using RADICAL

Change		Conc. at Core Outlet (582 cm)		Conc. at Liquid Sample Line (661 cm)	
parameter	description	H_2O_2 (ppb)	O_2 (ppb)	H_2O_2 (ppb)	O_2 (ppb)
	Base case	199.0	91.4	47.1	101.0
In-core dose rate profile	Uniform	194.0	92.2	47.0	100.0
O_2 injection into feedwater	50 ppb	207.0	97.7	48.8	110.0
	100 ppb	215.0	104.0	50.5	119.0
	150 ppb	223.0	111.0	52.2	129.0
	200 ppb	231.0	119.0	53.9	138.0
	250 ppb	240.0	126.0	55.7	148.0
	300 ppb	249.0	134.0	57.4	159.0
	500 ppb	285.0	165.0	63.9	201.0

Change		Conc. at Core Outlet (582 cm)		Conc. at Liquid Sample Line (661 cm)	
parameter	description	H_2O_2 (ppb)	O_2 (ppb)	H_2O_2 (ppb)	O_2 (ppb)
H_2 injection into feedwater	100 ppb	118.0	39.0	25.3	22.2
	200 ppb	77.9	19.1	7.23	3.36
	300 ppb	60.3	9.93	5.28	0.631
	500 ppb	50.2	3.66	5.26	0.291
	1000 ppb	38.9	0.70	4.61	0.0773
	2000 ppb	14.8	0.0609	2.96	0.0133
Mass flow rate	1/2 mass flow rate	175.0	123.0	32.0	107.0
	2x mass flow rate	241.0	66.3	88.7	92.3
Out-of-core dose rates	0 everywhere ex-core	199.0	91.4	47.9	106.0
	10x ex-core dose rates	282.0	122.0	73.8	112.0
	100x ex-core dose rates	754.0	289.0	175.0	203.0

Change		Conc. at Core Outlet (582 cm)		Conc. at Liquid Sample Line (661 cm)	
parameter	description	H_2O_2 (ppb)	O_2 (ppb)	H_2O_2 (ppb)	O_2 (ppb)
Gamma dose rate effect	1/4 of base case	340.0	84.9	65.2	142.0
	1/2 of base case	252.0	86.4	52.7	116.0
	2x base case	180.0	102.0	49.6	96.5
	4x base case	189.0	118.0	57.7	101.0
	6x base case	207.0	131.0	64.8	107.0
Neutron dose rate effect	1/4 of base case	137.0	64.3	33.1	71.6
	1/2 of base case	155.0	73.2	37.4	80.7
	2x base case	322.0	129.0	71.3	152.0
	4x base case	678.0	202.0	132.0	289.0
	6x base case	1130.0	272.0	198.0	462.0

Change		Conc. at Core Outlet (582 cm)		Conc. at Liquid Sample Line (661 cm)	
parameter	description	H_2O_2 (ppb)	O_2 (ppb)	H_2O_2 (ppb)	O_2 (ppb)
gamma-neutron ratio	Dg = 1/3 Dn (reduce gamma)	228.0	91.0	49.5	108.0
exit quality effect	exit quality = 0	107.0	63.7	37.0	39.0
	exit quality = 5%	191.0	121.0	65.9	103.0
	exit quality = 10%	195.0	107.0	55.5	104.0
	exit quality = 20%	205.0	79.6	41.4	99.4
	exit quality = 25%	212.0	70.6	37.3	98.9
Quality profile	polynomial (2nd order)	224.0	143.0	59.0	159.0
Boiling length effect	increase 20 cm	204.0	99.2	50.0	107.0
	decrease 20 cm	195.0	83.2	44.1	95.9

Change		Conc. at Core Outlet (582 cm)		Conc. at Liquid Sample Line (661 cm)	
parameter	description	H_2O_2 (ppb)	O_2 (ppb)	H_2O_2 (ppb)	O_2 (ppb)
G-values	New (1992) GE G-values	163.0	106.0	31.6	102.0
	New (1992) IBE G-values	274.0	92.8	58.7	127.0
Wall decomp-osition effect	No wall decomposition	206.0	91.5	161.0	79.7
Reaction Constants	New Ibe (1992) Reaction Constants (MIT G-Values)	394.0	196.0	94.0	246.0
Ibe data set (1992)	G-values and reaction constants	353.0	194.0	80.3	241.0
Stoichiometric injection in the feedwater	25 ppb H_2 + 200 ppb O_2	199.0	91.4	47.1	101.0
Peroxide injection	425 ppb H_2O_2 (equivalent to 200 ppb O_2)	231.0	119.0	53.9	138.0

Table 4.2 System temperature parametric study results

Liquid Density	Temperature	H_2O_2 (551 cm / 646 cm)	O_2 (551 cm / 646 cm)
ρ_f=0.675 g/cc	553 K	219.0 / 93.3	24.5 / 21.1
	563 K	223.0 / 98.9	32.0 / 26.3
	573 K	228.0 / 105.0	40.9 / 32.2
ρ_f=0.825 g/cc	553 K	189.0 / 73.3	20.0 / 17.2
	563 K	192.0 / 77.2	26.2 / 21.3
	573 K	196.0 / 81.3	33.5 / 25.9

Note: 551 cm location is core exit.
646 cm location is liquid plenum exit.
all concentrations are ppb.

Table 4.3 Liquid density parametric study results

Temperature	Liquid Density	H_2O_2 (551 cm / 646 cm)	O_2 (551 cm / 646 cm)
553 K	0.675 g/cc	219.0 / 93.3	24.5 / 21.1
	0.750 g/cc	203.0 / 82.0	22.0 / 18.9
	0.825 g/cc	189.0 / 73.7	20.0 / 17.2
563 K	0.675 g/cc	223.0 / 98.9	32.0/ 26.3
	0.732 g/cc	210.0 / 88.9	29.5 / 24.1
	0.825 g/cc	192.0 / 77.2	26.2 / 21.3
573 K	0.675 g/cc	228.0 / 105.0	40.9 / 32.2
	0.712 g/cc	219.0 / 97.9	38.8 / 30.4
	0.825 g/cc	196.0 / 81.3	33.5 / 25.9

Note: 551 cm location is core exit.
646 cm location is liquid plenum exit.
all concentrations are ppb

Table 4.4 Gas Mass Transfer Coefficient (Liquid → Gas) Parametric Study Results

Parameter	O_2 (ppb)		H_2O_2 (ppb)	
	551 cm	646 cm	551 cm	646 cm
2 x μH_2G	150.0	119.0	387.0	228.0
1/2 x μH_2G	80.0	62.9	269.0	137.0
base case	111.0	87.3	322.2	179.0
2 x μO_2G	66.5	52.4	291.0	138.0
1/2 x μO_2G	179.0	142.0	378.0	243.0
1/10 x μH_2G, μO_2G	113.0	96.0	270.0	176.0
1/5 x μH_2G, μO_2G	124.0	103.0	288.0	186.0
1/2 x μH_2G, μO_2G	126.0	100.0	309.0	186.0
2 x μH_2G, μO_2G	88.0	69.7	344.0	176.0
5 x μH_2G, μO_2G	57.3	46.0	394.0	188.0
10 x μH_2G, μO_2G	38.0	31.0	439.0	204.0

* Change liquid → gas mass transfer coefficient only.

*Note: 551 cm location is core exit.
646 cm location is liquid plenum exit.

Table 4.4 Gas Mass Transfer Coefficient (Liquid ↔ Gas) Parametric Study Results (continued)

Parameter	O_2 (ppb)		H_2O_2 (ppb)	
	551 cm	646 cm	551 cm	646 cm
1/2 x μH_2	95.8	76.3	297.0	161.0
1/2 x μO_2	138.0	85.9	345.0	196.0
base case	111.0	87.3	322.2	179.0
2 x μH_2	121.0	94.8	338.0	191.0
2 x μO_2	97.8	89.0	311.0	173.0
1/10 x μH_2, μO_2	123.0	72.0	289.0	171.0
1/5 x μH_2, μO_2	127.0	66.1	305.0	173.0
1/2 x μH_2, μO_2	119.0	75.1	317.0	175.0
2 x μH_2, μO_2	107.0	96.5	326.0	184.0
5 x μH_2, μO_2	105.0	103.0	328.0	190.0
10 x μH_2, μO_2	104.0	106.0	329.0	192.0

* Change both liquid → gas and gas → liquid mass transfer coefficients.

* Note: 551 cm location is core exit.
646 cm location is liquid plenum exit.

Table 4.5. Comparison of G-values

Species	Neutron			Gamma		
	RADICAL (1991)	GE (1992)	Ibe (1992)	RADICAL (1991)	GE (1992)	Ibe (1992)
$e(aq)^-$	0.93	1.395	1.08	4.15	3.76	2.17
H^+	0.93	1.395	1.08	4.15	3.76	2.17
H	0.5	0.75	0.66	1.08	0.70	1.47
H_2	0.88	1.32	0.	0.62	0.80	1.16
H_2O_2	0.99	1.485	0.74	1.25	0.28	0.81
HO_2	0.04	0.06	0.	0.	0.	0.
OH	1.09	1.635	0.26	3.97	5.50	4.34
O	0.	0.	0.	0.	0.	0.

Table 4.6 Comparison of Thermochemical Constants

Reaction	k0(Ibe, 1992) water explicit	k0 (Ibe, 1992) water implicit	Ea (Ibe, 1992)	k0 (MIT, 1991)	Ea (MIT, 1991)	k (Ibe, 1992) water implicit at 563 K	k (MIT 1991) water implicit at 563 K
$e^- + H_2O \rightarrow H + OH^-$	16.000	888.96	12.600	40.000	12.600	9737.4	438.14
$e^- + H^+ \rightarrow H$	3.0000e+10	3.0000e+10	13.800	6.0000e+10	12.600	4.1275e+11	6.5722e+11
$e^- + OH \rightarrow OH^-$	3.0000e+10	3.0000e+10	12.600	7.5000e+10	12.600	3.2861e+11	8.2152e+11
$e^- + H_2O_2 \rightarrow OH + OH^-$	2.5000e+10	2.5000e+10	9.6200	3.2000e+10	12.600	1.5547e+11	3.5052e+11
$e^- + HO_2 \rightarrow HO_2^-$	2.0000e+10	2.0000e+10	12.600	5.0000e+10	12.600	2.1907e+11	5.4768e+11
$e^- + O_2 \rightarrow O_2^-$	6.5000e+10	6.5000e+10	11.300	4.7000e+10	12.600	5.5618e+11	5.1482e+11
$2e^- + 2H_2O \rightarrow H_2 + 2OH^-$	1.6400e+06	5.0600e+09	12.600	1.2000e+10	12.600	5.5426e+10	1.3144e+11
$H + H \rightarrow H_2$	1.0000e+10	1.0000e+10	12.600	2.5000e+10	12.600	1.0954e+11	2.7384e+11
$OH + OH \rightarrow H_2O_2$	1.0000e+10	1.0000e+10	3.8000	1.1000e+10	12.600	2.0583e+10	1.2049e+11
$HO_2 + OH \rightarrow O_2 + H_2O$	1.2000e+10	1.2000e+10	12.600	3.0000e+10	12.600	1.3144e+11	3.2861e+11
$O_2^- + OH \rightarrow O_2 + OH^-$	1.0000e+10	1.0000e+10	17.600	3.0000e+10	12.600	2.8320e+11	3.2861e+11
$H + OH^- \rightarrow e^- + H_2O$	2.0000e+07	2.0000e+07	12.600	7.8000e+07	18.800	2.1907e+08	2.7745e+09
$H + e^- + H_2O \rightarrow H_2 + OH^-$	4.5000e+08	2.5000e+10	12.600	6.2000e+10	12.600	2.7384e+11	6.7912e+11
$HO_2^- + e^- + H_2O \rightarrow OH + 2OH^-$	6.3000e+07	3.5000e+09	12.600	8.7000e+09	12.600	3.8338e+10	9.5296e+10
$H + OH \rightarrow H_2O$	2.0000e+10	2.0000e+10	12.600	5.0000e+10	12.600	2.1907e+11	5.4768e+11
$H_2 + OH \rightarrow H + H_2O$	3.4000e+07	3.4000e+07	19.200	1.1000e+08	12.600	1.3049e+09	1.2049e+09
$H_2O_2 + OH \rightarrow HO_2 + H_2O$	2.7000e+07	2.7000e+07	14.200	4.1000e+07	8.2000	4.0081e+08	1.9468e+08
$H_2O_2 + H \rightarrow OH + H_2O$	5.0000e+07	5.0000e+07	16.700	2.4000e+08	14.000	1.1934e+09	3.4298e+09
$O_2 + H \rightarrow HO_2$	3.3000e+10	3.3000e+10	6.3000	4.7000e+10	12.600	1.0922e+11	5.1482e+11
$O_2^- + HO_2 \rightarrow O_2 + HO_2^-$	1.5000e+07	1.5000e+07	18.800	5.8000e+10	18.800	5.3356e+08	2.0631e+12
$2HO_2 \rightarrow O_2 + H_2O_2$	8.4000e+05	8.4000e+05	20.100	1.1000e+07	18.800	3.8250e+07	3.9127e+08
$2O_2^- + 2H_2O \rightarrow O_2 + H_2O_2 + 2OH^-$	5600.0	1.7300e+07	18.800	6.6000e+07	18.800	6.1537e+08	2.3476e+09
$HO_2 + H \rightarrow H_2O_2$	2.0000e+10	2.0000e+10	12.600	5.0000e+10	12.600	2.1907e+11	5.4768e+11
$O_2^- + H \rightarrow HO_2^-$	2.0000e+10	2.0000e+10	12.600	5.0000e+10	12.600	2.1907e+11	5.4768e+11
$O_2^- + e^- + H_2O \rightarrow HO_2^- + OH^-$	1.8000e+08	1.0000e+10	18.800	5.1000e+10	18.800	3.5571e+11	1.8141e+12
$H_2O_2 + OH^- \rightarrow HO_2^- + H_2O$	1.0000e+08	1.0000e+08	18.800	7.0000e+08	18.800	3.5571e+09	2.4899e+10
$HO_2^- + H_2O \rightarrow H_2O_2 + OH^-$	10000	5.5600e+05	12.600	2.2000e+06	18.800	6.0903e+06	7.8254e+07
$HO_2^- + OH \rightarrow HO_2 + OH^-$	7.5000e+09	7.5000e+09	12.600	0.0000	0.0000	8.2153e+10	0.0000
$H_2O_2 \rightarrow 2OH$	2.4000e-07	2.4000e-07	54.000	2.0000e-08	7.2800	0.0068466	7.9738e-08
$H^+ + OH^- \rightarrow H_2O$	1.4400e+11	1.4400e+11	12.600	1.4000e+11	12.600	1.5773e+12	1.5335e+12
$H^+ + HO_2^- \rightarrow H_2O_2$	5.0000e+10	5.0000e+10	12.600	0.0000	0.0000	5.4769e+11	0.0000
$H^+ + O_2^- \rightarrow HO_2$	2.0000e+10	2.0000e+10	12.600	1.2000e+11	12.600	2.1907e+11	1.3144e+12
units : for k, sec-1; for Ea, kJ/mol K							

chemical reactions used and the corresponding rate constants. For peroxide concentration in the ex-core region, it is observed that the decomposition reaction is the dominant factor.

Several of the parametric variations were made to investigate modeling approximations and experimental uncertainties:

- We have already noted the lack of sensitivity to exit quality (which is probably underestimated in Ref. (R-1): see appendix I)

- The use of the same dose in all in-core nodes instead of a 3-node axial profile has virtually no effect at all.

- Out-of-core dose rates would have to be higher than currently estimated by a factor of 5 or so to have a significant effect

- Use of a polynomial quality profile increases radiolysis sufficiently to warrant upgrading the model in this respect

- Wall-induced H_2O_2 decomposition is not important in the core zone, but extremely important to sample point peroxide concentration.

- Stoichiometric H_2 and O_2 in the feedwater has no effect on exit concentrations

- Stoichiometrically equivalent H_2O_2 in feedwater has the same effect as O_2

- These last two findings suggest that a single input variable will correlate all results: ppb net O_2=ppb O_2 - 8·ppb H_2 + $\frac{8}{17}$·ppb H_2O_2, as shown in Figures 4.1 and 4.2.

- System temperature (±10° C) and liquid density (within ±15%) have very little effect on exit concentrations.

- Liquid ↔ vapor mass transfer coefficients are important, if subjected to large changes – as might be appropriate in view of the uncertainty in these parameters.

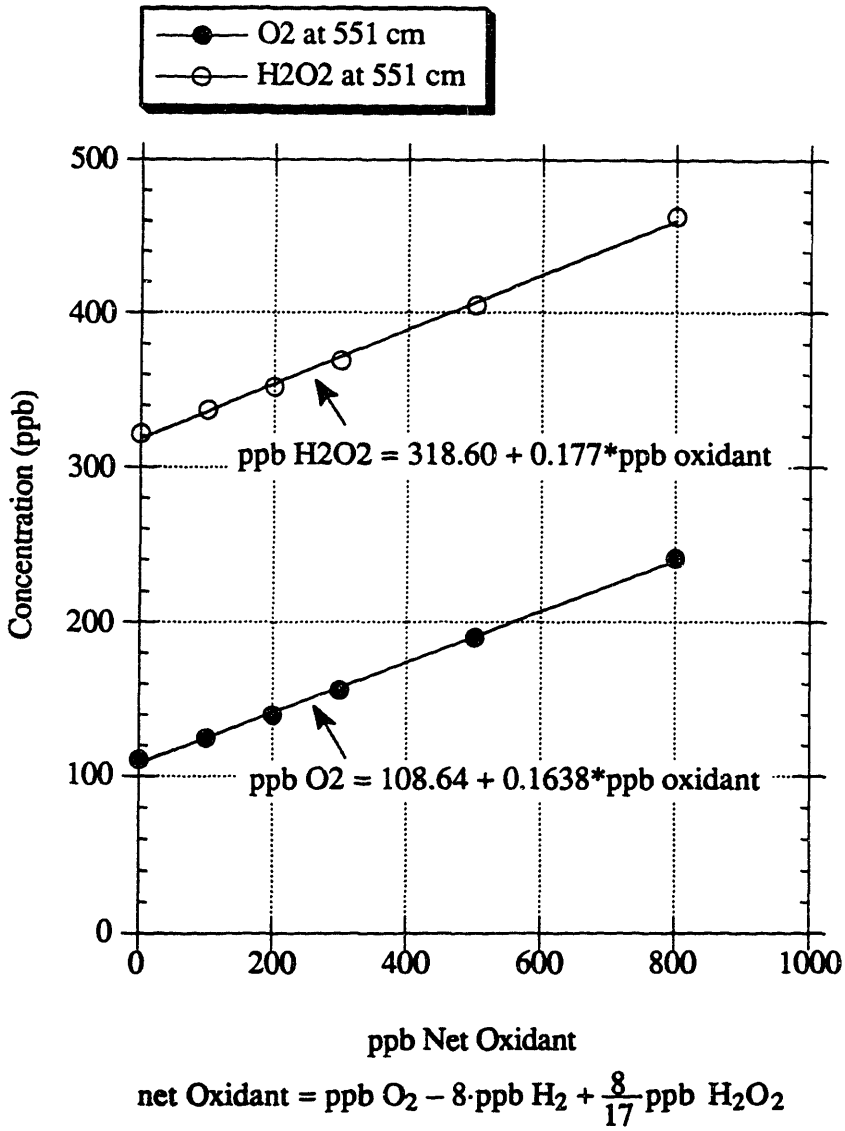

Figure 4.1 Concentrations of H_2O_2 and O_2 at 551 cm as functions of net oxidant (for net oxidant greater than zero).

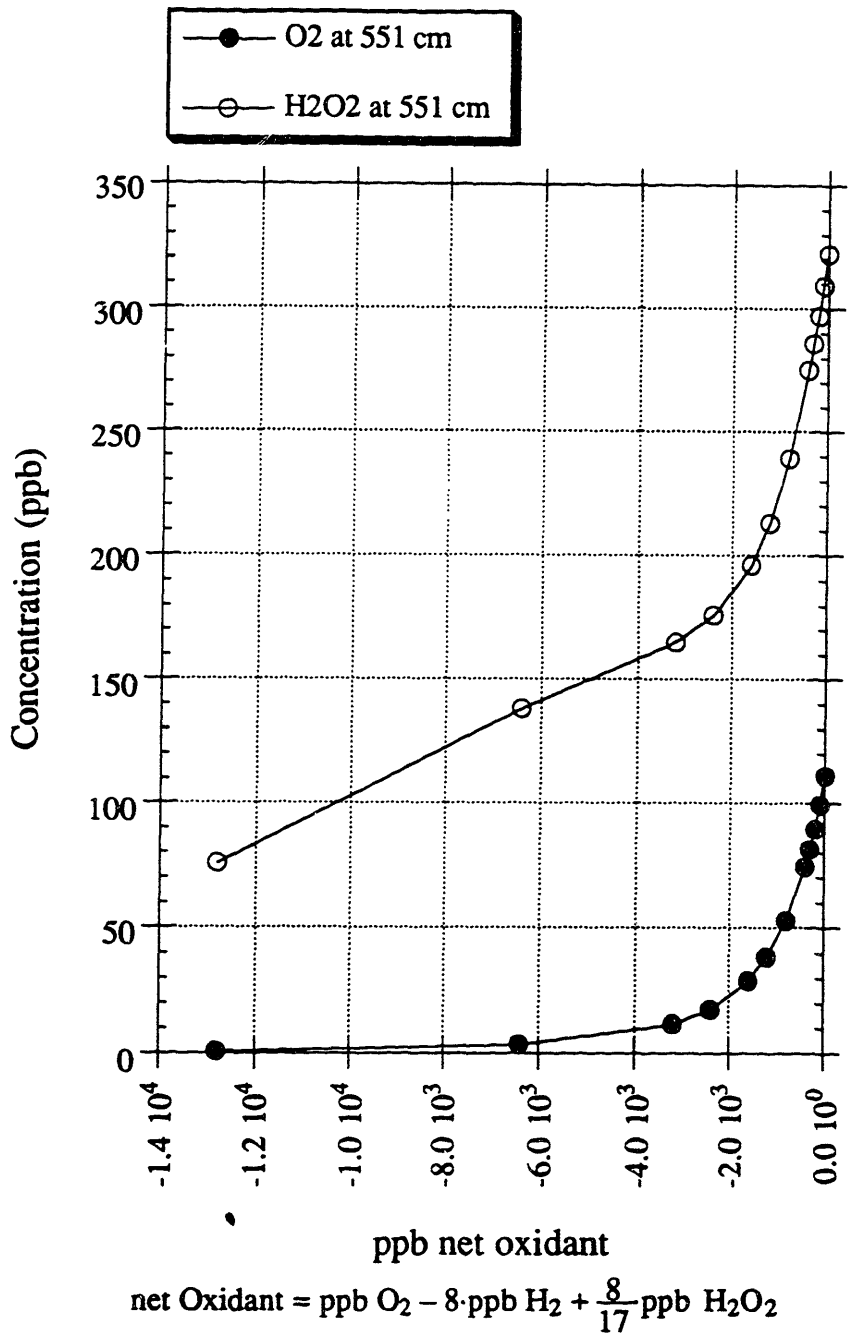

Figure 4.2 Concentrations of H_2O_2 and O_2 at 551 cm as functions of net oxidant (for net oxidant less than zero)

The foregoing parametric study points the way to a number of upgrades, which will be implemented in the "consensus" version of the BCCL in the next chapter. It must be noted, however, that none of the plausible changes in the array of Table 4.1, singly or in combination, can account for the levels of H_2O_2 measured in the Fall 1991 or Summer 1992 campaigns.

4.3 Sensitivity Study

A unique feature of RADICAL is its incorporation of a sensitivity analysis as a supplement to radiolysis calculations. This feature enables the user to determine which of the input parameters among G-values, concentrations of chemical species and reaction rate constants has the most significant influence on a particular species concentration in a certain component under examination. Among many numerical methods for sensitivity analysis for a system of equations, a straight-forward method of adjoint implementation is used in RADICAL. This method requires evaluation of the adjoint of the radiolysis equations, which in turn is used in evaluation of response equations. These response equations give the sensitivity of the concentration of a species under examination with respect to a number of input parameters. Therefore the sensitivity routine requires two steps; the first routine evaluates the adjoint using a backward integration of the concentration profile, and the second routine evaluates the response from the concentration and adjoint profiles. A detailed derivation of the sensitivity equations is given in Chapter 6 of J. Chun's thesis (C-1).

The sensitivity of the results to basic radiolysis and thermochemical data was investigated, to identify specific parameters which might account for differences among results computed by MIT and others. A sensitivity study has been made to see the effect of G-values, chemical reaction constants and chemical species concentrations. The results are shown as both relative sensitivity and absolute sensitivity. Figures 4.3, 4.4 and 4.5 show the relative sensitivity results and Figs. 4.6, 4.7 and 4.8 show the absolute sensitivity, both for the base case BCCL simulation at the core outlet for chemical reactions, G-values and species concentrations, The definition of absolute sensitivity and relative sensitivity are as follows (C-1):

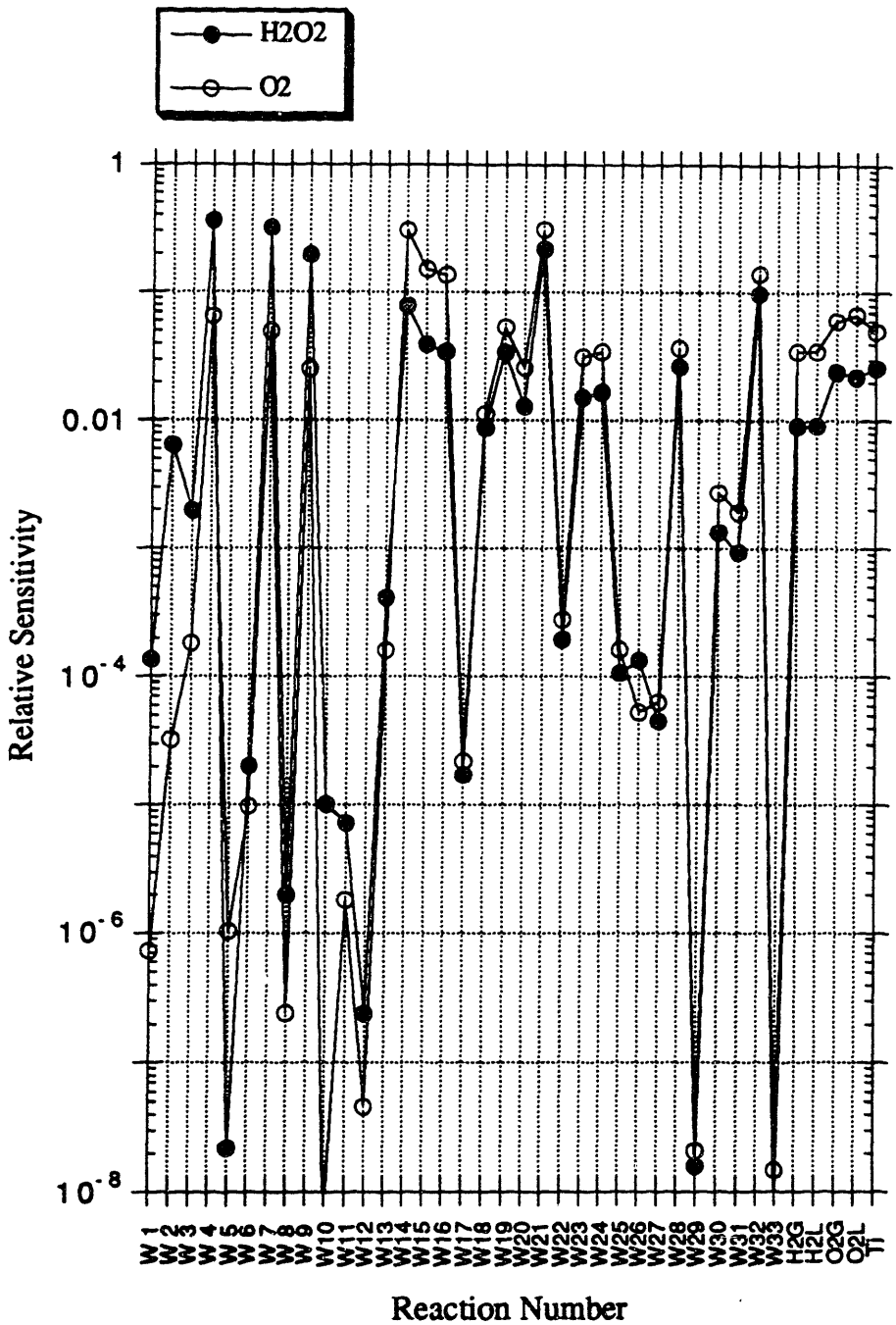

Figure 4.3 Relative sensitivities of O_2 and H_2O_2 concentrations with respect to reaction rate constants in the core outlet region.

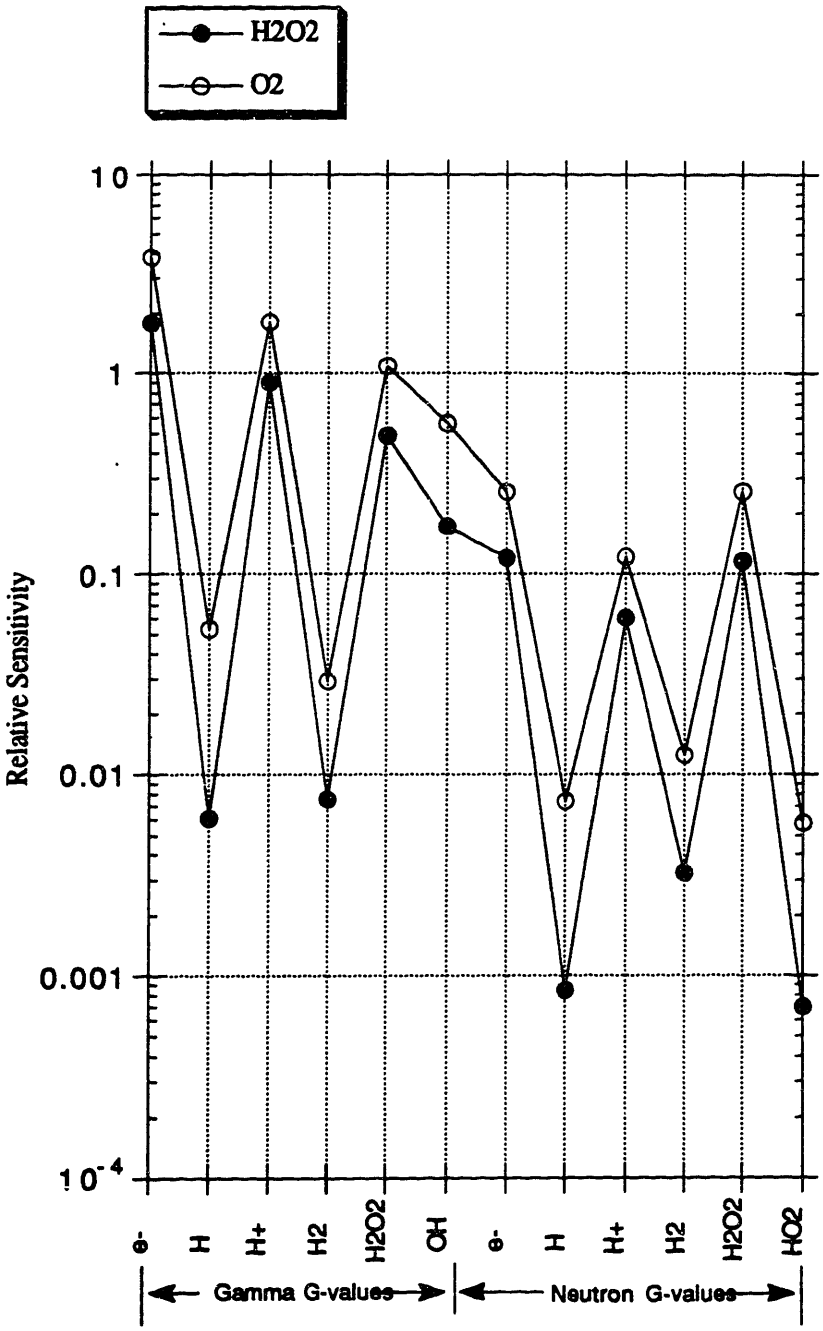

Figure 4.4 Relative sensitivities of O_2 and H_2O_2 concentrations with respect to G-values in the core outlet region.

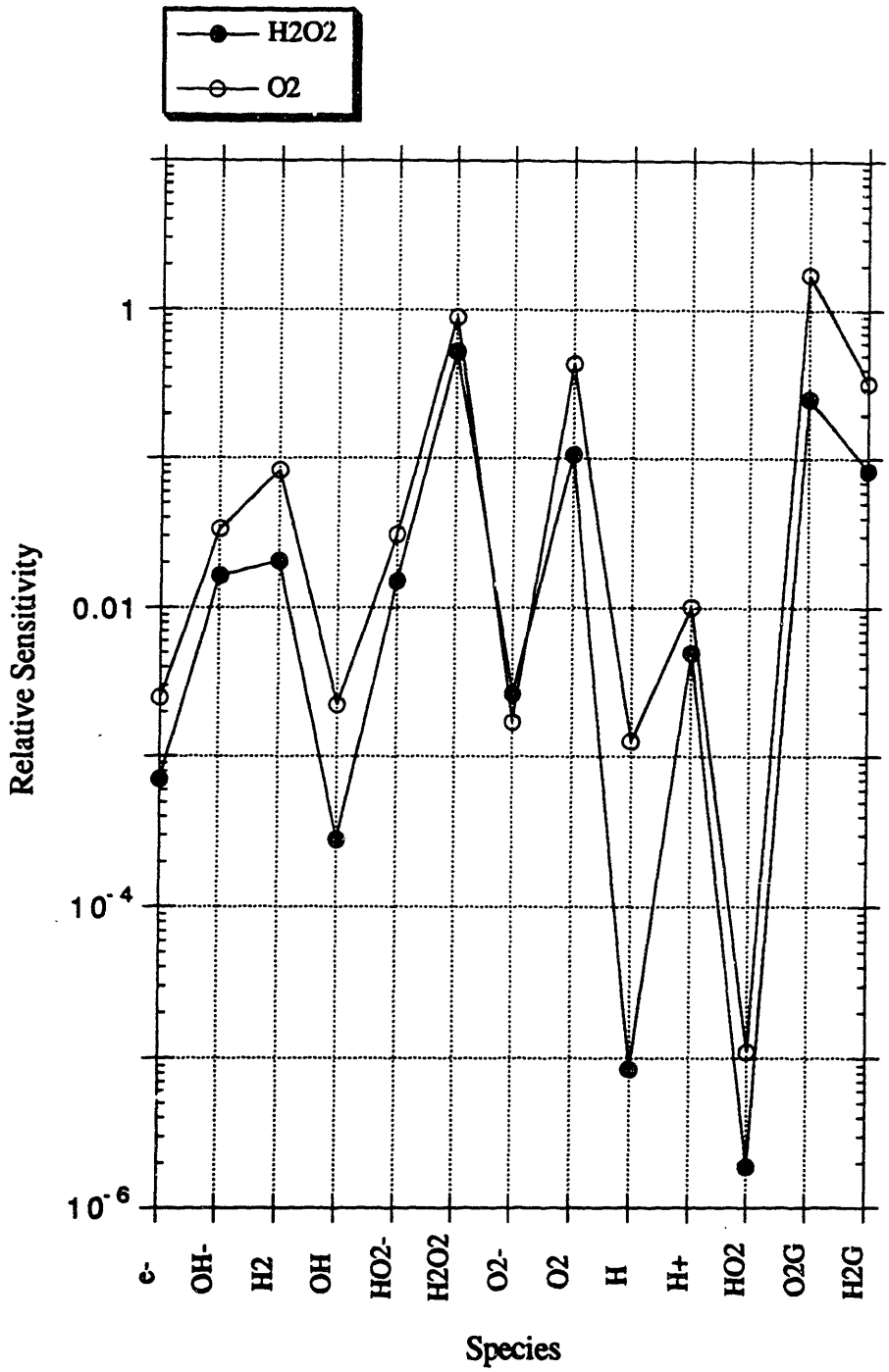

Figure 4.5 Relative sensitivities of O_2 and H_2O_2 concentrations with respect to inlet concentrations in the core outlet region.

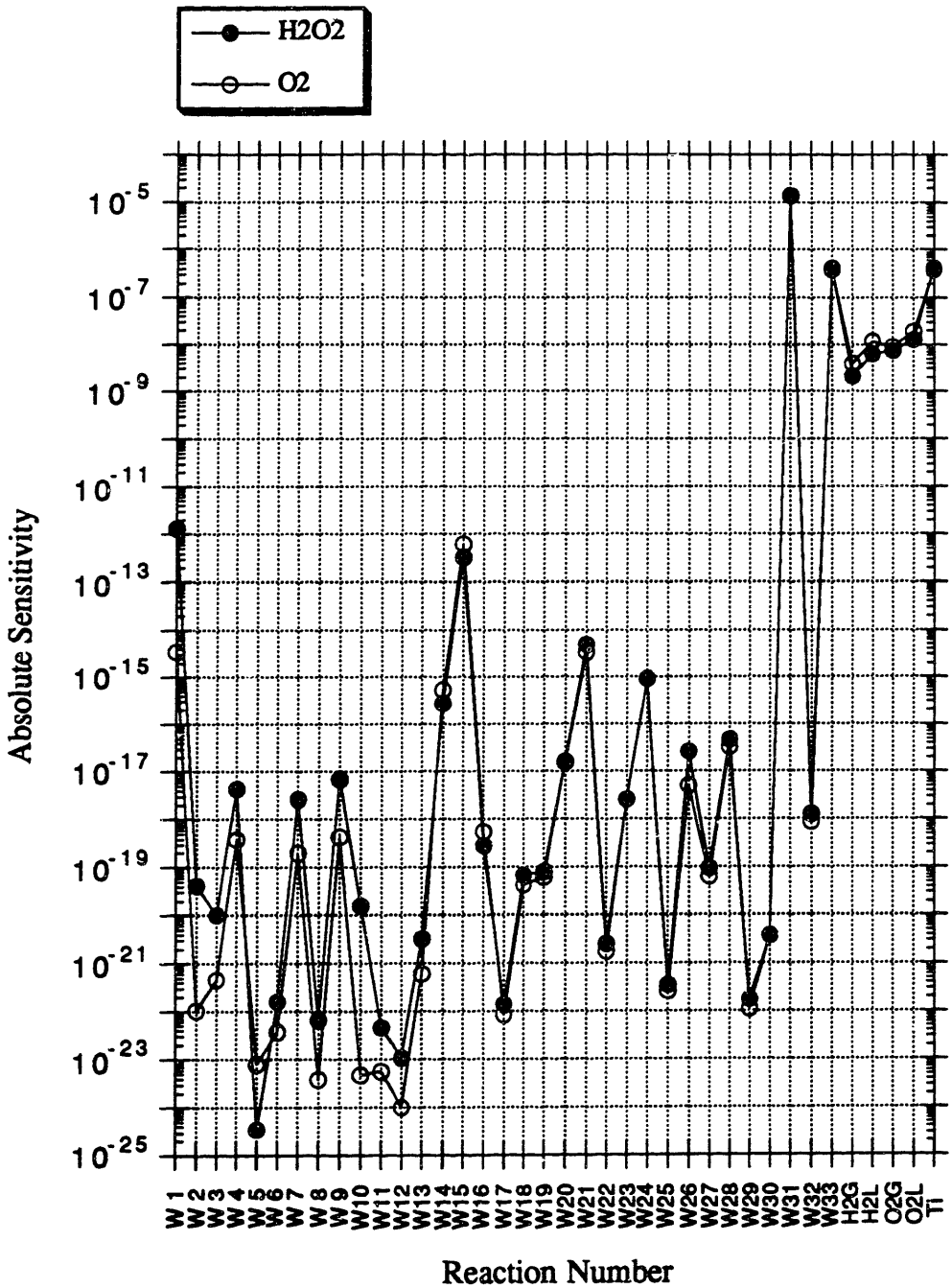

Figure 4.6 Absolute sensitivities of O_2 and H_2O_2 concentrations with respect to reaction rate constants in the core outlet region.

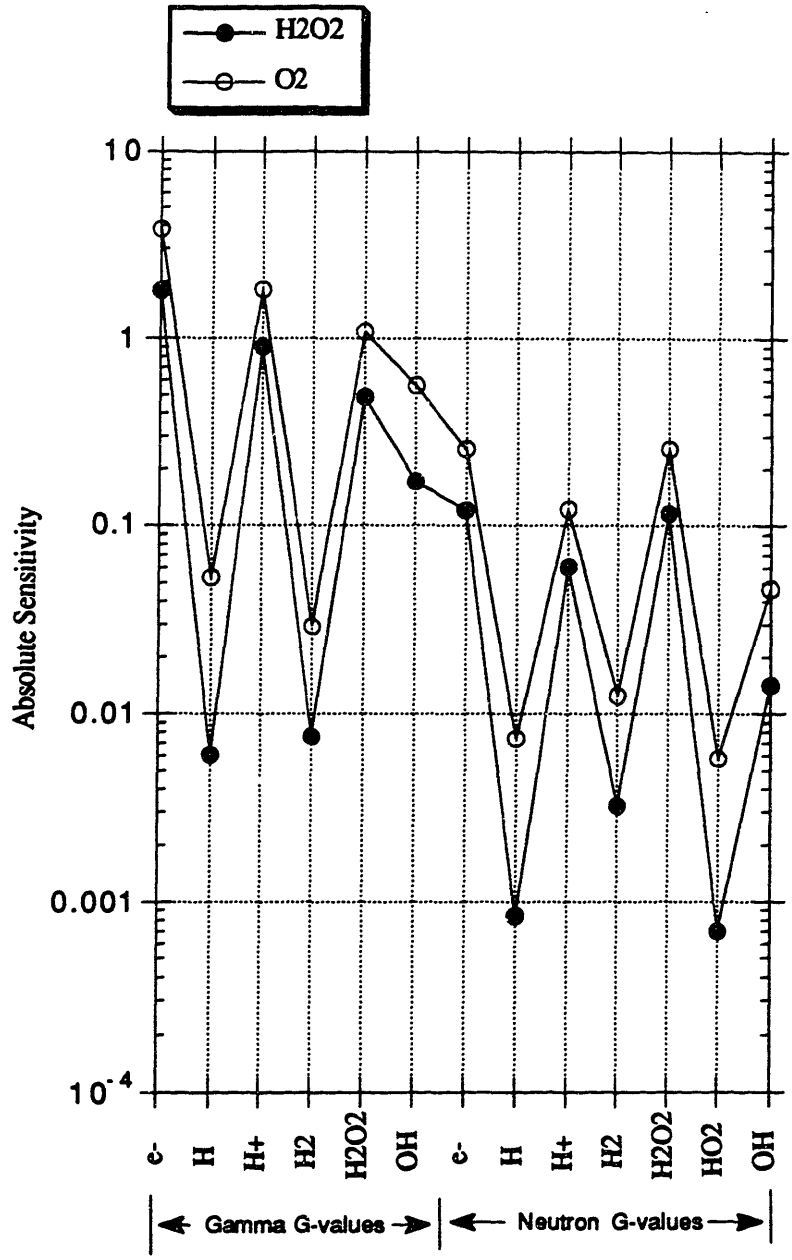

Figure 4.7 Absolute sensitivities of O_2 and H_2O_2 concentrations with respect to G-values in the core outlet region.

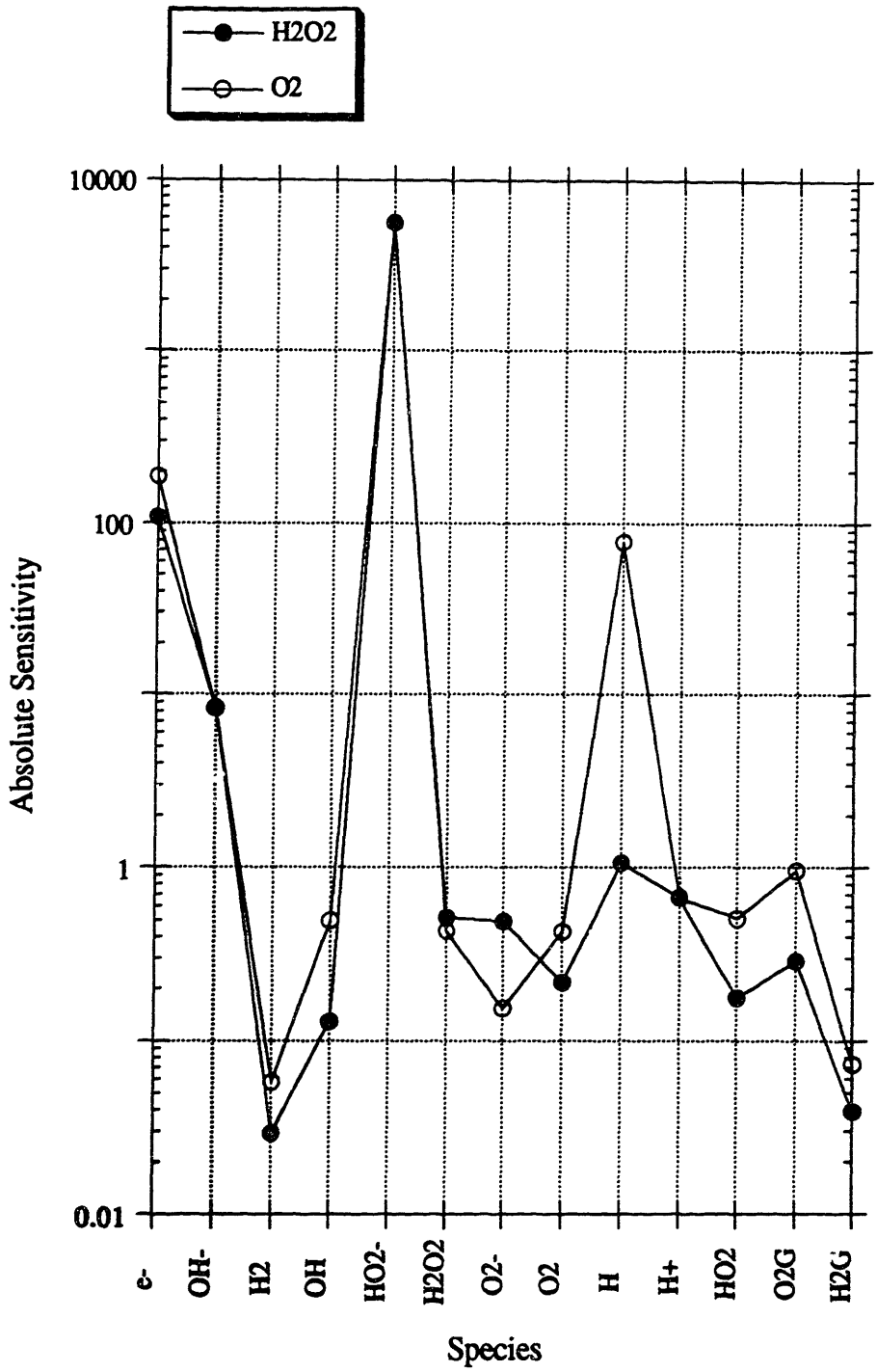

Figure 4.8 Absolute sensitivities of O_2 and H_2O_2 concentrations with respect to inlet concentrations in the core outlet region.

If a curve is plotted in an x-y plane and the slope of the curve at x_0 and y_0 is measured, this slope is the absolute sensitivity. The slope gives a measure of how much y changes for a small change in x about x_0, i.e., Dy and Dx. If the slope is multiplied by x_0 and divided by y_0. this gives a dimensionless value, which is the relative sensitivity. Relative sensitivity gives the percent change in y_0 for a percent change in x_0, i.e., Dy/y_0 and Dx/x_0. The larger the value of the sensitivity, the more sensitive is the response of y to a change in x.

The above description can be summarized as follows:

Absolute Sensitivity= Dy / Dx at (x_0 , y_0)
Relative Sensitivity = $(Dy/y_0) / (Dx/x_0)$

where the unit of absolute sensitivity depends on the parameters examined and the relative sensitivity is dimensionless.

Relative Sensitivity

(1) chemical reactions:
Among the chemical reactions, reactions W4, W7, W9, and W21, as summarized in Table 4.7, have the most significant effect on peroxide concentration at the core outlet. For O_2 concentration, W14, W15, W16 and W21 are the dominant reactions

(2) G-values
e^-, H^+ and H_2O_2 gamma G-values are the most important for both H_2O_2 and O_2 concentrations. The same result has been obtained for neutron G-values.

(3) Species concentrations
H_2O_2, O_2, O_2G and H_2G concentrations at the core outlet have the most significant effect on both H_2O_2 and O_2 concentration at the core outlet.

Table 4.7

Summary of Sensitivity Studies (Relative Sensitivity)

H_2O_2 in Liquid at Core Outlet

Most Sensitive to Reactions

W4	$e^-aq + H_2O_2 \rightarrow OH + OH^-$
W7	$e^-aq + O_2 \rightarrow O2^-$
W9	$OH + OH \rightarrow H_2O_2$
W21	$OH + H_2O_2 \rightarrow HO_2 + H_2O$

G-Values

γ and n of e^-, H^+, H_2O_2

Species

H_2O_2, O_2, O_2 (gas), H_2 (gas)

O_2 in Liquid at Core Outlet

Most Sensitive to Reactions

W14	$OH + H_2 \rightarrow H + H_2O$
W15	$H + H_2O \rightarrow H_2 + OH$
W16	$H + O_2 \rightarrow HO_2$
W21	$OH + H_2O_2 \rightarrow HO_2\, H_2O$

G-Values

γ and n of e^-, H^+, H_2O_2

Species

H_2O_2, O_2, O_2 (gas), H_2 (gas)

Absolute Sensitivity

(1) chemical reactions;

Surface decomposition and reactions W31 and W33, as summarized in Table 4.8, have the most significant effect on both oxygen and hydrogen peroxide concentrations at the core outlet.

(2) G-values

The results are the same as for the relative sensitivity study.

(3) Species concentrations

For peroxide at the core outlet, HO_2^-, e^-, and OH^-, have the most important effect. And for oxygen, HO_2^-, e^-, and H are the most important.

Table 4.8

Summary of Sensitivity Studies (Absolute Sensitivity)

H_2O_2 in Liquid at Core Outlet

Most Sensitive to Reactions

W31 $H_2O \rightarrow H^+ + OH^-$

Surface decomposition (Titanium)

W33 $H_2O_2 \rightarrow OH + OH$

G-Values

γ and n of e^-, H^+, H_2O_2

Species

HO_2^-, e^-, OH^-

O_2 in Liquid at Core Outlet

Most Sensitive to Reactions

W31 $H_2O \rightarrow H^+ + OH^-$

Surface decomposition (Titanium)

W33 $H_2O_2 \rightarrow OH + OH$

G-Values

γ and n of e^-, H^+, H_2O_2

Species

HO_2^-, e^-, H

4.4 Chapter Summary

This chapter has been concerned with parametric studies carried out to:

(a) establish the adequacy of the approximate nodal representation adopted to describe the BCCL.

(b) identify key variables governing the performance of the BCCL with respect to generation of the radiolytic species H_2O_2, O_2 and H_2.

(c) help establish uncertainty bands for both the computed and measured results.

(d) examine the degree to which the BCCL simulates an actual BWR.

(e) aid in the development of a consensus estimate nodal representation and data set for the comparisons with experimental results reported in Chapter 5.

Among the more significant findings are that:

(a) as expected, the magnitude of in-core gamma and neutron dose rates rank high on the list of dominant loop characteristics.

(b) surface-induced decomposition of H_2O_2 significantly affects the concentration of this species downstream of the separator plenum.

(c) considering likely uncertainties in system parameters and basic data (radiolysis yields and thermodynamic data), computed concentrations of H_2O_2, O_2 and H_2 are probably credible to within $\pm$ 25% or so.

(d) a similar degree of difference between the BCCL and a BWR is to be expected in terms of core exit values.

(e) net oxidant (or reductant) concentration at the core inlet is the principal determinant of core and loop exit concentrations of H_2O_2, O_2 and H_2 (other variables held constant).

As will be seen in Chapter 5, none of the plausible variations examined in this chapter can account for the differences between calculated and measured radiolysis product concentrations. Additional work to resolve this dilemma is suggested in chapter 7.

Chapter 5
Best-Estimate Results

5.1 Introduction

In this chapter the current best-estimate results are reported resulting from use of the RADICAL program to simulate the reference case normal water chemistry (NWC), and hydrogen water chemistry (HWC), runs of the Summer 1992 campaign. The major changes from the version used for the parametric studies of Chapter 4 are:

(1) the use of current best-estimate neutron and gamma dose rates for the MITR, as established in Chapter 2.

(2) the use of a more up-to-date set of high temperature G values provided by GE (R-2) and a consensus reaction rate set agreed to in the MIT August 1992 workshop (M-3): see Chapter 4 for a comparison of results using these values and our earlier data set.

The initial task addressed in this chapter is establishment of the experimental results which are to be simulated. This is followed by the nominal case RADICAL results, including a brief discussion of some likely reasons for the discrepancies. Chapter 7 suggests a course of action to resolve these differences.

5.2 Experimental Results

The thesis by Rozier (R-1) documents the results of the Fall 1991 experimental campaign. However, final correction of the peroxide measurements for decomposition in the sampling system was deferred pending post-run calibration of the system. This has since been accomplished by B. Hilton, who will report the details in his SM Thesis which is principally concerned with the Summer 1992 campaign (H-1).

In the comparison between computations and experiment, greater reliance will be placed upon Summer 1992 results, because of the improved instrumentation available for this campaign – notably a stable, well-calibrated Hydran H_2 analyzer. In general, however, the H_2O_2 and O_2 data is comparable for these two campaigns. Representative measurements are summarized later in this chapter in Table 5.3.

The following important points must be appreciated with respect to this data:

(1) The H_2O_2 values are measured at the sample point in the liquid effluent line exiting the loops' core outlet plenum. Inlet H_2O_2 concentrations are negligible in the runs cited here (but not in runs following long periods of cold standby operation).

(2) The O_2 and H_2 values show the inlet/outlet concentrations: "inlet" was measured in the bypass return line from the charging pump; "outlet" was measured in the line which returns mixed water plus steam effluent to the makeup tank. As such it also contains oxygen from decomposition of water effluent H_2O_2.

(3) The uncertainty of the exit quality in the BCCL has been estimated as shown in Appendix I. The error will be as large as 4% for an operating temperature of 290°C if the heat loss in lines to the heat exchanger is approximate to 10°C. Thus for a measured quality of 10% using an energy balance, the real exit quality could be as much as 14%.

5.3 Calculation of Summer 1992 Runs

Best-estimate calculations have been made to compare with data from the Summer 1992 runs. Figure 5.1 is the current nodal diagram used in the simulation. The dose rates, chemical reaction data sets and G-values have already been discussed (also see Appendices C and A). They have been updated to improve the simulation of the experiments. Table 5.1 shows the components and their corresponding positions with respect to the inlet of the BCCL. Table 5.2 presents the conditions for the best-estimate base case. All conditions are kept the same for the calculations except for the inlet chemical concentrations and the boiling conditions, depending on the experiments simulated.

Table 5.1

BCCL Components and their Corresponding Positions

Component	Inlet/Outlet	Position (cm)
Feedwater Plus Chemical Injection	Inlet	0
Charging Line	Outlet	400
Core Inlet Zone	Inlet	400
	Outlet	431
Core Subcooled	Inlet	431
	Outlet	451
Core Boiling 1	Inlet	451
	Outlet	471
Core Boiling 2	Inlet	471
	Outlet	491
Core Boiling 3	Inlet	491
	Outlet	511
Core Boiling 4	Inlet	511
	Outlet	531
Core Boiling 5	Inlet	531
	Outlet	551
Core Outlet Zone	Inlet	551
	Outlet	582
Plenum Inlet Line	Inlet	582
	Outlet	646
Liquid Phase in	Inlet	646
Outlet Plenum	Outlet	661
Liquid Return Line	Inlet	661
	Outlet	686
Sampling Line	Inlet	686

Table 5.2

Conditions of the Best-Estimate Base Case

- Loop Geometry/Temperature/Dose Rates: as in Figure 5.1
- Exit Quality: 15%
- Mass Flow Rate: 25 g/s
- Reaction set: a consensus reaction set as agreed to in the MIT August 1992 workshop (Set No.2 in Appendix A)
- G-values: New GE high temperature G-values (Set No.2 in Appendix A)
- H_2O_2 Decomposition: $H_2O_2 \rightarrow H_2O + 1/2\ O_2$

  $k_{total} = 0.3\ sec^{-1}$ (diameter and velocity independent)

  Ea= 0.0 kJ/mol K (hence temperature independent)
- Inlet O_2 , H_2 concentrations: measured experimental values

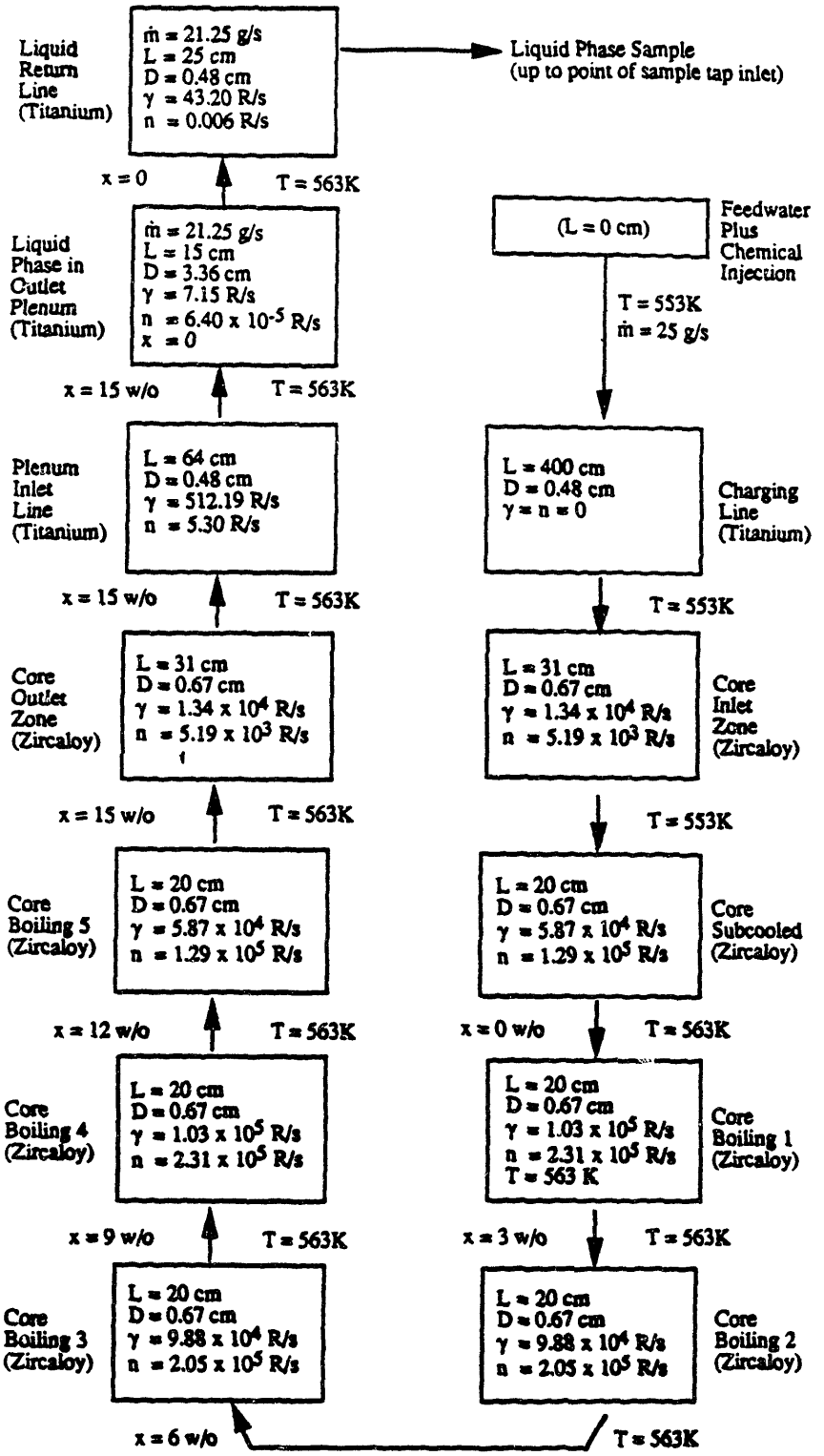

Figure 5.1 Best-Estimate Revised Nodal Diagram of BCCLL as of 9/15/92

Special attention must be paid to the usage of the set No.2 H_2O_2 decomposition reaction in RADICAL. The H_2O_2 decomposition reaction can be expressed as thermal (homogeneous) and surface (heterogeneous) decomposition in RADICAL. For the surface decomposition term, a factor of $\frac{1}{D}$ multiplies k'_{surf} to account for the area/volume ratio effect (see Appendix H). For the subject calculations, this more sophisticated treatment was not utilized to simplify matters and thereby provide results which are easier to compare with those of other modelers. H_2O_2 decomposition, in the form of an ordinary chemical reaction, is used in the best-estimate calculation input files with a reaction rate of 0.3 s^{-1} and zero activation energy; this gives a constant decomposition rate (0.3 s^{-1}) for all components and all temperatures (~ 290°C). Note the analysis by Hilton (H-1),which suggests that this approximation greatly overestimates decomposition in the exit plenum.

Table 5.3 compares the experimental results and the simulation results for Summer 1992 runs (see Appendix E for detailed results of the best-estimate simulation). As for the experimental data, the H_2O_2 values are those at the sample point in the liquid effluent line exiting the loop's core outlet plenum, which corresponds to the position of 686 cm. The inlet concentrations of the O_2 and H_2 were measured in the bypass return line from the charging pump; outlet concentrations were measured in the line which returns mixed water plus steam effluent to the makeup tank. The accuracy of the colorimeter, orbisphere and Hydran/orbisphere instruments used to measure H_2O_2, O_2 and H_2 concentrations is within 5% depending on when and how the instruments are calibrated. The predicted O_2 and H_2 mixed return concentrations were calculated from the following equations, using the quality-weighted concentrations calculated in the vapor (g) and liquid (l) phases at 686 cm:

$$O_2 \text{ mixed return} = X \cdot \text{ppb } O_2(g) + (1-X) \cdot \text{ppb } O_2(l) + \frac{8}{17} \text{ppb } H_2O_2(l) \qquad (5.1)$$

$$H_2 \text{ mixed return} = X \cdot \text{ppb } H_2(g) + (1-X) \cdot \text{ppb } H_2(l) \qquad (5.2)$$

For NWC, the predicted H_2O_2 concentrations are only about 1/10 to 1/4 of the experimental data, while the mixed return O_2 and H_2 are closer to the experimental values. The problem of the discrepancy of the H_2O_2 concentrations is still unsolved. One of the possibilities suggested is that H_2O_2 is produced in the sampling system, which is not included in the present model. A simplified sampling system model has been investigated, which will be presented in the next section. The result tends to discredit this hypothesis. Another factor which decreases the H_2O_2 concentration in the simulation is the H_2O_2

Table 5.3 Comparisons between experimental data and predicted results for NWC, HWC, boiling and non-boiling cases

			O_2 (ppb) inlet	H_2 (ppb) inlet	H_2O_2 (ppb) sample extraction (at 686 cm)	O_2 (ppb) mixed return*	H_2 (ppb) mixed return*
Boiling cases (X_{exit} = 15%)	NWC	experimental	202 ± 104	18 ± 6	1155 ± 417	1048 ± 225	165 ± 23
		predicted	202.0	18.0	90.6	554.1	61.3
	HWC	experimental	0.± 5**	966 ± 38	560 ± 557	0 ± 5**	896 ± 45
		predicted	0.	966.0	0.12	0.06	964.7
Non-boiling cases	NWC	experimental	150 ± 37	5.± 1	272 ± 79	359 ± 59	41 ± 11
		predicted	150.0	5.0	69.0	194.6	10.7
	HWC	experimental	0.± 5**	419 ± 10	410 ± 224	0 ± 5**	407 ± 4
		predicted	0.	419.0	0.095	0.045	419.1

* H_2O_2 decomposition is included in all of the runs. (k_{total} = 0.3 sec^{-1}, Ea=0.)

* Input to code set equal to preliminary measured values reported prior to complete data reduction of Summer 1992 results.

* Mixed return values are calculated from values at 686 cm (entrance to liquid sample line) assuming complete dissociation of remaining H_2O_2.

** The ± values shown represent statistical variation for data collected during different runs (the noted ** values had zero standard deviation, so an estimate for systematic error is reported). The given measurement for all parameters, except for H_2O_2, during one run is more accurate, typically within ±5%.

Table 5.4 Comparisons between experimental data and predicted results without thermal and surface H_2O_2 decomposition

			O_2 (ppb) inlet	H_2 (ppb) inlet	H_2O_2 (ppb) sample extraction (at 686 cm)	O_2 (ppb) mixed return*	H_2 (ppb) mixed return*
Boiling cases (X_{exit} = 15%)	NWC	experimental	202 ± 104	18 ± 6	1155 ± 417	1048 ± 225	165 ± 23
		predicted	202.0	18.0	386.0	574.0	61.0
	HWC	experimental	0.± 5**	966 ± 38	560 ± 557	0 ± 5**	896 ± 45
		predicted	0.	966.0	0.13	0.06	964.7
Non-boiling cases	NWC	experimental	150 ± 37	5.± 1	272 ± 79	359 ± 59	41 ± 11
		predicted	150.0	5.0	249.0	194.5	10.6
	HWC	experimental	0.± 5**	419 ± 10	410 ± 224	0 ± 5**	407 ± 4
		predicted	0.	419.0	0.1	0.048	419.1

* H_2O_2 decomposition is not included in these runs. (k_{total} = 0. sec^{-1})

* Mixed return values are calculated from values at 686 cm (entrance to liquid sample line) assuming complete dissociation of remaining H_2O_2.

** The ± values shown represent statistical variation for data collected during different runs (the noted ** values had zero standard deviation, so an estimate for systematic error is reported). The given measurement for all parameters, except for H_2O_2, during one run is more accurate, typically within ±5%.

decomposition in the loop, especially in the exit plenum. Table 5.4 lists the simulation results without any decomposition of H_2O_2: at the current state of affairs, these values are probably to be preferred for comparison with Hilton's experimental data. Under this limiting condition predicted H_2O_2 concentrations are increased by about four times those for NWC in Table 5.3. It was also observed in the parametric study discussed in chapter 4 that different decomposition reactions and constants will result in significant differences in predicted H_2O_2 concentrations. Several aspects of H_2O_2 decomposition (homogeneous and heterogeneous) are still in dispute among the experts in this field. Thus both theory and experiment require further study.

Although there is a discrepancy between the predicted and experimental results, comparison with other collaborating workers' calculations is quite satisfactory. Table 5.5 is a comparison between MIT (RADICAL) and GE (FACSIMILE) simulation of what is essentially a non-boiling base case but with 30 ppb O_2 injection at the inlet.

Table 5.5 Comparison of MIT and GE simulations
(non-boiling base case with 30 ppb O_2 injection)

Position	551 cm	646 cm
GE result O_2 / H_2O_2 / Total O_2* (ppb)	40.9 / 331.0 / 196.7	44.8 / 80.4 / 82.6
MIT result O_2 / H_2O_2 / Total O_2* (ppb)	41.0 / 325.0 / 193.9	38.5 / 137.0 / 103.0

*Total $O_2 = O_2 + \frac{8}{17} H_2O_2$

5.4 Sampling System Simulation

H_2O_2 production in the sampling system in the BCCL has been investigated because of the high H_2O_2 concentrations measured in experiments. It is suspected that there might be a significant amount of H_2O_2 produced in the sampling line, which is at a low temperature (~ 70°C) compared to the temperature of the BCCL in-core region. A simplified sampling system model as shown in Figure 5.2 has been devised to simulate the H_2O_2 generation in this region using RADICAL. In the sampling system a loop sample stream (at 686 cm in Fig. 5.1) is mixed with cold injection water, and the resulting mixture is extracted through a heat exchanger.

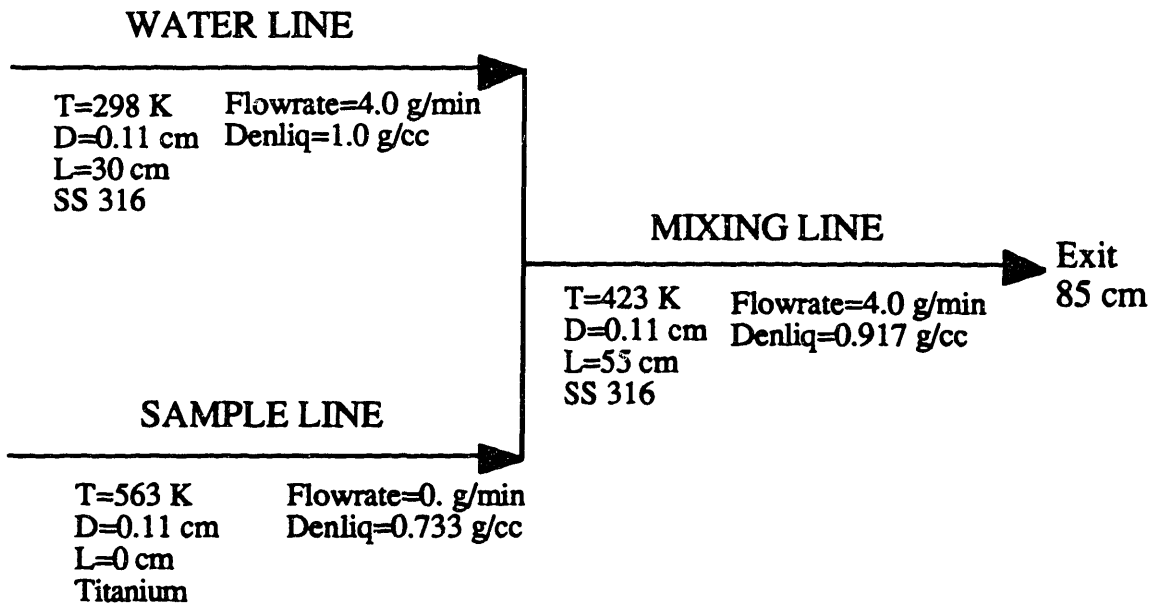

Figure 5.2 Simplified Sampling System Model of the BCCL

A constant temperature of the mixing line is assumed in this model: an approximation justified by the fact that decomposition is negligible below about 450°K. The flowrate of the sample line has been set to zero to maximize the effect of the H_2O_2 production in the water line. Gamma and neutron dose rates are 43.20 R/s and 0.006 R/s respectively for all three components. These values are obtained from the new MCNP calculations (conservatively assumed equal to the dose rates in the liquid return line, see Fig. 5.1). A calculation of the flow rate effect in the water line has been carried out. Figure 5.3 shows the results: H_2O_2 generation in the water line approaches 27 ppb at very low rates (~ 0.04 g/min), which are considerably less than those employed in practice (~ 2 g/min).

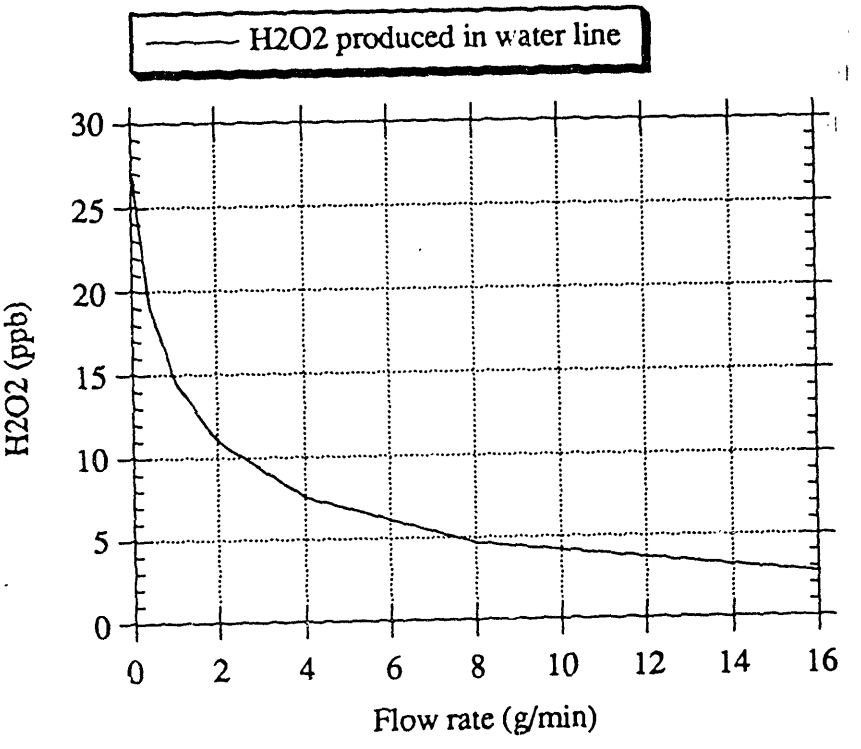

Figure 5.3 H_2O_2 production in the water line as a function of flow rate.

5.5 Chapter Summary

This chapter presents the best-estimate results of RADICAL calculations simulating Summer 1992 runs. A new nodal diagram of the BCCL has been constructed to simulate the environment of the experiment. The dose rates used in this nodal diagram are calculated using MCNP: detailed information on the dose rates is presented in Appendix C.

Tables 5.3 and 5.4 compare the simulations results and experimental results for Summer 1992 runs. A H_2O_2 thermal/surface decomposition rate of 0.3 sec^{-1} is assumed in the calculations shown in Table 5.3. For the calculation results shown in Table 5.4, thermal/surface decomposition is assumed to be zero, as a limiting case. The results show that the decomposition rate has a crucial effect on H_2O_2 concentrations at the sample extraction point for NWC, but has little effect on O_2 and H_2 mixed return concentrations. The simulation results show the importance of H_2O_2 decomposition in the plenum. Hilton (H-1) has also pointed out that use of the same decomposition rate constant for loop tubing

and the outlet plenum probably grossly overestimates decomposition in the latter component; hence no-decomposition results are probably closer to reality. The predicted results also show that the decomposition has little effect on mixed return O_2 and H_2 concentrations (less than 1%). Thus the following discussion on the comparison between calculation and experimental results are based on no-decomposition simulations. H_2O_2 is underpredicted by a factor of three, return O_2 and H_2 concentrations are underpredicted by factors of two and three, respectively, for boiling NWC condition. For non-boiling NWC, the calculation predicts the H_2O_2 concentration, but still underpredicts return O_2 and H2 by factors of two and four, respectively. The oxygen to hydrogen ratio for the experimental results is about 5.8, compared to 8 for stoichiometry.

H_2O_2 is significantly underpredicted for HWC in both boiling and non-boiling cases. Appreciable H_2O_2 is measured in the experiments, but no O_2 from its decomposition appears in the mixed return water. A calculation of the H_2O_2 production in the sampling system has been carried out. The predicted H_2O_2 concentration in the water line is negligible (< 10 ppb) at its normal flow rate (~ 4 g/min).

Possible factors for the discrepancy between experimental / predicted data are summarized as follows:

(a) G-values
(b) Chemical reaction rate data sets
(c) H_2O_2 decomposition reactions
(d) Errors in dose rate estimates
(e) Over-simplified thermal hydraulic model (e.g., neglect of the effect of downflow)
(f) H_2O_2 production in sampling system
(g) Bias in the experimental measurements
(h) Catalytic production of H_2O_2 by TiO_2, the predominant surface oxide film in the MIT loop.

Among these factors, (a) through (e) apply to simulation, while (f) through (h) are experiment related.

Hilton will report on tests done on the peroxide analysis method and loop sampling system in his thesis (H-1). All indications to date seem to rule out items (f) and (g), however considerable additional investigations of these points are planned for the Summer 1993 campaign.

Chapter 6

Hydrogen Peroxide Measurements

6.1 Introduction

There are eleven major chemical species (e^-, OH^-, H_2, OH, HO_2^-, H_2O_2, O_2^-, O_2, H, H^+ and HO_2) produced both directly and indirectly in BCCL coolant due to the in-core gamma and neutron irradiation. Only the three stable species among them, H_2, O_2 and H_2O_2, are readily measurable and the others are comparatively short-lived ($T_{1/2}$ ~ 0.1 second) (M-5). Radiolysis analyses of BCCL experiments are focused on concentrations of dissolved hydrogen peroxide, oxygen and hydrogen in the coolant. Dissolved oxygen and hydrogen are measured by Orbisphere® O_2 analyzer and Hydran® H_2 analyzer, respectively. Colorimetry was the only method used to measure H_2O_2 concentration during the 1990, 1991 and 1992 campaigns. Since a wide variety of chemical additives were injected into the BCCL to examine the effect on N-16 carryover/carryunder, there is the possibility that the chemical additives react with the ampoule solution used for colorimetry and give a "false concentration" reading. This is one of the possible reasons which contribute to the significant discrepancy between predicted and measured hydrogen peroxide concentrations in the Summer 1992 campaign, as described in chapter 5. Table 6.1 is a summary of chemical additive effects on H_2O_2 measurement (H-1). Other alternatives for H_2O_2 measurement are now under investigation to improve reliability and accuracy. Among these, a method in which MnO_2 is used to dissociate H_2O_2 into O_2 has been proposed and tested. Results to date show that the accuracy of the MnO_2 method is within 20%.

This chapter mainly focuses on H_2O_2 measurement for the following reasons:

(1) There is not yet an intrumental method to measure H_2O_2 concentration for BCCL experiments, as one has for dissolved oxygen and hydrogen.
(2) H_2O_2 decomposes fairly rapidly at high temperatures (≥ 200 °C), especially in contact with metallic surfaces. Care must be taken to account for the thermal/surface-induced decomposition in the sampling system.
(3) A significant discrepancy is observed between computation and experiment, as described in chapter 5.

Table 6.1 Summary on Chemical Additive Effect on H_2O_2 Measurements (Reference H-1)

Additive	w/ H_2O_2	Effect on H_2O_2 Measurements
Oxidizing		
KNO_2	no	increase
KNO_2	yes	increase
K_2CO_3	no	none
K_2CO_3	yes	none
K_2CrO_4	no	increase
K_2CrO_4	yes	increase
K_2MnO_4	no	increase
K_2MnO_4	yes	increase
Reducing		
$N(CH_3)_3HCl$	no	none
$N(CH_3)_3HCl$	yes	none
$C_6H_5SO_3Na$	no	none
$C_6H_5SO_3Na$	yes	none
NH_3OHCl	no	none
NH_3OHCl	yes	none
C_2H_5OH	no	none
C_2H_5OH	yes	none
pH Agent		
KOH	no	none
KOH	yes	none
HCl	no	none
HCl	yes	none
NH_4OH(reducing)	no	none
NH_4OH(reducing)	yes	none
Complex Forming		
$PdCl_2$	no	none
$PdCl_2$	yes	none

Notes:

(1) additive concentrations were ~ 10^{-4} M, H_2O_2 at ~ 1000 ppb.
(2) the observed increases were equivalent to ~ 2000 ppb H_2O_2.
(3) Tests were carried out on two different colorimetric methods: Chemetrics kits No.5503 and No.5543: both responded similarly.

6.2 Hydrogen Peroxide Sampling System

The H_2O_2 sampling system consists of a sample cooler, tube-in-tube heat exchanger, mixed injection cooling system , sample line, and sample tap as shown in Fig. 6.1. The purpose of this system is to permit sampling of the water return line inside the BCCL thimble, just downstream of the outlet plenum, for H_2O_2 concentration measurement (R-1). It is crucial that the sample is cooled with cold water as soon as it is drawn from the water return line because H_2O_2 decomposes rapidly at high temperatures, especially when in contact with hot metal surfaces. To achieve this, a sample cooler is used which injects a stream of cold water into the sample at the sampling point, followed immediately by a tube-in-tube heat exchanger to cool the sample further. The cooling water is salted with a known concentration of KNO_3 (potassium nitrate) to enable determination of the ratio of sample to cooling water by measuring loop sample conductivity and mixed sample conductivity.

The hydrogen peroxide sample cooler was calibrated to determine the decomposition of the hydrogen peroxide sample from the sample point in the thimble to the ex-thimble point. Samples were drawn and analyzed with colorimetry at room temperature to obtain the baseline peroxide concentration. Then the water inlet stream was heated to 280°C to obtain the hydrogen peroxide concentration at the BCCL operating temperature. The fractional decomposition D was then computed as

$$D = \frac{\text{baseline concentration} - \text{concentration at operating temperature}}{\text{baseline concentration}}$$

The measured sample line fractional decomposition is 62 %, i.e., one should increase all measured H_2O_2 concentrations by a factor of 2.6 to account for the thermal decomposition at the sample line.

An overall correction factor of ~ 9, to account for both dilution and decomposition effects, was typically applied to the measured H_2O_2 concentrations in the BCCL experiments.

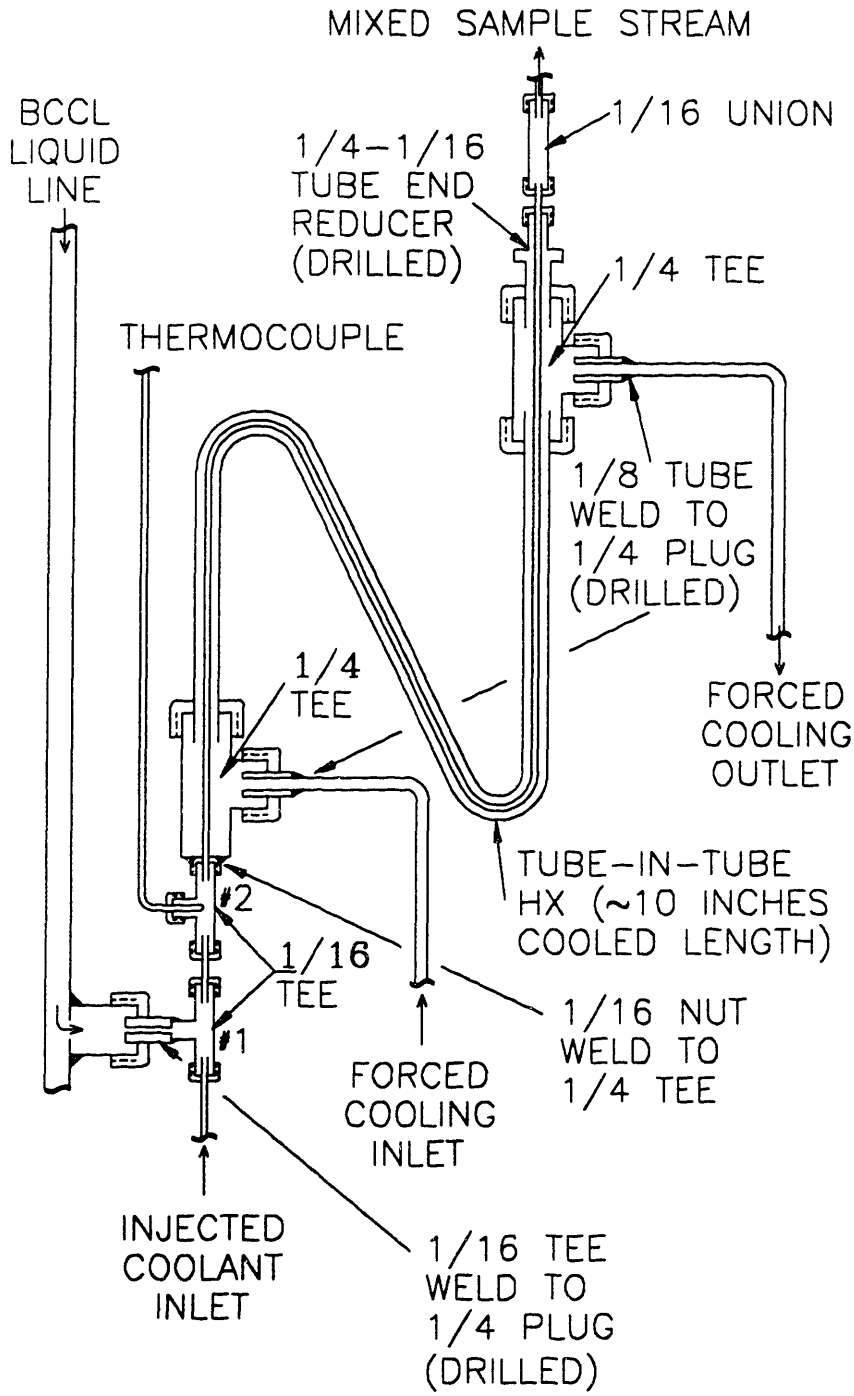

Figure 6.1 Hydrogen Peroxide Sampling System (R-1)

6.3 MnO_2 Method

MnO_2 is a fine, black powder which is used as a catalyst in this H_2O_2 measurement method. Hydrogen peroxide concentration is measured indirectly via the following decomposition reaction that is catalyzed by MnO_2.

$$H_2O_2 \rightarrow \frac{1}{2}O_2 + H_2O \qquad (6.1)$$

By measuring the O_2 concentration downstream of the decomposition bed and the O_2 concentration bypassing the decomposition bed, the H_2O_2 concentration can be calculated by the following equation.

$$\text{ppb } H_2O_2 = \frac{17}{8}\left(\text{ppb } O_2^{decomp} - \text{ppb } O_2^{bypass}\right) \qquad (6.2)$$

where ppb H_2O_2 = H_2O_2 concentration in the sample liquid.

ppb O_2^{decomp} = O_2 concentration in liquid measured downstream of the decomposition bed (originally existing O_2 plus O_2 produced from decomposition)

ppb O_2^{bypass} = O_2 concentration in the liquid bypassing the decomposition bed (background O_2 concentration in the sample liquid)

The oxygen concentration can be measured directly using an Orbisphere® meter. Appendix J shows the details of the Orbisphere® principle/calibration/operation.

This method has been demonstrated by running a series of experiments. Two kinds of loop configuration, recirculation and once-through, have been tested. The considerations of running in these different modes are:

- sample liquid flow rate (~ 10 cc/min permited in the sample line) and O_2 concentration measurement limits of different membranes. A higher flow rate can be obtained by circulating the sample liquid in the recirculation line, a membrane sensitive to lower O_2 concentration can then be used in the Orbsphere® (see Table J-1) for better O_2 measurement accuracy.

- the decomposition ability of the decomposition bed. A known decomposition ratio, or complete decomposition of the H_2O_2 sample, is required for the hydrogen peroxide measurement. Complete decomposition is more certain under the multiple-pass operation in the recirculation mode.
- system response time. The system response time includes membrane response time and loop response time. Long response time is undesirable for on-line measurements since the measurement will not promptly reflect the current hydrogen peroxide level during BCCL operation.

6.3.1 Recirculation Mode

The recirculation mode for the measurement system was first proposed because recirculatory flow permits a higher flow rate, which enables the use of a membrane having a lower O_2 concentration limit (see Table J-1), and also because it assures maximum hydrogen peroxide decomposition through the decomposition bed, given a high recirculation ratio.

– Setup

Figure 6.2 is a schematic of the design of the MnO_2 analyzer operated in its recirculation mode. The system was made using 1/4" Teflon tubing and the decomposer was 20 cm long 1/2" Teflon tubing filled with about 25 cc of fine MnO_2 particles. Oxygen analyzing membrane 2952A was used in the Orbisphere® sensor.

– Operation

The sample liquid is first purged with helium in a plastic bottle to reduce the oxygen concentration (air-saturated oxygen concentration in water is about 8 ppm). There are three options to run this system: bypass (to measure background O_2 concentration), bypass in recirculation line (to measure background O_2 concentration in the recirculation line) and recirculation (to measure total oxygen concentration including both background and H_2O_2 decomposition). Background O_2 concentration was at first measured in the bypass line with high flow rate. Then the loop was operated in a recirculation mode with a low recirculation ratio to purge air/pre-existing sample liquid in the decomposition bed. The recirculation ratio (ratio of recirculation flowrate to inlet sample flow rate) was raised to ~ 15 to enhance H_2O_2 decomposition in the recirculation line.

Data were taken when the Orbisphere® reading reached steady-state. The definition of "steady-state" here is repetitive small range oscillation (~ 10 to 30 ppb) observed for a reasonably long period of time (at least 5 minutes). The system was frequently perturbed by bubbles which influenced both flow rates and orbisphere readings. The emergence of bubbles in the recirculation line was due to high pumping power (hence pressure drop) which possibly sucks in air through the joints, or helium gas from the charging tank.

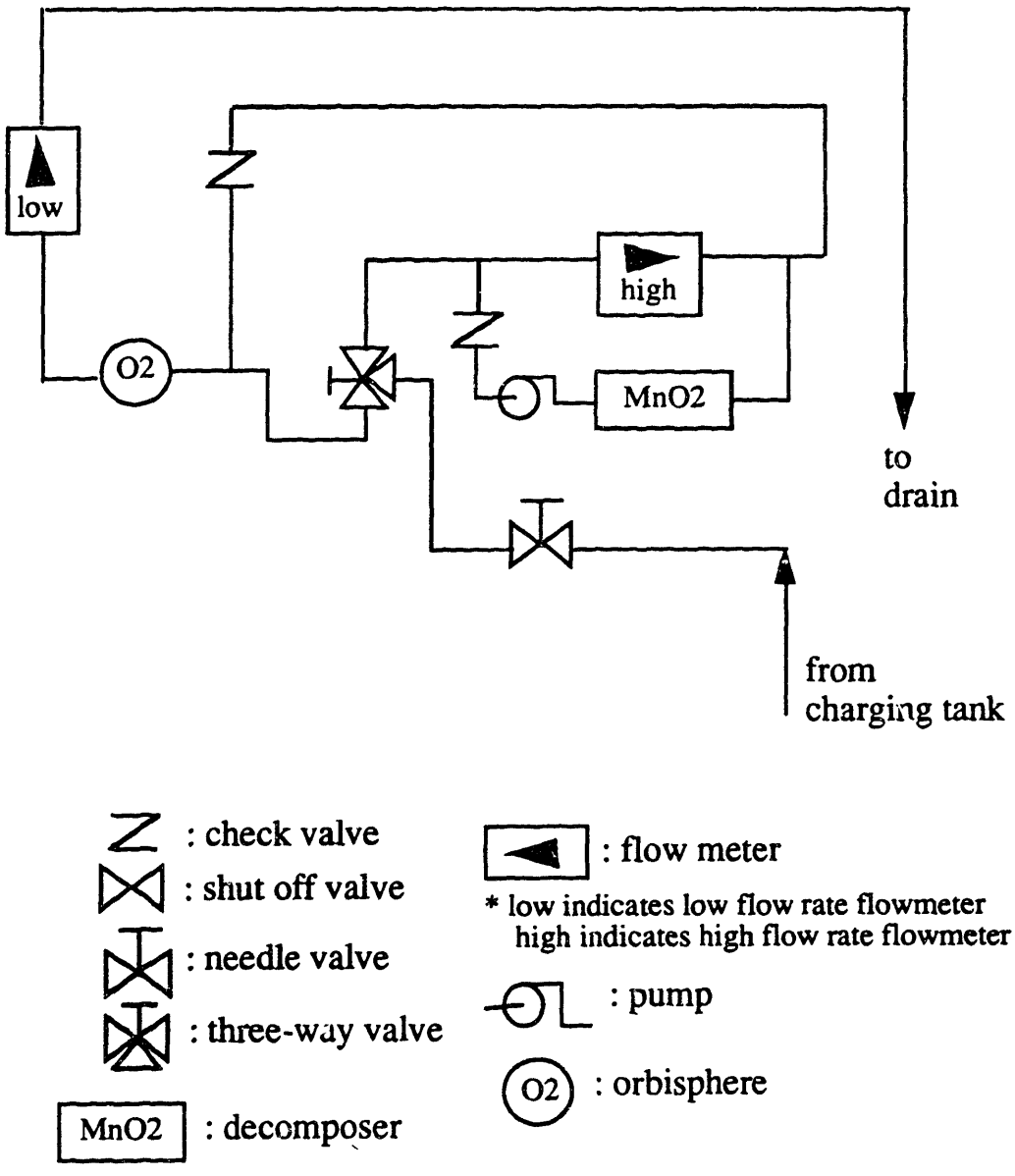

Figure 6.2 Schematic of H_2O_2 analyzer (recirculation mode)

– Experimental Results

Due to the long response time (see derivation in Appendix K) and oscillatory readings of the orbisphere, only two sets of experiments were carried out.

Experimental results are shown in Fig. 6.3 to Fig. 6.9. Figure 6.3 through Fig. 6.5 are tests for a H_2O_2 concentration of 1019 ppb and Fig. 6.6 through Fig. 6.7 are for a H_2O_2 concentration of 636 ppb. It was discovered that air was suctioned into the recirculation loop in the second set of runs; the background O_2 concentration of 66 ppb was at first measured in the bypass line (Fig. 6.8) and was measured as 155 ppb (Fig. 6.9) in the recirculation bypass line. This explains why measured O_2 concentrations are higher than they should be.

The experimental results are summarized in Table 6.2. The accuracy of the tests is within 20 %. The response time (> 1 hour, see Appendix K), however, is too long for an on-line measurement. Another concern with using the recirculation mode is the O_2 consumption through the Orbisphere sensor, due to the oxygen reduction reaction. This effect was not found significant in this series of runs because of the combined effect of the high O_2 concentration in the loop and air suction in the recirculation line. But it could become significant when the O_2 concentration is at a few ppb level.

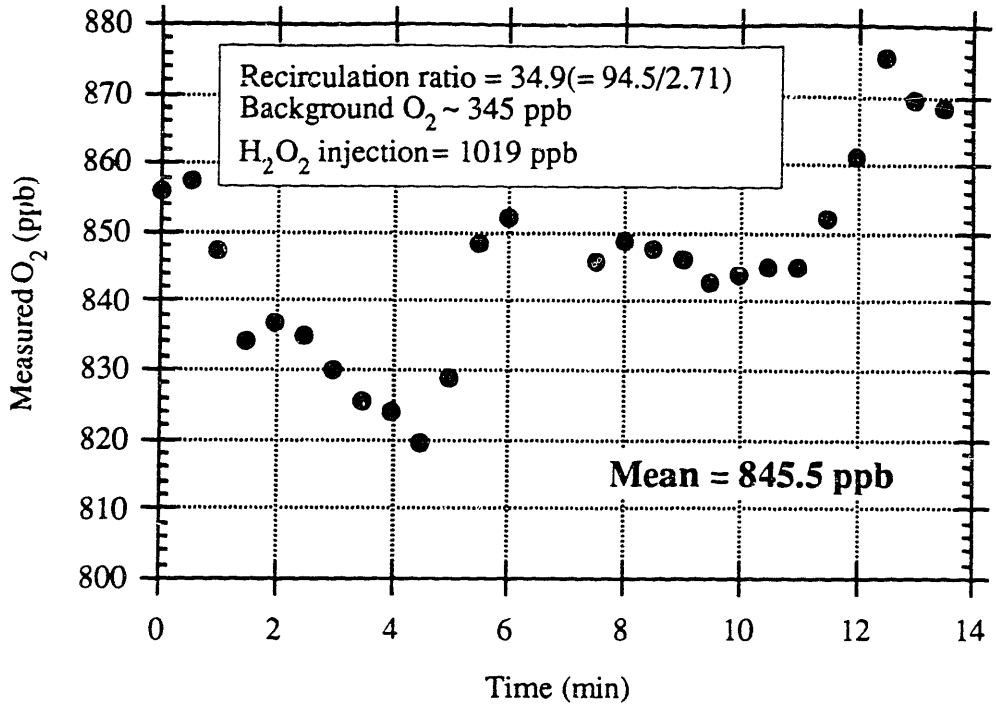

Figure 6.3 Total O_2 concentration measured for 1019 ppb H_2O_2 injection (recirculation mode), Run 1.

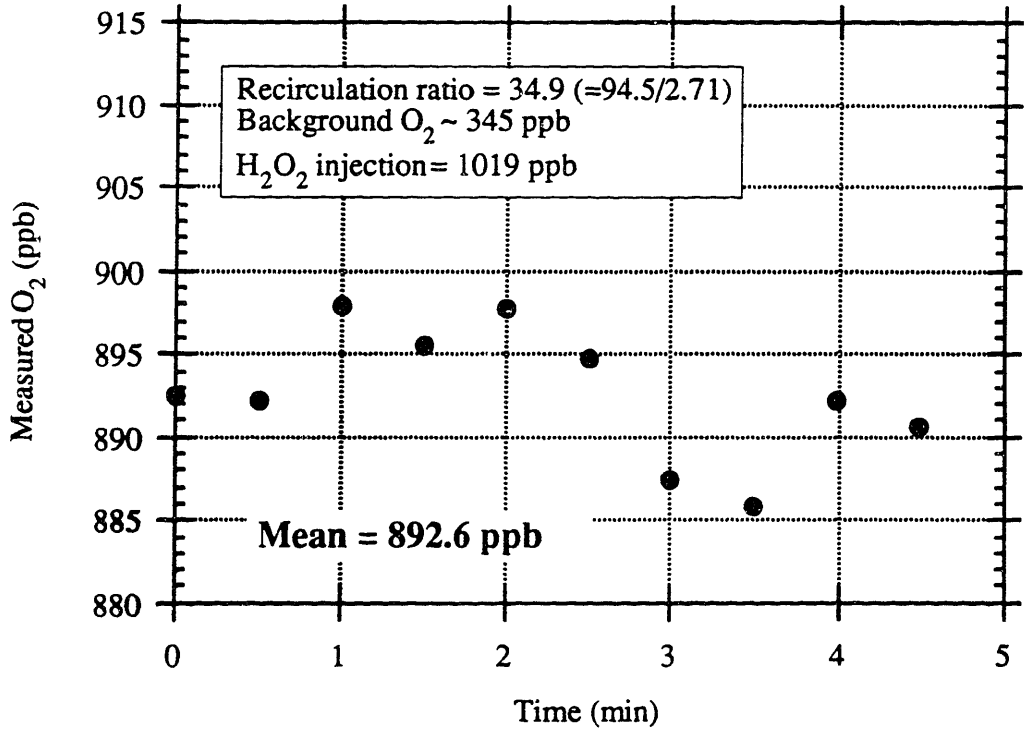

Figure 6.4 Total O_2 concentration measured for 1019 ppb H_2O_2 injection (recirculation mode), Run 2.

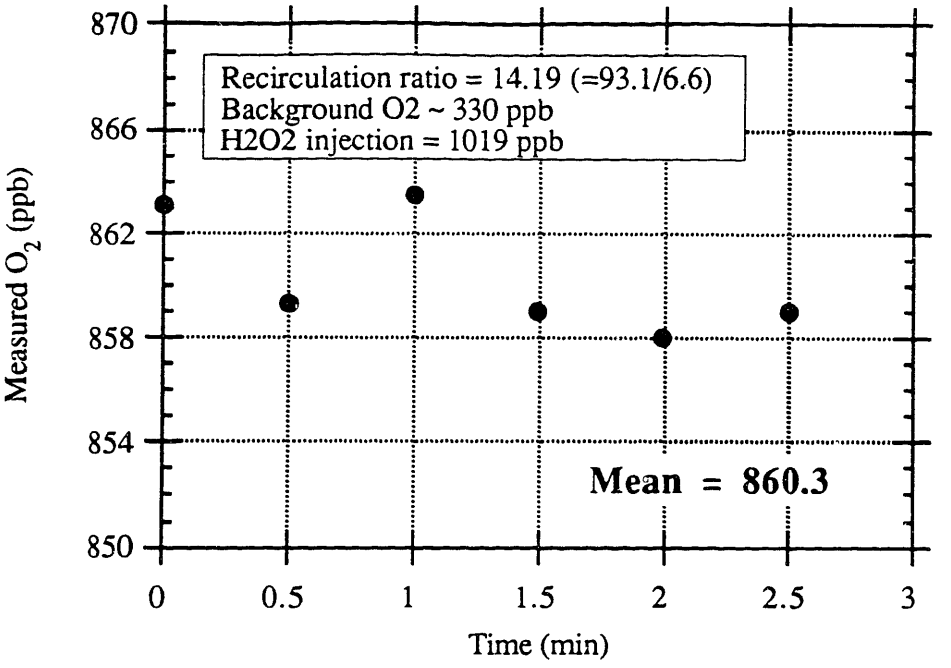

Figure 6.5 Total O_2 concentration measured for 1019 ppb H_2O_2 injection (recirculation mode), Run 3.

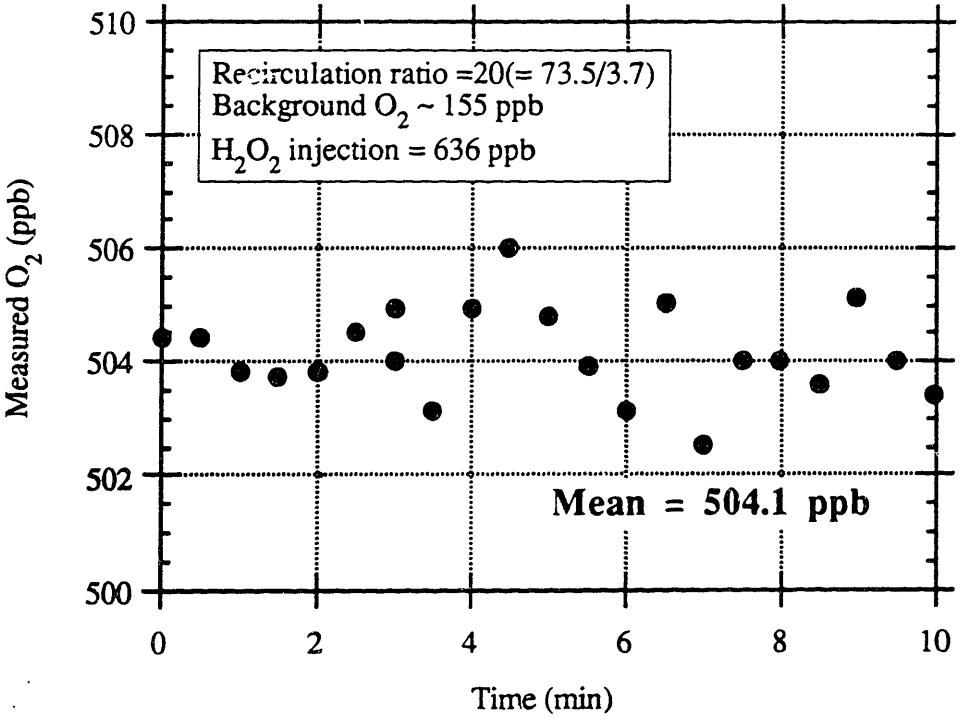

Figure 6.6 Total O_2 concentration measured for 636 ppb H_2O_2 injection (recirculation mode), Run 4.

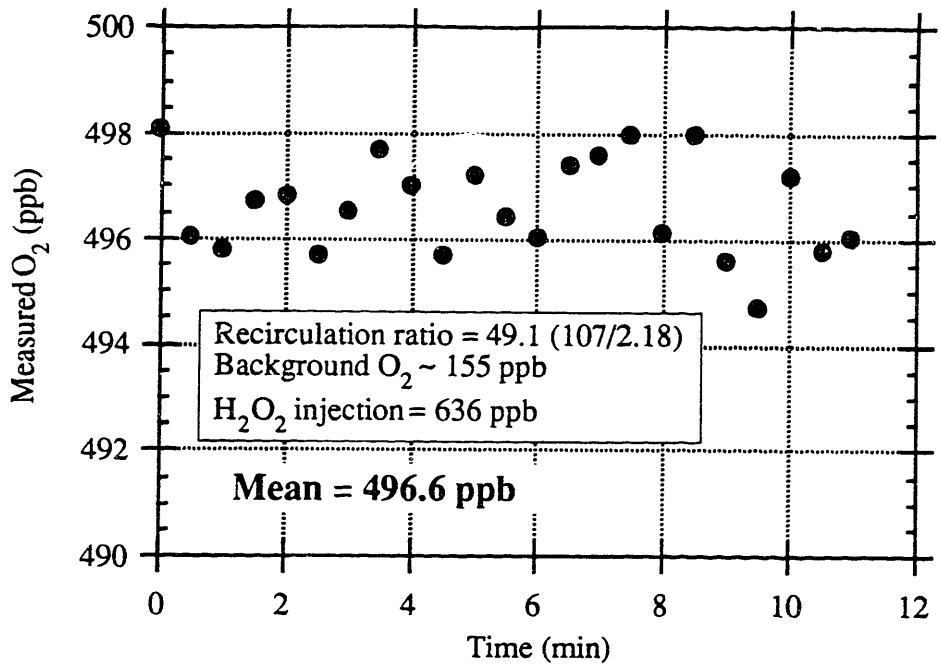

Figure 6.7 Total O_2 concentration measured for 636 ppb H_2O_2 injection (recirculation mode), Run 5.

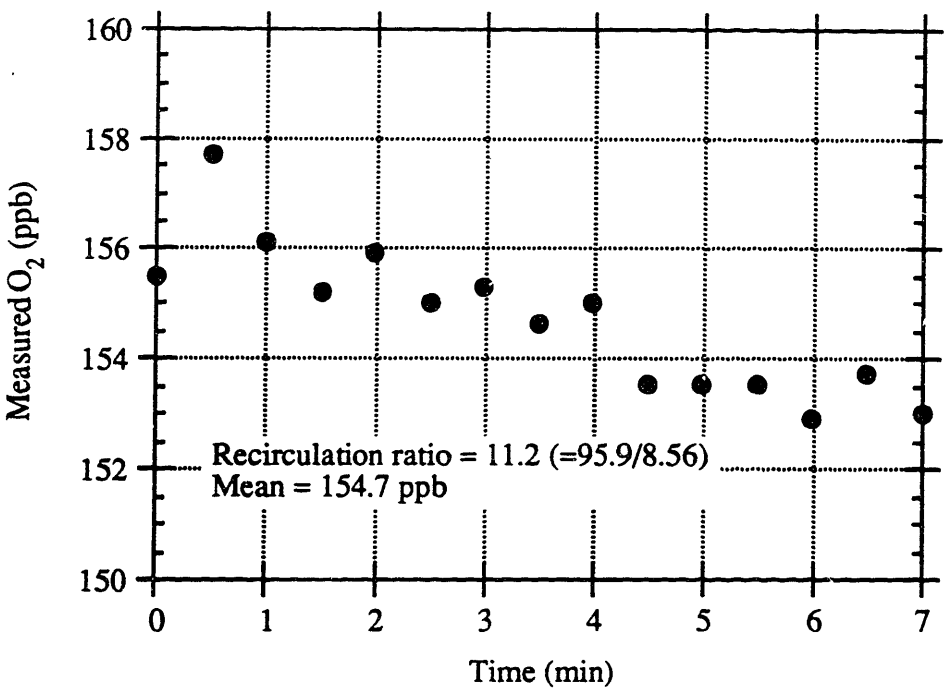

Figure 6.8 Background O_2 concentration measured in bypass line for second set of runs.

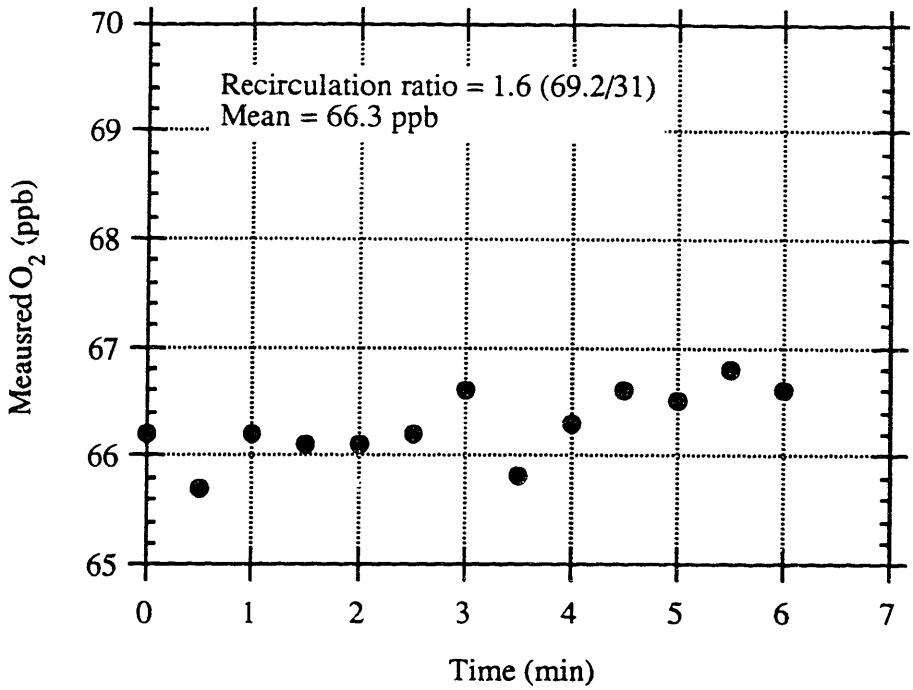

Figure 6.9 Background O_2 concentration measured in recirculation bypass line for second set of runs.

Table 6.2 H_2O_2 Analyzer Experimental Results (Recirculation Mode)

H_2O_2 injection (ppb)	ID	Measured O_2 conc.(ppb)	Background O_2 conc.(ppb)	Predicted H_2O_2 conc. (ppb)	Error
1019	Run 1	845.5	345	1063.6	4.4%
	Run 2	892.6	345	1163.7	14.2%
	Run 3	860.3	330	1126.9	10.6%
636	Run 4	504.1	155*	741.8	16.6%
	Run 5	496.6	155*	725.9	14.1%

* This is the background O_2 concentration in a high recirculation ratio bypass loop.

6.3.2 Once-Through Mode

The MnO_2 method was switched to a once-through mode (Figure 6.10) due to the long response time of the H_2O_2 measurement using the recirculation mode. The response time, defined as the time required for the Orbisphere to reach a steady-state reading of the O_2 concentration, is influenced by the sample liquid mass existing in the loop, sample liquid flow rate and the type of membrane used. The long response time of the recirculation mode is mainly due to the large volume of the system, which may initially hold liquid with O_2 concentration higher or lower than the O_2 concentration analyzed. A substantial amount of time is thus spent on purging the system with the sample liquid. The system volume, also the response time, will be greatly reduced in the once-through design.

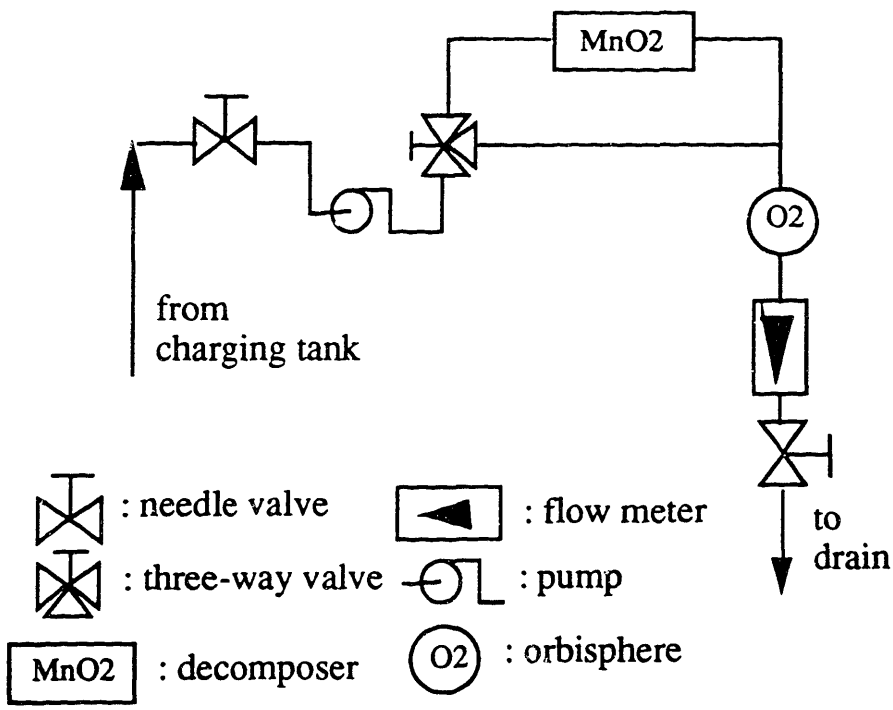

Figure 6.10 Schematic of H_2O_2 analyzer (once-through mode)

For the Orbisphere, membrane 2935A, which has a response time of 138 seconds, is used since a maximum flow rate of 10 cc/min is allowed for sample liquid measurement from the BCCL sample line. The response time of the once-through system is about 20 to 30 minutes, which is a combined result of its small flow rate and the reduced total system volume.

Another concern was the decomposition ability of the MnO_2 bed. A series of tests have been done which proved that the H_2O_2 can be completely decomposed in one pass with ~ 40 cc of MnO_2 powder (occupying ~ 14 cm of length in a 3/4"OD SS tubing) at a flow rate of ~ 10 cc/min. H_2O_2 sample concentrations ranging from about 100 ppb to 3.5 ppm have been tested (H_2O_2 concentrations measured during the summer 1992 campaign were up to ~ 1 ppm) . The sample liquid H_2O_2 concentrations were measured through the bypass line, and the decomposed H_2O_2 concentrations were measured through the decomposer, both using colorimetry. The decomposition ratio of the MnO_2 bed is 100% ± 0.5% as shown in Fig. 6.11; the uncertainty of the decomposition ratio measurement is mainly due to the sensitivity of the colorimetric method, its detection limit level is ~ 10 ppb. The H_2O_2 sample is then assumed completely decomposed by the MnO_2 bed in the following tests.

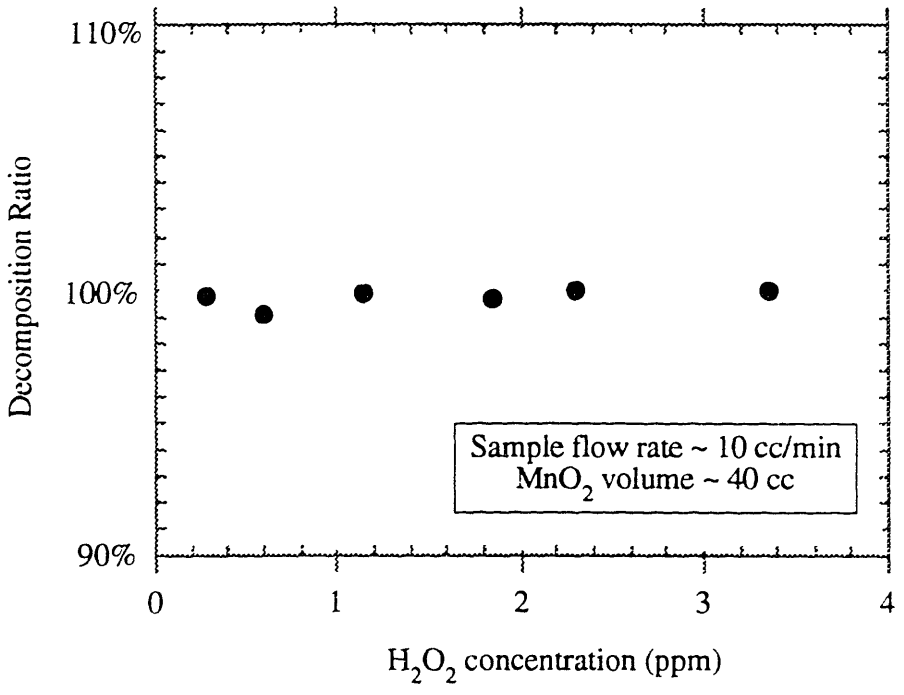

Figure 6.11 Tests of MnO_2 bed decomposition ability

– Setup

The prototype loop next constructed and tested is made of 1/4" stainless steel tubing, and the decomposer is made of 1/2" stainless steel tubing filled with about 40 cc of MnO_2. Great efforts have been made in reducing the system volume. The total volume of the system is about 75 cc, and about 2/3 of it is occupied by the decomposer. Joints are sealed with duct tape to prevent air leakage.

– Operation

The sample liquid was purged with helium to reduce the background O_2 concentration. The loop itself was also purged with helium to reduce the influence of air or pre-existing O_2 concentration in the liquid. Both needle valves were closed after purging until the sample liquid flows in. The flow rate was kept at ~ 10 cc/min using the inlet needle valve. Orbisphere® readings were taken when the instrument reading reached steady-state.

– Experimental Results

The experimental results are shown in Fig. 6.12 through Fig. 6.25. The H_2O_2 sample concentrations are measured by colorimetry. The accuracy of colorimetry is ~ 10 ppb in the range of interest. The oscillatory behavior of the Orbisphere readings during steady-state is the same as in recirculation mode operation, but the range is reduced to ~ 5 ppb.

The results are summarized in Table 6.3. The accuracy of this set of experiments is within 20%. One interesting phenomenon is that the predicted H_2O_2 concentrations are all lower than the sample H_2O_2 concentrations. Possible reasons for the discrepancy are:

- Background O_2 concentrations are decreasing when the system is operated in its decomposition mode since the changing tank is pressurized with helium. Background O_2 concentrations at the beginning and at the end of the loop operation were measured for one of the tests; it was found that the background O_2 was decreased by ~ 2 ppb.
- The Orbisphere sensor may not be well-calibrated. The Orbisphere sensor was calibrated at the beginning of the test. There is the possibility that the sensor itself has a certain degree of error. The accuracy of the Orbisphere sensor is ±1% or ±0.1 ppb/0.05 Pa whichever is greater, according to the system specifications (O-3).

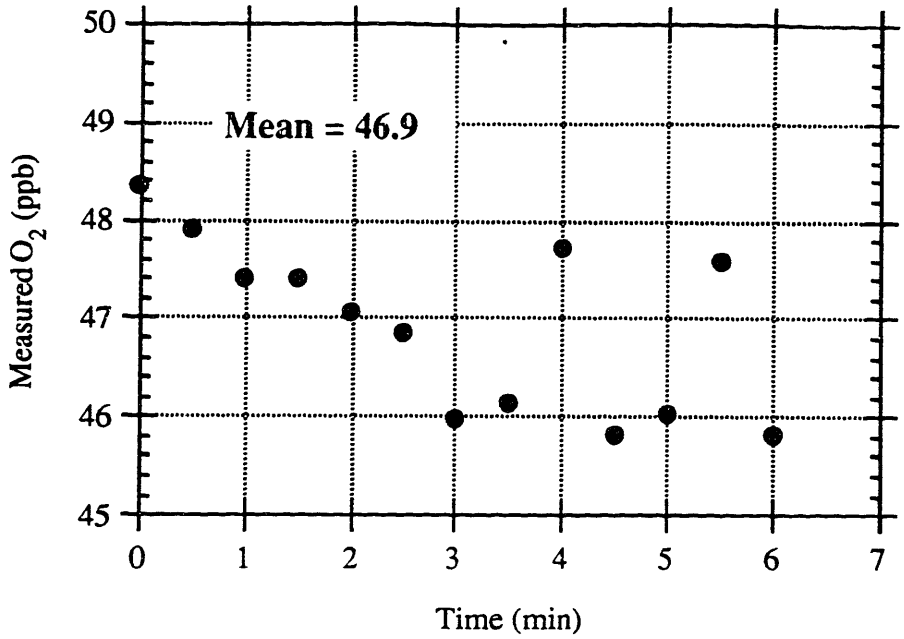

Figure 6.12 Background O_2 concentration measured for 80 ppb H_2O_2 injection (once-through mode), Run 6.

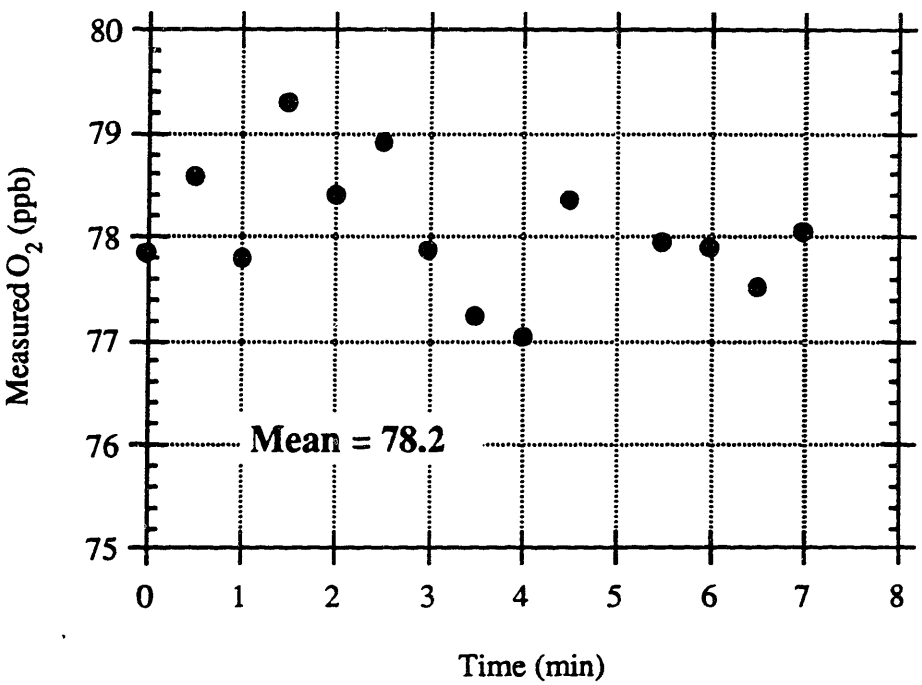

Figure 6.13 Total O_2 concentration measured for 80 ppb H_2O_2 injection (once-through mode), Run 6.

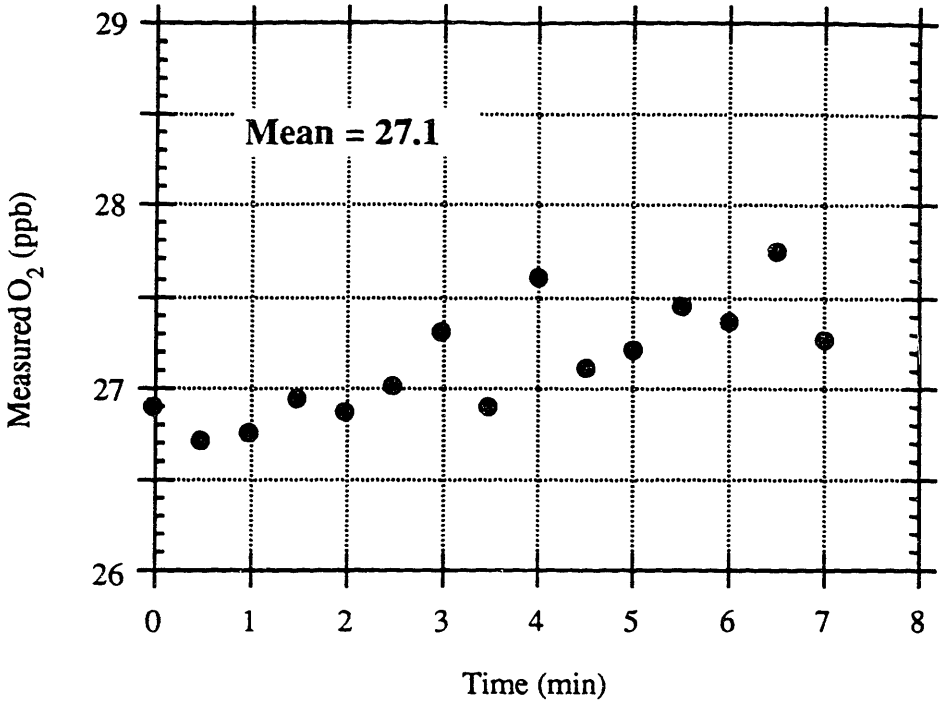

Figure 6.14 Background O_2 concentration measured for 210 ppb H_2O_2 injection (once-through mode), Run 7.

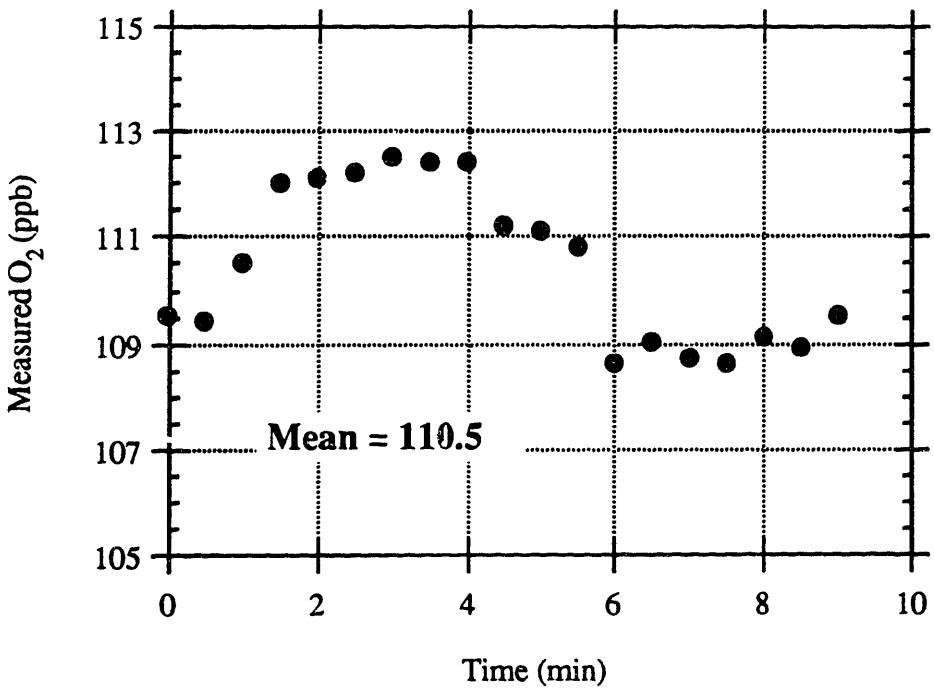

Figure 6.15 Total O_2 concentration measured for 210 ppb H_2O_2 injection (once-through mode), Run 7.

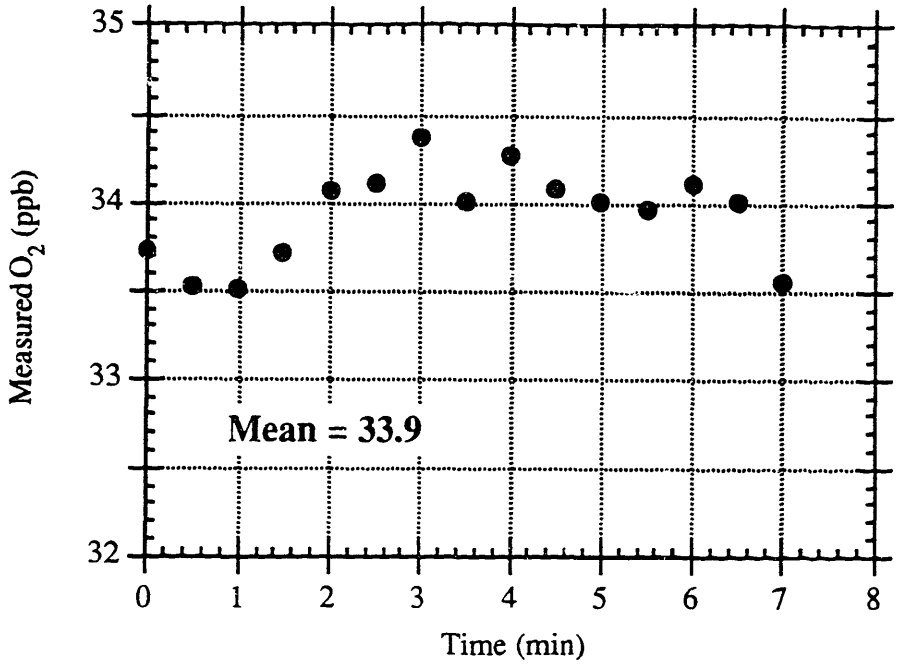

Figure 6.16 Background O_2 concentration measured for 230 ppb H_2O_2 injection (once-through mode), Run 8.

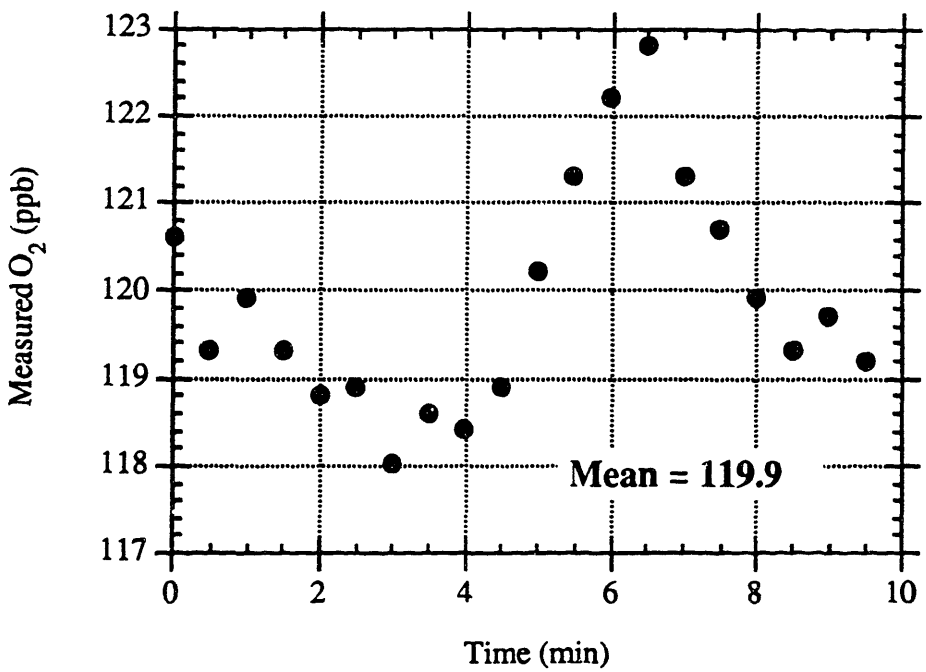

Figure 6.17 Total O_2 concentration measured for 230 ppb H_2O_2 injection (once-through mode), Run 8.

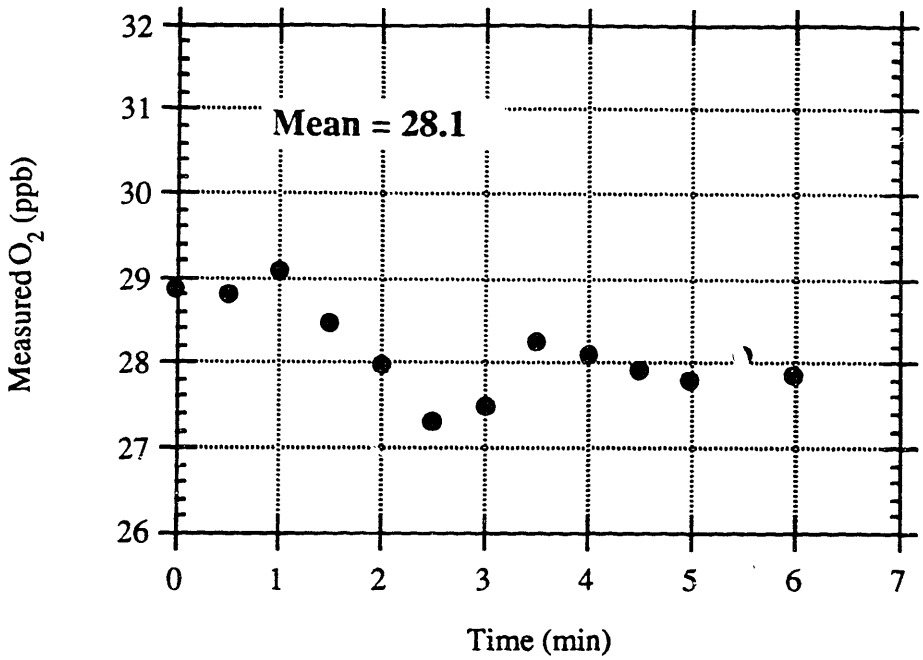

Figure 6.18 Background O_2 concentration measured for 260 ppb H_2O_2 injection (once-through mode), Run 9.

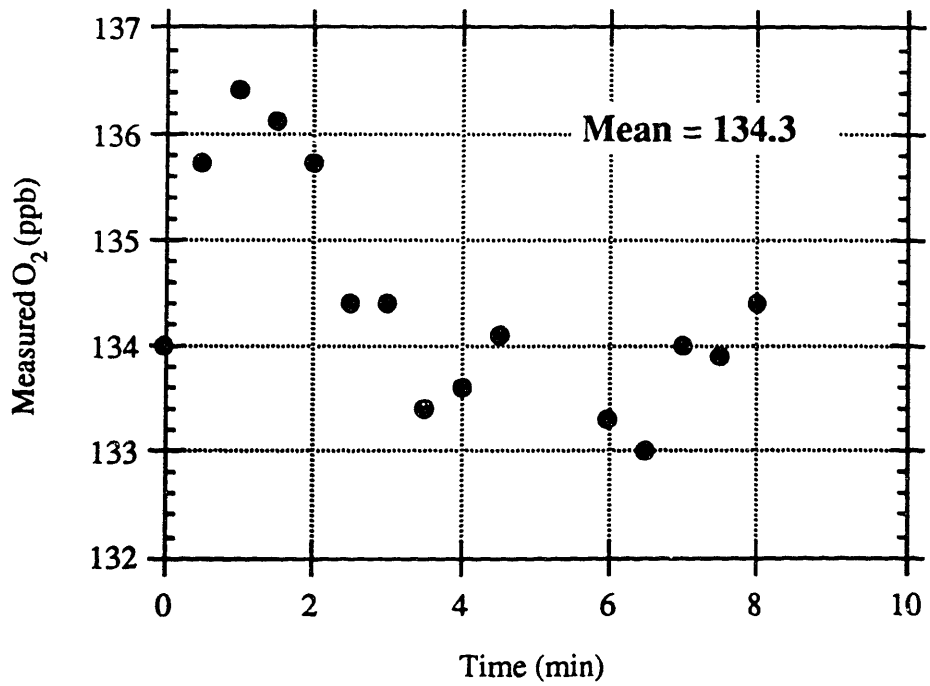

Figure 6.19 Total O_2 concentration measured for 260 ppb H_2O_2 injection (once-through mode), Run 9.

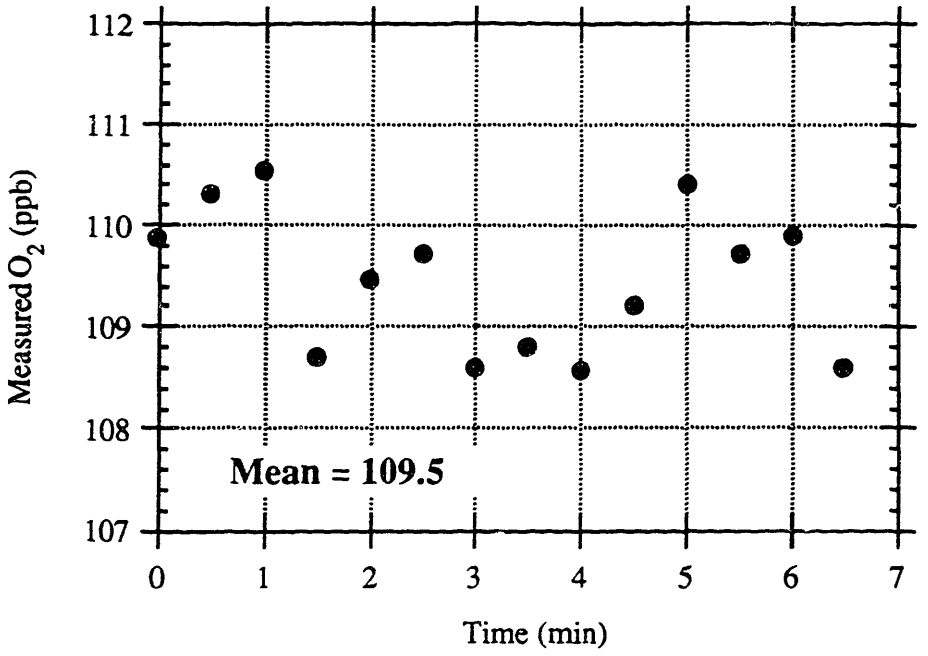

Figure 6.20 Background O_2 concentration measured for 360 ppb H_2O_2 injection (once-through mode), Run 10.

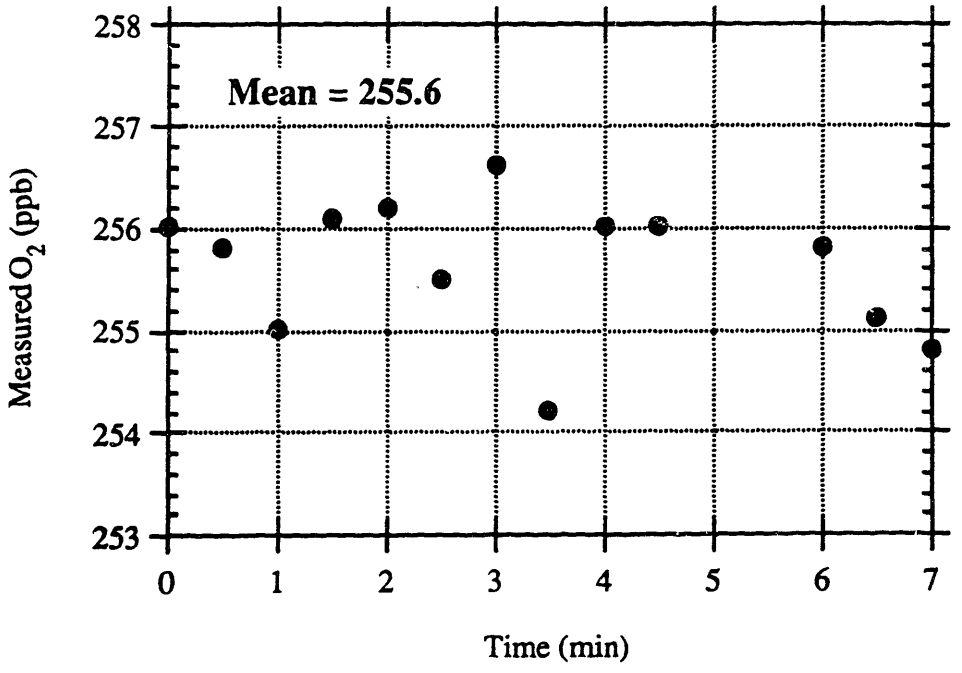

Figure 6.21 Total O_2 concentration measured for 360 ppb H_2O_2 injection (once-through mode), Run 10.

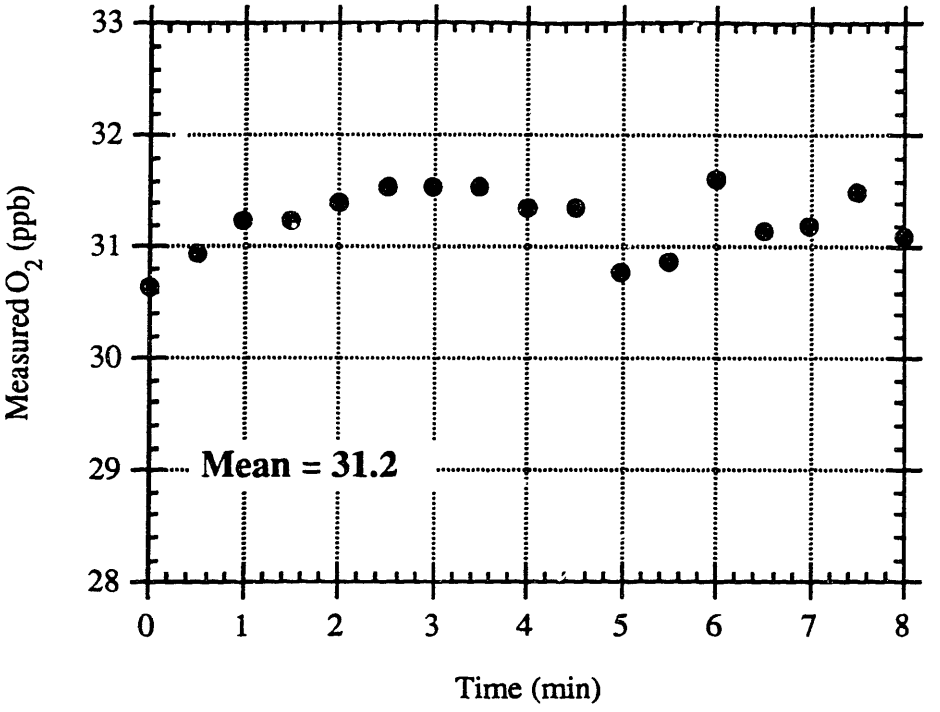

Figure 6.22 Background O_2 concentration measured for 400 ppb H_2O_2 injection (once-through mode), Run 11.

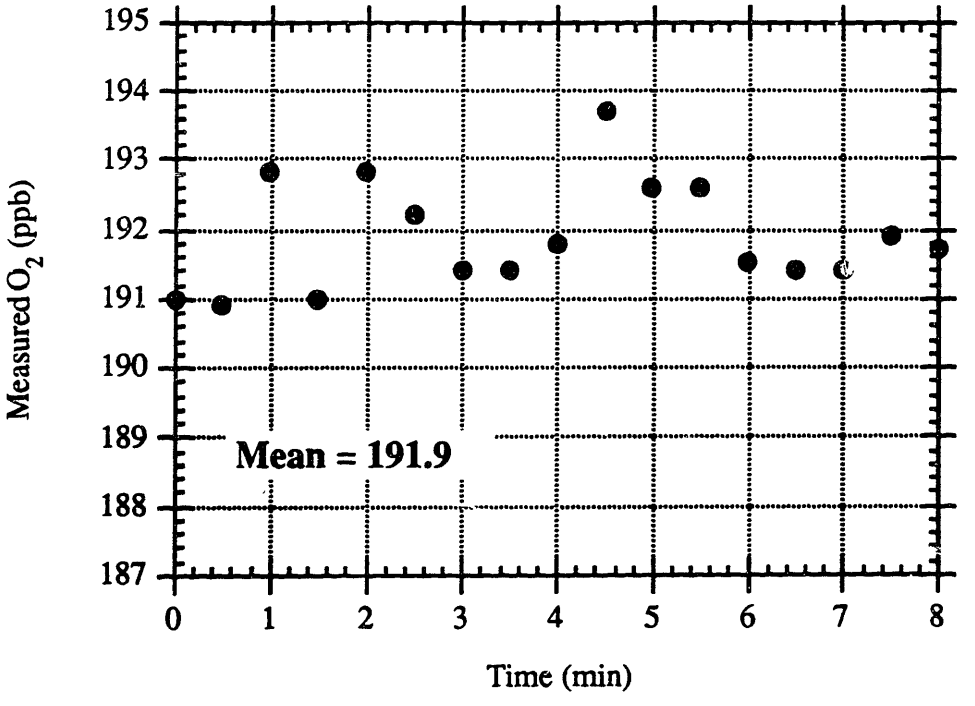

Figure 6.23 Total O_2 concentration measured for 400 ppb H_2O_2 injection (once-through mode), Run 11.

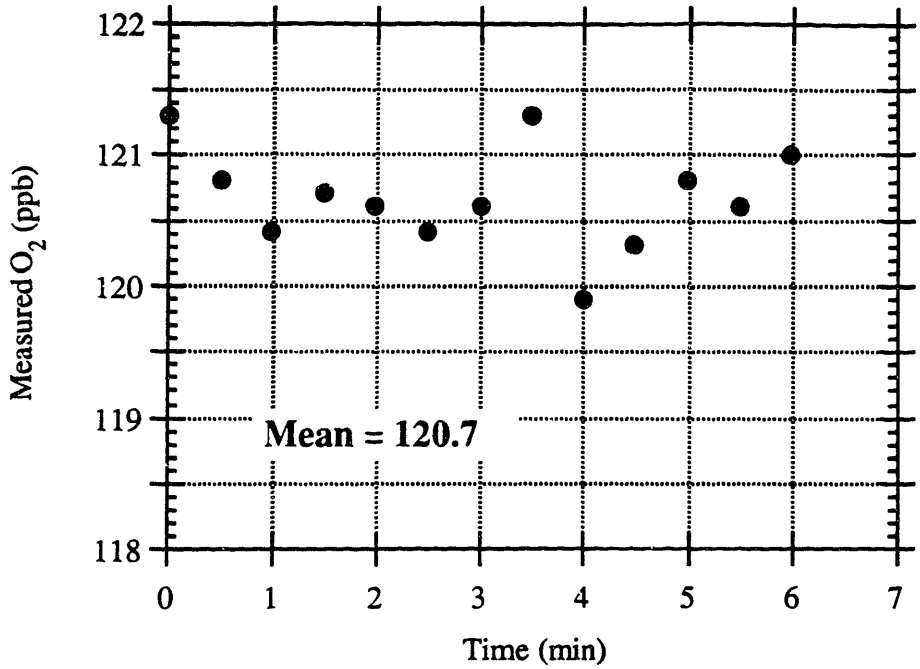

Figure 6.24 Background O_2 concentration measured for 230 ppb H_2O_2 injection (once-through mode), Run 12.

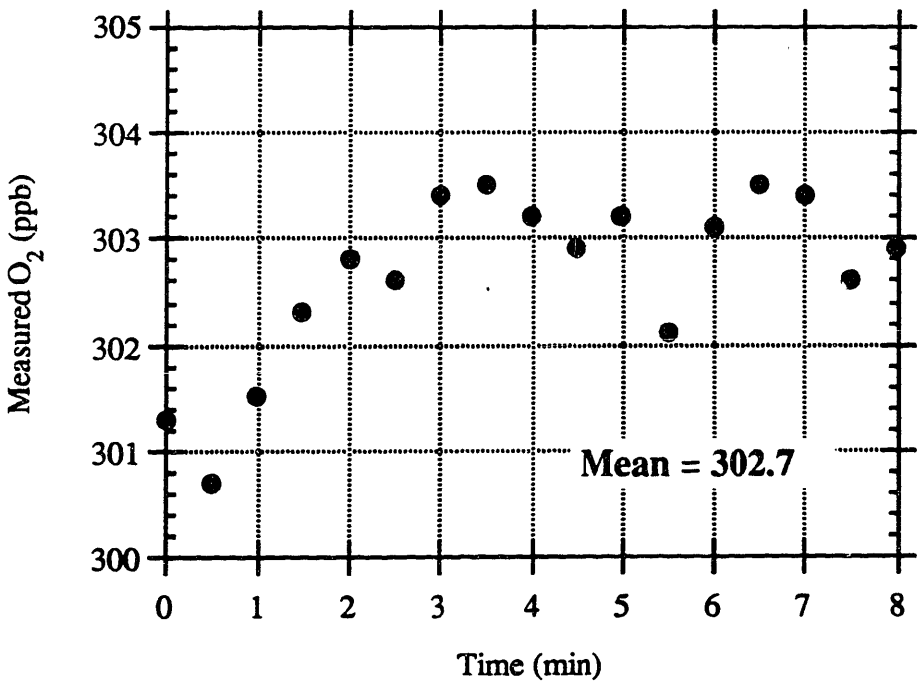

Figure 6.25 Total O_2 concentration measured for 230 ppb H_2O_2 injection (once-through mode), Run 12.

Table 6.3 H_2O_2 Analyzer Experimental Results (Once-Through Mode)

ID	H_2O_2 injection (ppb)	Measured O_2 conc.(ppb)	Background O_2 conc.(ppb)	Predicted H_2O_2 conc. (ppb)	Error
Run 6	80	78.2	46.9	66.5	-16.9 %
Run 7	210	110.5	27.1	177.2	-15.6 %
Run 8	230	119.9	33.9	181.9	-20.9 %
Run 9	260	134.4	28.1	225.9	-13.1 %
Run 10	360	255.6	109.5	310.5	-13.8 %
Run 11	400	191.9	31.2	341.5	-14.6 %
Run 12	480	302.7	120.7	386.8	-19.4 %

6.4 Reagent Injection

A reagent injection method is to be evaluated using colorimetric reagent in the sample cooling line. This would cause H_2O_2 to react on the spot and avoid, or greatly reduce, thermal/surface decomposition. Colorimetry can then be used to measure H_2O_2 concentration without taking into account the thermal/surface decomposition effect. The chemical composition of a typical one-step colorimetric reagent is as follows:

Major chemical	FeSCN
pH	1.3
conductivity	0.7 mS/cm
FeSCN concentration*	6.5×10^{-3} mol/l
* measured using ICP method	

Hydrogen peroxide oxidizes sulfur compounds, and the rate of the reaction increases with increasing acidity (K-1). A red-orange color is produced from the chemical reaction between hydrogen peroxide and FeSCN, and the concentration of hydrogen peroxide in the sample liquid can then be measured using colorimetry.

This method will be used independently of the MnO_2 method, so that experimental results can be verified, particularly if an abnormal hydrogen peroxide concentration is measured.

6.5 Chapter Summary

This chapter introduced the hydrogen peroxide measurement method used in the summer 1992 campaign, and possible alternatives as supplementary methods. Colorimetry, which was the only method used to measure hydrogen peroxide at MIT in the 1990 to 1992 time frame, has the possibility of giving false concentration readings resulting from reagent and chemical additive interactions.

A "MnO_2 method" was tested for two different configurations – recirculation and once-through. Both are shown to be accurate within ± 20 % for H_2O_2 concentration ranging from 100 ppb to 1000 ppb. The once-through mode, however, has the advantage of shorter (20 to 30 minutes) system response time, which enables on-line measurement of the H_2O_2 production in the BCCL. Colorimetric reagent injection is also proposed to improve H_2O_2 measurement by reducing thermal/surface decomposition in the sample line. The reagent would cause H_2O_2 to react on the spot and avoid decomposition. This method will be further investigated by testing the oxidizing rate with H_2O_2, and its reaction with chemical additives.

Chapter 7

Summary, Conclusions and Recommendations

7.1 Introduction

This thesis has been written to document the work carried out at MIT during 1992 to compare the results of radiolysis calculations, using the in-house RADICAL program, to experimental data measured in the in-pile BWR Coolant Chemistry Loop (BCCL) and to document the experimental results for the MnO_2 decomposition method for hydrogen peroxide measurement.

Work was carried out in three major areas for the radiolysis calculations: characterization of the neutron and gamma radiation environment in and above the MITR core, and inside the BCCL itself; parametric studies to evaluate the influence of design and operational variables; all leading to a set of best-estimate calculations corresponding to reference chemistry runs carried out during the Summer 1992 BCCL campaign. To a considerable extent the work was also carried out, and reported herein, in the above order, the latter stages benefiting considerably from an MIT workshop in August 1992 and the technical advisory committee meeting in October 1992, also at MIT.

As for hydrogen peroxide measurement, a method, using MnO_2 powder to dissociate H_2O_2 into O_2, which can then be measured using an Orbisphere detector), was proposed and tested as a supplement to the colorimetric method. Experiments were carried out for both recirculation mode and once-through mode operation of the instrument train. The accuracy is within $\pm$ 20% for both setups. The once-through mode, however, has the advantage of shorter system response time.

7.2 Summary and Evaluation

7.2.1 Radiolysis Calculations

One of the more important goals of the present calculation work was to better define the gamma and neutron dose rates in the BCCL. Available experimental data was reviewed, and analytic bounds were established, but principal reliance was placed on monte carlo calculations using the MCNP program. In general the different calculational methods were consistent, but only the MCNP results accounted for important effects such as neutron and gamma attenuation by the BCCL structure – which makes doses in loop water significantly lower than in MITR core water. Table 2.4 summarizes and compares pertinent results.

Detailed spatial profiles in and above the core were also developed, and are documented earlier in this report. It is also worth calling attention to the experiments discussed in Appendix D, which showed that there is no gamma (actually secondary electron) dose enhancement due to the metal tubing walls. In parallel to the above, RADICAL code runs were being made using an earlier set of dose rate estimates, as embodied in the nodal diagram of Fig. 2.11.

The model was exercised in an extensive series of parametric studies to help judge the impact of approximations and uncertainties. Table 7.1 ranks the various effects in three categories: strong, moderate and weak. Items in the first category have been given the most attention in our overall plan of attack.

It should be noted that the parametric studies, while extensive, were by no means exhaustive. A number of potentially important variations were not fully explored because of code or time limitations, for example:

(1) In-core two-phase-flow thermal hydraulics
The presence of downflow and small diameter tubing complicate the thermal hydraulic simulation of the BCCL. Deviation between the currently used Bankoff equation and reality might introduce a significant uncertainty in the residence time (hence integrated dose) of the liquid phase in core. The liquid-to-gas mass transfer rate may also be affected.

(2) liquid-vapor interactions in the separator plenum
The partition of radiolytic species between the vapor and liquid phases is sensitive to phenomena such as carryunder.

(3) Internally consistent variations in radiolysis yields
One can not arbitrarily change a single G-value without violating charge conservation or stoichiometry.

In defense of deferring a more intensive investigation in these areas, the following mitigating factors should be noted:

(1) Substantial differences between calculation and experiment are also present for the non-boiling (zero-quality) mode of operation. Hence liquid-vapor dynamics may not be the principal contributor.

Table 7.1

Summary of Parametric Studies

Effect on H_2O_2, O_2, H_2 concentrations

Strong

- neutron and gamma dose rate in core
- net oxidant or reductant in feedwater
- surface-induced H_2O_2 decomposition ex-core
- non-boiling vs boiling mode operation
- loop flow rate (residence time, dose)
- decomposition reaction and rate constant
- reaction rate data sets

Moderate

- neutron and gamma dose rate above core exit
- G-values and reaction rate data sets
- exit quality (greater than a few %)
- length of subcooled zone in core
- gas $\leftrightarrow$ liquid mass transfer coefficients
- polynomial v.s. linear quality profile

Weak

- neutron and gamma dose rate in vicinity of plenum
- shape of dose rate profile
- neutron and gamma dose rate above core entrance
- surface induced H_2O_2 decomposition in-core
- loop temperature ($\pm 10°C$)
- stoichiometric mixtures of $2H_2 + O_2$ in feedwater
- stoichiometrically equivalent O_2 or H_2O_2 in feedwater

(2) The vapor and liquid effluents from the BCCL are remixed prior to measurement of H_2 and O_2, because the instruments only operate satisfactorily at high flow rates; the separate steam and water samples are bled off at too low a rate. Also at the measurement point all H_2O_2 has decomposed. Hence plenum performance is irrelevant until such time as measurement methods are upgraded (e.g., addition of a gas chromatograph).

(3) Other collaborating researchers (sponsors and TAC members) are more knowledgeable on the subject of radiolysis yields and reaction rate constants, and periodically update their data sets, taking into account the results of their own research and that of others. We have, therefore, taken the role of user rather than originator in this area.

Most of the work just summarized was completed prior to September 1992. Subsequently, two meetings (a radiolysis workshop and the 1992 TAC review) provided significant new input, and, in addition, the Summer 1992 BCCL experimental campaign provided new sets of reference case data (i.e., NWC, HWC, boiling, non-boiling). Consequently a "consensus" update of RADICAL code input was prepared to enable us to make a final set of comparisons. Figure 5.1 shows the best-estimate nodal diagram. Major changes were as follows:

(a) MCNP dose rate estimates, both in and above core
(b) a reduction in the length of the liquid return line to reflect changes in the BCCL between its Fall 1991 and Summer 1992 campaigns
(c) use of a new consensus data set (G-values, reaction rate constants: Set 2 of Appendix A)
(d) H_2O_2 decomposition was simplified, using a constant rate constant (k_{total} = 0.3 sec^{-1}). The value specified probably represents an overestimate of decomposition, particularly in-plenum.

Table 5.3 compares experimental data and RADICAL calculations. The ± values shown for the experimental data give the range bracketing measurements over a period of several hours; at the concentrations of interest the colorimetric H_2O_2, the Orbisphere O_2 analyzer and the Hydran H_2 analyzer are accurate to about 5% depending on when and how the analyzers are calibrated. In interpreting the subject results, the following important points must be appreciated:

(1) The H_2O_2 values are measured at the sample point in the liquid effluent line exiting the loop's core outlet plenum. Inlet H_2O_2 concentrations are negligible in the runs cited here (but not in runs following long periods of cold standby operation).

(2) The O_2 and H_2 values show the inlet/outlet concentrations: "inlet" was measured in the bypass return line from the charging pump; "outlet" was measured in the line which returns mixed water plus steam effluent to the makeup tank. As such it also contains oxygen from decomposition of water effluent H_2O_2.

Tables 5.3 and 5.4 compare the simulations results and experimental results for Summer 1992 runs. A H_2O_2 thermal/surface decomposition rate of 0.3 sec^{-1} is assumed in the calculations shown in Table 5.3. For the calculation results shown in Table 5.4, thermal/surface decomposition is assumed to be zero, as a limiting case. The results show that the decomposition rate has a crucial effect on H_2O_2 concentrations at the sample extraction point for NWC, but has little effect on O_2 and H_2 mixed return concentrations. One thing worth noticing is that the decomposition effect is important only for out-of-core regions, as shown in Tables E.1 to E.8. The simulation results show the importance of H_2O_2 decomposition in the plenum. Hilton (H-1) has also pointed out that use of the same decomposition rate constant for loop tubing and the outlet plenum probably grossly overestimates decomposition in the latter component; hence no-decomposition results are probably closer to reality. The predicted results also show that the decomposition has little effect on mixed return O_2 and H_2 concentrations (less than 1%). Thus the following discussion on the comparison between calculation and experimental results are based on no-decomposition simulations.

H_2O_2 is underpredicted by a factor of three, return O_2 and H_2 concentrations are underpredicted by factors of two and three, respectively, for boiling NWC condition. For non-boiling NWC, the calculation predicts the H_2O_2 concentration, but still underpredicts return O_2 and H2 by factors of two and four, respectively. The oxygen to hydrogen ratio for the experimental results is about 5.8, compared to 8 for stoichiometry.

H_2O_2 is significantly underpredicted for HWC in both boiling and non-boiling cases. Appreciable H_2O_2 is measured in the experiments, but no O_2 from its decomposition appears in the mixed return water. One could postulate that the missing oxygen has catalytically recombined with hydrogen, since the measured effluent H_2 is less (by roughly the amount required) than input H_2. Other suggested factors are (a) radiolysis

in the H_2O_2 sample line, (b) false indication by the colorimetric H_2O_2 analysis methods (two different), (c) or even the creation of some heretofore unexpected ephemeral oxidizing species. Reference (H-1) addresses some of these possibilities, and presents evidence tending to discredit the first two hypotheses.

In conclusion, we can not yet account for the high measured values of H_2O_2: this topic will be a major focus of the 1993 experimental/analytical campaign.

7.2.2 Hydrogen Peroxide Measurement Methods

A hydrogen peroxide measurement method, using MnO_2 to dissociate H_2O_2, and then to measure O_2 using the Orbisphere, was tested for the Summer 1993 campaign. The method has been demonstrated by running a series of experiments. Two kinds of detection loop configuration, recirculation and once-through, have been tested. The accuracy of this method is within 20% for both loop configurations, as shown in Tables 6.1 and 6.2. The results show that the once-through mode operation has a shorter response time (20 to 30 minutes), compared to a response time of > 1 hour for the recirculation mode operation, which will be more suitable for on-line measurements for BCCL experiments.

A reagent injection method, using colorimetric reagent in the sample cooling line, will also be evaluated as an alternative H_2O_2 measurement method. This would cause H_2O_2 to react at the injection point and avoid, or greatly reduce, thermal/surface decomposition. Better accuracy can then be attained by eliminating the need of taking into account the thermal/surface decomposition inccurred in the sample line, as has been described in section 6.2.

7.3 Plans for Future Work

Various changes in BCCL components are planned prior to the Summer 1993 campaign. Our interest here is limited to those which might have a non-negligible effect on radiolysis, in particular:

(1) relocation of the H_2O_2 sampling system to reduce its ambient gamma dose rate
(2) qualification of an on-line H_2O_2 measurement system: e.g., decomposition using an MnO_2 catalyst bed followed by O_2 measurement using a low-flow-rate Orbisphere® detector as described in chapter 6
(3) other alternative H_2O_2 measurement methods
(4) changing from titanium to stainless steel as the principal material of construction
(5) adaptation of the sample cooling heat exchanger to permit use of the cooling water as a gamma dose / H_2O_2 generation monitor

In parallel, MIT radiolysis calculations will be upgraded in several respects:

(1) a new consensus data set will be used, when available
(2) some additional model upgrading will be carried out, to evaluate the potential effects of downflow boiling and the high surface-to-volume ratio in the BCCL on radiolysis
(3) a limited series of parametric studies will be carried out using consistently-modified G data sets (i.e., preserving charge and a 2 H:1 O total atom product ratio)

As is evident, the emphasis will now turn to perfection and validation of the experimental methods, especially hydrogen peroxide measurements, deferring major initiatives on the computational/modeling front until after Summer 1993 campaign results are evaluated.

One specific initiative is in order, however. During the Summer 1993 campaign, substantial operation in the recirculation mode is scheduled. Hence, a nodal RADICAL representation of this configuration must be developed and exercised to predict results, as an aid to planning for such runs, and to serve as the basis for another set of experiment vs calculation comparisons.

References

(B-1) S. Boerigter, *An Investigation of Neutron-Irradiation Induced Segregation in Austenitic Stainless Steels*, Sc.D Thesis, MIT Nuclear Engineering Department, Dec. 1992.

(B-2) G. G. Bartolomei, V. G. Brantov, Ju. S. Molochnikov, Yu. V. Kharitonov, V. A. Solodkii, G. N. Batashova and V. N. Mikhailov, *An Experimental Investigation of True Volumetric Vapour Content with Subcooled Boiling in Tubes* , Thermal Engineering, 29(3), 1.

(C-1) J. Chun, *Modelling of BWR Chemistry* , SM Thesis, MIT Nuclear Engineering Department, September 1990.

(C-2) J. G. Collier, *Convective Boiling and Condensation* (2nd ed.) New York: McGraw-Hill, 1980.

(D-1) J. M. Delhaye, M. Giot and M. L. Riethmuller, *Thermohydraulics of Two-Phase Systems for Industrial Design and Nuclear Engineering* , McGraw-Hill Book Company, 1981.

(H-1) B. Hilton, *Improvement and Use of an In-pile Loop for BWR Chemistry Studies* , SM Thesis, MIT Department of Nuclear Engineering, May 1993.

(H-2) Lin-Wen Hu, Michael J. Dricoll and Scott A. Simonson, *Radiolysis Calculations for the MIT BWR Coolant Chemistry Loop*, MITRL-050, Dec. 1992.

(I-1) M. Ishii and K. Mishima, *Two-Fluid Model and Hydrodynamic Constitutive Relations* , Nuclear Engineering and Design 82 (1984), 107-126.

(K-1) Tadeusz E. Kleindlenst, Paul B. Shepson, Dennis N. Hodges, and Chris M. Nero, *Comparison of Techniques for Measurement of Ambient Levels of Hydrogen Peroxide* , Environ. Sci. Technol., 1988, 22, 53-61.

(L-1) R. T. Lahey, Jr. and F. J. Moody, *The Thermal Hydraulics of a Boiling Water Reactor*, American Nuclear Society, 1977.

(L-2) C.C. Lin, F.R. Smith, N. Ichikawa, T. Baba and M. Itow, *Decomposition of Hydrogen Peroxide in Aqueous Solutions at Elevated Temperatures*, International Journal of Chemical Kinetics, Vol. 23, 971-987 (1991).

(M-1) V. Mason, *Chemical Characterization of Simulated Boiling Water Reactor Coolant* , SM Thesis, MIT Departments of Nuclear and Chemical Engineering, May 1990.

(M-2) R. Medina, *Measurement of Neutron Flux and Spectrum-Averaged Cross Sections for an In-Pile PWR Loop* , SM Thesis, MIT Nuclear Engineering Department, May 1990.

(M-3) Minutes of MIT Radiolysis Workshop, August 1992.

(M-4) Minutes of MITNRL Technical Advisory Committee Meeting, October 1992.

(M-5) MIT Nuclear Reactor Laboratory, *Development and Use of an In-Pile Loop for BWR Chemistry Studies* , EPRITR-102248, 1993 (to be published).

(O-1) J. O. Outwater, *Design, Construction and Commissioning of an In-Pile BWR Coolant Chemistry Loop* , ScD Thesis, MIT Nuclear Engineering Department, January 1991.

(O-2) J. O. Outwater, unpublished report, MITNRL, 1990.

(O-3) Orbisphere Laboratories, *Microprocessor – based One Channel Analyzer (M.O.C.A) for Oxygen Measurement*, 1992

(R-1) R. Rozier, *Modification and Operation of an In-Pile Loop for BWR Chemistry Studies* , SM Thesis, MIT Nuclear Engineering Department, May 1992.

(S-1) S. A. Simonson, *Modeling of Radiation Effects on Nuclear Waste Package Materials* , Ph.D Thesis, MIT Nuclear Engineering Department, 1988.

(S-2) P. Saha and N. Zuber, *Point of Vapor Generation and Vapor Void Fraction in Subcooled Boiling* , Proc. of the 5th International Heat Transfer Conference, vol. 4, 1974.

(T-1) Y. Taitel and A. E. Dukler, *Flow Regime Transitions for Vertical Upward Gas-Liquid Flow: a Preliminary Approach*, presented at the AIChE 70th Annual Meeting, New York, 1977.

(V-1) J. Vergara, *The Development of a Facility for the Evaluation of Environmentally Assisted Cracking of In-Core Structural Materials in Light Water Reactors* , Ph.D Thesis, MIT Nuclear Engineering Department, May 1992.

(Z-1) M. Zaker, *Dose Rate Measurements in the MITR-II Facilities* , SM Thesis, MIT Nuclear Engineering Department, May 1987.

Appendix A

Radiolysis Data Sets

A.1 Introduction

MIT experience, and we believe general consensus, is that the data set (G values and thermochemical properties) is the source of most of the differences in computations among the various participants in such endeavors, and between calculation and experiment. Furthermore, most data sets are "hand tailored" by the cognizant researcher, using input from a number of preferred sources. Thus it is important to clearly document the specific data set used for a particular calculation. The theses by Chun (C-1) and Mason (M-1) compare the results of using several different sets available in the literature, or through personal communication at the time of their work. The set found to give the best agreement with BWR measurements by Chun (sometimes referred to as the "Burns" set in-house) was used for most of the BCCL/IASCC/Sensor project work at MIT through July 1992. Hence this set is listed in this Appendix as Set No. 1. The improved versions of reaction rate data and G-values agreed to in the August 1992 Radiolysis Workshop are shown in Tables A.3 and A.4, respectively. They were used in the best-estimate cases to simulate Summer 1992 runs (see chapter 5).

A.2 Commentary on Listing

The data set listing is for the most part self-explanatory. A few points of clarification are in order:

(1) The last three peroxide decomposition reactions are fictitious in reaction data set No.1 because RADICAL can not deal with fractional stoichiometric coefficients directly: i.e., the code will not accept $1/2O_2$ as a valid product. The formation of OH will lead to the production of O_2 through a rapid sequence of reactions.

(2) A realistic H_2O_2 decomposition reaction is used in reaction data set No.2, that is, $H_2O_2 \rightarrow 1/2\ O_2 + H_2O$. The way to solve the problem of dealing with a fractional stoichiometric coefficient is to assume $1/2O_2$ as a fictitious species, say, X. Thus we can write the reactions as

Table A.1 Set No. 1 Radiolysis-Generated Species and Their Reaction Rate Constants at Room Temperature

Name	Reactants					Products				Rate Constant s^{-1}	Activation Energy KJ/mol^{o}K
W1	e_{aq}^-	+	H_2O		→	H	+	OH^-		0.400E+02	0.126E+02
W2	e_{aq}^-	+	H^+		→	H				0.600E+11	0.126E+02
W3	e_{aq}^-	+	OH		→	OH^-				0.750E+11	0.126E+02
W4	e_{aq}^-	+	H_2O_2		→	OH	+	OH^-		0.320E+11	0.126E+02
W5	H	+	H		→	H_2				0.250E+11	0.126E+02
W6	e_{aq}^-	+	HO_2		→	HO_2^-				0.500E+11	0.126E+02
W7	e_{aq}^-	+	O_2		→	O_2^-				0.470E+11	0.126E+02
W8	$2e_{aq}^-$	+	$2H_2O$		→	$2OH^-$	+	H_2		0.120E+11	0.126E+02
W9	OH	+	OH		→	H_2O_2				0.110E+11	0.126E+02
W10	OH^-	+	H		→	e_{aq}^-	+	H_2O		0.780E+08	0.188E+02
W11	e_{aq}^-	+	H	+ H_2O	→	H_2	+	OH^-		0.620E+11	0.126E+02
W12	e_{aq}^-	+	HO_2^-	+ H_2O	→	OH	+	$2OH^-$		0.870E+10	0.126E+02
W13	H	+	OH		→	H_2O				0.500E+11	0.126E+02
W14	OH	+	H_2		→	H	+	H_2O		0.110E+09	0.126E+02
W15	H	+	H_2O		→	H_2	+	OH		0.490E-01	0.850E+02
W16	H	+	O_2		→	HO_2				0.470E+11	0.126E+02
W17	H	+	HO_2		→	H_2O_2				0.500E+11	0.126E+02
W18	H	+	O_2^-		→	HO_2^-				0.500E+11	0.126E+02
W19	e_{aq}^-	+	O_2^-		→	HO_2^-	+	OH^-		0.510E+11	0.188E+02
W20	H	+	H_2O_2		→	OH	+	H_2O		0.240E+09	0.140E+02
W21	OH	+	H_2O_2		→	HO_2	+	H_2O		0.410E+08	0.820E+01
W22	OH	+	HO_2		→	O_2	+	H_2O		0.300E+11	0.126E+02
W23	OH^-	+	H_2O_2		→	HO_2^-	+	$2H_2O$		0.700E+09	0.188E+02
W24	HO_2^-	+	H_2O		→	OH^-	+	H_2O_2		0.220E+07	0.188E+02
W25	H^+	+	O_2^-		→	HO_2				0.120E+12	0.126E+02
W26			HO_2		→	H^+	+	O_2^-		0.200E+07	0.126E+02
W27	HO_2	+	O_2^-		→	HO_2^-	+	O_2		0.580E+08	0.188E+02
W28	$2O_2^-$	+	H_2O		→	H_2O_2	+	O_2 +	$2OH^-$	0.660E+08	0.188E+02
W29	HO_2	+	HO_2		→	H_2O_2	+	O_2		0.110E+08	0.188E+02
W30	H^+	+	OH^-		→	H_2O				*0.144E+12	0.126E+02
W31			H_2O		→	H^+	+	OH^-		*0.260E-04	0.126E+02
W32	OH	+	O_2^-		→	O_2	+	OH^-		0.300E+11	0.126E+02
W33			H_2O_2		→	OH	+	OH		0.200E-07	0.730E+01
SS			H_2O_2		→	OH	+	OH		5.322E-07	66.90E+00
Ti			H_2O_2		→	OH	+	OH		5.322E-07	66.90E+00

*Rate constants modified to fit entire temperature range of interest.

Table A.2 Summary of G-values for Neutron and Gamma Radiolysis

SPECIES	Neutron (LET ~ 4 eV/Å)				Gamma (LET ~ 0.02 eV/Å)			
	Set 1n	Set 2n	Set 3n	Set 4n	Set 1g	Set 2g	Set 3g	Set 4g
e^-_{aq}	0.93	0.37	0.40	1.08	2.70	0.40	2.17	4.15
H^+	0.93	0.37	0.40	1.08	2.70	0.40	2.17	4.15
H	0.50	0.36	0.30	0.66	0.62	0.30	1.47	1.08
H_2	0.88	1.12	2.00	0.00	0.43	2.00	1.16	0.62
H_2O_2	0.99	1.00	0.00	0.74	0.62	0.00	0.81	1.25
HO_2	0.04	0.17	0.00	0.00	0.03	0.00	0.00	0.00
OH	1.09	0.46	0.70	0.26	2.9	0.70	4.34	3.97
O	0.00	0.00	2.00	0.00	0.00	2.00	0.00	0.00
$-H_2O$	3.12	3.17	2.70	1.74	4.20	2.70	4.21	6.47

Set 1n: G. Burns' for room temperature (1976). (Used in this study)*

Set 2n: H. Christensen's for room temperature (1988).

Set 3n: G. Burns' for 573-683°K (1976).

Set 4n: E. Ibe's for 558°K (1991).

Set 1g: G. Burns' for room temperature (1976)

Set 2g: G. Burns' for 573-683°K (1976).

Set 3g: E. Ibe's for 558°K (1991).

Set 4g: A. Elliot's for 558°K (1989). (Used in this study)*

*Set No. 1 in the present work

Table A.3. Reaction Rate Data Set No.2.(Consensus Reaction Constant Set Agreed to in August 1992 Radiolysis Workshop)

Name	Reaction	k_o (s^{-1})	Ea	Name	Reaction	k_o (s^{-1})	Ea
F3	$e^- + H_2O \rightarrow H + OH^-$	1.6e1	12.55	F19	$H + O_2^- \rightarrow HO_2^-$	2.e10	12.55
F4	$e^- + H^+ \rightarrow H$	3.5e11	0.e0	*F20	$O_2^- + e^- \rightarrow HO_2^- + OH^-$	1.3e8	18.83
F5	$e^- + OH \rightarrow OH^-$	2.0e10	12.55	F21	$H + H_2O_2 \rightarrow OH + H_2O$	9.e7	16.61
F6	$e^- + H_2O_2 \rightarrow OH + OH^-$	1.3e11	0.e0	F22	$H_2O_2 + OH \rightarrow H_2O + HO_2$	3.e7	13.01
F7	$H + H \rightarrow H_2$	8.5e10	0.e0	F23	$HO_2 + OH \rightarrow O_2 + H_2O$	8.6e10	0.e0
F8	$e^- + HO_2 \rightarrow HO_2^-$	2.0e10	12.55	F24	$H_2O_2 + OH^- \rightarrow HO_2^- + H_2O$	1.8e10	12.55
F9	$e^- + O_2 \rightarrow O_2^-$	2.6e11	0.e0	*R24	$HO_2^- \rightarrow H_2O_2 + OH^-$	5.7e5	18.83
*F10	$e^- + e^- \rightarrow OH^- + OH^- + H_2$	5.e9	12.55	F25	$HO_2 + HO_2 \rightarrow O_2 + H_2O_2$	8.5e5	22.82
F11	$OH + OH \rightarrow H_2O_2$	1.7e10	0.e0	F26	$HO_2 \rightarrow H^+ + O_2^-$	2.57e4	12.55
F12	$H + OH^- \rightarrow e^- + H_2O$	2.0e7	18.83	R26	$O_2^- + H^+ \rightarrow HO_2$	5.e10	12.55
F13	$H + e^- \rightarrow H_2 + OH^-$	2.5e10	12.55	F27	$HO_2 + O_2^- \rightarrow HO_2^- + O_2$	5.e9	0.e0
F14	$HO_2^- + e^- \rightarrow OH + OH^- + OH^-$	3.5e9	12.55	F29	$H^+ + OH^- \rightarrow H_2O$	1.44e11	12.55
F15	$H + OH \rightarrow H_2O$	5.5e10	0.e0	*R29	$\rightarrow H^+ + OH^-$	0.71	12.55
F16	$OH + H_2 \rightarrow H + H_2O$	4.e7	18.02	F30	$OH + O_2^- \rightarrow O_2 + OH^-$	8.6e10	0.e0
R16	$H + H_2O \rightarrow OH + H_2$	1.04e-4	85.17	TIF	$1/2O_2 + 1/2O_2 \rightarrow O_2$	1.e15	0.e0
F17	$H + O_2 \rightarrow HO_2$	8.6e10	0.e0	TI	$H_2O_2 \rightarrow 1/2O_2$	0.3	0.0
F18	$H + HO_2 \rightarrow H_2O_2$	2.e10	12.55	* water implicit reactions, unit of Ea is kJ/mol °K			

Table A.4 Set No. 2 G-values (New GE High Temperature G-values, 1992)

Species	Neutron (#/100 ev)	Gamma (#/100 ev)
$e(aq)^-$	1.395	3.76
H^+	1.395	3.76
H	0.75	0.70
H_2	1.32	0.80
H_2O_2	1.485	0.28
HO_2	0.06	0.
OH	1.635	5.50
O	0.	0.
H_2O	-4.725	-6.06

$$H_2O_2 \rightarrow H_2O + X,$$

and

$$X + X \rightarrow O_2$$

The reaction rate of the second reaction is assumed to be 1×10^{15} s^{-1}, so that whenever X is generated, O_2 will be produced immediately.

(3) Units are as follows

$$A + B \rightarrow C + D$$

$$\frac{d[A]}{dt} = -k[A][B]$$

All concentrations, [ ], are in moles per liter (units are omitted on the k column in the listings) and

$$k = ko \exp\left\{\frac{Ea}{R}\left(\frac{1}{To} - \frac{1}{T}\right)\right\}$$

for Ea in kilojoules per mole per degree Kelvin, where ko is the room temperature (To = 293 K) value listed in the table.

Appendix B

Sample RADICAL Input/Output

Sample input and output files used for BCCL loop simulation are listed in this appendix. The sample shows what RADICAL needs and produces. Plot files can also be obtained from RADICAL for generating graphs in KaleidaGraph, showing the spatial variation in the concentration of chemical species. They are not included here, since the format of the plot files is very easy to understand.

B.1 BCCLW.in

BCCLW.in is the input file employed to simulate the BCCL experiments at MIT. Table B.1 is a summary of the parameters of BCCLW.in corresponding to the model diagram shown in Fig. 2.8.

Table B.1 Summary of BCCLW.in parameters for base case calculations

system pressure	70 atm
mass flow rate	25 g/sec
exit quality	15%
quality distribution profile	linear
dose rates and shapes	gamma and neutron dose rates are uniform in each component.
boiling region	six components (20 cm each), one subcooled and five boiling.
number of simulation cycles	one
chemical injection	none
sensitivity calculation	no

Table B.2 is a checklist of the main control and system parameters for constructing an input file which corresponds to the users' needs. For detailed descriptions for the parameters used in the input files please refer to Appendix A and comments in RADICAL program printouts in John Chun's thesis (C-1). It is suggested that users double check the input parameters shown in the printout of the output file to verify that the input parameters are correct.

Table B.2 Check list for constructing an input file for RADICAL

Categories	Items	Descriptions
Radiation and chemical reaction constants	G-values	in #/100 ev
	Reaction rate set	Check for consisiency between the reactions and the rate constants is water concentration implicit or explicit ?
Control Parameters	output concentration units	PPBOUT, users' choice of ppb or mol/l for output concentrations. (if the concentrations are given in ppb, users should modify H2G and O2G concentrations by multiplying them by the ratio between liquid and vapor densities. See section 3.3)
	void or quality distribution	Users can give either void or quality distribution for the system by setting VOIDFLAG=T for void fraction distribution or VOIDFLAG=F for quality distribution in $FLAG. RADICAL will calculate the other one using the Bankoff equation.
	sensitivity calculation	Set SENS=T to enter sensitivity routine.
	onset of bulk boiling	Set XBOIL=position where boiling begins. RADICAL won't do its two-phase routine before this point.
	surface decomposition	set CALCSENS=T in $FLAG for surface decomposition calculations. Also set NSURFRX=number of surface reactions in $SIZE
	reference temperature	TempRef, at which reaction rate constants are given
	output files	set PlotOut=T to create plot file (the file name should be given in $FILENAME). RADICAL 1.11 Mac version can't create a sensitivity plot output file, so users should get the sensitivity results from the output file.
System geometry	diameter	set tube diameters for each component.
	length (position)	XLength=length of the component. XInitial=initial position of the component. XFinal=final position of the component. Users can also define Xstep for step size at which to print concentration output.

Table B.2 Check list for constructing an input file for RADICAL (continued)

Categories	Items	Descriptions
Operating conditions	pressure and temperature	pressure in atm, temperature in Kelvin
	densities	vapor and liquid densities in g/cm^3.
	mass flow rates	total (liquid plus vapor) mass flow rate for each component. Users should ensure that mass flow rate and velocity are consistent even though they are independent parameters in RADICAL.
	velocities	To ensure continuity of flow velocities for the connections of components, refer to section 3.3 to see how to define VelInlet.
Environment	tube materials	specify the materials for surface decomposition in $REACTION.
	dose rates	in Rad/sec
	dose shapes	fitted by polynomials, functions of distance from loop inlet.
Sensitivity study	components	define the components examined in the sensitivity study by setting CALCSENS=T in $FLAG in components.
	species	define the species for a sensitivity study by setting SENSSPECIES=species names. (also NSENS=number of species)

BCCLW.IN

```
                BCCL LOOP CHEMISTRY (BURNS DATA SET)  7/12/1992
This input file is modified by Lin-Wen Hu from BCCLH2Conc0.in

 $FILENAME
 OUTFILE  = ':Woutput:BCCLW.OUT',
 PLOTFILE = ':Wplot:BCCLW.PLOT',
 $END

 $SIZE
 NSPECIES =          13,
 NRX      =          39,
 NSURFRX  =           2,
 NCOMP    =          13,
 NNODE    =          14,
 NCYCLE   =           1,
 $END

*************************************************************************

 $CONTROL
 NodeStart=           1,
 Tempref  =      298.0,
 PlotOut  = T,
 LinLin   = F,
 Sens     = F,
 NORMALIZE= F,
 PPBOUT   = T,
 CYCLEOUT = 40*T,60*T,
 $END

*************************************************************************

 123456789012345*1234123412341234
 $COMPONENT
 Chemical Inject    1   2   1
 Charging Line      2   3
 Core Inlet         3   4
 Core Subcooled     4   5
 Core Boiling1      5   6
 Core Boiling2      6   7
 Core Boiling3      7   8
 Core Boiling4      8   9
 Core Boiling5      9   10
 Core Outlet        10  11
 Plenum Inlet       11  12
 Liq Plenum Out     12  13
 Liq Sample Line    13  14
 $END
 ***************************************************************

 NOTRE.DAT  NOTREDAME REACTIONS GIVEN ON P. 166 OF SIMONSONS'
 THESIS 4 APRIL 1990 Tuesday, July 9, 1991:Two gas species are removed.

 NSPECIES = 13,
 NSURFACE =  2,
 NRX      = 39,
```

```
 H2O IMPLICIT IN RX.

*GAMMA AND NEUTRON G-VALUES
 McCRACKEN'S 300 K GAMMA G-VALUES FROM ELLIOT, ET. AL.;"G-VALUES FOR
 GAMMA- IRRADIATED...",1990 BURNS' LO-T NEUTRON G-VALUES   RUIZ, ET.
AL.;
"MODELING HYDROGEN WATER CHEMISTRY...",P. 3-1, 1989

 $GVALUE
*e-          4.15000
             0.930D+00
             5.490D-04
 OH-            0.0000
             0.000D+00
             1.700D+01
*H2             0.6200
             0.880D+00
             2.000D+00
*OH          3.97000
             1.090D+00
             1.700D+01
 HO2-           0.0000
             0.000D+00
             3.300D+01
*H2O2           1.2500
             0.990D+00
             3.400D+01
 O2-            0.0000
             0.000D+00
             3.200D+01
 O2             0.0000
             0.000D+00
             3.200D+01
*H           1.08000
             0.500D+00
             1.000D+00
*H+          4.15000
             0.930D+00
             1.000D+00
@HO2            0.0000
             0.040D-00
             3.300D+01
O2G             0.0000
             0.000D+00
             3.200D+01
H2G             0.0000
             0.000D+00
             2.000D+00
 $END OF GVALUE

 $NAME
 SPECIESNAME  = 'e- '   ,'OH-',   'H2 ',   'OH ',  'HO2-', 'H2O2 ',
            'O2- ', 'O2 ',     'H ',   'H+ ',   'HO2 ','O2G','H2G'
 $END

*REACTION NAME, REACTION, RATE CONSTANT AND ACTIVATION ENERGY
 WATER EXPLICITLY DECLARED
```

```
$REACTION
W 1      1  0  0  9  2  0  0    0.400000E+02    0.126000E+02
W 2      1 10  0  9  0  0  0    0.600000E+11    0.126000E+02
W 3      1  4  0  2  0  0  0    0.750000E+11    0.126000E+02
W 4      1  6  0  4  2  0  0    0.320000E+11    0.126000E+02
W 5      9  9  0  3  0  0  0    0.250000E+11    0.126000E+02
W 6      1 11  0  5  0  0  0    0.500000E+11    0.126000E+02
W 7      1  8  0  7  0  0  0    0.470000E+11    0.126000E+02
W 8      1  1  0  2  2  3  0    0.120000E+11    0.126000E+02
W 9      4  4  0  6  0  0  0    0.110000E+11    0.126000E+02
W10      2  9  0  1  0  0  0    0.780000E+08    0.188000E+02
W11      1  9  0  3  2  0  0    0.620000E+11    0.126000E+02
W12      1  5  0  4  2  2  0    0.870000E+10    0.126000E+02
W13      9  4  0  0  0  0  0    0.500000E+11    0.126000E+02
W14      4  3  0  9  0  0  0    0.110000E+09    0.126000E+02
W15      9  0  0  3  4  0  0    0.490000E-01    0.850000E+02
W16      9  8  0 11  0  0  0    0.470000E+11    0.126000E+02
W17      9 11  0  6  0  0  0    0.500000E+11    0.126000E+02
W18      9  7  0  5  0  0  0    0.500000E+11    0.126000E+02
W19      1  7  0  5  2  0  0    0.510000E+11    0.188000E+02
W20      9  6  0  4  0  0  0    0.240000E+09    0.140000E+02
W21      4  6  0 11  0  0  0    0.410000E+08    0.820000E+01
W22      4 11  0  8  0  0  0    0.300000E+11    0.126000E+02
W23      2  6  0  5  0  0  0    0.700000E+09    0.188000E+02
W24      5  0  0  2  6  0  0    0.220000E+07    0.188000E+02
W25     10  7  0 11  0  0  0    0.120000E+12    0.126000E+02
W26     11  0  0 10  7  0  0    0.200000E+07    0.126000E+02
W27     11  7  0  5  8  0  0    0.580000E+08    0.188000E+02
W28      7  7  0  6  8  2  2    0.660000E+08    0.188000E+02
W29     11 11  0  6  8  0  0    0.110000E+08    0.188000E+02
W30     10  2  0  0  0  0  0    0.140000E+12    0.126000E+02
W31      0  0  0 10  2  0  0    0.261000E-04    0.126000E+02
W32      4  7  0  8  2  0  0    0.300000E+11    0.126000E+02
W33      6  0  0  4  4  0  0    0.200000E-07    7.280000E+00
H2G      3  0  0 13  0  0  0    0.300000E+02    -0.1E+01
H2L     13  0  0  3  0  0  0    0.100000E+02    -0.1E+01
O2G      8  0  0 12  0  0  0    0.230000E+02    -0.1E+01
O2L     12  0  0  8  0  0  0    0.120000E+02    -0.1E+01
SS       6  0  0  4  4  0  0    5.322000E-07    66.90000E+00
Ti       6  0  0  4  4  0  0    5.322000E-07    66.90000E+00
$END OF REACTION

************************************************
@Chemical Inject

$POSITION
XINITIAL =      0.0,
XLENGTH  =      0.0,
$END

$STATE $
$DOSESHAPE $
$VOIDFRACTION $

$INITIALCONC
Conc =    2*0.D0,   0.0D0,   2*0.D0,   0.0d0,   1*0.D0,   0.0d0,   5*0.D0
$END
```

```
$FLAG
CALCSURF = T,
WRITEPARA= T,
VoidFlag = F,
$END

$SENSITIVITY $
$LSODEDATA $
$ADJDATA $

@END OF Chemical Inject

************************************************
@Charging Line

$POSITION
XLENGTH  =     400.0,
XSTEP    =     400.0,
$END

$STATE
TempIn   =   553.00,
TempOUT  =   553.00,
VELINLET =   184.2,
Pressure =    68.0,
DENSLIQ  =   0.750,
GAMMARATE=   0.0E0,
NEUTRATE =   0.0E0,
Flowrate =   25.0,
Diameter =   0.48,
Surface  =   'Ti',
$END

$DOSESHAPE $
$VOIDFRACTION $
$INITIALCONC $
$FLAG $
$SENSITIVITY $

@END OF Charging Line

************************************************
@Core Inlet

$POSITION
XLENGTH   =   31.0,
XSTEP     =   31.0,
$END

$STATE
VELINLET =   94.44,
GAMMARATE=   2.2D4,
NEUTRATE =   6.6D3,
Diameter =   0.67,
$END

$DOSESHAPE
```

```
GammaC = 1.0,
NeutronC = 1.0,
$END

$VOIDFRACTION $
$INITIALCONC $
$FLAG $
$SENSITIVITY $

@END OF Core Inlet

************************************************
@Core Subcooled

$POSITION
XLENGTH= 20.0,
XSTEP  = 20.0,
$END

$STATE
VELINLET =   94.44,
GAMMARATE=   1.19D5,
NEUTRATE =   1.19D5,
$END

$DOSESHAPE $
$VOIDFRACTION $
$INITIALCONC $
$FLAG $
$SENSITIVITY $

@END OF Core Subcooled


************************************************
@Core Boiling1

$POSITION
XLENGTH=   20.0,
XSTEP  =   20.0,
XBoil  =  451.0,
$END

$STATE
VELINLET = 96.6,
TempOUT  = 563.0,
DensLiq  = 0.733,
DensGas  = 0.039,
Pressure  = 68.0,
GAMMARATE=   1.43D5,
NEUTRATE =   1.43D5,
$END

$DOSESHAPE $

$VOIDFRACTION
VoidC = -.6765, 0.0015,
$END
```

```
$INITIALCONC $
$FLAG $
$SENSITIVITY $

@END OF Core Boiling1

************************************************
@Core Boiling2

$POSITION
XLENGTH=   20.0,
XSTEP  =   20.0,
$END

$STATE
VELINLET =   96.6,
GAMMARATE=   0.70D5,
NEUTRATE =   0.70D5,
$END

$VOIDFRACTION $
$DOSESHAPE $
$INITIALCONC $
$FLAG $
$SENSITIVITY $

@END OF Core Boiling2

************************************************
@Core Boiling3

$POSITION
XLENGTH=   20.0,
XSTEP  =   20.0,
$END

$STATE
VELINLET =   96.6,
GAMMARATE=   0.70D5,
NEUTRATE =   0.70D5,
$END

$DOSESHAPE $
$VOIDFRACTION $
$INITIALCONC $
$FLAG $
$SENSITIVITY $

@END OF Core Boiling3

************************************************
@Core Boiling4

$POSITION
XLENGTH=   20.0,
XSTEP  =   20.0,
$END
```

```
$STATE
VELINLET =   96.6,
GAMMARATE=   1.43D5,
NEUTRATE =   1.43D5,
$END

$DOSESHAPE $
$VOIDFRACTION $
$INITIALCONC $
$FLAG $
$SENSITIVITY $

@END OF Core Boiling4

************************************************
@Core Boiling5

$POSITION
XLENGTH=   20.0,
XSTEP  =   20.0,
$END

$STATE
VELINLET =   96.6,
GAMMARATE=   1.19D5,
NEUTRATE =   1.19D5,
$END

$DOSESHAPE $
$VOIDFRACTION $
$INITIALCONC $
$FLAG $
$SENSITIVITY $

@END OF Core Boiling5

************************************************
@Core Outlet

$POSITION
XLENGTH=    31.0,
XSTEP  =    31.0,
$END

$STATE
GAMMARATE=   2.2D4,
NEUTRATE =   6.6D3,
$END

$DOSESHAPE $

$VOIDFRACTION
VoidC = 0.15, 0.0,
$END
$INITIALCONC $
$FLAG $
$SENSITIVITY $
```

```
@END OF Core Outlet

************************************************
@Plenum Inlet

$POSITION
XLENGTH= 64.0,
XSTEP  = 64.0,
$END

$STATE
Diameter = 0.48,
GAMMARATE=   2.2D3,
NEUTRATE =   1.1D3,
$END

$DOSESHAPE $
$VOIDFRACTION $
$INITIALCONC $
$FLAG $
$SENSITIVITY $

@END OF Plenum Inlet


************************************************
@Liq Plenum Out

$POSITION
XLENGTH=      15.0,
XSTEP  =      15.0,
XBOIL  =     99999,
$END

$STATE
VELINLET =   3.270,
Diameter =    3.36,
FLOWRATE =    21.25,
GAMMARATE=   220.0,
NEUTRATE =    0.22,
$END

$DOSESHAPE $
$VOIDFRACTION
VOIDC = 0.00,
$END
$INITIALCONC $
$FLAG $
$SENSITIVITY $

@END OF Liq Plenum Out


************************************************
@Liq Sample Line

$POSITION
```

```
XLENGTH=      56.0,
XSTEP  =      56.0,
$END

$STATE
Diameter =    0.48,
VELINLET =   160.2,
GAMMARATE=    2.2D3,
NEUTRATE =    1.1D3,
$END

$DOSESHAPE $
$VOIDFRACTION $
$INITIALCONC $
$FLAG $
$SENSITIVITY $

@END OF Liq Sample Line

*****************************************************
```

B.2 BCCLW.out

The output file of RADICAL includes the input parameters given in the input file and the detailed calculation results for each component. It is worthwhile to double-check the input parameters shown in the output file since sometimes incorrect results are obtained because of the inadvertent use of the wrong format for the input data.

RADICAL CODE PACKAGE OUTPUT
VERSION: 1.1

08/25/1992 19:50:47

INPUT

INPUT FILE NAME	=	:winput:bcclw.in
OUTPUT FILE NAME	=	:Woutput:BCCLW.OUT
PLOT FILE NAME	=	:Wplot:BCCLW.PLOT
NUMBER OF SPECIES EVALUATED	=	13
NUMBER OF CHEMICAL REACTIONS	=	39
NUMBER OF SURFACE REACTIONS	=	2
NUMBER OF COMPONENTS	=	13
NUMBER OF NODES	=	14
NUMBER OF CYCLES	=	1
STARTING NODE	=	1
REFERENCE TEMPERATURE	=	298.00000 Kelvin
PlotOut	=	T
LinLin	=	F
SENS	=	F
NORMALIZE	=	F
PPBOUT	=	T

COMPONENT NAME	FLOW-IN NODE	FLOW-OUT NODE	INITIAL CONC
Chemical Inject	1	2	1
Charging Line	2	3	0
Core Inlet	3	4	0
Core Subcooled	4	5	0
Core Boiling1	5	6	0
Core Boiling2	6	7	0
Core Boiling3	7	8	0
Core Boiling4	8	9	0
Core Boiling5	9	10	0
Core Outlet	10	11	0
Plenum Inlet	11	12	0
Liq Plenum Out	12	13	0
Liq Sample Line	13	14	0

SPECIES	GAMMA G-VALUES (#/100eV)	NEUTRON G-VALUES (#/100eV)	MOLECULAR WEIGHT (g/mole)
e-	0.42D+01	0.93D+00	0.55D-03

OH-	0.00D+00	0.00D+00	0.17D+02
H2	0.62D+00	0.88D+00	0.20D+01
OH	0.40D+01	0.11D+01	0.17D+02
HO2-	0.00D+00	0.00D+00	0.33D+02
H2O2	0.13D+01	0.99D+00	0.34D+02
O2-	0.00D+00	0.00D+00	0.32D+02
O2	0.00D+00	0.00D+00	0.32D+02
H	0.11D+01	0.50D+00	0.10D+01
H+	0.42D+01	0.93D+00	0.10D+01
HO2	0.00D+00	0.40D-01	0.33D+02
O2G	0.00D+00	0.00D+00	0.32D+02
H2G	0.00D+00	0.00D+00	0.20D+01

CHEMICAL REACTIONS, RATE CONSTANTS, AND ACTIVATION ENERGIES

	REACTIONS					RATE CONSTANT	ACTIVATION ENERGIES (KJ/MOL-K)
W 1 e-		>H	OH-			0.40E+02	0.13E+02
W 2 e-	H+	>H				0.60E+11	0.13E+02
W 3 e-	OH	>OH-				0.75E+11	0.13E+02
W 4 e-	H2O2	>OH	OH-			0.32E+11	0.13E+02
W 5 H	H	>H2				0.25E+11	0.13E+02
W 6 e-	HO2	>HO2-				0.50E+11	0.13E+02
W 7 e-	O2	>O2-				0.47E+11	0.13E+02
W 8 e-	e-	>OH-	OH-	H2		0.12E+11	0.13E+02
W 9 OH	OH	>H2O2				0.11E+11	0.13E+02
W10 OH-	H	>e-				0.78E+08	0.19E+02
W11 e-	H	>H2	OH-			0.62E+11	0.13E+02
W12 e-	HO2-	>OH	OH-	OH-		0.87E+10	0.13E+02
W13 H	OH	>				0.50E+11	0.13E+02
W14 OH	H2	>H				0.11E+09	0.13E+02
W15 H		>H2	OH			0.49E-01	0.85E+02
W16 H	O2	>HO2				0.47E+11	0.13E+02
W17 H	HO2	>H2O2				0.50E+11	0.13E+02
W18 H	O2-	>HO2-				0.50E+11	0.13E+02
W19 e-	O2-	>HO2-	OH-			0.51E+11	0.19E+02
W20 H	H2O2	>OH				0.24E+09	0.14E+02
W21 OH	H2O2	>HO2				0.41E+08	0.82E+01
W22 OH	HO2	>O2				0.30E+11	0.13E+02
W23 OH-	H2O2	>HO2-				0.70E+09	0.19E+02
W24 HO2-		>OH-	H2O2			0.22E+07	0.19E+02
W25 H+	O2-	>HO2				0.12E+12	0.13E+02
W26 HO2		>H+	O2-			0.20E+07	0.13E+02
W27 HO2	O2-	>HO2-	O2			0.58E+08	0.19E+02
W28 O2-	O2-	>H2O2	O2	OH-	OH-	0.66E+08	0.19E+02
W29 HO2	HO2	>H2O2	O2			0.11E+08	0.19E+02
W30 H+	OH-	>				0.14E+12	0.13E+02
W31		>H+	OH-			0.26E-04	0.13E+02
W32 OH	O2-	>O2	OH-			0.30E+11	0.13E+02
W33 H2O2		>OH	OH			0.20E-07	0.73E+01
H2G H2		>H2G				0.30E+02	-0.10E+01

H2L	H2G	>H2		0.10E+02	-0.10E+01
O2G	O2	>O2G		0.23E+02	-0.10E+01
O2L	O2G	>O2		0.12E+02	-0.10E+01
SS	H2O2	>OH	OH	0.53E-06	0.67E+02
Ti	H2O2	>OH	OH	0.53E-06	0.67E+02

OUTPUT FOR CYCLE 1 AT Charging Line

INITIAL POSITION	=	.00000	cm
FINAL POSITION	=	400.00000	cm
FLOW LENGTH	=	400.00000	cm
POSITION INCREMENT	=	400.00000	cm
POSITION OF ONSET OF BOILING	=	9999.00000	cm
INLET TEMPERATURE	=	553.00000	Kelvin
OUTLET TEMPERATURE	=	553.00000	Kelvin
INLET LIQUID VELOCITY	=	184.20000	cm/s
PIPE INTERNAL DIAMETER	=	.48000	cm
WATER DENSITY	=	.75000	g/cc
VAPOR DENSITY	=	.03620	g/cc
PRESSURE	=	68.00000	atm
MASS FlowRate	=	0.25000E+02	g/s
SURFACE MATERIAL	= Ti		
GAMMA DOSE RATE MULTIPLIER	=	0.00000E+00	Rad/s
NEUTRON DOSE RATE MULTIPLIER	=	0.00000E+00	Rad/s
GConvert	=	0.77850E-09	
CalcSurf	=	T	
VoidFlag	=	F	
CalcSens	=	F	
WriteRx	=	F	
WritePara	=	T	
RADIOLYSIS ABSOLUTE TOLERANCE	=	0.10000E-14	
RELATIVE TOLERANCE	=	0.10000E-04	

CYCLE 1 POSITION IN Charging Line = .0000 cm
CONCENTRATIONS[ppb] AT POSITION = .0000 cm

e-	= 0.000000E+00 **		OH-	= 0.000000E+00 **	
H2	= 0.000000E+00 **		OH	= 0.000000E+00 **	
HO2-	= 0.000000E+00 **		H2O2	= 0.000000E+00 **	
O2-	= 0.000000E+00 **		O2	= 0.000000E+00 **	
H	= 0.000000E+00 **		H+	= 0.000000E+00 **	
HO2	= 0.000000E+00 **		O2G	= 0.000000E+00 **	
H2G	= 0.000000E+00 **				

NO. STEPS	=	0
TEMPERATURE (K)	=	.00000
LIQUID VELOCITY (CM/S)	=	184.20000

```
GAS VELOCITY  (CM/S)        =          .00000
VOID FRACTION               =          .00000
QUALITY                     =          .00000
GAMMA DOSE RATE (RAD/S)     =     0.00000E+00
NEUTRON DOSE RATE (RAD/S)   =     0.00000E+00
```

```
CYCLE    1        POSITION IN Charging Line    =     400.0000 cm
              CONCENTRATIONS[ppb]  AT POSITION =     400.0000 cm

e-       =    0.000000E+00 **     OH-      =    0.309488E+00 **
H2       =    0.000000E+00 **     OH       =    0.000000E+00 **
HO2-     =    0.000000E+00 **     H2O2     =    0.000000E+00 **
O2-      =    0.000000E+00 **     O2       =    0.000000E+00 **
H        =    0.000000E+00 **     H+       =    0.182052E-01 **
HO2      =    0.000000E+00 **     O2G      =    0.000000E+00 **
H2G      =    0.000000E+00 **

NO. STEPS                   =       74
TEMPERATURE (K)             =      553.00000
LIQUID VELOCITY (CM/S)      =      184.20000
GAS VELOCITY  (CM/S)        =          .00000
VOID FRACTION               =          .00000
QUALITY                     =          .00000
GAMMA DOSE RATE (RAD/S)     =     0.00000E+00
NEUTRON DOSE RATE (RAD/S)   =     0.00000E+00
```

RUN STATISTICS FOR CYCLE 1 AT Charging Line

```
REQUIRED RWORK SIZE   =       308
IWORK SIZE            =        33
NUMBER OF STEPS       =        74
# OF FUNC.- EVALS.    =        93
# OF JACOB.- EVALS    =        18
COMPONENT JOB TIME    =         8. seconds

CONCENTRATION PROFILE OF Charging Line    HAS BEEN EVALUATED SUCCESSFULLY!
```

OUTPUT FOR CYCLE 1 AT Core Inlet

```
INITIAL POSITION                =     400.00000 cm
FINAL POSITION                  =     431.00000 cm
FLOW LENGTH                     =      31.00000 cm
POSITION INCREMENT              =      31.00000 cm
POSITION OF ONSET OF BOILING    =    9999.00000 cm

INLET TEMPERATURE               =     553.00000 Kelvin
```

```
OUTLET TEMPERATURE                =      553.00000 Kelvin
INLET LIQUID VELOCITY             =       94.44000 cm/s
PIPE INTERNAL DIAMETER            =         .67000 cm
WATER DENSITY                     =         .75000 g/cc
VAPOR DENSITY                     =         .03620 g/cc
PRESSURE                          =       68.00000 atm
MASS FlowRate                     =   0.25000E+02 g/s

SURFACE MATERIAL                  = Ti

GAMMA DOSE RATE MULTIPLIER        =   0.22000E+05 Rad/s
NEUTRON DOSE RATE MULTIPLIER      =   0.66000E+04 Rad/s
GConvert                          =   0.77850E-09

GAMMA DOSE SHAPE FUNCTION COEFFICIENTS
GAMMA COEFFICIENT  0              =   0.10000E+01
GAMMA COEFFICIENT  1              =   0.00000E+00
GAMMA COEFFICIENT  2              =   0.00000E+00
GAMMA COEFFICIENT  3              =   0.00000E+00
GAMMA COEFFICIENT  4              =   0.00000E+00
GAMMA COEFFICIENT  5              =   0.00000E+00

NEUTRON DOSE SHAPE FUNCTION COEFFICIENTS
NEUTRON COEFFICIENT  0            =   0.10000E+01
NEUTRON COEFFICIENT  1            =   0.00000E+00
NEUTRON COEFFICIENT  2            =   0.00000E+00
NEUTRON COEFFICIENT  3            =   0.00000E+00
NEUTRON COEFFICIENT  4            =   0.00000E+00
NEUTRON COEFFICIENT  5            =   0.00000E+00

CalcSurf                          =          T
VoidFlag                          =          F
CalcSens                          =          F
WriteRx                           =          F
WritePara                         =          T

RADIOLYSIS ABSOLUTE TOLERANCE     =   0.10000E-14
           RELATIVE TOLERANCE     =   0.10000E-04
```

```
CYCLE    1        POSITION IN Core Inlet       =        .0000 cm
              CONCENTRATIONS[ppb]  AT POSITION =     400.0000 cm

e-      =   0.000000E+00 **     OH-      =   0.309488E+00 **
H2      =   0.000000E+00 **     OH       =   0.000000E+00 **
HO2-    =   0.000000E+00 **     H2O2     =   0.000000E+00 **
O2-     =   0.000000E+00 **     O2       =   0.000000E+00 **
H       =   0.000000E+00 **     H+       =   0.182052E-01 **
HO2     =   0.000000E+00 **     O2G      =   0.000000E+00 **
H2G     =   0.000000E+00 **

NO. STEPS                 =          0
TEMPERATURE (K)           =    553.00000
LIQUID VELOCITY (CM/S)    =     94.44000
GAS VELOCITY  (CM/S)      =       .00000
VOID FRACTION             =       .00000
QUALITY                   =       .00000
GAMMA DOSE RATE (RAD/S)   =  0.00000E+00
```

NEUTRON DOSE RATE (RAD/S) = 0.00000E+00

CYCLE 1 POSITION IN Core Inlet = 31.0000 cm
CONCENTRATIONS[ppb] AT POSITION = 431.0000 cm

e-	=	0.549169E-07 **	OH-	=	0.224293E+00 **
H2	=	0.884681E+01 **	OH	=	0.276752E+00 **
HO2-	=	0.236575E-03 **	H2O2	=	0.768443E+02 **
O2-	=	0.712548E+00 **	O2	=	0.339485E+02 **
H	=	0.118493E-03 **	H+	=	0.355680E-01 **
HO2	=	0.125766E-02 **	O2G	=	0.000000E+00 **
H2G	=	0.000000E+00 **			

NO. STEPS	=	286
TEMPERATURE (K)	=	553.00000
LIQUID VELOCITY (CM/S)	=	94.44000
GAS VELOCITY (CM/S)	=	.00000
VOID FRACTION	=	.00000
QUALITY	=	.00000
GAMMA DOSE RATE (RAD/S)	=	0.22000E+05
NEUTRON DOSE RATE (RAD/S)	=	0.66000E+04

RUN STATISTICS FOR CYCLE 1 AT Core Inlet

REQUIRED RWORK SIZE	=	308
IWORK SIZE	=	33
NUMBER OF STEPS	=	286
# OF FUNC.- EVALS.	=	406
# OF JACOB.- EVALS	=	50
COMPONENT JOB TIME	=	16. seconds

CONCENTRATION PROFILE OF Core Inlet HAS BEEN EVALUATED SUCCESSFULLY!

OUTPUT FOR CYCLE 1 AT Core Subcooled

INITIAL POSITION	=	431.00000 cm
FINAL POSITION	=	451.00000 cm
FLOW LENGTH	=	20.00000 cm
POSITION INCREMENT	=	20.00000 cm
POSITION OF ONSET OF BOILING	=	9999.00000 cm
INLET TEMPERATURE	=	553.00000 Kelvin
OUTLET TEMPERATURE	=	553.00000 Kelvin
INLET LIQUID VELOCITY	=	94.44000 cm/s
PIPE INTERNAL DIAMETER	=	.67000 cm
WATER DENSITY	=	.75000 g/cc

```
VAPOR DENSITY                        =         .03620 g/cc
PRESSURE                             =       68.00000 atm
MASS FlowRate                        =    0.25000E+02 g/s

SURFACE MATERIAL                     = Ti

GAMMA DOSE RATE MULTIPLIER           =    0.11900E+06 Rad/s
NEUTRON DOSE RATE MULTIPLIER         =    0.11900E+06 Rad/s
GConvert                             =    0.77850E-09

GAMMA DOSE SHAPE FUNCTION COEFFICIENTS
GAMMA COEFFICIENT  0                 =    0.10000E+01
GAMMA COEFFICIENT  1                 =    0.00000E+00
GAMMA COEFFICIENT  2                 =    0.00000E+00
GAMMA COEFFICIENT  3                 =    0.00000E+00
GAMMA COEFFICIENT  4                 =    0.00000E+00
GAMMA COEFFICIENT  5                 =    0.00000E+00

NEUTRON DOSE SHAPE FUNCTION COEFFICIENTS
NEUTRON COEFFICIENT  0               =    0.10000E+01
NEUTRON COEFFICIENT  1               =    0.00000E+00
NEUTRON COEFFICIENT  2               =    0.00000E+00
NEUTRON COEFFICIENT  3               =    0.00000E+00
NEUTRON COEFFICIENT  4               =    0.00000E+00
NEUTRON COEFFICIENT  5               =    0.00000E+00

CalcSurf                             =       T
VoidFlag                             =       F
CalcSens                             =       F
WriteRx                              =       F
WritePara                            =       T

RADIOLYSIS ABSOLUTE TOLERANCE        =    0.10000E-14
           RELATIVE TOLERANCE        =    0.10000E-04
```

```
CYCLE    1        POSITION IN Core Subcooled   =        .0000 cm
              CONCENTRATIONS[ppb]  AT POSITION =     431.0000 cm

e-       =    0.549169E-07 **     OH-      =    0.224293E+00 **
H2       =    0.884681E+01 **     OH       =    0.276752E+00 **
HO2-     =    0.236575E-03 **     H2O2     =    0.768443E+02 **
O2-      =    0.712548E+00 **     O2       =    0.339485E+02 **
H        =    0.118493E-03 **     H+       =    0.355680E-01 **
HO2      =    0.125766E-02 **     O2G      =    0.000000E+00 **
H2G      =    0.000000E+00 **

NO. STEPS                    =       0
TEMPERATURE (K)              =     553.00000
LIQUID VELOCITY (CM/S)       =      94.44000
GAS VELOCITY  (CM/S)         =        .00000
VOID FRACTION                =        .00000
QUALITY                      =        .00000
GAMMA DOSE RATE (RAD/S)      =   0.11900E+06
NEUTRON DOSE RATE (RAD/S)    =   0.11900E+06
```

```
CYCLE    1        POSITION IN Core Subcooled   =      20.0000 cm
```

CONCENTRATIONS[ppb] AT POSITION = 451.0000 cm

e-	=	0.136961E-06 **	OH-	=	0.270825E+00 **
H2	=	0.215133E+02 **	OH	=	0.638748E+00 **
HO2-	=	0.803228E-03 **	H2O2	=	0.213870E+03 **
O2-	=	0.201190E+01 **	O2	=	0.696517E+02 **
H	=	0.453071E-03 **	H+	=	0.790766E-01 **
HO2	=	0.801371E-02 **	O2G	=	0.000000E+00 **
H2G	=	0.000000E+00 **			

NO. STEPS	=	181
TEMPERATURE (K)	=	553.00000
LIQUID VELOCITY (CM/S)	=	94.44000
GAS VELOCITY (CM/S)	=	.00000
VOID FRACTION	=	.00000
QUALITY	=	.00000
GAMMA DOSE RATE (RAD/S)	=	0.11900E+06
NEUTRON DOSE RATE (RAD/S)	=	0.11900E+06

RUN STATISTICS FOR CYCLE 1 AT Core Subcooled

REQUIRED RWORK SIZE	=	308
IWORK SIZE	=	33
NUMBER OF STEPS	=	181
# OF FUNC.- EVALS.	=	229
# OF JACOB.- EVALS	=	35
COMPONENT JOB TIME	=	12. seconds

CONCENTRATION PROFILE OF Core Subcooled HAS BEEN EVALUATED SUCCESSFULLY!

OUTPUT FOR CYCLE 1 AT Core Boiling1

INITIAL POSITION	=	451.00000 cm
FINAL POSITION	=	471.00000 cm
FLOW LENGTH	=	20.00000 cm
POSITION INCREMENT	=	20.00000 cm
POSITION OF ONSET OF BOILING	=	451.00000 cm
INLET TEMPERATURE	=	553.00000 Kelvin
OUTLET TEMPERATURE	=	563.00000 Kelvin
INLET LIQUID VELOCITY	=	96.60000 cm/s
PIPE INTERNAL DIAMETER	=	.67000 cm
WATER DENSITY	=	.73300 g/cc
VAPOR DENSITY	=	.03900 g/cc
PRESSURE	=	68.00000 atm
MASS FlowRate	=	0.25000E+02 g/s

```
SURFACE MATERIAL                    = Ti

GAMMA DOSE RATE MULTIPLIER          =    0.14300E+06 Rad/s
NEUTRON DOSE RATE MULTIPLIER        =    0.14300E+06 Rad/s
GConvert                            =    0.76085E-09

GAMMA DOSE SHAPE FUNCTION COEFFICIENTS
GAMMA COEFFICIENT  0                =    0.10000E+01
GAMMA COEFFICIENT  1                =    0.00000E+00
GAMMA COEFFICIENT  2                =    0.00000E+00
GAMMA COEFFICIENT  3                =    0.00000E+00
GAMMA COEFFICIENT  4                =    0.00000E+00
GAMMA COEFFICIENT  5                =    0.00000E+00

NEUTRON DOSE SHAPE FUNCTION COEFFICIENTS
NEUTRON COEFFICIENT  0              =    0.10000E+01
NEUTRON COEFFICIENT  1              =    0.00000E+00
NEUTRON COEFFICIENT  2              =    0.00000E+00
NEUTRON COEFFICIENT  3              =    0.00000E+00
NEUTRON COEFFICIENT  4              =    0.00000E+00
NEUTRON COEFFICIENT  5              =    0.00000E+00

VOID FRACTION FUNCTION COEFFICIENTS
VOID FRACTION  COEFFICIENT  0   =   -0.67650E+00
VOID FRACTION  COEFFICIENT  1   =    0.15000E-02
VOID FRACTION  COEFFICIENT  2   =    0.00000E+00
VOID FRACTION  COEFFICIENT  3   =    0.00000E+00
VOID FRACTION  COEFFICIENT  4   =    0.00000E+00
VOID FRACTION  COEFFICIENT  5   =    0.00000E+00

CalcSurf                            =        T
VoidFlag                            =        F
CalcSens                            =        F
WriteRx                             =        F
WritePara                           =        T

RADIOLYSIS ABSOLUTE TOLERANCE       =    0.10000E-14
           RELATIVE TOLERANCE       =    0.10000E-04
```

```
CYCLE    1        POSITION IN Core Boiling1    =         .0000 cm
              CONCENTRATIONS[ppb]  AT POSITION =     451.0000 cm

e-       =    0.140138E-06 **     OH-      =    0.277106E+00 **
H2       =    0.220123E+02 **     OH       =    0.653562E+00 **
HO2-     =    0.821856E-03 **     H2O2     =    0.218830E+03 **
O2-      =    0.205856E+01 **     O2       =    0.712671E+02 **
H        =    0.463579E-03 **     H+       =    0.809105E-01 **
HO2      =    0.819957E-02 **     O2G      =    0.000000E+00 **
H2G      =    0.000000E+00 **

NO. STEPS                    =        0
TEMPERATURE (K)              =      553.00000
LIQUID VELOCITY (CM/S)       =       96.60000
GAS VELOCITY  (CM/S)         =      119.66701
VOID FRACTION                =        0.00000
QUALITY                      =        0.00000
GAMMA DOSE RATE (RAD/S)      =   0.14300E+06
```

NEUTRON DOSE RATE (RAD/S) = 0.14300E+06

CYCLE 1 POSITION IN Core Boiling1 = 20.0000 cm
CONCENTRATIONS[ppb] AT POSITION = 471.0000 cm

e-	=	0.125370E-06 **	OH-	=	0.296521E+00 **
H2	=	0.186833E+02 **	OH	=	0.736843E+00 **
HO2-	=	0.108321E-02 **	H2O2	=	0.271317E+03 **
O2-	=	0.201935E+01 **	O2	=	0.934288E+02 **
H	=	0.359940E-03 **	H+	=	0.808082E-01 **
HO2	=	0.807762E-02 **	O2G	=	0.794068E+02 **
H2G	=	0.257326E+02 **			

O2G = 0.571E-04 ATM
H2G = 0.296E-03 ATM

NO. STEPS	=	141
TEMPERATURE (K)	=	563.00000
LIQUID VELOCITY (CM/S)	=	133.24018
GAS VELOCITY (CM/S)	=	193.55079
VOID FRACTION	=	.29674
QUALITY	=	.03000
GAMMA DOSE RATE (RAD/S)	=	0.14300E+06
NEUTRON DOSE RATE (RAD/S)	=	0.14300E+06

RUN STATISTICS FOR CYCLE 1 AT Core Boiling1

REQUIRED RWORK SIZE	=	308
IWORK SIZE	=	33
NUMBER OF STEPS	=	141
# OF FUNC.- EVALS.	=	174
# OF JACOB.- EVALS	=	33
COMPONENT JOB TIME	=	11. seconds

CONCENTRATION PROFILE OF Core Boiling1 HAS BEEN EVALUATED SUCCESSFULLY!

OUTPUT FOR CYCLE 1 AT Core Boiling2

INITIAL POSITION	=	471.00000 cm
FINAL POSITION	=	491.00000 cm
FLOW LENGTH	=	20.00000 cm
POSITION INCREMENT	=	20.00000 cm
POSITION OF ONSET OF BOILING	=	451.00000 cm
INLET TEMPERATURE	=	563.00000 Kelvin
OUTLET TEMPERATURE	=	563.00000 Kelvin

```
INLET LIQUID VELOCITY                =       96.60000 cm/s
PIPE INTERNAL DIAMETER               =         .67000 cm
WATER DENSITY                        =         .73300 g/cc
VAPOR DENSITY                        =         .03900 g/cc
PRESSURE                             =       68.00000 atm
MASS FlowRate                        =    0.25000E+02 g/s

SURFACE MATERIAL                     = Ti

GAMMA DOSE RATE MULTIPLIER           =    0.70000E+05 Rad/s
NEUTRON DOSE RATE MULTIPLIER         =    0.70000E+05 Rad/s
GConvert                             =    0.76085E-09

GAMMA DOSE SHAPE FUNCTION COEFFICIENTS
GAMMA COEFFICIENT  0                 =    0.10000E+01
GAMMA COEFFICIENT  1                 =    0.00000E+00
GAMMA COEFFICIENT  2                 =    0.00000E+00
GAMMA COEFFICIENT  3                 =    0.00000E+00
GAMMA COEFFICIENT  4                 =    0.00000E+00
GAMMA COEFFICIENT  5                 =    0.00000E+00

NEUTRON DOSE SHAPE FUNCTION COEFFICIENTS
NEUTRON COEFFICIENT  0               =    0.10000E+01
NEUTRON COEFFICIENT  1               =    0.00000E+00
NEUTRON COEFFICIENT  2               =    0.00000E+00
NEUTRON COEFFICIENT  3               =    0.00000E+00
NEUTRON COEFFICIENT  4               =    0.00000E+00
NEUTRON COEFFICIENT  5               =    0.00000E+00

VOID FRACTION FUNCTION COEFFICIENTS
VOID FRACTION  COEFFICIENT  0    =   -0.67650E+00
VOID FRACTION  COEFFICIENT  1    =    0.15000E-02
VOID FRACTION  COEFFICIENT  2    =    0.00000E+00
VOID FRACTION  COEFFICIENT  3    =    0.00000E+00
VOID FRACTION  COEFFICIENT  4    =    0.00000E+00
VOID FRACTION  COEFFICIENT  5    =    0.00000E+00

CalcSurf                             =         T
VoidFlag                             =         F
CalcSens                             =         F
WriteRx                              =         F
WritePara                            =         T

RADIOLYSIS ABSOLUTE TOLERANCE        =    0.10000E-14
           RELATIVE TOLERANCE        =    0.10000E-04
```

```
CYCLE    1        POSITION IN Core Boiling2    =         .0000 cm
              CONCENTRATIONS[ppb]  AT POSITION =      471.0000 cm

e-       =    0.125370E-06 **     OH-      =    0.296521E+00 **
H2       =    0.186833E+02 **     OH       =    0.736843E+00 **
HO2-     =    0.108321E-02 **     H2O2     =    0.271317E+03 **
O2-      =    0.201935E+01 **     O2       =    0.934288E+02 **
H        =    0.359940E-03 **     H+       =    0.808082E-01 **
HO2      =    0.807762E-02 **     O2G      =    0.794068E+02 **
H2G      =    0.257326E+02 **
```

```
O2G        =    0.571E-04 ATM
H2G        =    0.296E-03 ATM

NO. STEPS                      =         0
TEMPERATURE (K)                =       563.00000
LIQUID VELOCITY (CM/S)         =       133.24018
GAS VELOCITY  (CM/S)           =       183.55079
VOID FRACTION                  =          .29674
QUALITY                        =          .03000
GAMMA DOSE RATE (RAD/S)        =     0.70000E+05
NEUTRON DOSE RATE (RAD/S)      =     0.70000E+05
```

```
CYCLE    1        POSITION IN Core Boiling2     =      20.0000 cm
                CONCENTRATIONS[ppb]  AT POSITION =     491.0000 cm

e-         =     0.684730E-07 **      OH-        =     0.244959E+00 **
H2         =     0.120214E+02 **      OH         =     0.512382E+00 **
HO2-       =     0.778019E-03 **      H2O2       =     0.237143E+03 **
O2-        =     0.145140E+01 **      O2         =     0.898248E+02 **
H          =     0.172696E-03 **      H+         =     0.599138E-01 **
HO2        =     0.426763E-02 **      O2G        =     0.104899E+03 **
H2G        =     0.242179E+02 **

O2G        =    0.754E-04 ATM
H2G        =    0.279E-03 ATM

NO. STEPS                      =       151
TEMPERATURE (K)                =       563.00000
LIQUID VELOCITY (CM/S)         =       162.22478
GAS VELOCITY  (CM/S)           =       247.43456
VOID FRACTION                  =          .44026
QUALITY                        =          .06000
GAMMA DOSE RATE (RAD/S)        =     0.70000E+05
NEUTRON DOSE RATE (RAD/S)      =     0.70000E+05
```

RUN STATISTICS FOR CYCLE 1 AT Core Boiling2

```
REQUIRED RWORK SIZE   =        308
IWORK SIZE            =         33
NUMBER OF STEPS       =        151
# OF FUNC.- EVALS.    =        183
# OF JACOB.- EVALS    =         31
COMPONENT JOB TIME    =         11. seconds
```

CONCENTRATION PROFILE OF Core Boiling2 HAS BEEN EVALUATED SUCCESSFULLY!

OUTPUT FOR CYCLE 1 AT Core Boiling3

```
INITIAL POSITION                    =      491.00000 cm
FINAL POSITION                      =      511.00000 cm
FLOW LENGTH                         =       20.00000 cm
POSITION INCREMENT                  =       20.00000 cm
POSITION OF ONSET OF BOILING        =      451.00000 cm

INLET TEMPERATURE                   =      563.00000 Kelvin
OUTLET TEMPERATURE                  =      563.00000 Kelvin
INLET LIQUID VELOCITY               =       96.60000 cm/s
PIPE INTERNAL DIAMETER              =         .67000 cm
WATER DENSITY                       =         .73300 g/cc
VAPOR DENSITY                       =         .03900 g/cc
PRESSURE                            =       68.00000 atm
MASS FlowRate                       =   0.25000E+02 g/s

SURFACE MATERIAL                    = Ti

GAMMA DOSE RATE MULTIPLIER          =   0.70000E+05 Rad/s
NEUTRON DOSE RATE MULTIPLIER        =   0.70000E+05 Rad/s
GConvert                            =   0.76085E-09

GAMMA DOSE SHAPE FUNCTION COEFFICIENTS
GAMMA COEFFICIENT  0                =   0.10000E+01
GAMMA COEFFICIENT  1                =   0.00000E+00
GAMMA COEFFICIENT  2                =   0.00000E+00
GAMMA COEFFICIENT  3                =   0.00000E+00
GAMMA COEFFICIENT  4                =   0.00000E+00
GAMMA COEFFICIENT  5                =   0.00000E+00

NEUTRON DOSE SHAPE FUNCTION COEFFICIENTS
NEUTRON COEFFICIENT  0              =   0.10000E+01
NEUTRON COEFFICIENT  1              =   0.00000E+00
NEUTRON COEFFICIENT  2              =   0.00000E+00
NEUTRON COEFFICIENT  3              =   0.00000E+00
NEUTRON COEFFICIENT  4              =   0.00000E+00
NEUTRON COEFFICIENT  5              =   0.00000E+00

VOID FRACTION FUNCTION COEFFICIENTS
VOID FRACTION  COEFFICIENT  0   =  -0.67650E+00
VOID FRACTION  COEFFICIENT  1   =   0.15000E-02
VOID FRACTION  COEFFICIENT  2   =   0.00000E+00
VOID FRACTION  COEFFICIENT  3   =   0.00000E+00
VOID FRACTION  COEFFICIENT  4   =   0.00000E+00
VOID FRACTION  COEFFICIENT  5   =   0.00000E+00

CalcSurf                            =         T
VoidFlag                            =         F
CalcSens                            =         F
WriteRx                             =         F
WritePara                           =         T

RADIOLYSIS ABSOLUTE TOLERANCE       =   0.10000E-14
           RELATIVE TOLERANCE       =   0.10000E-04
```

```
CYCLE    1        POSITION IN Core Boiling3    =        .0000 cm
```

CONCENTRATIONS[ppb] AT POSITION = 491.0000 cm

e-	=	0.684730E-07 **	OH-	=	0.244959E+00 **
H2	=	0.120214E+02 **	OH	=	0.512382E+00 **
HO2-	=	0.778019E-03 **	H2O2	=	0.237143E+03 **
O2-	=	0.145140E+01 **	O2	=	0.898248E+02 **
H	=	0.172696E-03 **	H+	=	0.599138E-01 **
HO2	=	0.426763E-02 **	O2G	=	0.104899E+03 **
H2G	=	0.242179E+02 **			

O2G = 0.754E-04 ATM
H2G = 0.279E-03 ATM

NO. STEPS	=	0
TEMPERATURE (K)	=	563.00000
LIQUID VELOCITY (CM/S)	=	162.22478
GAS VELOCITY (CM/S)	=	247.43456
VOID FRACTION	=	.44026
QUALITY	=	.06000
GAMMA DOSE RATE (RAD/S)	=	0.70000E+05
NEUTRON DOSE RATE (RAD/S)	=	0.70000E+05

CYCLE 1 POSITION IN Core Boiling3 = 20.0000 cm
CONCENTRATIONS[ppb] AT POSITION = 511.0000 cm

e-	=	0.676382E-07 **	OH-	=	0.254540E+00 **
H2	=	0.105502E+02 **	OH	=	0.539031E+00 **
HO2-	=	0.830662E-03 **	H2O2	=	0.243866E+03 **
O2-	=	0.134972E+01 **	O2	=	0.889992E+02 **
H	=	0.165975E-03 **	H+	=	0.573000E-01 **
HO2	=	0.382196E-02 **	O2G	=	0.113640E+03 **
H2G	=	0.223175E+02 **			

O2G = 0.817E-04 ATM
H2G = 0.257E-03 ATM

NO. STEPS	=	17
TEMPERATURE (K)	=	563.00000
LIQUID VELOCITY (CM/S)	=	185.01583
GAS VELOCITY (CM/S)	=	311.31834
VOID FRACTION	=	.52487
QUALITY	=	.09000
GAMMA DOSE RATE (RAD/S)	=	0.70000E+05
NEUTRON DOSE RATE (RAD/S)	=	0.70000E+05

RUN STATISTICS FOR CYCLE 1 AT Core Boiling3

REQUIRED RWORK SIZE	=	308
IWORK SIZE	=	33
NUMBER OF STEPS	=	17
# OF FUNC.- EVALS.	=	23

```
# OF JACOB.- EVALS     =          6
COMPONENT JOB TIME     =          6. seconds

CONCENTRATION PROFILE OF Core Boiling3     HAS BEEN EVALUATED SUCCESSFULLY!
```

OUTPUT FOR CYCLE 1 AT Core Boiling4

INITIAL POSITION	=	511.00000	cm
FINAL POSITION	=	531.00000	cm
FLOW LENGTH	=	20.00000	cm
POSITION INCREMENT	=	20.00000	cm
POSITION OF ONSET OF BOILING	=	451.00000	cm
INLET TEMPERATURE	=	563.00000	Kelvin
OUTLET TEMPERATURE	=	563.00000	Kelvin
INLET LIQUID VELOCITY	=	96.60000	cm/s
PIPE INTERNAL DIAMETER	=	.67000	cm
WATER DENSITY	=	.73300	g/cc
VAPOR DENSITY	=	.03900	g/cc
PRESSURE	=	68.00000	atm
MASS FlowRate	=	0.25000E+02	g/s
SURFACE MATERIAL	= Ti		
GAMMA DOSE RATE MULTIPLIER	=	0.14300E+06	Rad/s
NEUTRON DOSE RATE MULTIPLIER	=	0.14300E+06	Rad/s
GConvert	=	0.76085E-09	

GAMMA DOSE SHAPE FUNCTION COEFFICIENTS

GAMMA COEFFICIENT 0	=	0.10000E+01
GAMMA COEFFICIENT 1	=	0.00000E+00
GAMMA COEFFICIENT 2	=	0.00000E+00
GAMMA COEFFICIENT 3	=	0.00000E+00
GAMMA COEFFICIENT 4	=	0.00000E+00
GAMMA COEFFICIENT 5	=	0.00000E+00

NEUTRON DOSE SHAPE FUNCTION COEFFICIENTS

NEUTRON COEFFICIENT 0	=	0.10000E+01
NEUTRON COEFFICIENT 1	=	0.00000E+00
NEUTRON COEFFICIENT 2	=	0.00000E+00
NEUTRON COEFFICIENT 3	=	0.00000E+00
NEUTRON COEFFICIENT 4	=	0.00000E+00
NEUTRON COEFFICIENT 5	=	0.00000E+00

VOID FRACTION FUNCTION COEFFICIENTS

VOID FRACTION COEFFICIENT 0	=	-0.67650E+00
VOID FRACTION COEFFICIENT 1	=	0.15000E-02
VOID FRACTION COEFFICIENT 2	=	0.00000E+00
VOID FRACTION COEFFICIENT 3	=	0.00000E+00
VOID FRACTION COEFFICIENT 4	=	0.00000E+00
VOID FRACTION COEFFICIENT 5	=	0.00000E+00
CalcSurf	=	T

```
VoidFlag                          =        F
CalcSens                          =        F
WriteRx                           =        F
WritePara                         =        T

RADIOLYSIS ABSOLUTE TOLERANCE     =    0.10000E-14
           RELATIVE TOLERANCE     =    0.10000E-04
```

```
CYCLE    1        POSITION IN Core Boiling4     =        .0000 cm
              CONCENTRATIONS[ppb]  AT POSITION =     511.0000 cm

e-       =    0.676382E-07 **      OH-       =    0.254540E+00 **
H2       =    0.105502E+02 **      OH        =    0.539031E+00 **
HO2-     =    0.830662E-03 **      H2O2      =    0.243866E+03 **
O2-      =    0.134972E+01 **      O2        =    0.889992E+02 **
H        =    0.165975E-03 **      H+        =    0.573000E-01 **
HO2      =    0.382196E-02 **      O2G       =    0.113640E+03 **
H2G      =    0.223175E+02 **

O2G       =   0.817E-04 ATM
H2G       =   0.257E-03 ATM

NO. STEPS                    =         0
TEMPERATURE (K)              =       563.00000
LIQUID VELOCITY (CM/S)       =       185.01583
GAS VELOCITY  (CM/S)         =       311.31834
VOID FRACTION                =          .52487
QUALITY                      =          .09000
GAMMA DOSE RATE (RAD/S)      =     0.14300E+06
NEUTRON DOSE RATE (RAD/S)    =     0.14300E+06
```

```
CYCLE    1        POSITION IN Core Boiling4     =      20.0000 cm
              CONCENTRATIONS[ppb]  AT POSITION =     531.0000 cm

e-       =    0.105998E-06 **      OH-       =    0.313862E+00 **
H2       =    0.127919E+02 **      OH        =    0.801228E+00 **
HO2-     =    0.137285E-02 **      H2O2      =    0.326403E+03 **
O2-      =    0.180379E+01 **      O2        =    0.110103E+03 **
H        =    0.271635E-03 **      H+        =    0.750656E-01 **
HO2      =    0.677497E-02 **      O2G       =    0.130190E+03 **
H2G      =    0.242294E+02 **

O2G       =   0.936E-04 ATM
H2G       =   0.279E-03 ATM

NO. STEPS                    =       141
TEMPERATURE (K)              =       563.00000
LIQUID VELOCITY (CM/S)       =       202.72538
GAS VELOCITY  (CM/S)         =       375.20211
VOID FRACTION                =          .58067
QUALITY                      =          .12000
GAMMA DOSE RATE (RAD/S)      =     0.14300E+06
NEUTRON DOSE RATE (RAD/S)    =     0.14300E+06
```

RUN STATISTICS FOR CYCLE 1 AT Core Boiling4

REQUIRED RWORK SIZE	=	308
IWORK SIZE	=	33
NUMBER OF STEPS	=	141
# OF FUNC.- EVALS.	=	172
# OF JACOB.- EVALS	=	28
COMPONENT JOB TIME	=	10. seconds

CONCENTRATION PROFILE OF Core Boiling4 HAS BEEN EVALUATED SUCCESSFULLY!

OUTPUT FOR CYCLE 1 AT Core Boiling5

INITIAL POSITION	=	531.00000 cm
FINAL POSITION	=	551.00000 cm
FLOW LENGTH	=	20.00000 cm
POSITION INCREMENT	=	20.00000 cm
POSITION OF ONSET OF BOILING	=	451.00000 cm
INLET TEMPERATURE	=	563.00000 Kelvin
OUTLET TEMPERATURE	=	563.00000 Kelvin
INLET LIQUID VELOCITY	=	96.60000 cm/s
PIPE INTERNAL DIAMETER	=	.67000 cm
WATER DENSITY	=	.73300 g/cc
VAPOR DENSITY	=	.03900 g/cc
PRESSURE	=	68.00000 atm
MASS FlowRate	=	0.25000E+02 g/s
SURFACE MATERIAL	=	Ti
GAMMA DOSE RATE MULTIPLIER	=	0.11900E+06 Rad/s
NEUTRON DOSE RATE MULTIPLIER	=	0.11900E+06 Rad/s
GConvert	=	0.76085E-09

GAMMA DOSE SHAPE FUNCTION COEFFICIENTS

GAMMA COEFFICIENT 0	=	0.10000E+01
GAMMA COEFFICIENT 1	=	0.00000E+00
GAMMA COEFFICIENT 2	=	0.00000E+00
GAMMA COEFFICIENT 3	=	0.00000E+00
GAMMA COEFFICIENT 4	=	0.00000E+00
GAMMA COEFFICIENT 5	=	0.00000E+00

NEUTRON DOSE SHAPE FUNCTION COEFFICIENTS

NEUTRON COEFFICIENT 0	=	0.10000E+01
NEUTRON COEFFICIENT 1	=	0.00000E+00
NEUTRON COEFFICIENT 2	=	0.00000E+00
NEUTRON COEFFICIENT 3	=	0.00000E+00
NEUTRON COEFFICIENT 4	=	0.00000E+00
NEUTRON COEFFICIENT 5	=	0.00000E+00

```
VOID FRACTION FUNCTION COEFFICIENTS
VOID FRACTION  COEFFICIENT  0   =   -0.67650E+00
VOID FRACTION  COEFFICIENT  1   =    0.15000E-02
VOID FRACTION  COEFFICIENT  2   =    0.00000E+00
VOID FRACTION  COEFFICIENT  3   =    0.00000E+00
VOID FRACTION  COEFFICIENT  4   =    0.00000E+00
VOID FRACTION  COEFFICIENT  5   =    0.00000E+00

CalcSurf                        =        T
VoidFlag                        =        F
CalcSens                        =        F
WriteRx                         =        F
WritePara                       =        T

RADIOLYSIS ABSOLUTE TOLERANCE   =    0.10000E-14
           RELATIVE TOLERANCE   =    0.10000E-04
```

```
CYCLE    1        POSITION IN Core Boiling5    =        .0000 cm
              CONCENTRATIONS[ppb]  AT POSITION =    531.0000 cm

e-       =    0.105998E-06 **     OH-      =    0.313862E+00 **
H2       =    0.127919E+02 **     OH       =    0.801228E+00 **
HO2-     =    0.137285E-02 **     H2O2     =    0.326403E+03 **
O2-      =    0.180379E+01 **     O2       =    0.110103E+03 **
H        =    0.271635E-03 **     H+       =    0.750656E-01 **
HO2      =    0.677497E-02 **     O2G      =    0.130190E+03 **
H2G      =    0.242294E+02 **

O2G       =   0.936E-04 ATM
H2G       =   0.279E-03 ATM

NO. STEPS                  =        0
TEMPERATURE (K)            =      563.00000
LIQUID VELOCITY (CM/S)     =      202.72538
GAS VELOCITY  (CM/S)       =      375.20211
VOID FRACTION              =         .58067
QUALITY                    =         .12000
GAMMA DOSE RATE (RAD/S)    =    0.11900E+06
NEUTRON DOSE RATE (RAD/S)  =    0.11900E+06
```

```
CYCLE    1        POSITION IN Core Boiling5    =      20.0000 cm
              CONCENTRATIONS[ppb]  AT POSITION =    551.0000 cm

e-       =    0.888898E-07 **     OH-      =    0.294098E+00 **
H2       =    0.115929E+02 **     OH       =    0.722090E+00 **
HO2-     =    0.126892E-02 **     H2O2     =    0.322294E+03 **
O2-      =    0.168504E+01 **     O2       =    0.111057E+03 **
H        =    0.222772E-03 **     H+       =    0.701578E-01 **
HO2      =    0.589239E-02 **     O2G      =    0.143423E+03 **
H2G      =    0.243951E+02 **

O2G       =   0.103E-03 ATM
H2G       =   0.281E-03 ATM

NO. STEPS                  =      116
```

TEMPERATURE (K)	=	563.00000
LIQUID VELOCITY (CM/S)	=	216.21429
GAS VELOCITY (CM/S)	=	439.08589
VOID FRACTION	=	.62024
QUALITY	=	.15000
GAMMA DOSE RATE (RAD/S)	=	0.11900E+06
NEUTRON DOSE RATE (RAD/S)	=	0.11900E+06

RUN STATISTICS FOR CYCLE 1 AT Core Boiling5

REQUIRED RWORK SIZE	=	308
IWORK SIZE	=	33
NUMBER OF STEPS	=	116
# OF FUNC.- EVALS.	=	142
# OF JACOB.- EVALS	=	26
COMPONENT JOB TIME	=	10. seconds

CONCENTRATION PROFILE OF Core Boiling5 HAS BEEN EVALUATED SUCCESSFULLY!

OUTPUT FOR CYCLE 1 AT Core Outlet

INITIAL POSITION	=	551.00000	cm
FINAL POSITION	=	582.00000	cm
FLOW LENGTH	=	31.00000	cm
POSITION INCREMENT	=	31.00000	cm
POSITION OF ONSET OF BOILING	=	451.00000	cm
INLET TEMPERATURE	=	563.00000	Kelvin
OUTLET TEMPERATURE	=	563.00000	Kelvin
INLET LIQUID VELOCITY	=	216.21429	cm/s
PIPE INTERNAL DIAMETER	=	.67000	cm
WATER DENSITY	=	.73300	g/cc
VAPOR DENSITY	=	.03900	g/cc
PRESSURE	=	68.00000	atm
MASS FlowRate	=	0.25000E+02	g/s
SURFACE MATERIAL	= Ti		
GAMMA DOSE RATE MULTIPLIER	=	0.22000E+05	Rad/s
NEUTRON DOSE RATE MULTIPLIER	=	0.66000E+04	Rad/s
GConvert	=	0.76085E-09	

GAMMA DOSE SHAPE FUNCTION COEFFICIENTS

GAMMA COEFFICIENT 0	=	0.10000E+01
GAMMA COEFFICIENT 1	=	0.00000E+00
GAMMA COEFFICIENT 2	=	0.00000E+00
GAMMA COEFFICIENT 3	=	0.00000E+00

```
GAMMA COEFFICIENT  4              =     0.00000E+00
GAMMA COEFFICIENT  5              =     0.00000E+00

NEUTRON DOSE SHAPE FUNCTION COEFFICIENTS
NEUTRON COEFFICIENT  0            =     0.10000E+01
NEUTRON COEFFICIENT  1            =     0.00000E+00
NEUTRON COEFFICIENT  2            =     0.00000E+00
NEUTRON COEFFICIENT  3            =     0.00000E+00
NEUTRON COEFFICIENT  4            =     0.00000E+00
NEUTRON COEFFICIENT  5            =     0.00000E+00

VOID FRACTION FUNCTION COEFFICIENTS
VOID FRACTION  COEFFICIENT  0     =     0.15000E+00
VOID FRACTION  COEFFICIENT  1     =     0.00000E+00
VOID FRACTION  COEFFICIENT  2     =     0.00000E+00
VOID FRACTION  COEFFICIENT  3     =     0.00000E+00
VOID FRACTION  COEFFICIENT  4     =     0.00000E+00
VOID FRACTION  COEFFICIENT  5     =     0.00000E+00

CalcSurf                          =         T
VoidFlag                          =         F
CalcSens                          =         F
WriteRx                           =         F
WritePara                         =         T

RADIOLYSIS ABSOLUTE TOLERANCE     =     0.10000E-14
           RELATIVE TOLERANCE     =     0.10000E-04
```

```
CYCLE    1        POSITION IN Core Outlet      =        .0000 cm
                CONCENTRATIONS[ppb]  AT POSITION =     551.0000 cm

e-       =    0.888898E-07 **     OH-      =    0.294098E+00 **
H2       =    0.115929E+02 **     OH       =    0.722090E+00 **
HO2-     =    0.126892E-02 **     H2O2     =    0.322294E+03 **
O2-      =    0.168504E+01 **     O2       =    0.111057E+03 **
H        =    0.222772E-03 **     H+       =    0.701578E-01 **
HO2      =    0.589239E-02 **     O2G      =    0.143423E+03 **
H2G      =    0.243951E+02 **

O2G       =   0.103E-03 ATM
H2G       =   0.281E-03 ATM

NO. STEPS                    =        0
TEMPERATURE (K)              =      563.00000
LIQUID VELOCITY (CM/S)       =      216.21429
GAS VELOCITY  (CM/S)         =      439.08589
VOID FRACTION                =         .62024
QUALITY                      =         .15000
GAMMA DOSE RATE (RAD/S)      =    0.22000E+05
NEUTRON DOSE RATE (RAD/S)    =    0.66000E+04
```

```
CYCLE    1        POSITION IN Core Outlet      =      31.0000 cm
                CONCENTRATIONS[ppb]  AT POSITION =     582.0000 cm

e-       =    0.209174E-07 **     OH-      =    0.194424E+00 **
H2       =    0.822251E+01 **     OH       =    0.216712E+00 **
```

HO2-	=	0.516764E-03 **	H2O2	=	0.199252E+03 **
O2-	=	0.100449E+01 **	O2	=	0.914181E+02 **
H	=	0.465308E-04 **	H+	=	0.428808E-01 **
HO2	=	0.204531E-02 **	O2G	=	0.163683E+03 **
H2G	=	0.249932E+02 **			

O2G = 0.118E-03 ATM
H2G = 0.287E-03 ATM

NO. STEPS	=	186
TEMPERATURE (K)	=	563.00000
LIQUID VELOCITY (CM/S)	=	216.21429
GAS VELOCITY (CM/S)	=	439.08589
VOID FRACTION	=	.62024
QUALITY	=	.15000
GAMMA DOSE RATE (RAD/S)	=	0.22000E+05
NEUTRON DOSE RATE (RAD/S)	=	0.66000E+04

RUN STATISTICS FOR CYCLE 1 AT Core Outlet

REQUIRED RWORK SIZE	=	308
IWORK SIZE	=	33
NUMBER OF STEPS	=	186
# OF FUNC.- EVALS.	=	226
# OF JACOB.- EVALS	=	32
COMPONENT JOB TIME	=	12. seconds

CONCENTRATION PROFILE OF Core Outlet HAS BEEN EVALUATED SUCCESSFULLY!

OUTPUT FOR CYCLE 1 AT Plenum Inlet

INITIAL POSITION	=	582.00000 cm
FINAL POSITION	=	646.00000 cm
FLOW LENGTH	=	64.00000 cm
POSITION INCREMENT	=	64.00000 cm
POSITION OF ONSET OF BOILING	=	451.00000 cm
INLET TEMPERATURE	=	563.00000 Kelvin
OUTLET TEMPERATURE	=	563.00000 Kelvin
INLET LIQUID VELOCITY	=	421.26126 cm/s
PIPE INTERNAL DIAMETER	=	.48000 cm
WATER DENSITY	=	.73300 g/cc
VAPOR DENSITY	=	.03900 g/cc
PRESSURE	=	68.00000 atm
MASS FlowRate	=	0.25000E+02 g/s
SURFACE MATERIAL	=	Ti

```
GAMMA DOSE RATE MULTIPLIER          =    0.22000E+04 Rad/s
NEUTRON DOSE RATE MULTIPLIER        =    0.11000E+04 Rad/s
GConvert                            =    0.76085E-09

GAMMA DOSE SHAPE FUNCTION COEFFICIENTS
GAMMA COEFFICIENT  0                =    0.10000E+01
GAMMA COEFFICIENT  1                =    0.00000E+00
GAMMA COEFFICIENT  2                =    0.00000E+00
GAMMA COEFFICIENT  3                =    0.00000E+00
GAMMA COEFFICIENT  4                =    0.00000E+00
GAMMA COEFFICIENT  5                =    0.00000E+00

NEUTRON DOSE SHAPE FUNCTION COEFFICIENTS
NEUTRON COEFFICIENT  0              =    0.10000E+01
NEUTRON COEFFICIENT  1              =    0.00000E+00
NEUTRON COEFFICIENT  2              =    0.00000E+00
NEUTRON COEFFICIENT  3              =    0.00000E+00
NEUTRON COEFFICIENT  4              =    0.00000E+00
NEUTRON COEFFICIENT  5              =    0.00000E+00

VOID FRACTION FUNCTION COEFFICIENTS
VOID FRACTION  COEFFICIENT  0       =    0.15000E+00
VOID FRACTION  COEFFICIENT  1       =    0.00000E+00
VOID FRACTION  COEFFICIENT  2       =    0.00000E+00
VOID FRACTION  COEFFICIENT  3       =    0.00000E+00
VOID FRACTION  COEFFICIENT  4       =    0.00000E+00
VOID FRACTION  COEFFICIENT  5       =    0.00000E+00

CalcSurf                            =         T
VoidFlag                            =         F
CalcSens                            =         F
WriteRx                             =         F
WritePara                           =         T

RADIOLYSIS ABSOLUTE TOLERANCE       =    0.10000E-14
           RELATIVE TOLERANCE       =    0.10000E-04
```

```
CYCLE    1        POSITION IN Plenum Inlet     =        .0000 cm
                CONCENTRATIONS[ppb]  AT POSITION =     582.0000 cm

e-       =    0.209174E-07 **     OH-      =    0.194424E+00 **
H2       =    0.822251E+01 **     OH       =    0.216712E+00 **
HO2-     =    0.516764E-03 **     H2O2     =    0.199252E+03 **
O2-      =    0.100449E+01 **     O2       =    0.914181E+02 **
H        =    0.465308E-04 **     H+       =    0.428808E-01 **
HO2      =    0.204531E-02 **     O2G      =    0.163683E+03 **
H2G      =    0.249932E+02 **

O2G      =   0.118E-03 ATM
H2G      =   0.287E-03 ATM

NO. STEPS                    =        0
TEMPERATURE (K)              =      563.00000
LIQUID VELOCITY (CM/S)       =      421.26126
GAS VELOCITY  (CM/S)         =      855.49329
VOID FRACTION                =         .62024
```

```
QUALITY                          =          .15000
GAMMA DOSE RATE (RAD/S)          =     0.22000E+04
NEUTRON DOSE RATE (RAD/S)        =     0.11000E+04
```

```
CYCLE    1        POSITION IN Plenum Inlet      =      64.0000 cm
                CONCENTRATIONS[ppb]  AT POSITION =     646.0000 cm

e-       =    0.238167E-08 **      OH-      =    0.188735E+00 **
H2       =    0.818807E+01 **      OH       =    0.385646E-01 **
HO2-     =    0.449944E-03 **      H2O2     =    0.179004E+03 **
O2-      =    0.694734E+00 **      O2       =    0.873358E+02 **
H        =    0.725991E-05 **      H+       =    0.328304E-01 **
HO2      =    0.104833E-02 **      O2G      =    0.166270E+03 **
H2G      =    0.248020E+02 **

O2G       =   0.120E-03 ATM
H2G       =   0.285E-03 ATM

NO. STEPS                        =        166
TEMPERATURE (K)                  =     563.00000
LIQUID VELOCITY (CM/S)           =     421.26126
GAS VELOCITY  (CM/S)             =     855.49329
VOID FRACTION                    =        .62024
QUALITY                          =        .15000
GAMMA DOSE RATE (RAD/S)          =     0.22000E+04
NEUTRON DOSE RATE (RAD/S)        =     0.11000E+04
```

RUN STATISTICS FOR CYCLE 1 AT Plenum Inlet

```
REQUIRED RWORK SIZE   =       308
IWORK SIZE            =        33
NUMBER OF STEPS       =       166
# OF FUNC.- EVALS.    =       197
# OF JACOB.- EVALS    =        29
COMPONENT JOB TIME    =        11. seconds
```

CONCENTRATION PROFILE OF Plenum Inlet HAS BEEN EVALUATED SUCCESSFULLY!

OUTPUT FOR CYCLE 1 AT Liq Plenum Out

```
INITIAL POSITION                 =     646.00000 cm
FINAL POSITION                   =     661.00000 cm
FLOW LENGTH                      =      15.00000 cm
POSITION INCREMENT               =      15.00000 cm
POSITION OF ONSET OF BOILING     =   99999.00000 cm
```

```
INLET TEMPERATURE                =      563.00000 Kelvin
OUTLET TEMPERATURE               =      563.00000 Kelvin
INLET LIQUID VELOCITY            =        3.27000 cm/s
PIPE INTERNAL DIAMETER           =        3.36000 cm
WATER DENSITY                    =         .73300 g/cc
VAPOR DENSITY                    =         .03900 g/cc
PRESSURE                         =       68.00000 atm
MASS FlowRate                    =    0.21250E+02 g/s

SURFACE MATERIAL                 = Ti

GAMMA DOSE RATE MULTIPLIER       =    0.22000E+03 Rad/s
NEUTRON DOSE RATE MULTIPLIER     =    0.22000E+00 Rad/s
GConvert                         =    0.76085E-09

GAMMA DOSE SHAPE FUNCTION COEFFICIENTS
GAMMA COEFFICIENT  0             =    0.10000E+01
GAMMA COEFFICIENT  1             =    0.00000E+00
GAMMA COEFFICIENT  2             =    0.00000E+00
GAMMA COEFFICIENT  3             =    0.00000E+00
GAMMA COEFFICIENT  4             =    0.00000E+00
GAMMA COEFFICIENT  5             =    0.00000E+00

NEUTRON DOSE SHAPE FUNCTION COEFFICIENTS
NEUTRON COEFFICIENT  0           =    0.10000E+01
NEUTRON COEFFICIENT  1           =    0.00000E+00
NEUTRON COEFFICIENT  2           =    0.00000E+00
NEUTRON COEFFICIENT  3           =    0.00000E+00
NEUTRON COEFFICIENT  4           =    0.00000E+00
NEUTRON COEFFICIENT  5           =    0.00000E+00

CalcSurf                         =         T
VoidFlag                         =         F
CalcSens                         =         F
WriteRx                          =         F
WritePara                        =         T

RADIOLYSIS ABSOLUTE TOLERANCE    =    0.10000E-14
           RELATIVE TOLERANCE    =    0.10000E-04
```

```
CYCLE    1        POSITION IN Liq Plenum Out   =        .0000 cm
              CONCENTRATIONS[ppb]  AT POSITION =     646.0000 cm

e-       =    0.238167E-08 **     OH-      =    0.188735E+00 **
H2       =    0.818807E+01 **     OH       =    0.385646E-01 **
HO2-     =    0.449944E-03 **     H2O2     =    0.179004E+03 **
O2-      =    0.694734E+00 **     O2       =    0.873358E+02 **
H        =    0.725991E-05 **     H+       =    0.328304E-01 **
HO2      =    0.104833E-02 **     O2G      =    0.166270E+03 **
H2G      =    0.248020E+02 **

NO. STEPS                  =         0
TEMPERATURE (K)            =       563.00000
LIQUID VELOCITY (CM/S)     =         3.27000
GAS VELOCITY  (CM/S)       =          .00000
VOID FRACTION              =          .00000
QUALITY                    =          .00000
```

```
GAMMA DOSE RATE (RAD/S)     =     0.22000E+03
NEUTRON DOSE RATE (RAD/S)   =     0.22000E+00
```

```
CYCLE    1          POSITION IN Liq Plenum Out    =      15.0000 cm
                CONCENTRATIONS[ppb]  AT POSITION =     661.0000 cm

e-        =    0.331109E-09 **      OH-       =    0.258441E+00 **
H2        =    0.211841E+01 **      OH        =    0.115491E-01 **
HO2-      =    0.162222E-03 **      H2O2      =    0.471383E+02 **
O2-       =    0.246893E+00 **      O2        =    0.101182E+03 **
H         =    0.521467E-06 **      H+        =    0.229233E-01 **
HO2       =    0.257826E-03 **      O2G       =    0.166270E+03 **
H2G       =    0.248020E+02 **

NO. STEPS                      =      178
TEMPERATURE (K)                =      563.00000
LIQUID VELOCITY (CM/S)         =        3.27000
GAS VELOCITY  (CM/S)           =         .00000
VOID FRACTION                  =         .00000
QUALITY                        =         .00000
GAMMA DOSE RATE (RAD/S)        =    0.22000E+03
NEUTRON DOSE RATE (RAD/S)      =    0.22000E+00
```

RUN STATISTICS FOR CYCLE 1 AT Liq Plenum Out

```
REQUIRED RWORK SIZE   =       308
IWORK SIZE            =        33
NUMBER OF STEPS       =       178
# OF FUNC.- EVALS.    =       220
# OF JACOB.- EVALS    =        33
COMPONENT JOB TIME    =        11. second
CONCENTRATION PROFILE OF Liq Plenum Out HAS BEEN EVALUATED SUCCESSFULLY!
```

OUTPUT FOR CYCLE 1 AT Liq Sample Line

```
INITIAL POSITION                =     661.00000 cm
FINAL POSITION                  =     717.00000 cm
FLOW LENGTH                     =      56.00000 cm
POSITION INCREMENT              =      56.00000 cm
POSITION OF ONSET OF BOILING    =   99999.00000 cm

INLET TEMPERATURE               =     563.00000 Kelvin
OUTLET TEMPERATURE              =     563.00000 Kelvin
INLET LIQUID VELOCITY           =     160.20000 cm/s
PIPE INTERNAL DIAMETER          =        .48000 cm
WATER DENSITY                   =        .73300 g/cc
```

```
VAPOR DENSITY                          =          .03900 g/cc
PRESSURE                               =        68.00000 atm
MASS FlowRate                          =     0.21250E+02 g/s

SURFACE MATERIAL                       = Ti

GAMMA DOSE RATE MULTIPLIER             =     0.22000E+04 Rad/s
NEUTRON DOSE RATE MULTIPLIER           =     0.11000E+04 Rad/s
GConvert                               =     0.76085E-09

GAMMA DOSE SHAPE FUNCTION COEFFICIENTS
GAMMA COEFFICIENT  0                   =     0.10000E+01
GAMMA COEFFICIENT  1                   =     0.00000E+00
GAMMA COEFFICIENT  2                   =     0.00000E+00
GAMMA COEFFICIENT  3                   =     0.00000E+00
GAMMA COEFFICIENT  4                   =     0.00000E+00
GAMMA COEFFICIENT  5                   =     0.00000E+00

NEUTRON DOSE SHAPE FUNCTION COEFFICIENTS
NEUTRON COEFFICIENT  0                 =     0.10000E+01
NEUTRON COEFFICIENT  1                 =     0.00000E+00
NEUTRON COEFFICIENT  2                 =     0.00000E+00
NEUTRON COEFFICIENT  3                 =     0.00000E+00
NEUTRON COEFFICIENT  4                 =     0.00000E+00
NEUTRON COEFFICIENT  5                 =     0.00000E+00

CalcSurf                               =         T
VoidFlag                               =         F
CalcSens                               =         F
WriteRx                                =         F
WritePara                              =         T

RADIOLYSIS ABSOLUTE TOLERANCE          =     0.10000E-14
           RELATIVE TOLERANCE          =     0.10000E-04
```

```
CYCLE    1        POSITION IN Liq Sample Line  =          .0000 cm
                CONCENTRATIONS[ppb]  AT POSITION =     661.0000 cm

e-       =    0.331109E-09 **     OH-      =    0.258441E+00 **
H2       =    0.211841E+01 **     OH       =    0.115491E-01 **
HO2-     =    0.162222E-03 **     H2O2     =    0.471383E+02 **
O2-      =    0.246893E+00 **     O2       =    0.101182E+03 **
H        =    0.521467E-06 **     H+       =    0.229233E-01 **
HO2      =    0.257826E-03 **     O2G      =    0.166270E+03 **
H2G      =    0.248020E+02 **

NO. STEPS                      =        0
TEMPERATURE (K)                =      563.00000
LIQUID VELOCITY (CM/S)         =      160.20000
GAS VELOCITY  (CM/S)           =         .00000
VOID FRACTION                  =         .00000
QUALITY                        =         .00000
GAMMA DOSE RATE (RAD/S)        =    0.22000E+04
NEUTRON DOSE RATE (RAD/S)      =    0.11000E+04
```

```
CYCLE    1        POSITION IN Liq Sample Line  =       56.0000 cm
```

CONCENTRATIONS[ppb] AT POSITION = 717.0000 cm

e-	=	0.338599E-08 **	OH-	=	0.202262E+00 **
H2	=	0.302627E+01 **	OH	=	0.425919E-01 **
HO2-	=	0.174896E-03 **	H2O2	=	0.649102E+02 **
O2-	=	0.589600E+00 **	O2	=	0.998100E+02 **
H	=	0.382110E-05 **	H+	=	0.303342E-01 **
HO2	=	0.819014E-03 **	O2G	=	0.166270E+03 **
H2G	=	0.248020E+02 **			

NO. STEPS	=	141
TEMPERATURE (K)	=	563.00000
LIQUID VELOCITY (CM/S)	=	160.20000
GAS VELOCITY (CM/S)	=	.00000
VOID FRACTION	=	.00000
QUALITY	=	.00000
GAMMA DOSE RATE (RAD/S)	=	0.22000E+04
NEUTRON DOSE RATE (RAD/S)	=	0.11000E+04

RUN STATISTICS FOR CYCLE 1 AT Liq Sample Line

REQUIRED RWORK SIZE	=	308
IWORK SIZE	=	33
NUMBER OF STEPS	=	141
# OF FUNC.- EVALS.	=	184
# OF JACOB.- EVALS	=	26
COMPONENT JOB TIME	=	11. seconds

CONCENTRATION PROFILE OF Liq Sample Line HAS BEEN EVALUATED SUCCESSFULLY!
**** ERROR IN INPUT NODE INFORMATION. SUM OF FLOWRATES IS ZERO.
PROGRAM TERMINATED AT SUBROUTINE AVERAGEFLOW.

Appendix C

Neutron and Gamma Dose Rates

C.1 Introduction

The function of this appendix is to summarize the analyses and computations carried out to establish the neutron and gamma dose rates in the BCCL and how they relate to those in a BWR.

First considered are rough bounds which can be established by simple energy balance considerations. This approach also helps to identify sources of error in other calculations and measurements, and to suggest reasons for the differences between the MITR and a full-scale BWR.

The next subtopic is the use of Monte Carlo computations to compare dose rates in the BWR and MITR.

A final subsection investigates the extent to which the dose rates inside the BCCL thimble may differ from those in MITR coolant.

C.2 Estimate of Gamma Dose Rate in H_2O in BWR AND MITR Cores

C.2.1 BWR

An energy balance can be employed to estimate the gamma dose rate.

Per fission, gamma energies are as follows:

	Mev	Ref
Prompt γ	6.97	(1)
Delayed γ	6.33	(1)
Capture γ	~ 6.72	(2)
Inelastic γ	$\leq$ 1.63	(3)
TOTAL	$\leq$21.65	

Hence, for a total energy per fission of 200 Mev, the fraction emitted as gammas is 0.11. This ignores the small contribution by bremsstrahlung and Cerenkov photons, leakage, and the differences among fissioning nuclides. (Prompt plus decay gamma

energies for U-235, U-238, Pu-239, Pu-241 are 13.30, 14.56, 12.93, 14.04 Mev, respectively). We also ignore spatial heterogeneity (hence attenuation of gammas in fuel during first-flight escape).

The fraction of this gamma energy absorbed in H_2O can be estimated using the following data:

	density ρ_i g/cm^3	volume fraction, v_i	$\mu a/\rho$, cm^2/g (5)
H_2O	$\bar{\rho} = 0.44$	0.654	0.023
UO_2	9.54	0.214	0.033
Zr	6.5	0.132	0.023

Thus the fraction absorbed in H_2O is 0.071; and at a power density of q''' kw/l

$$D\gamma \approx 3.6 \times 10^8 (0.11) (0.071) q'''/[(0.44)(0.654)] = 9.77 \times 10^6 q''' \text{ R/hr}$$

or if q''' = 51 kw/l,

$$D\gamma \approx \underline{4.98 \times 10^8 \text{ R/hr}} \approx \underline{1.38 \times 10^5 \text{ R/s}}$$

which compares favorably to values of $4 \pm 1 \times 10^8$ R/hr quoted by BWR vendors (GE/Hitachi/ABB, normalized to 51 Kw/l) (6).

C.2.2 MITR

The MITR-II employs fully enriched fuel in an element which is essentially 57% H_2O, 43% Al in volume (only ~ 1% is U). Hence we may neglect capture in or inelastic scattering by U-238. The coolant is also at low temperature (~50°C). Removal of fast neutrons by Al is small; hence we assume all neutron downscattering is by H_2O. Hence with the above assumptions, inelastic gamma contributions are negligible. Per fission there are roughly 0.05 captures each in Al and H_2O.

For capture gammas we take, per fission (neglecting captures in U-238 and control poison):

U-235: 6.4 α Mev = 6.4 (0.2) = 1.28 Mev
where α is the capture to fission ratio

Al: 7.7 (0.05)
H_2O: 2.2 (0.05)
} 0.5 Mev

Hence per fission, gamma energies are:

Prompt γ	6.97
Delayed γ	6.33
Capture γ	~1.78
TOTAL	15.08

which, at 200 Mev per fission, is a fractional yield of 0.075.

Assuming $\mu a/\rho$ is 0.021 cm^2/g for Al, which has a density of 2.7 g/cc, and that the core contains equal volumes of Al and H_2O (at ρ = 1.0 g/cc), gives a fraction absorbed in H_2O of 0.35.

Finally, at a power density of 70 kw/l, the dose rate is:

$$D\gamma \cong 3.6 \times 10^8 \, (0.075) \, (0.35) \, (70)/(0.5) \times 1, \text{ R/hr, or}$$
$$D\gamma \cong 13 \times 10^8 \text{ R/hr} = 3.7 \times 10^5 \text{ R/s}$$

which is a factor of three higher than we have earlier estimated for a BWR, and also higher than prior estimates for the MITR.

It should be noted, however, that several factors suggest that the above dose rate is an overestimate:

(1) Where the BWR core is large, the MITR core is small, hence leakage is important for the MITR. The effective spherical radius of the MITR core is only 25 cm.

(2) The BWR results are for sustained operation at 100% power, such that fission product decay gammas attain their asymptoptic value; the MITR normally operates weekdays, and shuts down weekends, yielding an effective capacity factor of ~60%. Hence the decay gamma contribution could be as much as 40% lower than used in our estimate.

(3) The BCCL experiment H_2O is isolated from the core by successive layers of Al, Ti, Pb, Zr, which will attenuate some of the core-produced gammas.

Hence a value as low as 2 x 10^5 R/s is plausible, which is roughly twice that in a BWR.

References and Footnotes

(1) EPRI NP-1771, Fission Energy Release For 16 Fissioning Nuclides, March 1981.

(2) Capture gamma energy is estimated by assuming:

(a) $\nu - 1 \equiv 1.4$ captures per fission.

(b) The capture γ energy corresponds to that for U-238, the dominant capturing species, ie. 4.8 Mev.
(other absorbers of some importance include H, Zr, B at ~2.2, 6.9, 0.48, Mev, respectively).

(3) An upper limit on de-excitation γ energy from inelastic neutron scattering is obtained by assuming:

(a) All of the energy deposited by the inelastically scattered neutrons is emitted as gammas.

(b) All neutron removal by materials other than H_2O is by inelastic removal and represented by U-238, the dominant inelastic scatterer.

(c) Following Ref. (4), inelastically scattered neutrons are assumed to have a Maxwellian energy distribution, with an average temperature of the residual nucleus, T = 0.33 Mev for U-238:

$$N(E) \sim E\, e^{-E/T}$$

Hence the average energy of the scattered neutrons is 2T = 0.66 Mev.

(d) From a previous note: 44% of removal is by other than H_2O, and E_n = 5.3 Mev; since $\nu = 2.4$, the average fission neutron energy is 2.2 Mev, of which (2.2 - 0.66) 1.54 Mev is inelastically deposited and re-emitted as gammas.

(e) Thus inelastic gamma energy is approximately (2.4) (1.54) (0.44) = 1.63 Mev.

(4) G. Szwarcbaum, M. Sieger and S. Yiftah, "Inelastic Scattering of High-Energy Neutrons in Fast Reactors", Vol. 6, ICPUAE, Geneva (1965).

(5) R. N. MacDonald and H. H. Baucon, "Nuclear Data for Reactor Studies", NUCLEONICS, Vol. 20, No. 8, August 1962.

(6) eg. GE(Ruiz) letter of 7/11/91 quotes 3.73 x 10^8 R/hr (normalized to 51 Kw/l)

C.3 Neutron Dose Rates in BWR and MITR

C.3.1 BWR

A. Upper Bound

If one assumes that all energy carried by the neutrons released in fission is deposited in H_2O, an upper bound on the neutron dose rate should be realized.

Reference (1) gives the following values for neutron energy/fission; also shown are approximate values for the relative contribution to fissions in a BWR core:

Isotope	Mev	% of fissions
U-235	4.79 ± 0.07	50
U-238	5.51 ± 0.10	8
Pu-239	5.9 ± 0.10	36
Pu-241	5.99 ± 0.13	6

Hence in a steady state core we take ~ 5.3 Mev/fission and a total energy/fission of 200 Mev.

Other parameters and conversion factors required are:

1 Mev = 1.6×10^{-13} watt sec = 1.6×10^{-6} erg

Core Avg. q''' = 51 Kw/l

Core Ave. water content: 0.288 Kg/l (at HFP)

1 R = 100 erg/g

$$\text{Thus max n dose} = \left(\frac{51\ \text{Kw/l}}{0.288\ \text{Kg/l}} \times \frac{5.3}{200}\right) \frac{\text{watts}}{\text{g}} \times 10^{+7} \frac{\text{erg}}{\text{watt sec}} \times \frac{1\text{R}}{100\ \text{erg/g}} \times \frac{3600\ \text{sec}}{\text{hr}}$$

or

$D\ n_{max} = 16.89 \times 10^8$ R/hr

which compares to the value of 10.3×10^8 R/hr quoted by GE in Ref. (2).

(1) EPRI NP-1771, Fission Energy Release for 16 Fissioning Nuclides, March 1981.

(2) C. Ruiz (GE) letter to M. Driscoll (MIT), dated 7/11/91.

B. Lower Bound

At high neutron energies heavy nuclei can remove considerable energy by inelastic scattering, which is much more effective than the elastic scattering which prevails at lower energies. Hence we can compute a lower bound on the energy deposited in H_2O by assuming that the fractional removal by heavy nuclei at high energy applies to neutrons of all energies.

Removal cross sections for fission spectrum neutrons are available in the literature Ref. (3), from which we may construct the following table:

Constituent	Σ_R, cm-1	Vol. % in BWR core
UO_2	0.075	21.4
Zr	0.038	13.2
H_2O (300°C)	0.073	65.4

Thus the fraction of removal by (energy deposition in) H_2O is computed to be (ignoring neutron leakage, which is only a few percent in a large BWR):

$$F \geq 0.69$$

Combined with our prior estimate for 100% deposition in H_2O, this gives:

$$D\, n_{min} = 11.65 \times 10^8 \text{ R/hr}$$

which is close to the GE estimate.

(3) M. K. Sheaffer et al., "A One-Group Method for Fast Reactor Calculations," MIT Nucl. Eng. Dept., MITNE-108, September 1970.
Other formulations are available, but would give roughly comparable relative results, eg: L, K. Zoller, "Fast Neutron Removal Cross Sections," Nucleonics, Vol. 22, No. 8, August 1964.

C.3.2 MITR

In the MIT Reactor virtually all fissions are in U-235, (hence giving 4.79 Mev/fission), the core average water content is ~ 0.57 Kg/l, and the core average power density, q''' = 70 Kw/l.

Hence the upper limit neutron dose, using the same prescription as earlier is:

$$D\,n_{max} = 10.6 \times 10^8 \text{ R/hr} = 2.9 \times 10^5 \text{ R/s}$$

Note, however, that a large fraction of fission-generated neutrons leak out of the small MITR core — predominantly at high energies. Hence the above value is a cruder upper limit than in a large BWR core.

As to the lower bound, the removal cross section for Al, $\Sigma_R = 0.028$ cm^{-1}, and that for H_2O at 50°C, $\Sigma_R = 0.10$ cm^{-1}. Hence for a 57/43 mixture, H_2O will absorb 83% of the neutron energy; thus:

$$D\,n_{min} = 8.8 \times 10^8 \text{ R/hr} = 2.4 \times 10^5 \text{ R/s}$$

which is comparable to BWR values.

The comment regarding leakage again applies, however.

C.4 Monte Carlo Calculations of a Representative BWR Unit Cell

The MCNP program was used to calculate neutron and gamma energy deposition in the typical unit cell (fuel, cladding, coolant) shown in Figure C.1. Note that the cladding thickness and water volume are augmented to account for non-fuel structure and bypass region water, to reproduce core-average composition.

MCNP output is given as Mev per gram H_2O per fission neutron. This was converted to R/s using 2.418 neutrons per U-235 fission to give:

$$D\,n = 3.02 \times 10^5 \text{R/s}$$

$$D\gamma = 7.64 \times 10^4 \text{ R/s}$$

This latter value, however, is for a fresh core, and does not account for fission product decay gammas. If one multiplies by the ratio with/without taken from the energy yield data cited earlier:

$$D\gamma = 1.12 \times 10^5 \text{ R/s}$$

This is in excellent agreement with the consensus vendor estimates of

$$D\gamma = 4 \pm 1 \times 10^8 \text{ R/hr} = 1.11 \pm 0.28 \times 10^5 \text{ R/s}$$

The neutron dose rate is also in good agreement with the GE estimates of 2.86×10^5 R/s.

Hence we have some confidence that MCNP can be used to establish core dose rates.

- core effective height = 3.8 m
- enrichment: 2.0 wt% U-235
- Temperatures:
  Coolant: 558K
  Pellet: 900K
- power per fuel rod = 83.4 kw
- density
  UO_2* = 9.54 g/cc
  Zr = 6.5 g/cc
  H_2O = 0.44 g/cc (averaged; including steam "voids")

* The gap has been homogenized with the fuel.

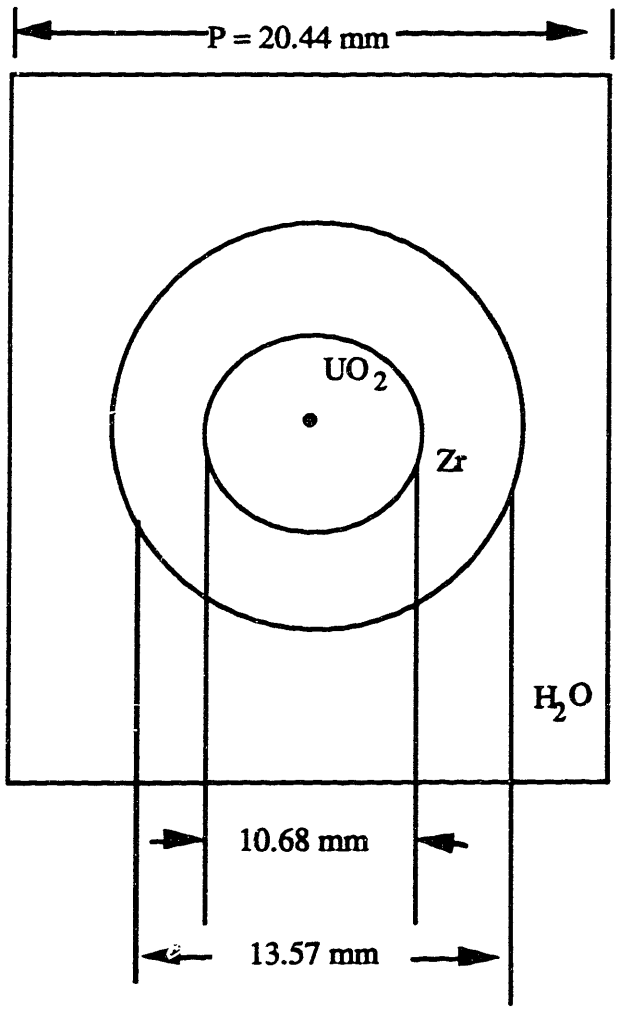

Figure C.1 A Representative BWR Core Unit Cell

C.5 MCNP Results for the MITR

The MCNP program was also used to calculate neutron and gamma energy deposition in the MIT reactor. Since the BCCL loop is located in the A-ring region of the MIT reactor, only the results for the A-ring are presented here as a comparison with the BCCL dose rates. Figure C.2 shows the dose rate distributions of the prompt gammas and neutrons in the MITR. Note that the neutron and gamma dose rates have essentially the same profile in-core. Figures C.3 and C.4 show the results of curve fitting the gamma and neutron dose rate distributions in the in-core region and above-core region, respectively.

C.6 Gamma Attenuation in BCCL

Most of the gamma flux to which BCCL H_2O is exposed originates in the MITR core. Hence one must account for attenuation. An approximate estimate follows. First the attenuation coefficient must be estimated; for the in-core section one has the following (where A is the cross sectional area in a horizontal slice):

Material	A, cm^2	ρ g/cm^3	μ/ρ cm^2/g	μA
Al (dummy)	12.0	2.7	0.021	0.680
Al (thimble)	5.07	2.7	0.021	0.287
Ti (can)	2.84	4.5	0.022	0.281
Pb (bath)	5.22	11.3	0.031	1.829
Zy (tubes)	0.29	6.4	0.023	0.043
MgO (heater)	1.20	3.6	0.022	0.095
Fe	0.80	7.8	0.025	0.156
	27.42			3.371

Thus $\bar{\mu} = 0.123\ cm^{-1}$

and R = effective cylindrical radius = 2.95 cm

The transport theory expression for attenuation of isotropically incident photons at the center of a cylinder is:

$$f \cong 1 - \frac{4}{3}\mu R = 0.52$$

Thus the gamma flux in the BCCL H_2O could be as much as a factor of two less than that in the MITR core H_2O.

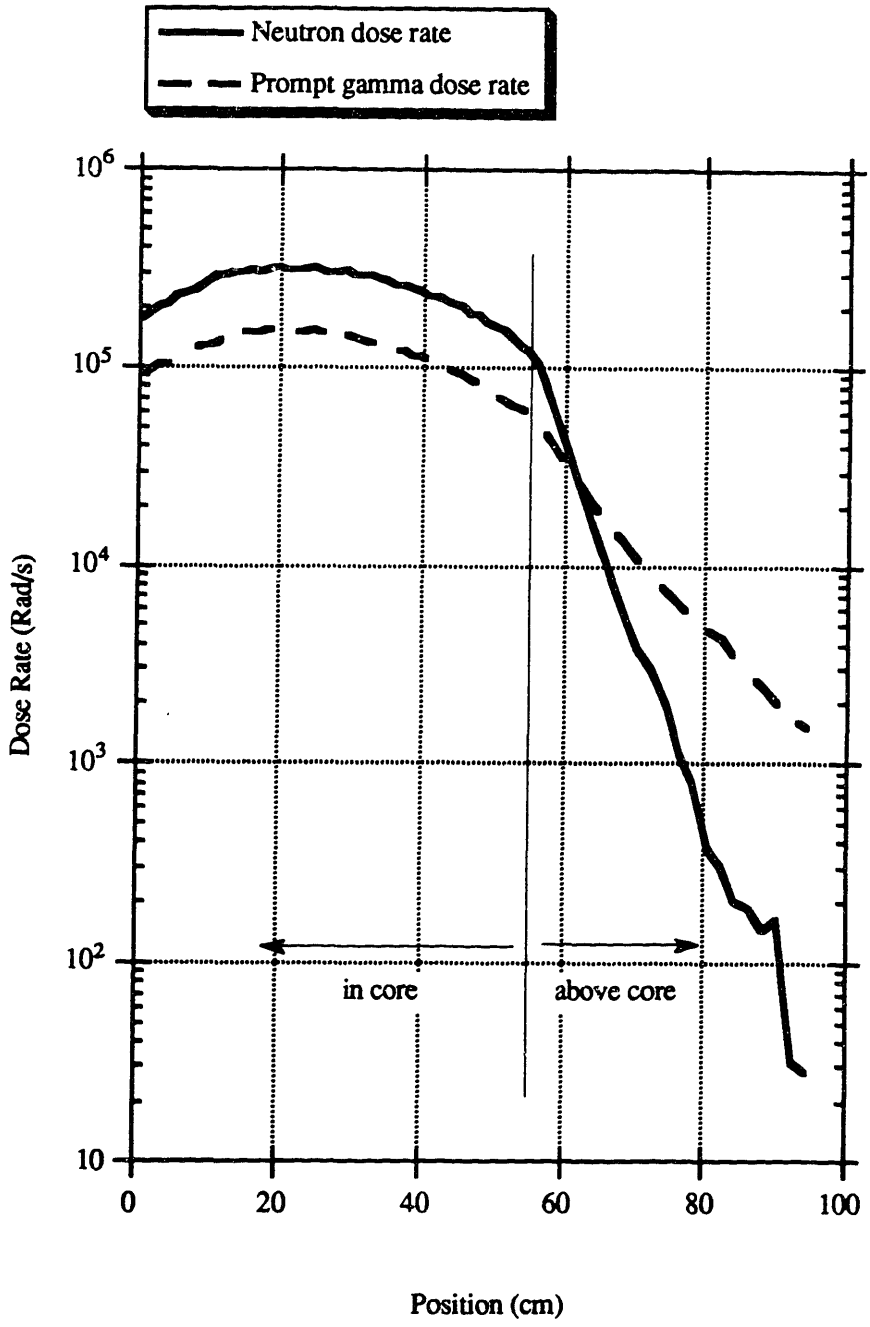

Figure C.2 Dose rate distributions in the MITR calculated by MCNP

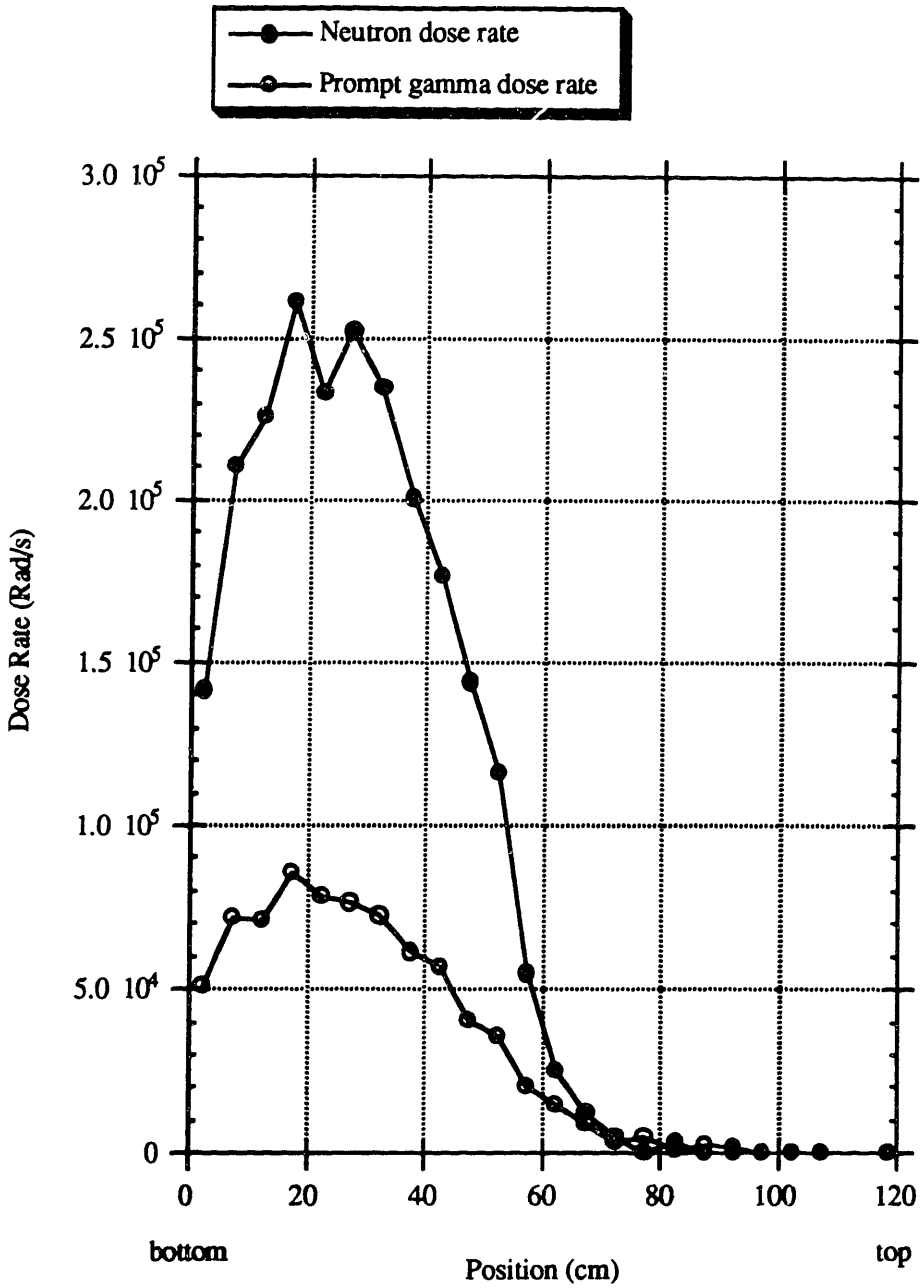

Figure C.3 Dose rate distributions in the BCCL calculated by MCNP

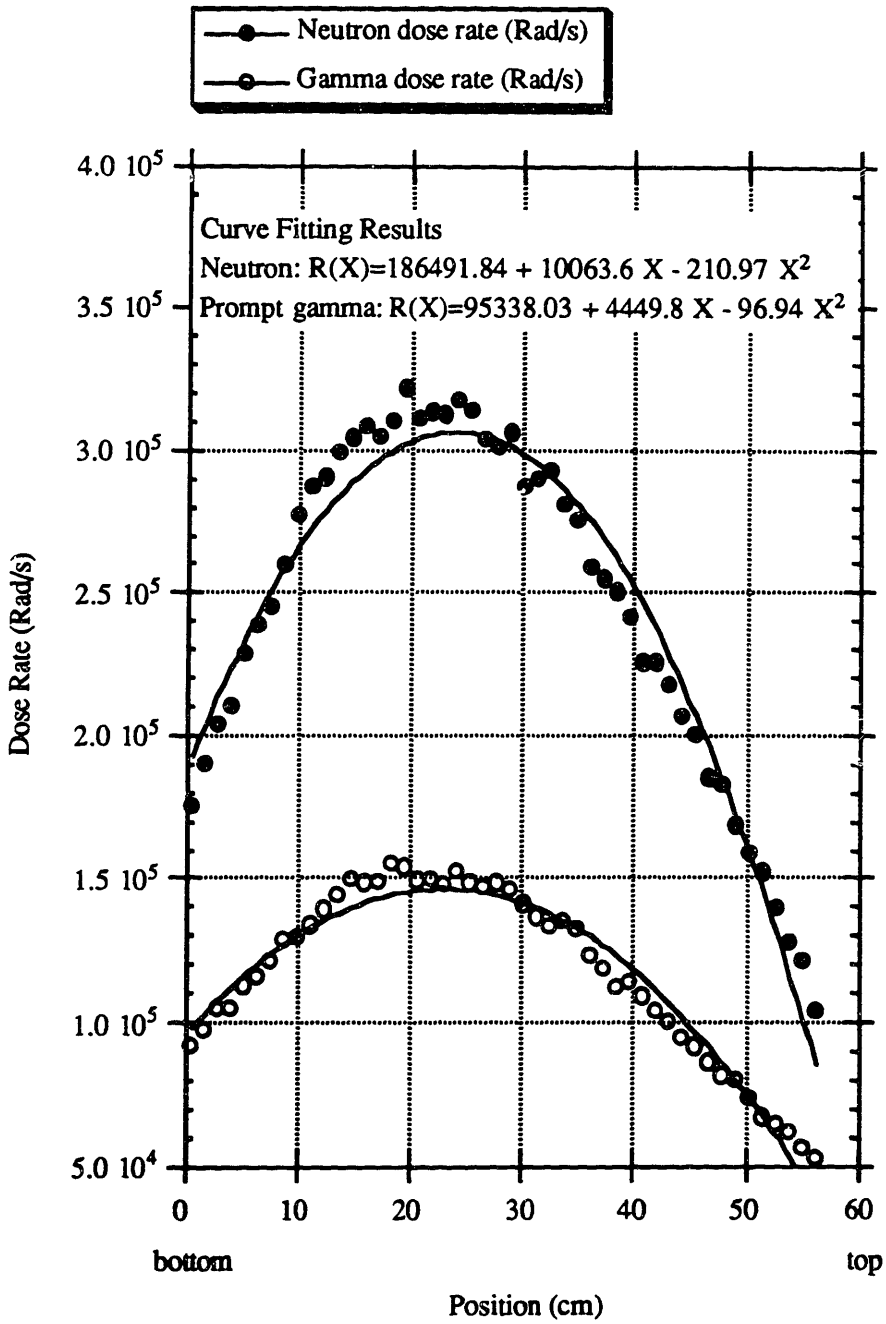

Figure C.4 Dose rate distributions in the MITR-II core region calculated by MCNP

Note that if Pb is replaced by Mg, the gamma flux will increase significantly; also note that the IASCC and SENSOR facilities, which do not have an in-pile Pb bath, will have higher gamma flux than the BCCL. Conversely, the attenuation by Pb makes the BCCL a better simulation of an actual BWR.

C.7 MCNP Results for the BCCL

The prompt gamma and neutron dose rates were calculated by MCNP. Both prompt gamma and neutron attenuation are taken into account. Figure C.5 shows the prompt gamma and neutron dose rates in the coolant of the BCCL loop. Notice that attenuation by the BCCL thimble and internals has a more significant effect on the prompt gamma dose rate. Since the MCNP calculation did not account for capture and fission product decay gammas, a correction has to be made to get the total gamma dose rate. For a capacity factor of 60% for the MITR (please refer to C.2.2), the total gamma dose rate can be calculated as follows:

$$R_\gamma = (R_{\gamma,\text{prompt fission}}+R_{\gamma,\text{prompt capture}})\cdot \frac{E_{\gamma,\text{prompt fission}}+E_{\gamma,\text{prompt capture}}+E_{\gamma,\text{decay}}\cdot 0.6}{E_{\gamma,\text{prompt fission}}+E_{\gamma,\text{prompt capture}}}$$

where $E_{\gamma,\text{prompt fission}}$ = 6.97 MeV, $E_{\gamma,\text{prompt capture}}$ = 1.78 MeV and $E_{\gamma,\text{decay}}$ = 6.33 MeV.

The dose rates in the coolant pool in the reactor and above the reactor core at the A-ring position were curve-fitted as shown in Figs. C.6 and C.7. The average dose rates in-core for the MITR and the BCCL are summarized in Table C.1.

Table C.1 Coolant average dose rates in the MITR A-ring and BCCL.

	avg. neutron dose rates	avg. prompt gamma dose rates	prompt plus decay gammas
MITR A-ring	2.453e+5	1.174e+5	1.684e+5
above core region (30 cm from 9 cm above active fuel)	0.0182e+5	0.0152e+5	0.0218e+5
BCCL (in core)	1.996e+5	0.636e+5	0.912e+5
all dose rates are in units of Rad/s.			

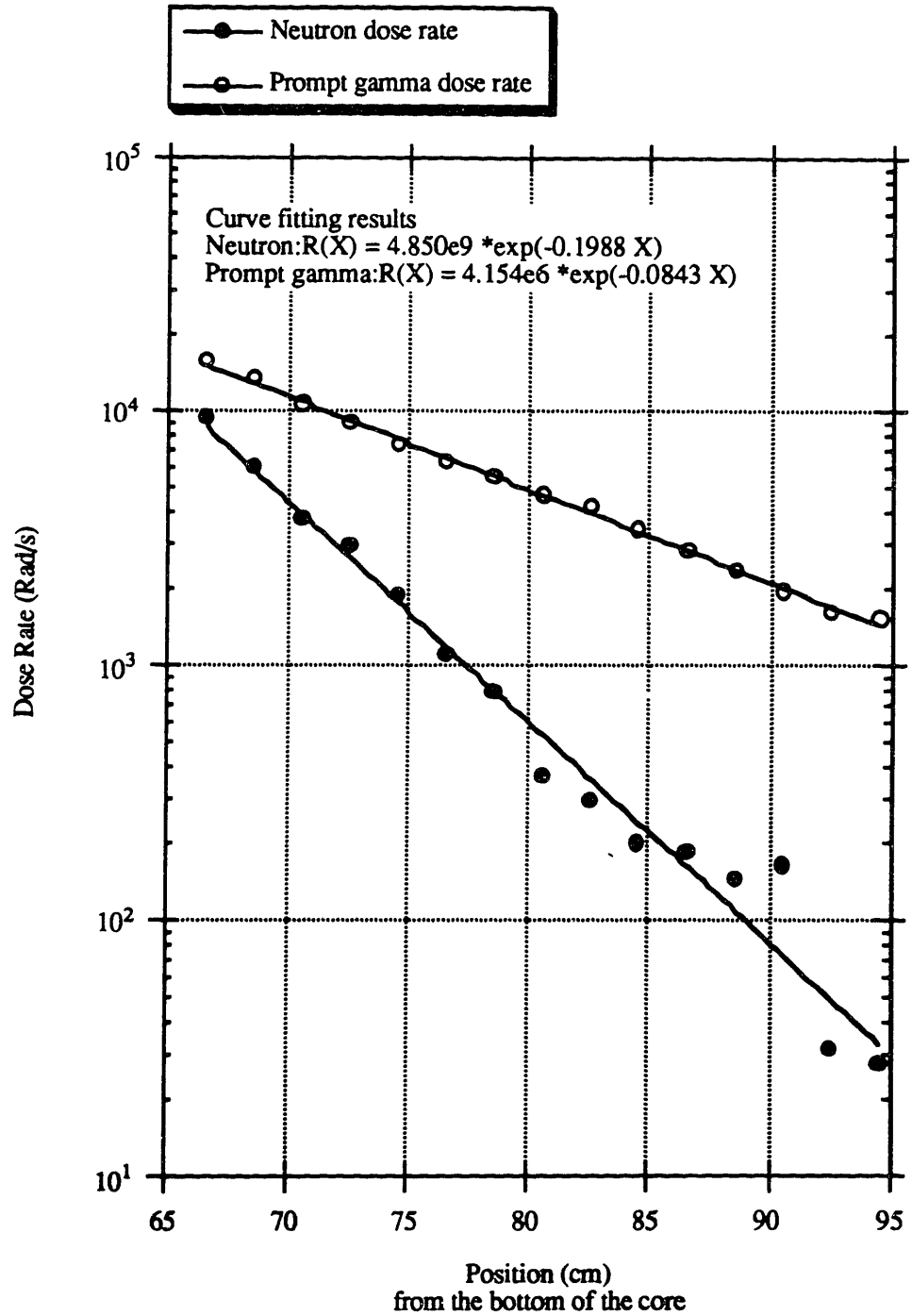

Figure C.5 Dose rate distributions above the MITR-II core region calculated by MCNP

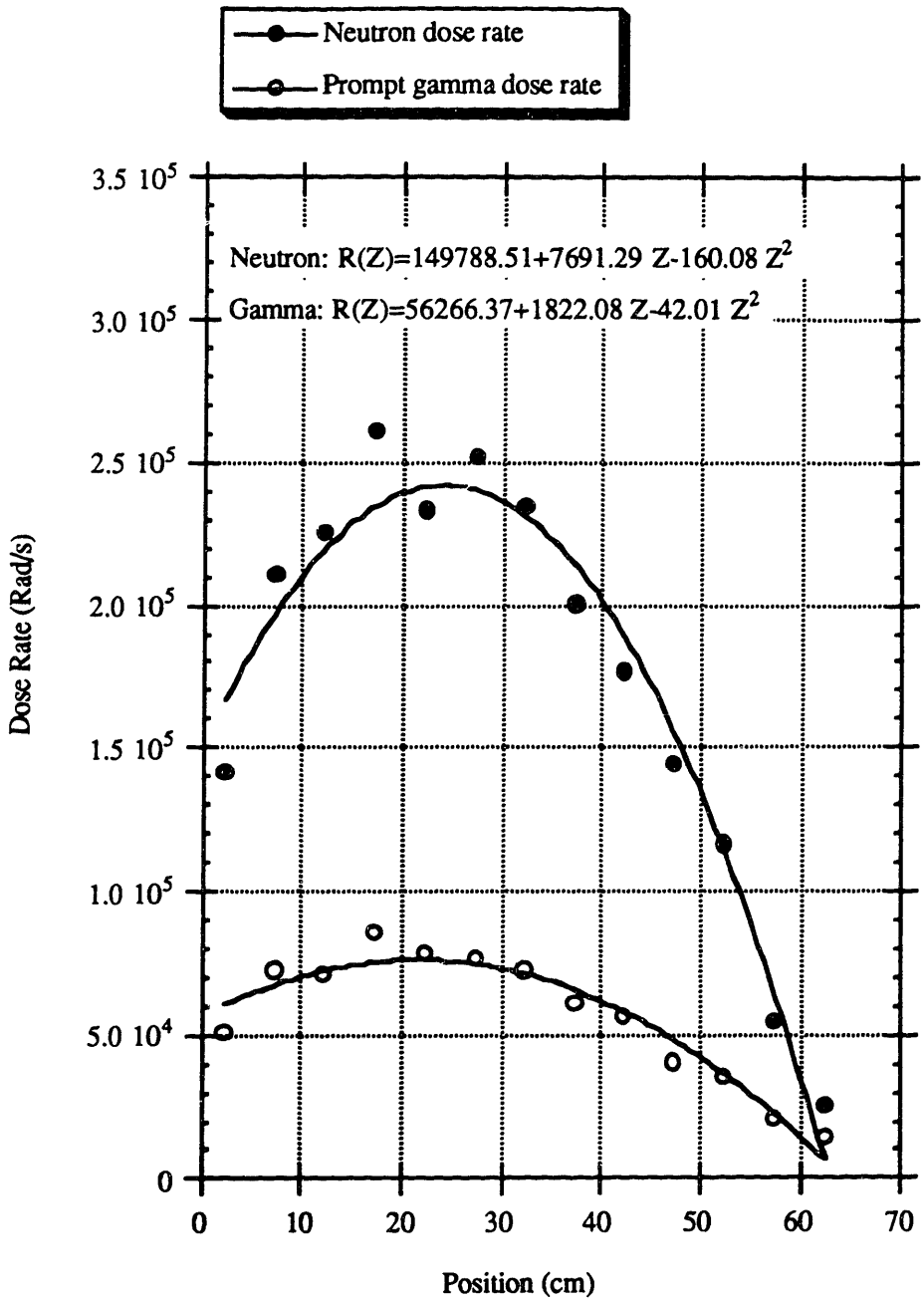

Figure C.6 Dose rate distributions in the BCCL in-core region calculated by MCNP

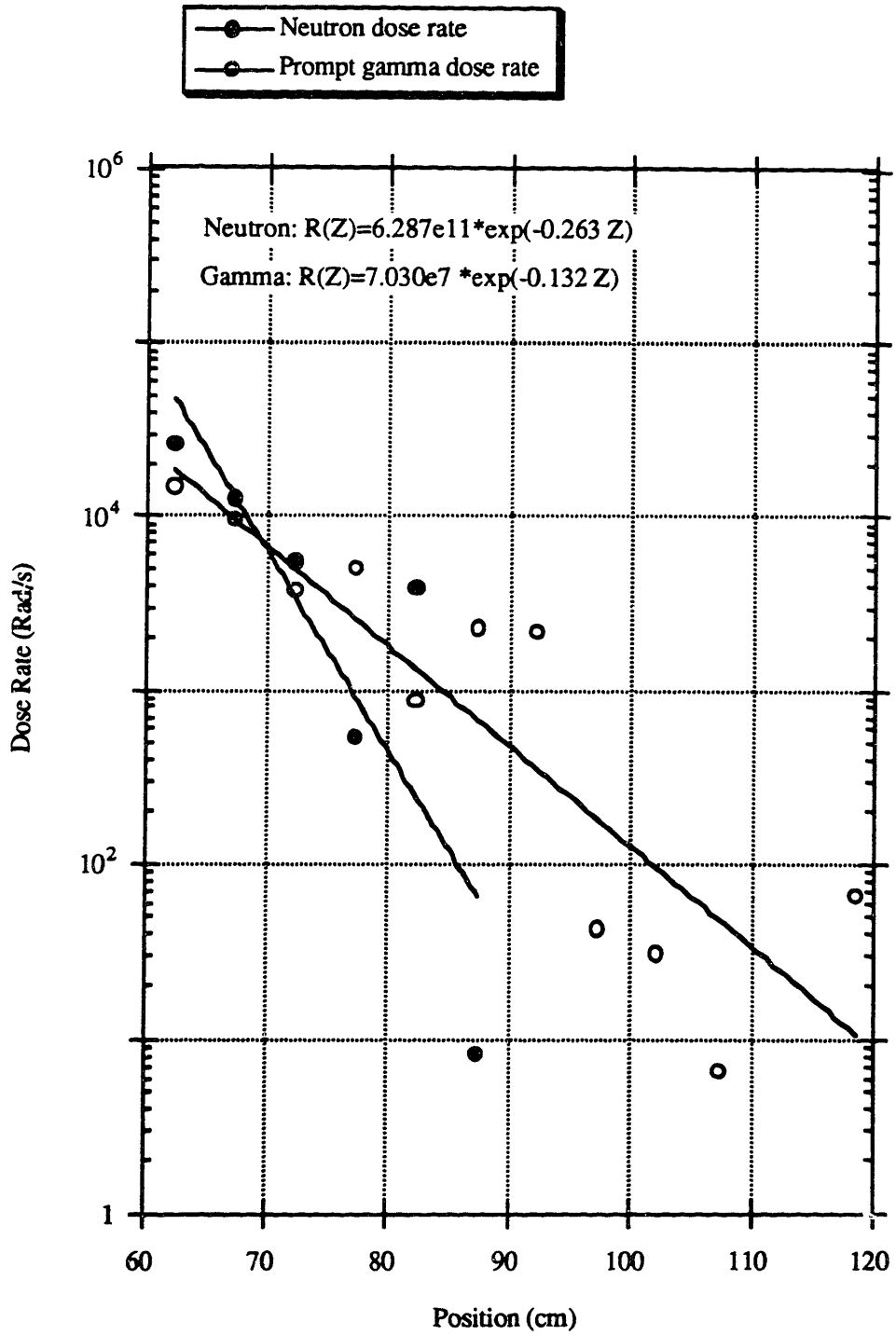

Figure C.7 Dose rate distributions calculated by MCNP in out-of-core region of the BCCL

The curve fitting results used to calculate BCCL dose rates are shown in Table C.2. Note that the MITR above-core dose rate equations are used since they have better statistics and are more conservative (i.e., a high-side estimate). Also note that the gamma dose rates are for total dose rates (prompt plus decay).

Table C.2 Neutron/Gamma dose rate equations used in BCCL Calculations

Items	Equations	Range
in-core total gamma	$80685.97 + 2612.86\ Z - 60.24\ Z^2$	Z=0 to 60 cm
above-core total gamma	$5.957 \times 10^6 \exp(-0.0843\ Z)$	Z> 60 cm
in-core neutron	$149788.51 + 7691.29\ Z - 160.08\ Z^2$	Z=0 to 60 cm
above-core neutron	$4.850 \times 10^9 \exp(-0.1988\ Z)$	Z> 60 cm
All dose rates are in units of Rad/s. Gamma doses have been augmented to account for the decay gamma contribution. Z is the distance from the bottom of the in-core Zircaloy U-tube, measured upwards.		

The polynomials can be used in RADICAL to simulate neutron and gamma dose rates in the best-estimate case. Note, however, that in RADICAL, all distances are measured from the inlet to the first node. Hence Z must be adjusted accordingly.

Appendix D

Interface Dose Experiment

The question has been raised as to whether important metal/water (i.e. high Z, A/low Z, A) interfacial effects on gamma doses are created by postulated differences in secondary electron spectra. As noted in Figure D.1, intra-fuel channels in a BWR (or tube ID in the BCCL) are on the same order as energetic electron range, hence such effects can not be ruled out.

To estimate the potential importance of the tube wall — water interface relative to our BWR experiments, the following experiment was carried out. Thin disk shaped dosimeters containing radiochromatic dyes were placed between pairs of disks, of steel, acrylic plastic, titanium, aluminium, graphite and lead. The arrangement is shown in the figure which follows. All discs were $1\frac{1}{8}$ inches in diameter, and all discs were sufficiently thick to assure secondary electron equilibrium.

The stack of dosimeters and disks of various materials were irradiated in an air-filled plastic capsule which was suspended above the core of the MITR-II. The reactor was shutdown for 74 hours prior to the gamma irradiation and was kept shutdown during this irradiation. The irradiation was performed about 12 inches above the upper grid plate of the core. Care was taken to rotate the capsule to insure uniform irradiation dose to all parts of the capsule.

The results are in the following table:

Material	Absorbed Dose (Gy)
Acrylic Samples 1	25
2	24
3	24
Pb	22
Ti	23
Fe	22
C	22
Al	23
Teflon	23

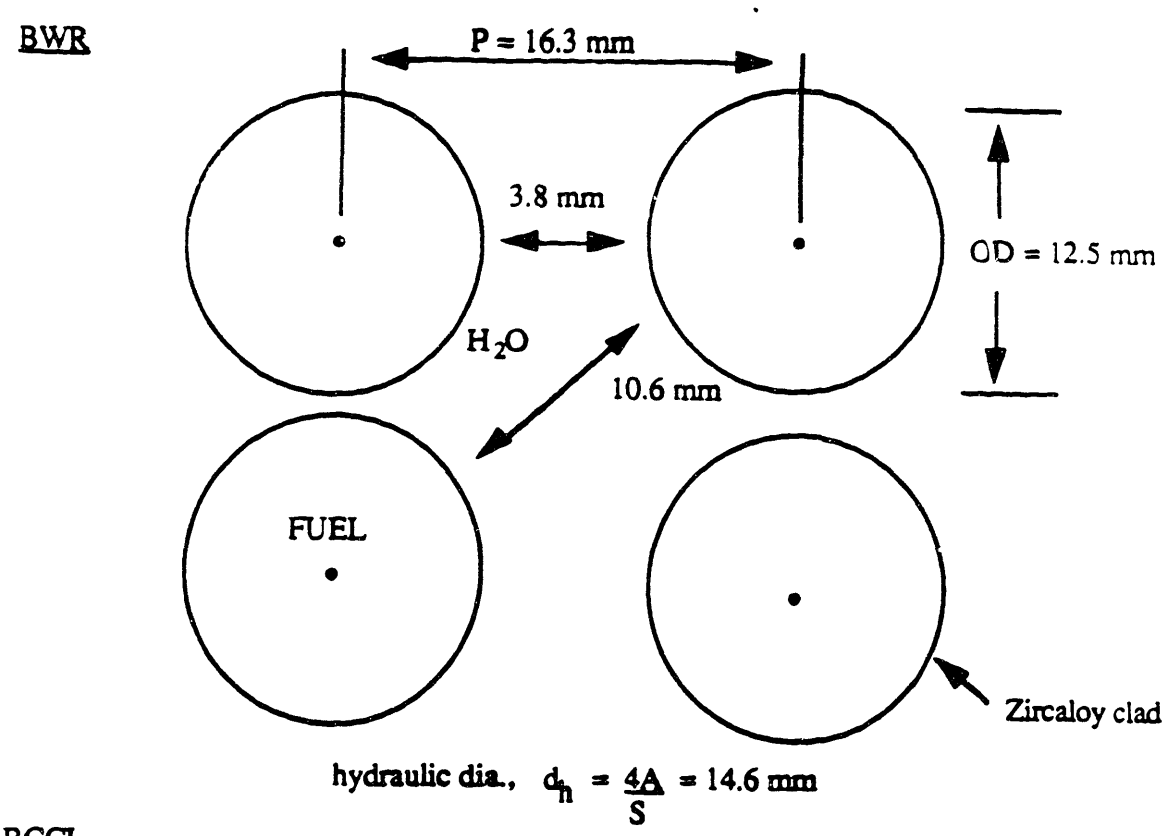

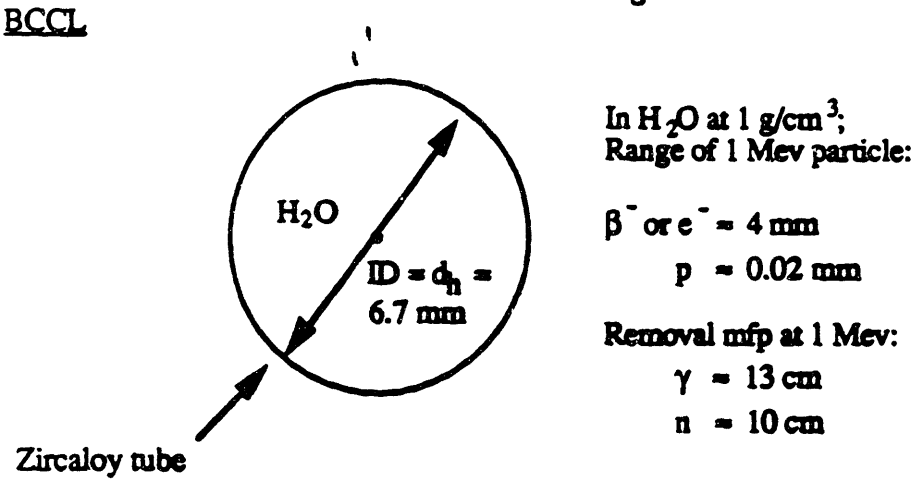

Note:
- mean density of liquid water at operating temperature = 0.7 g/cm^3
- mean density of liquid/vapor mixture ≈ 0.45 g/cm^3
- hence e^- range will be approximately double the value quoted above at 1 g/cm^3

Figure D.1. Geometric Configuration of Water Cells in a BWR and the BCCL Relative to Particle Ranges.

The absorbed doses for the acrylic disks are the same, within a small difference, indicating that a uniform dose distribution was obtained across the capsule. The absorbed doses for the dosimeters placed between the other disks are all the same within ~ 4% which is judged to be the uncertainty of the measurement method.

****

Arrangement of dosimeter disks irradiated in the gamma-ray field above the core of the MITR-II with the reactor shutdown.

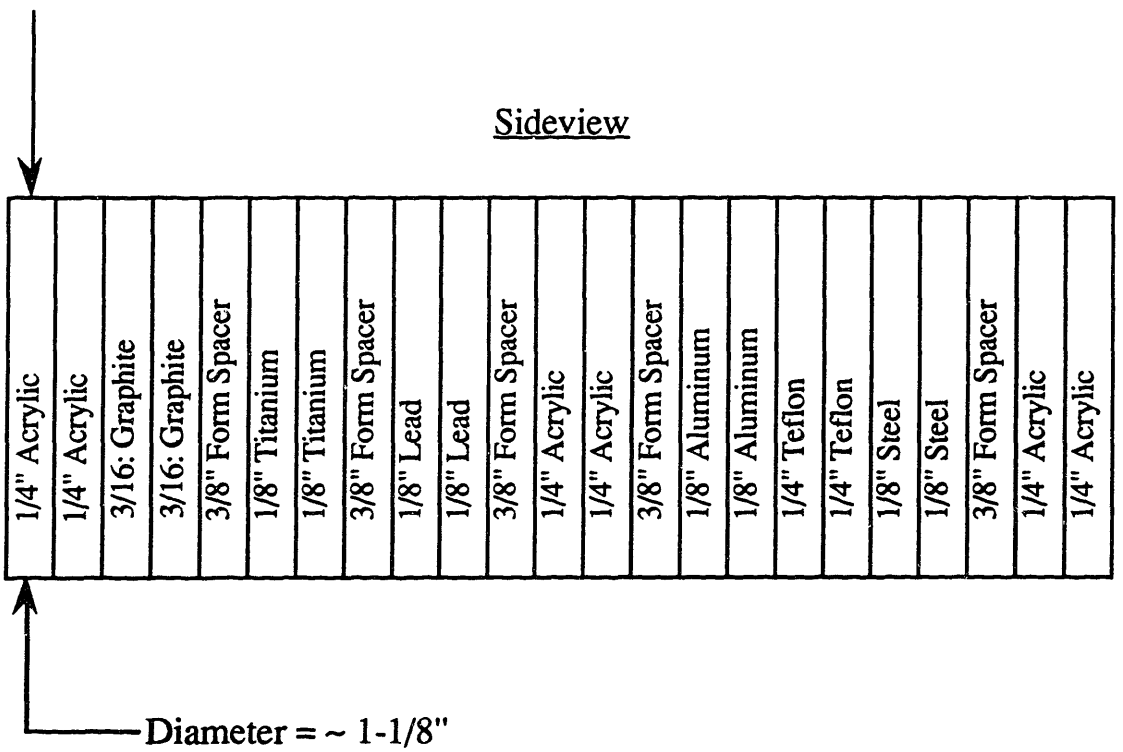

Note: Thin diachrometric dosimeter (dimensions: 1-$^1/_8$" diameter, ~ 0.010" thick) placed between each set of disks, centered on the axis of disk.

To further examine this phenomenon, a set of 0.175-0.300 inch ID tubes of Nylon, Inconel, Ti, SS, Zy-2, and Al were filled with ferrous ion solution in H_2O (Fricke dosimeter), and irradiated in a cluster above the MITR core after shutdown, following which depletion (oxidation) of $Fe^{+2} \rightarrow Fe^{+3}$ was measured colorimetrically. The Nylon/Ti/Inconel/Zy tube data showed that the contained H_2O experienced the same absorbed dose. However Al/SS and some Inconel tube data showed an apparent chemical interaction to restore $Fe^{+3} \rightarrow Fe^{+2}$. Based upon these experiments it is concluded that:

- The water tube experiment and the stacked disc experiment show no wall effect on gamma dose in H_2O (ie. materials with Z higher than H_2O cause no significant enhancement in secondary electron flux)

- We can calculate BCCL and BWR gamma doses in H_2O using a homogeneous infinite-medium model (current practice)

Appendix E

Compilation of Best-Estimate Runs

Simulation of the BCCL Summer 1992 campaign was carried out using a consensus data set and MCNP predicted dose rates (see chapter 5 and Appendix C). Results of simulation with and without decomposition reactions are presented in Tables 5.3 and 5.4, where H_2O_2 concentration at the inlet of the sample line (686 cm) and the H_2 and O_2 mixed return concentrations are compared with experimental data. The aim of this appendix is to present the simulation results in detail, tabulating the evolution of the concentrations along the loop. The following matrix shows the Tables corresponding to each of the runs.

			O2 (ppb) injection	H2 (ppb) injection	Table
Boiling Cases (Xexit=15%)	NWC	w/ P.D.	202.0	18.0	E.1
		w/o P.D.			E.2
	HWC	w/ P.D.	0.	966.0	E.3
		w/o P.D.			E.4
Non-boiling cases	NWC	w/ P.D.	150.0	5.	E.5
		w/o P.D.			E.6
	HWC	w/ P.D.	0.	419.0	E.7
		w/o P.D.			E.8

* P.D. = Peroxide Decomposition

Tables E.1 through E.8 show the major species (O_2, H_2, H_2O_2 and O_2G, H_2G for boiling cases) and the quality generated in the simulation of the BCCL loop. H_2 and O_2 mixed return concentrations are calculated using eqs. (5.1) and (5.2). Data reported are for each node (inlet and exit of each component) corresponding to the nodal diagram of Figure 5.1. Note that the results shown in Tables E.1 through E.8 have been modified according to RADICAL fine points (a) and (i) in chapter 3.

Table E.1 Prediction of NWC boiling case (with H_2O_2 decomposition reaction)

Component	Distance (cm)	Quality (%)	H_2 (l)	H_2(g)	O_2 (l)	O_2 (g)	H_2O_2	H_2 mixed return	O_2 mixed return
Charging Line	0.0000	0.0000	18.000	0.0000	202.00	0.0000	0.0000	18.000	202.00
Charging Line	400.00	0.0000	18.000	0.0000	202.00	0.0000	0.0000	18.000	202.00
Core Inlet	400.00	0.0000	18.000	0.0000	202.00	0.0000	0.0000	18.000	202.00
Core Inlet	431.00	0.0000	10.300	0.0000	70.200	0.0000	141.00	10.300	136.55
Core Subcooled	431.00	0.0000	10.300	0.0000	70.200	0.0000	141.00	10.300	136.55
Core Subcooled	451.00	0.0000	20.700	0.0000	58.300	0.0000	336.00	20.700	216.42
Core Boiling 1	451.00	0.0000	20.700	0.0000	58.300	0.0000	343.00	20.700	219.71
Core Boiling 1	471.00	0.0300	21.481	334.09	83.983	998.60	414.00	30.859	306.25
Core Boiling 2	471.00	0.0300	21.481	334.09	83.983	998.60	414.00	30.859	306.25
Core Boiling 2	491.00	0.0600	20.505	341.43	102.54	1424.5	427.00	39.760	382.79
Core Boiling 3	491.00	0.0600	20.505	341.43	102.54	1424.5	427.00	39.760	382.79
Core Boiling 3	511.00	0.0900	20.212	345.10	115.23	1688.8	447.00	49.452	467.21
Core Boiling 4	511.00	0.0900	20.212	345.10	115.23	1688.8	447.00	49.452	467.21
Core Boiling 4	531.00	0.12000	20.993	357.95	128.90	1909.1	489.00	61.428	572.64
Core Boiling 5	531.00	0.12000	20.993	357.95	128.90	1909.1	489.00	61.428	572.64
Core Boiling 5	551.00	0.15000	18.942	335.93	122.07	1945.8	472.00	66.490	617.75
Core Outlet	551.00	0.15000	18.942	335.93	122.07	1945.8	472.00	66.490	617.75
Core Outlet	582.00	0.15000	16.599	319.40	110.35	2074.3	369.00	62.020	578.59
Plenum Inlet	582.00	0.15000	16.599	319.40	110.35	2074.3	369.00	62.020	578.59
Plenum Inlet	646.00	0.15000	16.697	315.73	111.33	2092.7	353.00	61.552	574.64
Liquid Plenum Out	646.00	0.15000	16.697	315.73	111.33	2092.7	353.00	61.552	574.64
Liquid Plenum Out	661.00	0.15000	16.501	315.73	232.42	2092.7	93.700	61.386	555.55
Liquid Sample Line	661.00	0.15000	16.501	315.73	232.42	2092.7	93.700	61.386	555.55
Liquid Sample Line	686.00	0.15000	16.404	315.73	232.42	2092.7	90.600	61.303	554.09
concentrations in ppb									

Table E.2 Prediction of NWC boiling case (without H_2O_2 decomposition reaction)

Component	Distance (cm)	Quality (%)	H_2 (l)	H_2(g)	O_2 (l)	O_2 (g)	H_2O_2	H_2 mixed return	O_2 mixed return
Charging Line	0.0000	0.0000	18.000	0.0000	202.00	0.0000	0.0000	18.000	202.00
Charging Line	400.00	0.0000	18.000	0.0000	202.00	0.0000	0.0000	18.000	202.00
Core Inlet	400.00	0.0000	18.000	0.0000	202.00	0.0000	0.0000	18.000	202.00
Core Inlet	431.00	0.0000	10.300	0.0000	67.900	0.0000	146.00	10.300	136.61
Core Subcooled	431.00	0.0000	10.300	0.0000	67.900	0.0000	146.00	10.300	136.61
Core Subcooled	451.00	0.0000	20.600	0.0000	57.200	0.0000	337.00	20.600	215.79
Core Boiling 1	451.00	0.0000	20.600	0.0000	57.200	0.0000	344.00	20.600	219.08
Core Boiling 1	471.00	0.0300	21.479	334.40	82.969	988.51	415.00	30.866	305.43
Core Boiling 2	471.00	0.0300	21.479	334.40	82.969	988.51	415.00	30.866	305.43
Core Boiling 2	491.00	0.0600	20.405	339.92	101.52	1411.1	429.00	39.575	381.97
Core Boiling 3	491.00	0.0600	20.405	339.92	101.52	1411.1	429.00	39.575	381.97
Core Boiling 3	511.00	0.0900	20.209	343.59	115.18	1675.7	449.00	49.314	466.92
Core Boiling 4	511.00	0.0900	20.209	343.59	115.18	1675.7	449.00	49.314	466.92
Core Boiling 4	531.00	0.12000	20.991	358.29	127.87	1892.5	493.00	61.466	571.63
Core Boiling 5	531.00	0.12000	20.991	358.29	127.87	1892.5	493.00	61.466	571.63
Core Boiling 5	551.00	0.15000	18.843	334.40	121.04	1929.3	477.00	66.177	616.74
Core Outlet	551.00	0.15000	18.843	334.40	121.04	1929.3	477.00	66.177	616.74
Core Outlet	582.00	0.15000	16.597	317.87	107.37	2021.1	385.00	61.788	575.61
Plenum Inlet	582.00	0.15000	16.597	317.87	107.37	2021.1	385.00	61.788	575.61
Plenum Inlet	646.00	0.15000	16.695	314.19	107.37	2021.1	385.00	61.320	575.61
Liquid Plenum Out	646.00	0.15000	16.695	314.19	107.37	2021.1	385.00	61.320	575.61
Liquid Plenum Out	661.00	0.15000	16.402	314.19	105.42	2021.1	386.00	61.071	574.42
Liquid Sample Line	661.00	0.15000	16.402	314.19	105.42	2021.1	386.00	61.071	574.42
Liquid Sample Line	686.00	0.15000	16.402	314.19	105.42	2021.1	386.00	61.071	574.42
concentrations in ppb									

Table E.3 Prediction of HWC boiling case (with H_2O_2 decomposition reaction)

Component	Distance (cm)	Quality (%)	H_2 (l)	H_2(g)	O_2 (l)	O_2 (g)	H_2O_2	H_2 mixed return	O_2 mixed return
Charging Line	0.0000	0.0000	966.00	0.0000	0.000	0.00	0.00	966.00	0.000
Charging Line	400.00	0.0000	966.00	0.0000	0.000	0.00	0.00	966.00	0.000
Core Inlet	400.00	0.0000	966.00	0.0000	0.000	0.00	0.00	966.00	0.000
Core Inlet	431.00	0.0000	966.00	0.0000	6.710e-4	0.00	6.54	966.00	3.078
Core Subcooled	431.00	0.0000	966.00	0.0000	6.710e-4	0.00	6.54	966.00	3.078
Core Subcooled	451.00	0.0000	968.00	0.0000	3.970e-3	0.00	38.5	968.00	18.12
Core Boiling 1	451.00	0.0000	968.00	0.0000	3.970e-3	0.00	39.4	968.00	18.55
Core Boiling 1	471.00	0.0300	662.26	10896	8.018e-3	0.0930	50.9	969.27	23.96
Core Boiling 2	471.00	0.0300	662.26	10896	8.018e-3	0.0930	50.9	969.27	23.96
Core Boiling 2	491.00	0.0600	484.49	8543.8	1.125e-2	0.145	48.9	968.05	23.03
Core Boiling 3	491.00	0.0600	484.49	8543.8	1.125e-2	0.145	48.9	968.05	23.03
Core Boiling 3	511.00	0.0900	381.93	6890.2	1.594e-2	0.211	50.5	967.67	23.80
Core Boiling 4	511.00	0.0900	381.93	6890.2	1.594e-2	0.211	50.5	967.67	23.80
Core Boiling 4	531.00	0.12000	315.50	5751.0	2.357e-2	0.312	56.0	967.77	26.41
Core Boiling 5	531.00	0.12000	315.50	5751.0	2.357e-2	0.312	56.0	967.77	26.41
Core Boiling 5	551.00	0.15000	268.62	4942.6	2.239e-2	0.322	45.3	969.71	21.38
Core Outlet	551.00	0.15000	268.62	4942.6	2.239e-2	0.322	45.3	969.71	21.38
Core Outlet	582.00	0.15000	263.73	4960.9	3.403e-3	0.120	7.90	968.32	3.739
Plenum Inlet	582.00	0.15000	263.73	4960.9	3.403e-3	0.120	7.90	968.32	3.739
Plenum Inlet	646.00	0.15000	262.76	4942.6	1.750e-3	0.0614	2.28	964.73	1.084
Liquid Plenum Out	646.00	0.15000	262.76	4942.6	1.750e-3	0.0614	2.28	964.73	1.084
Liquid Plenum Out	661.00	0.15000	262.76	4942.6	3.207e-4	0.0614	0.0813	964.73	0.04774
Liquid Sample Line	661.00	0.15000	262.76	4942.6	3.207e-4	0.0614	0.0813	964.73	0.04774
Liquid Sample Line	686.00	0.15000	262.76	4942.6	1.995e-4	0.0614	0.119	964.73	0.06537
concentrations in ppb									

Table E.4 Prediction of HWC boiling case (without H_2O_2 decomposition reaction)

Component	Distance (cm)	Quality (%)	H_2 (l)	H_2(g)	O_2 (l)	O_2 (g)	H_2O_2	H_2 mixed return	O_2 mixed return
Charging Line	0.0000	0.0000	966.00	0.0000	0.000	0.00	0.0000	966.00	0.0000
Charging Line	400.00	0.0000	966.00	0.0000	0.000	0.00	0.0000	966.00	0.0000
Core Inlet	400.00	0.0000	966.00	0.0000	0.000	0.00	0.0000	966.00	0.0000
Core Inlet	431.00	0.0000	966.00	0.0000	2.410e-4	0.00	6.5500	966.00	3.0826
Core Subcooled	431.00	0.0000	966.00	0.0000	2.410e-4	0.00	6.5500	966.00	3.0826
Core Subcooled	451.00	0.0000	968.00	0.0000	2.990e-3	0.00	38.500	968.00	18.121
Core Boiling 1	451.00	0.0000	968.00	0.0000	2.990e-3	0.00	38.500	968.00	18.121
Core Boiling 1	471.00	0.0300	662.26	10896	7.016e-3	0.0803	49.737	969.27	23.415
Core Boiling 2	471.00	0.0300	662.26	10896	7.016e-3	0.0803	49.737	969.27	23.415
Core Boiling 2	491.00	0.0600	484.49	8543.8	1.016e-2	0.130	47.783	968.05	22.503
Core Boiling 3	491.00	0.0600	484.49	8543.8	1.016e-2	0.130	47.783	968.05	22.503
Core Boiling 3	511.00	0.0900	381.93	6890.2	1.485e-2	0.195	49.444	967.67	23.299
Core Boiling 4	511.00	0.0900	381.93	6890.2	1.485e-2	0.195	49.444	967.67	23.299
Core Boiling 4	531.00	0.12000	315.50	5751.0	2.228e-2	0.292	54.721	967.77	25.806
Core Boiling 5	531.00	0.12000	315.50	5751.0	2.228e-2	0.292	54.721	967.77	25.806
Core Boiling 5	551.00	0.15000	268.62	4924.2	2.101e-2	0.299	44.363	966.95	20.939
Core Outlet	551.00	0.15000	268.62	4924.2	2.101e-2	0.299	44.363	966.95	20.939
Core Outlet	582.00	0.15000	263.73	4960.9	2.765e-3	0.104	7.7391	968.32	3.6599
Plenum Inlet	582.00	0.15000	263.73	4960.9	2.765e-3	0.104	7.7391	968.32	3.6599
Plenum Inlet	646.00	0.15000	262.76	4942.6	6.752e-4	0.0331	2.2572	964.73	1.0678
Liquid Plenum Out	646.00	0.15000	262.76	4942.6	6.752e-4	0.0331	2.2572	964.73	1.0678
Liquid Plenum Out	661.00	0.15000	262.76	4942.6	2.072e-5	0.0331	0.09273	964.73	0.048617
Liquid Sample Line	661.00	0.15000	262.76	4942.6	2.072e-5	0.0331	0.09273	964.73	0.048617
Liquid Sample Line	686.00	0.15000	262.76	4942.6	2.755e-5	0.0331	0.12703	964.73	0.064763
concentrations in ppb									

Table E.5 Prediction of NWC non-boiling case (with H_2O_2 decomposition reaction)

Component	Distance (cm)	H_2 (l)	O_2 (l)	H_2O_2	H_2 mixed *return*	O_2 mixed *return*
Charging Line	0.0000	5.0000	150.00	0.0000	5.0000	150.00
Charging Line	400.00	5.0000	150.00	0.0000	5.0000	150.00
Core Inlet	400.00	5.0000	150.00	0.0000	5.0000	150.00
Core Inlet	431.00	5.8100	103.00	105.00	5.8100	152.41
Core Subcooled	431.00	5.8100	103.00	105.00	5.8100	152.41
Core Subcooled	451.00	22.100	89.000	401.00	22.100	277.71
Core Boiling 1	451.00	22.100	89.000	410.00	22.100	281.94
Core Boiling 1	471.00	25.425	91.540	459.00	25.425	307.54
Core Boiling 2	471.00	25.425	91.540	459.00	25.425	307.54
Core Boiling 2	491.00	24.154	92.419	436.00	24.154	297.60
Core Boiling 3	491.00	24.154	92.419	436.00	24.154	297.60
Core Boiling 3	511.00	24.154	92.419	435.00	24.154	297.13
Core Boiling 4	511.00	24.154	92.419	435.00	24.154	297.13
Core Boiling 4	531.00	25.425	91.540	460.00	25.425	308.01
Core Boiling 5	531.00	25.425	91.540	460.00	25.425	308.01
Core Boiling 5	551.00	23.078	88.707	426.00	23.078	289.18
Core Outlet	551.00	23.078	88.707	426.00	23.078	289.18
Core Outlet	582.00	11.735	88.023	241.00	11.735	201.43
Plenum Inlet	582.00	11.735	88.023	241.00	11.735	201.43
Plenum Inlet	646.00	10.952	93.982	218.00	10.952	196.57
Liquid Plenum Out	646.00	10.952	93.982	218.00	10.952	196.57
Liquid Plenum Out	661.00	10.757	162.17	71.300	10.757	195.73
Liquid Sample Line	661.00	10.757	162.17	71.300	10.757	195.73
Liquid Sample Line	686.00	10.659	162.17	69.000	10.659	194.64
concentrations in ppb						

Table E.6 Prediction of NWC non-boiling case (without H_2O_2 decomposition reaction)

Component	Distance (cm)	H_2 (l)	O_2 (l)	H_2O_2	H_2 mixed return	O_2 mixed return
Charging Line	0.0000	5.0000	150.00	0.0000	5.0000	150.00
Charging Line	400.00	5.0000	150.00	0.0000	5.0000	150.00
Core Inlet	400.00	5.0000	150.00	0.0000	5.0000	150.00
Core Inlet	431.00	5.8000	102.00	109.00	5.8000	153.29
Core Subcooled	431.00	5.8000	102.00	109.00	5.8000	153.29
Core Subcooled	451.00	22.000	87.300	403.00	22.000	276.95
Core Boiling 1	451.00	22.000	87.300	412.00	22.000	281.18
Core Boiling 1	471.00	25.324	90.331	460.00	25.324	306.80
Core Boiling 2	471.00	25.324	90.331	460.00	25.324	306.80
Core Boiling 2	491.00	24.053	91.113	437.00	24.053	296.76
Core Boiling 3	491.00	24.053	91.113	437.00	24.053	296.76
Core Boiling 3	511.00	23.956	91.210	436.00	23.956	296.39
Core Boiling 4	511.00	23.956	91.210	436.00	23.956	296.39
Core Boiling 4	531.00	25.324	90.331	460.00	25.324	306.80
Core Boiling 5	531.00	25.324	90.331	460.00	25.324	306.80
Core Boiling 5	551.00	22.880	86.909	428.00	22.880	288.32
Core Outlet	551.00	22.880	86.909	428.00	22.880	288.32
Core Outlet	582.00	11.636	82.803	250.00	11.636	200.45
Plenum Inlet	582.00	11.636	82.803	250.00	11.636	200.45
Plenum Inlet	646.00	10.853	79.088	248.00	10.853	195.79
Liquid Plenum Out	646.00	10.853	79.088	248.00	10.853	195.79
Liquid Plenum Out	661.00	10.658	77.817	249.00	10.658	194.99
Liquid Sample Line	661.00	10.658	77.817	249.00	10.658	194.99
Liquid Sample Line	686.00	10.560	77.328	249.00	10.560	194.50
concentrations in ppb						

Table E.7 Prediction of NWC non-boiling case (with H_2O_2 decomposition reaction)

Component	Distance (cm)	H_2 (l)	O_2 (l)	H_2O_2	H_2 mixed return	O_2 mixed return
Charging Line	0.0000	419.00	0.000	0.00	419.00	0.000
Charging Line	400.00	419.00	0.000	0.00	419.00	0.000
Core Inlet	400.00	419.00	0.000	0.00	419.00	0.000
Core Inlet	431.00	419.00	1.320e-3	7.00	419.00	3.295
Core Subcooled	431.00	419.00	1.320e-3	7.00	419.00	3.295
Core Subcooled	451.00	421.00	1.120e-2	41.3	421.00	19.45
Core Boiling 1	451.00	421.00	1.120e-2	42.2	421.00	19.87
Core Boiling 1	471.00	421.98	1.503e-2	53.4	421.98	25.14
Core Boiling 2	471.00	421.98	1.503e-2	53.4	421.98	25.14
Core Boiling 2	491.00	421.98	1.385e-2	49.8	421.98	23.45
Core Boiling 3	491.00	421.98	1.385e-2	49.8	421.98	23.45
Core Boiling 3	511.00	421.98	1.385e-2	49.8	421.98	23.45
Core Boiling 4	511.00	421.98	1.385e-2	49.8	421.98	23.45
Core Boiling 4	531.00	421.98	1.503e-2	53.4	421.98	25.14
Core Boiling 5	531.00	421.98	1.503e-2	53.4	421.98	25.14
Core Boiling 5	551.00	421.00	1.110e-2	41.8	421.00	19.68
Core Outlet	551.00	421.00	1.110e-2	41.8	421.00	19.68
Core Outlet	582.00	419.05	1.660e-3	6.96	419.05	3.277
Plenum Inlet	582.00	419.05	1.660e-3	6.96	419.05	3.277
Plenum Inlet	646.00	419.05	3.694e-4	0.748	419.05	0.3524
Liquid Plenum Out	646.00	419.05	3.694e-4	0.748	419.05	0.3524
Liquid Plenum Out	661.00	419.05	2.211e-4	0.0634	419.05	0.03006
Liquid Sample Line	661.00	419.05	2.211e-4	0.0634	419.05	0.03006
Liquid Sample Line	686.00	419.05	1.356e-4	0.0952	419.05	0.04494
concentrations in ppb						

Table E.8 Prediction of NWC non-boiling case (without H_2O_2 decomposition reaction)

Component	Distance (cm)	H_2 (l)	O_2 (l)	H_2O_2	H_2 mixed return	O_2 mixed return
Charging Line	0.0000	419.00	0.0000	0.0000	419.00	0.0000
Charging Line	400.00	419.00	0.0000	0.0000	419.00	0.0000
Core Inlet	400.00	419.00	0.0000	0.0000	419.00	0.0000
Core Inlet	431.00	419.00	0.00082	7.0200	419.00	3.3043
Core Subcooled	431.00	419.00	0.00082	7.0200	419.00	3.3043
Core Subcooled	451.00	421.00	0.01000	41.300	421.00	19.445
Core Boiling 1	451.00	421.00	0.01000	42.200	421.00	19.869
Core Boiling 1	471.00	421.98	0.013922	53.400	421.98	25.143
Core Boiling 2	471.00	421.98	0.013922	53.400	421.98	25.143
Core Boiling 2	491.00	421.98	0.012745	49.800	421.98	23.448
Core Boiling 3	491.00	421.98	0.012745	49.800	421.98	23.448
Core Boiling 3	511.00	421.98	0.012745	49.800	421.98	23.448
Core Boiling 4	511.00	421.98	0.012745	49.800	421.98	23.448
Core Boiling 4	531.00	421.98	0.013922	53.400	421.98	25.143
Core Boiling 5	531.00	421.98	0.013922	53.400	421.98	25.143
Core Boiling 5	551.00	421.00	0.009902	41.800	421.00	19.680
Core Outlet	551.00	421.00	0.009902	41.800	421.00	19.680
Core Outlet	582.00	419.05	0.001147	6.9800	419.05	3.2859
Plenum Inlet	582.00	419.05	0.001147	6.9800	419.05	3.2859
Plenum Inlet	646.00	419.05	6.9804e-5	0.76300	419.05	0.35913
Liquid Plenum Out	646.00	419.05	6.9804e-5	0.76300	419.05	0.35913
Liquid Plenum Out	661.00	419.05	6.2745e-6	0.072900	419.05	0.034312
Liquid Sample Line	661.00	419.05	6.2745e-6	0.072900	419.05	0.034312
Liquid Sample Line	686.00	419.05	8.6373e-6	0.10300	419.05	0.048479
concentrations in ppb						

Here are some points worth noting in the results:

(1) H_2O_2 reaches its maximum concentration at the components "core boiling 4" or "core boiling 5", and the concentration drops abruptly in the core outlet when decomposition is accounted for.

(2) Under NWC the elimination of H_2O_2 decomposition keeps H_2O_2 concentration almost constant from the core outlet region (582 cm) to the liquid sample line (686 cm). For HWC H_2O_2 decreases even in the absence of decomposition.

(3) Net H_2 and O_2 production (mixed return - inlet) is stoichiometric if we allow for the likely errors from code convergence tolerances, and data round-off error. For example, for Table E.1 line 24; using mixed return data:

$$\frac{O_{2,out} - O_{2,in}}{H_{2,out} - H_{2,in}} = 8.13 \approx 8$$

Appendix F

Supplementary Guide to Use of RADICAL

by John H. Chun

September 11, 1991

I. Introduction

This manual contains a tutorial on how to use RADICAL 1.11, the first version of RADICAL for the Macintosh®. The user should be familiar with the Macintosh operating system such as using the menu and windows.

RADICAL 1.11 was originally developed on the DEC MicroVax-III® and was ported to the Macintosh using the MacFortran II® compiler under system 6.0.5. Hence RADICAL 1.11 requires the math coprocessor, i.e., RADICAL 1.11 runs on Mac II or above. Successful use under system 7 has also been demonstrated.

There is no need to mention that the user should be familiar with radiolysis and workings of the loop to be analyzed. For more technical discussions, the user is referred to my thesis* which describes the physics and chemistry behind radiolysis as well as code development in detail.

II. What You Need

Here's a list of things that you need to run RADICAL:

1. A Macintosh computer of Mac II or above with the math coprocessor (e.g. Mac II, IIx, IIci, IIfx, SE30).

2. Macintosh operating system 6.0.5 or above with MultiFinder (RADICAL may or may not work with System 7).

3. At least 1 Mbyte of free RAM and 1 Mbyte of free disk space.

---

* John H. Chun; "Modeling of BWR Water Chemistry", SM Thesis - Nuclear Engineering, MIT, Cambridge, MA, 1990.

4. A copy of Microsoft Word 4.0® in the harddisk (to edit input files and view output files). A suitable substitution is acceptable if you know what you are doing.

5. A copy of KaleidaGraph 2.1.11® if you want to plot data. A suitable substitution is acceptable if you know what you are doing.

II. Installing RADICAL

RADICAL 1.11 is supplied on one double density 3.5" disk. The disk contains a folder named 'RADICAL'. Copy the folder to any place in the harddisk. The folder occupies about 400 kbytes of disk space.

III. Running RADICAL

After installation, open the RADICAL folder. It should look like Fig. III-1.

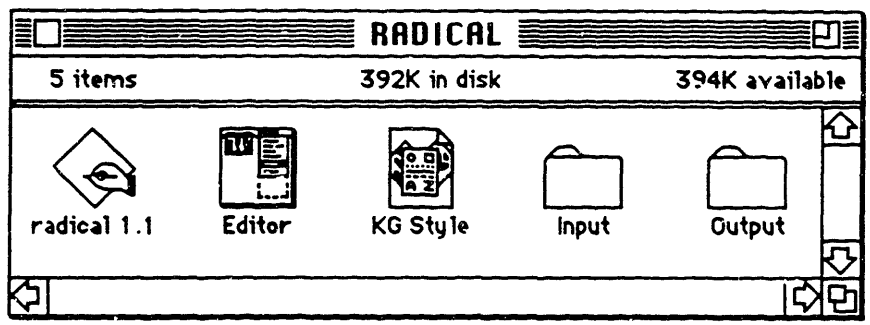

Figure III-1 Contents of the RADICAL folder.

To run RADICAL, simply double click on the 'radical 1.11' icon. A runtime window will pop up and ask for an input file name. First, we will run a short diagnostic input file. Upon the prompt, type ':input:bateman.in', followed by a return. This means we want to use the 'bateman.in' input file within the input folder. A colon separates folders and files. Don't forget the first colon in front of 'input', which tells the input folder is within the folder in which the radical 1.11 program is in (think about it slowly, one at a time. This is an example of the hierarchical directory system).

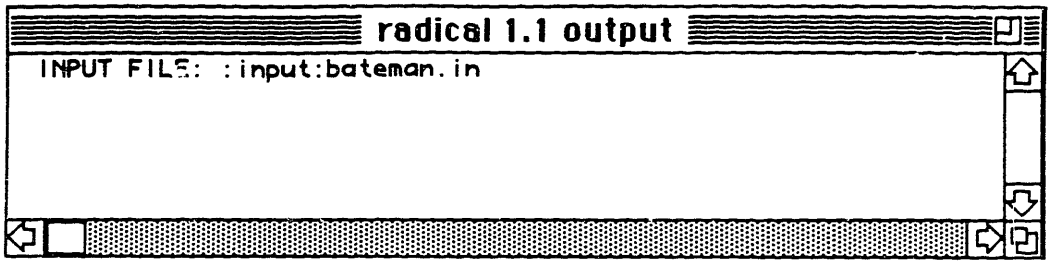

Figure III-2 The runtime window at the input prompt.

The program should start execution immediately and some messages should appear in the runtime window. When a dialog box prompts "Save text before quitting", click on the 'Discard' button. And upon the "Press RETURN to quit the program." prompt, just press return. The runtime window will disappear and the program terminates.

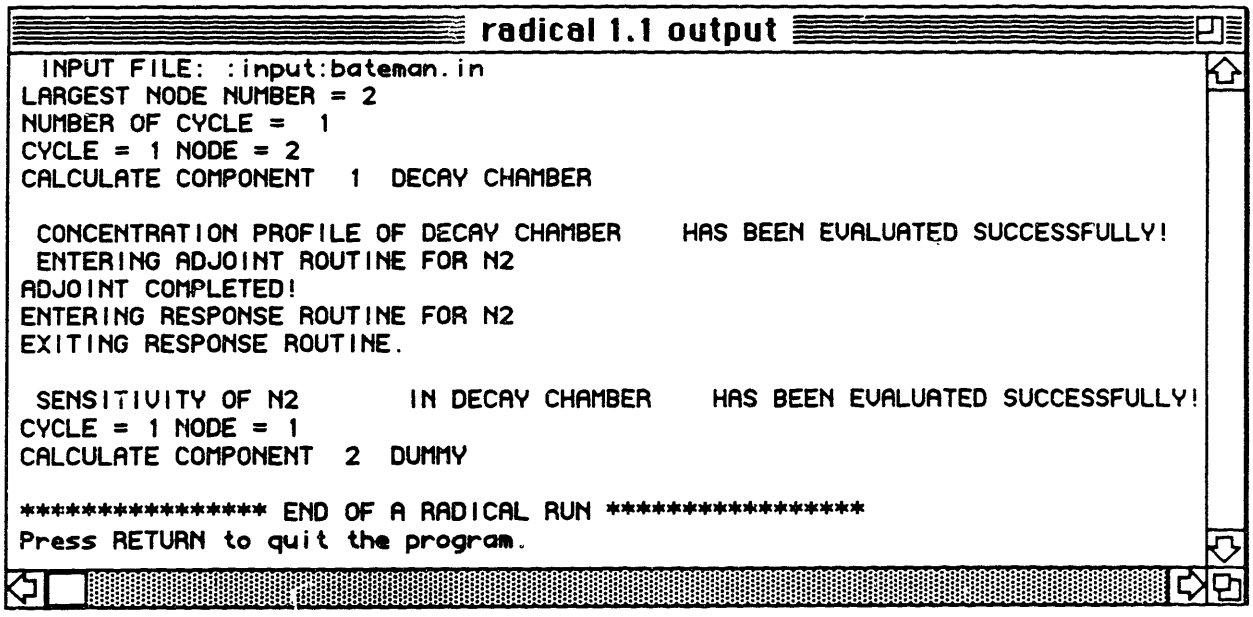

Figure III-3 The runtime window after execution.

IV. The Output File

This RADICAL run produced an output file called 'BATEMAN.OUT' within the Output folder. We can take a look at this file using the Editor. The Editor is nothing but a

style sheet for Microsoft Word 4.0. Therefore you must have a copy of Microsoft Word 4.0 somewhere in your harddisk and you must be familiar with the wordprocessor.

Note to Computer Gurus: RADICAL produces output files in plain text file format (aka an ASCII file). It also takes input files in strictly plain text format. Therefore when using a text editor to view and modify RADICAL files, the format must always remain in plain text. If the provided Editor style sheet is used there won't be any complications.

Double click on the Editor icon. MS Word should start and a blank window should appear on the screen. Open the 'BATEMAN.OUT' output file by reaching into the Output folder (this may take some effort depending on where the actual MS Word application is in your harddisk).

The output file can be viewed by scrolling the scroll bars to the right and bottom of the window. (For those who are curious this diagnostic output file describes the radioactive decay of parent and daughter elements.) The file also contains the sensitivity results. Be acquainted with the output format by inspecting every page of the file.

V. Plotting Data

The RADICAL run not only produced the output file 'BATEMAN.OUT' (simply called an output file), but also another output file called 'BATEMAN.PLOT' (called a plot file). Whereas the former contains detailed information of the run the latter is a compact, columnar output of concentrations at each spatial (or time) node. The primary purpose of the plot file is to generate plots using KaleidaGraph.

To run KaleidaGraph (of course you must have the software somewhere in your harddisk) double click on the Plotter icon. As in the Editor case, the Plotter icon is a style sheet which indirectly runs KaleidaGraph. Now KaleidaGraph should start up with a blank data window.

Open the plot file 'BATEMAN.PLOT' using the regular Open command under the File menu. A dialog box which looks like this should pop up since we are reading in a text file.

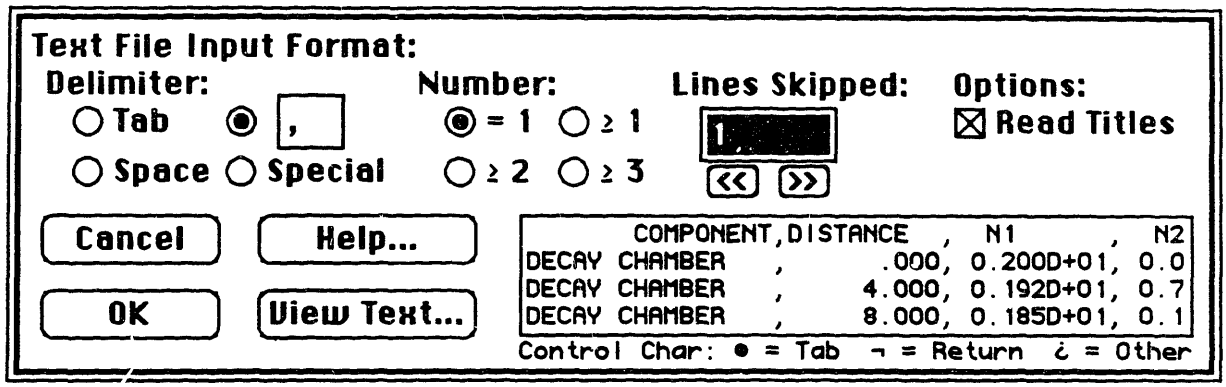

Set the Delimiter to comma, Lines Skipped to 1 as shown above and click OK. The data should be read into a data window. Go from here to make your own pretty plots.

VI. Modifying an Input File

Now that you know how to run RADICAL and manipulate its output files, it's time to learn to modify an input file and see what comes out of it.

In the Input folder there are two more files of interest: dresden0.in is a simulation of the primary circuit of a BWR power plant and pwr.in is a PWR shutdown chemistry simulation. You can make a copy of these files and start playing with them by changing input parameters and flow configuration, etc., and see how they affect the overall chemistry of the loop.

When you have to create your own input file, I suggest that you don't start from scratch, which would be more prone to making a lot of mistakes, but modify a sample input file in a major way. For detailed description of input format and parameters, please refer to my thesis. Appendix A of the thesis would be a good starting point before you jump into theoretical derivations.

Good luck!

Appendix G

Carryover and Carryunder

G.1 INTRODUCTION

Carryover and carryunder are of interest in the present instance because they "contaminate" the vapor phase and liquid phase return line samples with liquid and vapor, respectively. Other objectives are important in full scale BWR units: for example, moisture carryover can have detrimental effects on steam turbines. Hence low carryover and carryunder are also important to the goal of maximizing similitude between the BCCL and actual BWRs.

Reference 1 reports the following for large BWR units:

	Design Specification	Actual Performance
Carryover		
separator	10% water	0.01 - 5%
dryer	0.1% water	0.01%
Carryunder	0.2% steam	0.1 - 0.7%

In concurrence with common practice, carryover is defined here as the weight percent liquid water in steam, and carryunder as the weight percent steam entrained in liquid water.

It is not likely that separations as good as those noted above can be achieved in a system having components as small as those in the BCCL, although credible bench scale data exists on somewhat larger models of BWR separators (refs. 2, 3, 4, and 5). In the present instance a reasonable goal of $\leq 5\%$ carryover would permit satisfactorily accurate measurements to be made of N-16 carryover, based upon our observations that N-16 activity per gram is roughly equal in steam and water (In an actual BWR, with internal coolant circulation, steam may contain considerably less N-16 per unit mass).

Carryunder, on the other hand, would have to be $\leq 0.1\%$ to permit meaningful measurement of gas concentrations in the water phase because the entrained vapor contains much more O_2 or H_2 per unit mass than does the liquid (see Section G.5).

G.2 EXPERIMENTAL APPROACH

To evaluate BCCL performance, the following experimental methods were considered:

Carryover

(1) Measure water and condensed steam conductivity after adding a highly soluble, nonvolatile ionic compound.

(2) Measure induced ionic activity in both effluents, such as F-18, Na-24 or K-42.

Carryunder

(1) Add air to the feedwater and measure O_2 in the water and condensed steam using the Orbisphere® detector or colorimetric analysis, both of which can measure down to the ppb level. This should be done with electric heat only to avoid water radiolysis.

(2) Measure Ar-41 activity in both effluents; some should be present naturally, but it is easily enhanced.

The conductivity and Ar-41 measurements were selected for application in the 1990 and 1991 campaigns.

G.3 MEASUREMENT OF CARRYUNDER USING ARGON-41

Consider steam and liquid water entering the BWR loop plenum at mass flow rates S and W, respectively. Let C be the carryunder ratio: mass of steam entrained per unit mass of liquid. Then a balance on the contained argon gas and its radioactive isotope Ar-41 can be written:

Steam Phase:

$$Sy - CWy = K A_S (S - CW) \quad (G.1)$$

Water Phase:

$$Wx + CWy = K A_W (W + CW) \quad (G.2)$$

where

A_S, A_W = Ar-41 activity per unit mass of steam, water sample

y, x= mass (or mole) fraction Ar-41 in steam, water

K= proportionality constant

Henry's Law gives

$$p = Hx \quad (G.3)$$

hence

$$y = \left(\frac{p}{P}\right) = \left(\frac{H}{P}\right)x \quad (G.4)$$

where

H = Henry's Law constant for Ar-41 in H_2O at the temperature of interest

P = system pressure

Let $R = A_S/A_W$ and divide Eq. (G-1) by Eq. (G-2), using Eq. (G-4) to eliminate x. The result, when solved for C is:

$$C = \frac{1 - R(P/H)}{R - 1} \quad (G.5)$$

thus, if $R >> 1$

$$C \Rightarrow \frac{1}{R} - \frac{P}{H} \approx \frac{1}{R} = \frac{Aw}{As} \quad (G.6)$$

Henry's Law constants for Ar-41 at high temperature are given in ref. 6, as follows:

T°C	H, atm
25	4.22×10^4
250	3.10×10^4
275	2.43×10^4
300	1.87×10^4

The BWR plenum is at 1000 psig (68 atm) and 285°C; hence P/H ≈ 0.003, or an apparent background carryunder of 0.3% will be measured due to dissolved gas. As noted in Eq. G.6, this can be subtracted out.

If carryunder is defined as the fraction of steam in water plus steam, i.e. F = C/(1 + C),

$$F = \frac{\left(\frac{1}{R}\right) - \left(\frac{P}{H}\right)}{1 - \left(\frac{P}{H}\right)} \approx \left(\frac{1}{R}\right) - \left(\frac{P}{H}\right) \qquad (G.7)$$

to an even better degree of approximation.

A measurement carried out during the initial BCCL run in 1990 gave $\left(1/_R\right) = 0.147$, which implies ~ 14% carryunder — an improbably high value, which suggested loss of Ar-41 during steam sample condensation.

During the 1991 campaign a set of samples were taken using deflated balloons attached to the sample taps to insure off-gas retention. Ar-41 activities, however, were too low to assay with sufficient accuracy. Likewise, O_2 concentrations in the steam and water samples could not be measured with the requisite precision (the Orbisphere® detector requires too high a flow rate, and the colorimetric approach is too susceptible to air ingress in the sampling process).

A more concerted effort will be made in the next series of BCCL runs. One possibility is the use of Kr-87 as a tracer: this species is produced as a high yield fission product from tramp uranium, which is present in virtually all materials. It was detected at useful levels in the aforementioned balloon sample of condensed steam sample line effluent.

G.4 MEASUREMENT OF CARRYOVER USING CONDUCTIVITY

The procedure here, and its analysis, are relatively straightforward: carryover is given by

$$F = \frac{C_S - C_{SO}}{C_W - C_{WO}} \tag{G.8}$$

where

C_S = conductivity of condensed steam (cooled to room temperature), measured after adding ionic salt to feedwater.

C_{SO} = background conductivity of condensed steam, in absence of additive

Cw, Cwo = like quantities for water sample

The above prescription would also apply if added or induced radioactivity of a nonvolatile species were used to measure carryover.

Note that the background conductivity in the above relation is not merely that of theoretically pure H_2O, since even in the absence of an intentional additive, tramp impurities may be present, and some, like NH_3, are sufficiently volatile to carry over at a different ratio than ionic salts such as KNO_3. Such species are in fact slightly volatile, but this is sufficiently small to be negligible under BCCL and BWR conditions (ref. 7). We also neglect the slight decrease in ionic conductivity as concentration is increased.

Outwater applied this approach to estimate carryover (ref. 8), using both conductivity and K-42 activity, and inferred a value of ~ 2% using both methods.

Measurements during the Fall 1991 campaign using KOH gave, for a typical data set (all values are μS/cm):

$$F = \frac{1.4 - 0.8}{31.5 - 1.2} = 0.02, \tag{G.9}$$

or again 2%. There is substantial uncertainty in this value because the additive-free steam background value varies over time, and the sample for this measurement is taken at a different time than the post-additive sample.

While carryover is somewhat less than the goal of ≤ 5%, in the future it may be worthwhile to install an external steam dryer on the steam return line. Commercial components are available, but a simple mesh-filled plenum should suffice.

Once the loop is operated in a recirculating mode, radionuclide concentrations should increase to the point where they can be used to obtain more precise carryover estimates.

G.5 CARRYUNDER IN THE BCCL: A FUNDAMENTAL PROBLEM

From Henry's Law the ratio of mole (or mass) - based concentrations in the vapor and liquid phases in the BCCL plenum is (for O_2, using data from Ref. (9))

$$\frac{y}{x} = \frac{H}{P} \approx 200$$

Thus 0.1 w/o vapor carryunder by the liquid leaving the plenum will add about 20% more O_2 to the fluid than is dissolved in the liquid phase. Since the density of water is about 20 times that of steam under BCCL conditions, 0.1 w/o corresponds to ~2 vol. % — a goal which is probably not attainable (3).

Thus, unless we can measure carryunder for every sample taken (which appears impractical), or unless it is very nearly constant, liquid effluent gas content measurements will be of little scientific value as regards validation of radiolysis yields. It would appear that in the future we should continue to place principal emphasis on measurements after the vapor and liquid streams are recombined. Less information is obtained thereby, but it is considerably less ambiguous and more reliable.

REFERENCES

(1) E. L. Burley, A. A. Kudirka and R. H. Moen, "Performance of Internal Steam Separation Systems in Large Boiling Water Reactor Plants," *ASME Publication* 72-PWR-6 (1972).

(2) T. Akiyama, T. Shida and A. Shibuya, "Significance of Steam Separator Models for BWR Water Level Transients," *Trans. Am. Nucl. Soc.*, **Vol. 57**, October 1988.

(3) M. Hidaka and H. Suzuki, "An Experimental Study on Gas Carryunder in Downflow from a Two-Phase Mixture Surface," *Trans. Am. Nucl. Soc.*, **Vol. 61**, June 1990.

(4) M. Petrick, "A Study of Vapor Carryunder and Associated Problems," ANL-6581, July 1962.

(5) P. L. Miller and C. P. Armstrong, "Reduction of Vapor Carryunder in Simulated Boiling", ANL-6674, February 1963.

(6) J. W. Cobble and S. W. Lin, Chapter 8 "Chemistry of Steam Cycle Solutions: Properties;" in the ASME Handbook on Water Technology of Thermal Power Systems, P. Cohen ed., ASME, N.Y. (1989).

(7) W. T. Lindsay, Jr., Chapter 7, "Chemistry of Steam Cycle Solutions: Principles"; in the ASME Handbook on Water Technology of Thermal Power Systems, P. Cohen ed., ASME, NY (1989).

(8) J. O. Outwater, "Design, Construction and Commissioning of an In-Pile BWR Coolant Chemistry Loop," Ph.D Thesis, Dept. of Nucl. Eng., M.I.T., (January 1991).

(9) ASME Handbook on Water Technology for Thermal Power Systems (1989), p. 602.

Appendix H

Hydrogen Peroxide Decomposition

The H_2O_2 decomposition reaction (including thermal and surface) is a very important part of the reaction data set used in radiolysis water chemistry. Several aspects of H_2O_2 decomposition are still in dispute among the experts in this field. Different approaches on this topic will be described here to supplement the discussions in the previous chapters.

H.1 Decomposition Mechanisms

Dr. Ibe summarized H_2O_2 decomposition mechanisms as follows (M-4).

H_2O_2	$\rightarrow 2OH$	Thermal (dominant in vapor phase)
	$\rightarrow H + HO_2$	Currently being evaluated by Dr. Ibe
	$\rightarrow O + H_2O$	Christiansen (1988 JAIF)
	$\rightarrow H^+ + HO_2^-$	At high pH
$H_2O_2 + 2e^- \rightarrow 2OH^-$		Electrochemical
$(H_2 \rightarrow 2H^+ + 2e^-)$		

Two H_2O_2 decomposition mechanisms have been employed in RADICAL to date:

$H_2O_2 \rightarrow OH + OH$ (prior to 9/1/92)
$H_2O_2 \rightarrow H_2O + 1/2\ O_2$ (after 9/1/92)

The OH radical produced in the first reaction will rapidly react with other species to generate O_2. So basically both reactions lead to the generation of O_2. However, experimental work shows that the second reaction accounts for more than 90% of the decomposition under BWR conditions, and the contribution of the first reaction is small. It should be pointed out that Chun employed this reaction primarily to satisfy RADICAL format restrictions; he and Dr. Burns devised a method to employ the second reaction during the August 1992 workshop: see section 3.3 of chapter 3 for details.

H.2 Decomposition Rates

Experiments have been carried out by C.C. Lin of GE and others to measure H_2O_2 decomposition rates for different materials (e.g., Titanium, stainless steel, glass and Teflon). The decomposition reaction was determined to be a first order reaction. The decomposition rate was measured as a function of tubing material, reaction (residence) time and the corresponding concentration. The reaction rate can be modeled as follows (L-2):

For a first order reaction,

$$\frac{dC}{dt} = -kC \tag{H.1}$$

and, upon integration,

$$C = C_0 \exp(-kt), \quad \text{or} \quad k = -\frac{1}{t} \ln \frac{C}{C_0} \tag{H.2}$$

where t = reaction time, s
k = reaction rate constant, s^{-1}
C = concentration of H_2O_2 in solution at time t
C_0 = initial concentration of H_2O_2 in solution at time t = 0

The rate constant at a certain reaction temperature be estimated from

$$k = \frac{0.693}{t_{1/2}} \tag{H.3}$$

where $t_{1/2}$ is the "half-life" (time for concentration to decrease by a factor of two) of H_2O_2.

Experiments have been made for both metallic materials and Teflon and glass. Figure H.1 shows the peroxide decomposition rate as a function of temperature in stainless steel tubing. Figure H.2 shows the results for glass and Teflon. There is a factor of 10 ~ 100 difference between the decomposition rates, depending on surface material. Table H.1 is a summary of the suggested first order H_2O_2 decomposition rate constants as a function of temperature (L-2).

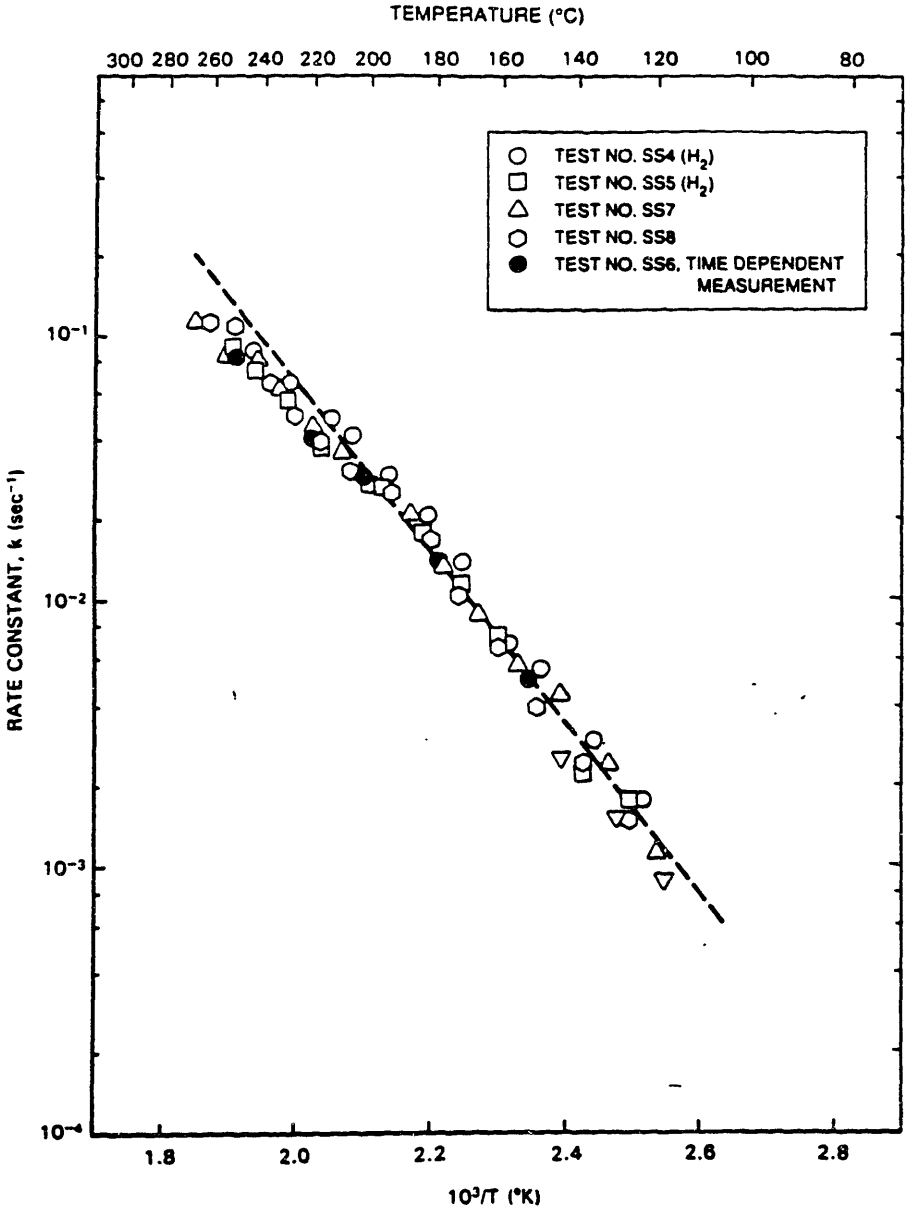

Figure H.1 Dependence of H_2O_2 decomposition rate constant on temperature for stainless steel tubing (L-2)

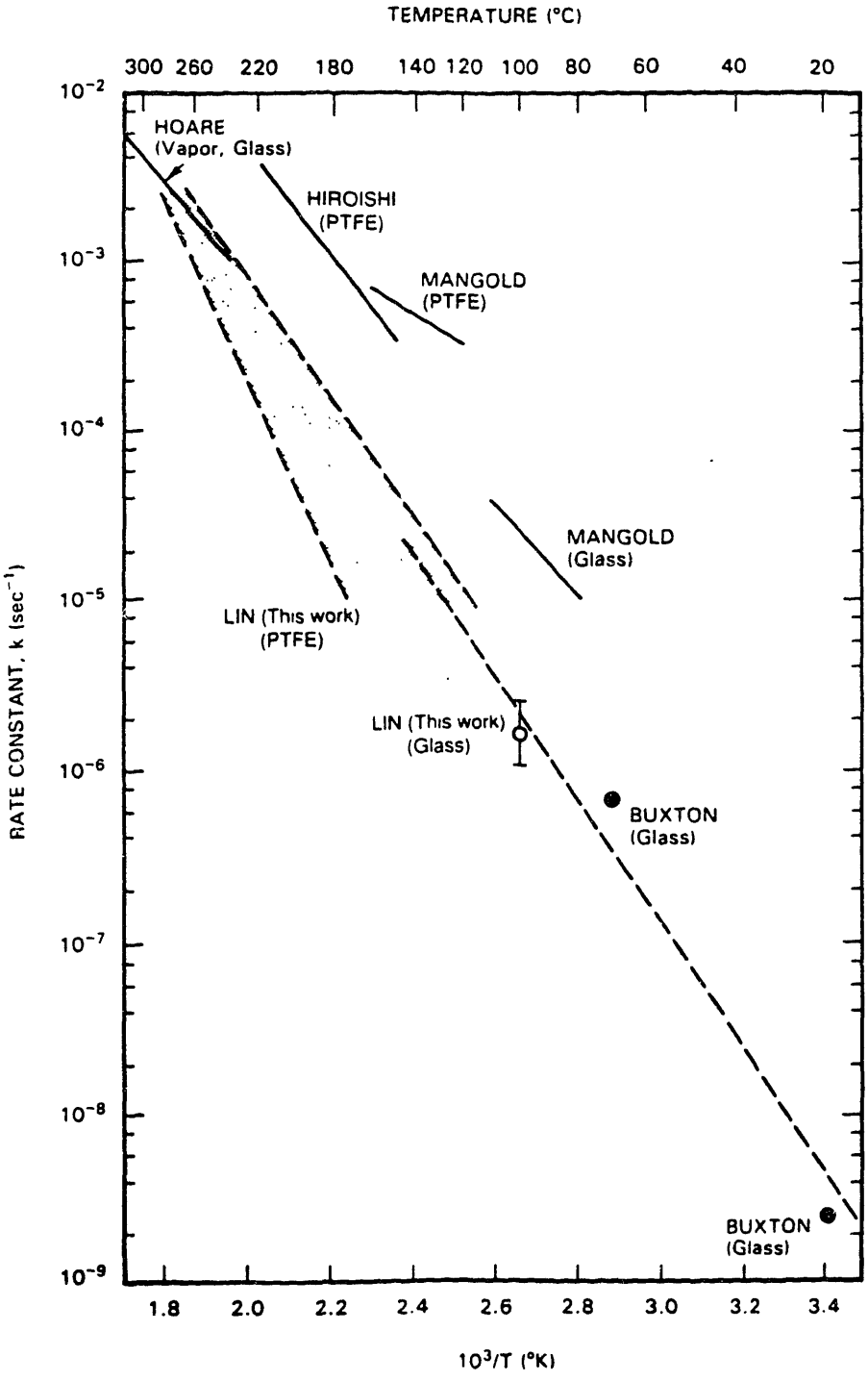

Figure H.2 H_2O_2 decomposition rate constants measured in glass and Teflon reaction vessels (L-2): i.e., in the presumed absence of wass decomposition.

Table H.1 Summary of the first order H_2O_2 decomposition rate constants for different materials

Reaction Vessel	Rate Constant
Teflon and Glass	k = 4.0 x 103 exp(-16000/RT)
Stainless Steel Tubing*	k = 2.5 x 105 exp(-14800/RT)
Titanium Tubing*	k = 7.2 x 105 exp(-16300/RT)
* 4.9 mmID R = 1.98 Kcal /mole/ °K, T in Kelvin	

It is suggested that the decomposition rate constant consists of two terms. One is for thermal (bulk) decomposition and the other one is for surface decomposition. The derivation is as follows:

$$- V \frac{d[H_2 O_2]}{dt} = V\, k_{bulk} [H_2 O_2] + S\, k_{surf} [H_2 O_2] \tag{H.4}$$

so,

$$- \frac{d[H_2 O_2]}{dt} = \left(k_{bulk} + \frac{S}{V} k_{surf}\right)[H_2 O_2] \tag{H.5}$$

where for a circular tube

$$V = \left(\frac{\pi d^2}{4}\right)\Delta z \text{, and } S = \pi d \Delta z$$

and eq.(H.5) becomes

$$- \frac{d[H_2 O_2]}{dt} = \left(k_{bulk} + \frac{4}{d} k_{surf}\right)[H_2 O_2] \tag{H.6}$$

The measured decomposition rate in the bulk water as measured in Teflon tubing is small compared to the surface decomposition measured either in stainless steel or titanium tubing. It was also found that the decomposition rate is approximately proportional to the S/V ratio.

It is suggested that not only the chemical reaction rate constant, but also the mass transfer rate, should be considered in the prediction of H_2O_2 decomposition. It is hypothesized that the decomposition process takes place on a catalytic surface following a mass transfer process (diffusion) from the bulk water to the surface. For lower

temperatures, the decomposition occurring on the surface is the dominant factor of the process, while for higher temperature, the mass transfer from the bulk water to the tubing surface is the dominant factor. The observed rate constant is related to the catalytic reaction rate constant and mass transfer coefficient as follows:

$$\frac{1}{k_{obs}} = \frac{1}{k_{dif}} + \frac{1}{k_{act}} \tag{H.7}$$

where k_{obs} = observed rate constant

k_{act} = rate constant attributed to chemical activation process that would be observed if there were no diffusion restriction on the reaction rate

k_{dif} = rate constant for diffusion (mass transfer) control

For a wide temperature range, there will be a mostly diffusion-controlled reaction ($k_{obs} \approx k_{dif}$) at one end, and a mostly activation-controlled reaction ($k_{obs} \approx k_{act}$) at the other end.

Figure H.3 shows a comparison of activation-controlled and diffusion-controlled decomposition rate constants as function of temperature. It can be seen that the H_2O_2 decomposition is activation-controlled ($k_{act} << k_{dif}$) at lower temperatures ($\leq$ 200°C) and is diffusion controlled for higher temperatures ($k_{dif} < k_{act}$). Both the theory and the experimental data suggest that a mass transfer coefficient be included in the determination of the H_2O_2 decomposition rate constant for higher temperatures.

The mass transfer coefficient (K) can be calculated from the following correlation.

$$Sh = 0.0023\ Re^{0.8}\ Sc^{0.33} \tag{H.8}$$

where Sh, Re and Sc are the Sherwood, Reynolds and Schmidt numbers, respectively. Their definitions are as follows:

$$Sh = \frac{Kd}{D},\ Re = \frac{dU}{\nu} \text{ and } Sc = \frac{\nu}{D}$$

d = diameter of tubing

D = diffusivity of H_2O_2

U = flow velocity

ν = kinematic viscosity

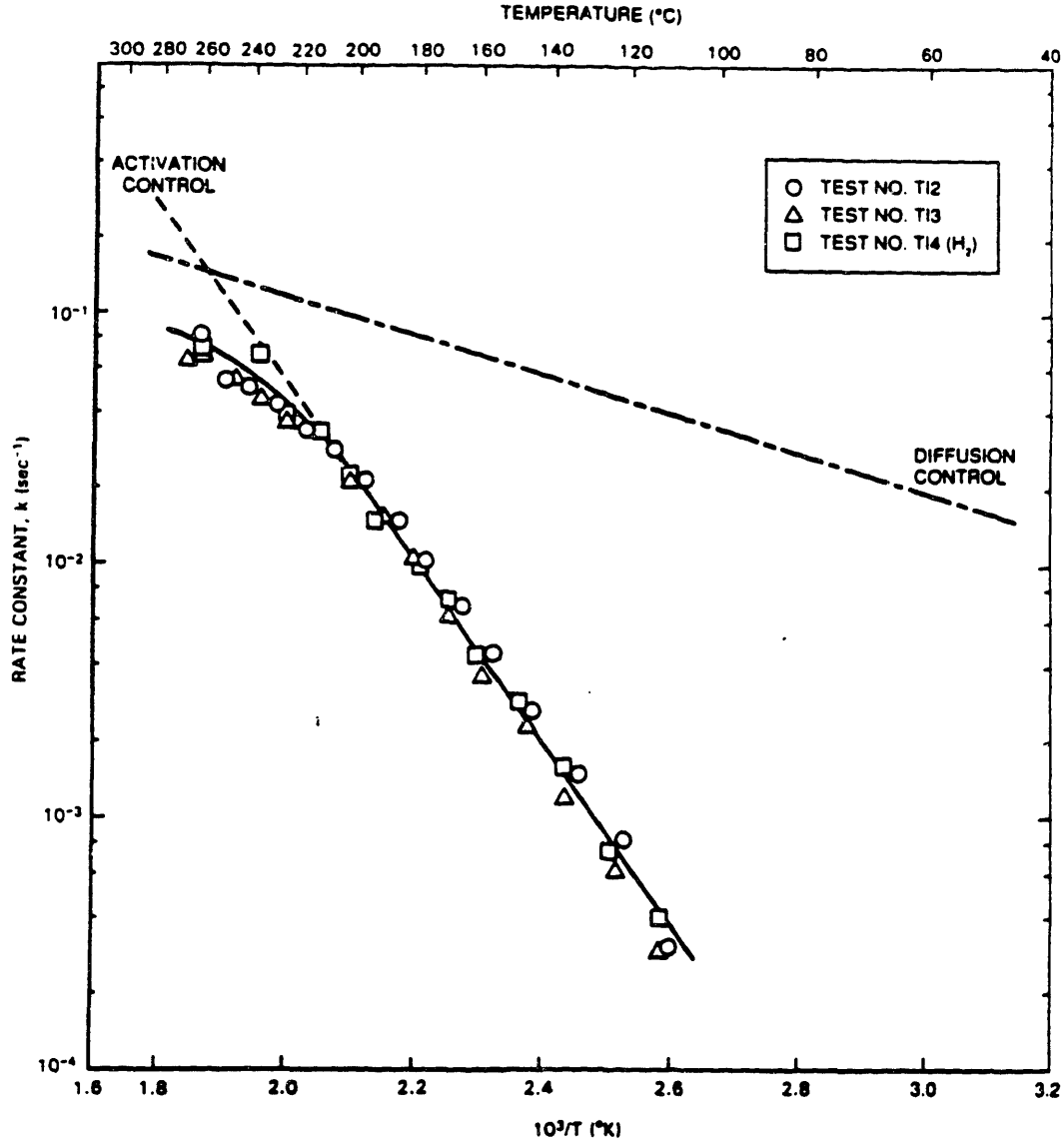

Figure H.3 Comparison of activation-controlled and diffusion-controlled decomposition rate constants as functions of temperature.

Thus K can be calculated from eq.(H.8), and k_{dif} is related to K as follows:

$$k_{dif} = K\left(\frac{S}{V}\right) = K \cdot \frac{4}{d} \qquad \text{(H.9)}$$

Note that this analysis is based upon a boundary condition of instantaneous decomposition at the wall (i.e., zero H_2O_2 concentration).

Thus Figures H.1 and H.3 suggest values for k for the BCCL in the range 0.1 to 0.5 sec^{-1}.

Appendix I

Error in Quality Measurement

Quality is measured in the BCCL by heat balance across the regenerative heat exchanger. Thermocouple errors are negligible, hence heat losses in the steam and water lines between the separator plenum and the RHX and from the RHX itself, are the principal source of error.

An enthalpy balance gives (basis = 1 unit mass flow):

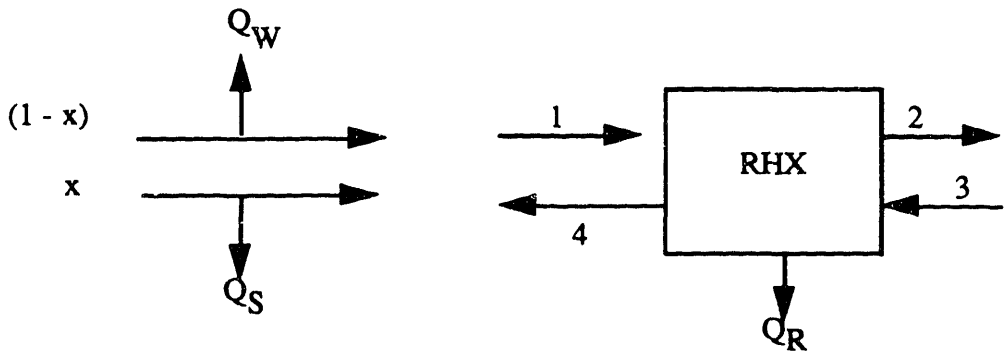

$$x H_{S1} + (1 - x) H_{W1} - H_2 - Q_W - Q_S = (H_4 - H_3) + Q_R \quad \text{(I.1)}$$

But

$$H_{S1} = \Delta H_{V1} + H_{L1} \quad \text{(I.2)}$$

where ΔH_{V1} is the latent heat of vaporization. Solving for x one obtains:

$$x = \frac{(H_4 + H_2) - (H_3 + H_{W1}) + Q_R + Q_W + Q_S}{\Delta H_{V1}} \quad \text{(I.3)}$$

Thus, compared to a system with no losses

$$\Delta x = \left(\frac{Q_R + Q_W + Q_S}{\Delta H_{V1}}\right) \quad \text{(I.4)}$$

The measured temperature loss between the plenum and RHX is ~ 10°C. Losses from the RHS itself are small, so we can neglect it for now in the calculation (i.e., $Q_R << Q_W + Q_S$). The errors as a function of operating temperature for a 10°C temperature loss can be calculated from equation (I.4) using

$$Q_W \approx (1-x)\cdot C_{pw}\cdot \Delta T \tag{I.5}$$

and

$$Q_S = x\cdot C_{ps}\cdot \Delta T \tag{I.6}$$

Thus Δx will be a function of operating quality. Due to the fact that C_{pw} and C_{ps} are close in the temperature range considered ($(C_{ps}-C_{pw})/C_{pw} = 0.2\%$ at 290°C, and within 15% for T = 200°C to 300°C), we assume that $\overline{C_p} \approx (C_{ps}+C_{pw})/2$ so the equation

$$Q_W + Q_S \approx \overline{C_p}\cdot \Delta T, \tag{I.7}$$

can replace eqs. (I.5) and (I.6).

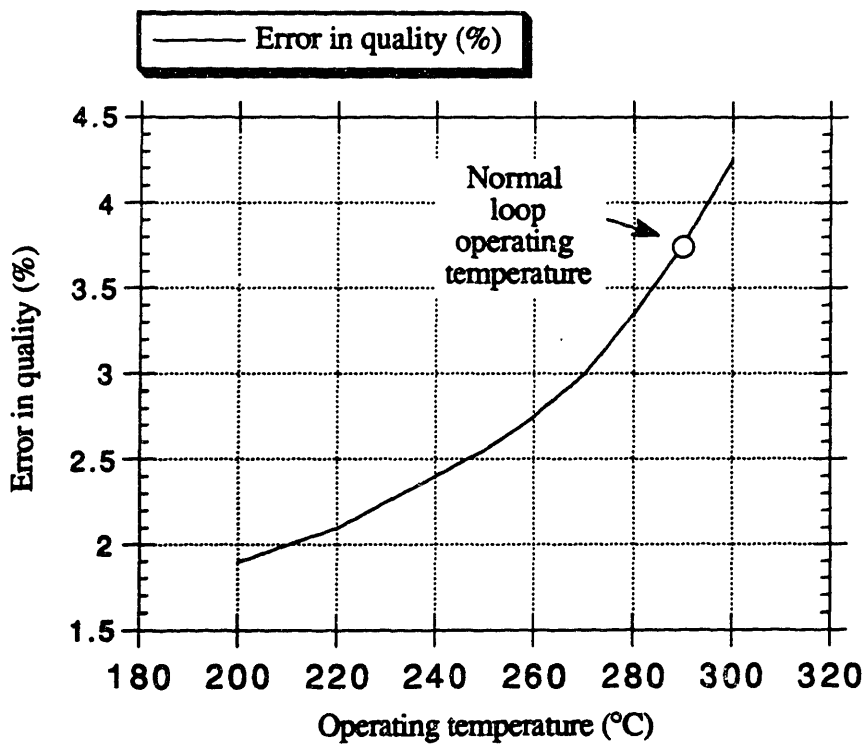

Figure I.1 Error in quality measurement as a function of operating temperature.

Based on the above estimate, the nominal quoted exit quality (e.g., 15%) is as much as 4% low. The parametric studies of chapter 4 show that this should not have a significant effect on radiolysis product concentrations. However, it does indicate that more direct measurements of steam flow rate using an accurate flowmeter be made in future loop campaigns.

Appendix J

Orbisphere Principle/Calibration/Operation

Orbisphere® detectors measure oxygen using reduction reaction. The anode of the Orbisphere sensor is held positive with respect to the cathode. Current flowing through the sensor due to oxygen reduction at the cathode is converted to a voltage by an amplifier, the proportionality between voltage and current being determined by the feedback resistance of this amplifier. The output voltage is essentially a function of oxygen activity (partial pressure), temperature and membrane permeability. Corrections for variations in membrane permeability are made when the sensor is calibrated. The temperature compensation circuit takes care of temperature variations automatically (O-3).

The Orbisphere sensor is calibrated in water-saturated air . The Orbisphere meter is first calibrated against a barometer. Then the sensor can be calibrated for known temperature and pressure (oxygen concentration in water-saturated air is a function of pressure and temperature). One should also check the Orbisphere sensor and perform sensor services (maintenance) periodically to make sure the sensor is operation normally.

The accuracy of Orbisphere detectors, as stated by the manufacturer, is ± 1% or ± 0.1 ppb/0.05Pa, whichever is greater. The response time (or signal drifting frequency) depends on the membrane used in the sensor. Also notice that the Orbsphere may be sensitive to the operating flow rates, so it is suggested that the flow rate be kept constant during experiments.

Table J-1 Orbisphere® membrane characteristics

Membrane	Response time: 90% of signal change @ 25°C	Upper/lower limits, DO2	Upper/lower limits, PO2	Recommended flow rate through flow chamber
2952A	38 sec.	80ppm/2ppb	200kPa/5Pa	50ml/min
2956A	7.2 sec.	20ppm/0.1ppb	30kPa/0.05Pa	180ml/min
2958A	9.5 sec.	60ppm/1ppb	125kPa/2Pa	120ml/min
29552A	90 sec.	80ppm/2ppb	200kPa/5Pa	50ml/min
2935A	137 sec.	200ppm/10ppb	200kPa/20Pa	10ml/min
2995A	80 sec.	2000ppm/40ppb	2000kPa/100Pa	1 ml/min
29521A	360 sec. at 65°C	200ppm/10ppb	200kPa/20Pa	60 cm/sec.

Appendix K

Recirculation System Response Time

For a recirculation system as below, assume H_2O_2 decomposes instantaneously as it goes into the loop so only one species, O_2, has to be considered.

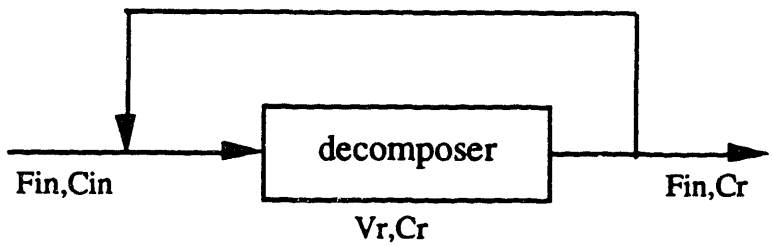

The following differential equation accounts for the O_2 concentration changes in the recirculation line

$$Vr\frac{\partial Cr}{\partial t} = Fin \cdot (Cin - Cr) \qquad (K.1)$$

The equation can be solved by assuming Fin, Cin and Vr are constants. So,

$$Cr(t) = (Cr0 - Cin) \cdot \exp(-\frac{Fin}{Vr} \cdot t) + Cin \qquad (K.2)$$

where Fin = inlet flow rate
Cin = inlet O_2 concentration (assume H_2O_2 decomposes instantaneously)
Cr = outlet O_2 concentration
Cr0 = initial O_2 concentration in the recirculation loop
Vr = total sample liquid volume in the recirculation loop

For the recirculation mode design of the MnO_2 method, the total volume of the recirculation loop occupied by sample liquid is ~ 90 cc. About 1/3 of the volume is occupied by the decomposer. The inlet flow rate is assumed to be 5 cc/min, which is about the average value of the experimental conditions in section 6.3.1. The half-life of the O_2 concentration originally existing in the recirculation loop is,

$$T1/2 = \frac{0.693}{Fin/Vr} = 12.5\,\text{min} \qquad \text{(K.3)}$$

So the half-life increases with system volume and decreases with inlet flow rate.

For Cin=500 ppb, Cr0=8 ppm

# of T1/2	Time (min)	Cr(t)/Cin
4	50	1.94
6	75	1.23
8	100	1.06
10	125	1.01

For Cin=500 ppb, Cr0=0 ppb

# of T1/2	Time (min)	Cr(t)/Cin
4	50	0.94
6	75	0.98
8	100	0.996

The above values are underestimates, because the membrane response time and the time required for 100% H_2O_2 decomposition are not included in this calculation. Hence for the system analyzed above, response times are on the order of 1 hour, which is too long to be useful in BCCL experiments.